TO REACH AND BEYOND: NEURAL MECHANISMS FOR MULTISENSORY INTEGRATION OF GRASPING AND PLACING MOVEMENTS

Gaëlle Nsamba Luabeya

A DISSERTATION SUBMITTED TO THE FACULTY OF GRADUATE STUDIES IN PARTIAL FULFILLMENT OF THE REQUIREMENTS FOR THE DEGREE OF DOCTOR OF PHILOSOPHY

GRADUATE PROGRAM IN BIOLOGY

YORK UNIVERSITY

TORONTO, ONTARIO, CANADA

June 2026

© Gaëlle N. Luabeya, 2026

ABSTRACT

For so many of us, our morning ritual involves hearing our alarm, opening our eyes, reaching to turn off the device, putting it back on our nightstand, and returning to sleep. As in this simple scenario, our brains rely on a multitude of sensory inputs to interact with the world around us. This thesis asks how this plethora of sensory information is integrated with our intention and verbal instructions received to execute a desired movement. To this end, I conducted three studies: a behavioural study (Chapter 2) and a functional Magnetic Resonance Imaging (fMRI) study (Chapter 3) of placement to understand how terminating our interaction with an object differs from initiating it. Returning to our example, this represents our action of grabbing the alarm clock to interact with it and placing it back on the nightstand. The third study used a cue-separation fMRI task (Chapter 4) to examine how we integrate multisensory cues into motor planning and execution (as required when incorporating the auditory cue of the alarm ringing with the visual cue of its light flashing). In the behavioural study, I varied the levels of visual feedback, gaze location, and saccade to investigate whether these factors affect placement errors in location and orientation. Similar to reach, placement overshoots the target location depending on the gaze location and the saccade performed. In addition, gaze influences the orientation of object placement, depending on the available visual information and the template orientation. In this fMRI study, there was a high degree of similarity in brain activation patterns for grasp and placement. However, I was able to differentiate these actions in reach-related regions of interest using a K-nearest neighbours classifier. Furthermore, grasp and place share a similar functional module topology but differ in their specific modularity. Finally, the cue-separation multisensory fMRI task revealed that multisensory input is processed by distinct subnetworks and integrated within the somatomotor regions. More specifically, visual information about object location followed the typical dorsal stream through an Occipital-Parietal-Somatomotor Module, whereas the verbal instructions were processed through a Temporal-Frontal-Somatomotor Module. Overall, these results implicate cortico-cerebellar subnetworks in the multisensory integration of visual, somatosensory, and auditory information for both grasping and placing, and frame goal-directed action as an intention-shaped process realized across distributed brain networks.

DEDICATION

In loving memory of Gustave Tshitala Luabeya,

a father like no other.

ACKNOWLEDGEMENTS

First and foremost, I would like to express my deepest gratitude to my supervisor, Dr. J. Douglas Crawford. Thank you for your patience, your generosity with your time, and the constant support that has shaped both this dissertation and the researcher I have become. Whether over lunch breaks, email threads, or Zoom meetings, you were always there to encourage me and keep me focused on my goal. You shared your wisdom freely, yet always let me make my own decisions. Your mentorship has made me a better scientist and deepened my curiosity. I am equally grateful to my co-supervisor, Dr. Erez Freud. Your insight and encouragement have been invaluable at every stage of this work. You gave feedback detailed enough to act on and never let me lose sight of the bigger picture. I am especially grateful for the way you invest in me. You made yourself available when I needed step-by-step clarification, and I left every one of our meetings with more ideas than I arrived with.

Thank you, Dr. Nikolaus F. Troje, for your thoughtful feedback over the years; your comments often opened new perspectives and sharpened my delivery and clarity. Furthermore, I would like to express my gratitude to my examining committee, Dr. Jody C. Culham, Dr. Denise Y. P. Henriques, and Dr. Jonathan A. Michaels, for the attention and time you dedicated to my dissertation. I am also grateful to Dr. Simona Monaco, Dr. Amirhosein Ghaderi, Dr. Xiaogang Yan, and Saihong Sun for the many meetings, the experience and the ideas you shared to guide my projects. I learned so much from each of you along the way. To my colleagues and friends in CrawLab and FreudLab, thank you for creating an environment where curiosity thrives. Your camaraderie and willingness to help brightened even the most challenging days. Over the years, we shared hopes, dreams, and laughter, and our work sessions were a constant source of encouragement. The time we shared and the memories we made remain treasured in my heart.

To my family and friends, here and abroad, thank you for a love that distance and time have never diminished. Oceans and busy schedules have stood between us, yet your encouragement reached me every single day, and it carried more weight than words can hold. Finally, my most heartfelt thanks go to my husband, John, and our wonderful children. You are my anchor and my constant source of strength. Your unwavering support, love, and flexibility carried me through every high and low. You are my greatest motivation and my deepest joy. As I have said time and time again, this is as much your accomplishment as it is mine.

TABLE OF CONTENTS

ABSTRACT ii
DEDICATION iii
ACKNOWLEDGEMENTS iv
TABLE OF CONTENTS v
LIST OF TABLES ix
LIST OF FIGURES x
CHAPTER 1: GENERAL INTRODUCTION 1
1.1 Multisensory Integration and the Dominance of the Visual System 2
1.2 Behavioural Aspects of Eye-hand Coordination in Goal-directed Action 3
1.3 Behavioural Dichotomy in Prehension 4
1.4 Functional Anatomy of the Reach and Grasp Systems 6
1.5 Behaviour and Neurophysiology of Object Placement 11
1.6 Neural Influence of Instructions on Action 13
1.7 Specific Aims and Hypotheses 15
CHAPTER 2: INFLUENCE OF GAZE, VISION, AND MEMORY ON HAND KINEMATICS IN A PLACEMENT TASK 18
2.1 Abstract 19
2.2 Introduction 19
2.3 Methods 22
2.3.1 Participants 22
2.3.2 Apparatus and Stimuli 23
2.3.3 General Task Design 25
2.3.4 Experiment 1 27
2.3.5 Experiment 2 28
2.3.6 Data Analysis and Exclusion Criteria 29
2.3.7 Statistical Analysis 31
2.4 Results 32
2.4.1 Experiment 1 32
2.4.2 Experiment 2 37
2.4.3 Influence of Initial Gaze Position During Saccades 40
2.5 Discussion 42
2.5.1 General Bias in Placement Location 43

2.5.2 Influence of Template Orientation on Placement Orientation 43
2.5.3 Influence of Gaze Position on Placement Location 44
2.5.4 Influence of Gaze Position on Placement Orientation 45
2.5.5 Influence of Visual Feedback and Memory Delay 46
2.5.6 Influence of Saccades 47
2.5.7 Caveats and limitations 47
2.5.8 Possible Neural substrates 48
2.5.9 Conclusions 49
CHAPTER 3: BEYOND REACH I: NEUROIMAGING REVEALS DIFFERENT CORTICO-CEREBELLAR NETWORKS FOR GRASP VS. OBJECT PLACEMENT 51
3.1 Abstract 52
3.2 Introduction 53
3.3 Methods 55
3.3.1 Participants 55
3.3.2 Apparatus and Stimuli 55
3.3.3 Experimental Task Design 57
3.3.4 Imaging Parameters 58
3.3.5 Preprocessing 59
3.3.6 Graph Theoretical Analysis 59
3.3.7 Statistical Analyses 62
3.3.7.1 Univariate Analysis 62
3.3.7.2 Regions-of-Interest and Classification Analyses 63
3.3.7.3 GTA Statistics 64
3.4 Results 64
3.4.1 Univariate Analysis 65
3.4.2 Region of Interest Analysis 70
3.4.3 Classification Analysis 71
3.4.4 Graph Theory Analysis 71
3.5 Discussion 78
3.5.1 Univariate BOLD Analysis during Planning and Execution 78
3.5.1.1 Common (Task-independent) Cortical and Subcortical Activation 78
3.5.1.2 Selective (Task-dependent) Cortical and Subcortical Activation 79
3.5.1.3 Region of Interest Analysis and Classification 80
3.5.2 Graph Theoretical Functional Connectivity Analysis 81

3.5.2.1 Macro-scale Network Features: Equivalence of Global Parameters 81
3.5.2.2 Meso-scale Network Features: Similar Modules, Different Community Strengths 82
3.5.2.3 Micro-scale Network Features: Local vs. Global Hubs 83
3.5.2.4 Limitations and Future Direction 84
3.5.2.5 General Implications for Sensorimotor Imaging Studies 85
3.5.2.6 Conclusion 86
CHAPTER 4: MODULAR INTEGRATION OF AUDITORY INSTRUCTIONS AND VISUAL CUES INTO THE CORTICAL REACH NETWORK 87
4.1 Abstract 88
4.2 Introduction 88
4.3 Methods 91
4.3.1 Participants 91
4.3.2 Apparatus and Stimuli 92
4.3.3 Experimental Task Design 94
4.3.4 Imaging Parameters 95
4.3.5 Preprocessing 95
4.3.6 Graph Theoretical Analysis 95
4.3.7 Statistical Analysis 100
4.4 Results 102
4.4.1 Whole-Brain Univariate Analyses 102
4.4.2 Region of Interest Analysis: Visual and Motor Components of the Reach Network 103
4.4.3 Functional Network Analysis 106
4.4.3.1 Global Network Properties. 106
4.4.3.2 Correlated Time Series Suggest Parallel Processing Streams 108
4.4.3.3 Modularity Analysis: Occipital-Parietal vs. Temporal-Frontal Modules 110
4.4.3.4 Classification Analysis: Cue Order-Dependence. 115
4.4.3.5 Eigenvector Centrality Hubs. 115
4.4.3.6 Betweenness Centrality Hubs. 119
4.5 Discussion 122
4.5.1 Univariate Analysis: Activation and Order Dependence 123
4.5.2 Graph Theory Analysis of Functional Network Properties 123
4.5.3 Order-Independent Integration at the Global Level 124

4.5.4 Network Integration: Modules and their Local Hubs 124
4.5.5 Lateral Integration: Betweenness Centrality 126
4.5.6 Caveats and Limitations 126
4.5.7 Possible Clinical Implications 127
4.5.8 Conclusion 127
CHAPTER 5: GENERAL DISCUSSION 129
5.1 General Summary of Results 129
5.2 Scientific Implications 131
5.3 Potential Applications 132
5.4 Limitations 133
5.5 Future Directions 134
5.6 Conclusion 136
REFERENCES 137
APPENDIX I: AUTHOR CONTRIBUTIONS 183
APPENDIX II: SUPPLEMENTARY FIGURES 184

LIST OF TABLES

Table 4.1 Glossary of Graph Theory Measures used for our weighted networks..... 99

Table 4.2 Summary of Means, Standard Errors, and FDR-corrected q-values for the significant difference in β weight 104

Table 4.3 Eigenvector Centrality Hubs.....117

Table 4.4 Betweenness Centrality Hubs 121

LIST OF FIGURES

Figure 1.1. Illustration of upper limb kinematics 6

Figure 1.2. A contrast of nonhuman primate and human parietal cortex 8

Figure 1.3. Schematic illustration of the cerebral cortex, the basal ganglia, and the cerebellum..11

Figure 1.4. Illustration of the auditory-motor pathway..... 15

Figure 2.1. Experimental Task 24

Figure 2.2. Experimental protocol 26

Figure 2.3. Typical placement kinematics for one participant in Experiment 1 30

Figure 2.4. Graph of Location Errors in *Experiment 1* 33

Figure 2.5. Orientation Errors in *Experiment 1* 36

Figure 2.6. Distribution of Location and Orientation Errors for *Experiment 2* 39

Figure 2.7. Mean Location Error and Orientation Errors in *Experiment 2* 41

Figure 3.1. Experimental setup 56

Figure 3.2. Illustration of the graph theoretical pipeline 61

Figure 3.3. Cortical activation maps for the *Grasp* & *Place* conditions during the *planning* phase 66

Figure 3.4. Cortical activation maps for the Grasp & *Place* conditions during the *execution* phase 68

Figure 3.5. Cortical activation maps for the *Grasp* vs *Place* comparison during the *planning* phase and the *execution* phase 69

Figure 3.6. Bar graphs of the beta weights from 7 ROIs in the left hemisphere 70

Figure 3.7. Trend unmodified network modularity analysis..... 72

Figure 3.8. Detrended Network modularity analysis for the *Grasp* and *Place* conditions..... 75

Figure 3.9. Brain maps showing local and global hubs for the *Grasp* and *Place* conditions..... 77

Figure 4.1. Experimental setup 93

Figure 4.2. Schematic representation of graph theoretical analysis (GTA) applied to fMRI data 97

Figure 4.3. Cortical activation maps 106

Figure 4.4. Violin plots displaying distributions of normalized global network parameters. 107

Figure 4.5. Medial and lateral views of the cortical activation maps 109

Figure 4.6. Network modularity analysis.....112

Figure 4.7. Modularity comparisons across experimental conditions and gamma values.....114

Figure 4.8. Eigenvector centrality hubs presented on brain maps 117

Figure 4.9. Betweenness centrality hubs are presented on brain maps..... 120

CHAPTER 1:

GENERAL INTRODUCTION

At first glance, goal-directed movements, such as toasting a piece of bread for breakfast, may appear trivial and effortless. However, like all complex actions we perform throughout the day, these movements require the integration of multiple sensory modalities and, in some cases, the combination of verbal instruction with visual information to perform the desired action (Neggers & Bekkering, 1999; Sedda et al., 2011; Tubaldi et al., 2008). Goal-directed movements are often studied in prehension, which is a specific type of movement used to reach and grasp objects (Van De Kamp & Zaal, 2007). Over the past forty years, prehension research has mapped how various processes in vision and motor control achieve the intended acquisition. Yet, the interaction with our surroundings does not end at acquisition. Indeed, after being picked up, the bread would need to be transported, rotated, and finally inserted into the toaster; any initiated prehension is often bound to terminate with an object placement movement. Despite its significance, the latter stage of the interaction has been relatively neglected in neuroscience. An additional layer of complexity is that the action is not solely guided by visual input. In our daily interactions as well as the laboratory experiments, verbal instruction often influences how the action is performed and what is done with what is seen, raising a follow-up question about how auditory instruction is integrated with vision by the cortical reach network. Therefore, this dissertation takes prehension as a starting point and expands its concept to investigate the behavioural and neural basis of object placement and examine how auditory instruction is merged with vision for action.

Taking a general-to-specific approach, the following chapter explores the general principles of multisensory integration, since each of these avenues depends on the brain's ability to combine information. This is further narrowed down to the importance of vision and explores the specific link between eye and hand coordination in action. Then, I present prehension and its two phases as models for studying goal-directed action at the behavioural and neural levels. To end things, I examine what we know about reach-to-placement and the influence of verbal instruction. Finally, I bring things back together and present the specific questions I investigated to expand our understanding of goal-directed action.

1.1 Multisensory Integration and the Dominance of the Visual System

As aforementioned, any interaction with our surroundings requires the coordination of the magnitude of sensory input received by the brain (Kawato et al., 1987; Sober & Sabes, 2003; Tagliabue & McIntyre, 2014). Indeed, the nervous system processes and deciphers the myriad of visual, auditory, haptic, and proprioceptive information readily available (Ladwig et al., 2013; Neggers & Bekkering, 1999; Sedda et al., 2011; Tubaldi et al., 2008). From the earliest evidence of multimodal sensory integration in the cat superior colliculus (SC) to more recent evidence of reciprocal communication between SC layers, multisensory interaction appears to be an intrinsic component of neuronal communication (Meredith et al., 1992; Wallace et al., 1996, 1998). In humans, studies have found that the brain is developmentally multisensory, with no clear cortical specialization until sensory experience prunes unnecessary connections. Indeed, early in development, touch could activate areas of the temporal cortex that would eventually be associated with auditory processing (Shibata et al., 2012). As they gain experience, this pruning reduces synaptic density throughout the cortex, thereby strengthening the cortical specialization we are familiar with.

Among the different sensory systems, the visual and auditory systems stand out for their ability to accumulate sensory information without requiring direct contact with the environment. Indeed, the other senses are limited to peripersonal space; evolutionarily speaking, they would pose a disadvantage when responding promptly to avoid danger. When presented in unison, visual and auditory information can optimize comprehension and movement output (Kenessy, 2021; Opoku-Baah et al., 2021). For instance, we usually understand our interlocutor better by watching them speak. In other cases, however, the two senses may interfere with each other, as in the peculiar habit of turning down the radio when searching for an address while driving (Ünal et al., 2013). Conversely, their absence in situations where they are expected could hinder the implementation of action. For instance, athletes' performance in table tennis and tennis decreases without auditory input (Hermann et al., 2006; Takeuchi, 1993). However, vision and audition do not carry the same weight in supporting the movement output.

Indeed, greater emphasis is placed on visual input, such that, in its presence, the other systems are often less influential (i.e., Hutmacher, 2019; Kritikos & Brasch, 2008). The visual capture phenomenon reflects this primacy of the visual system over the other senses (Bosen et al., 2017;

Radeau & Bertelson, 1977; Spence, 2007). For example, in the ventriloquism effect, the source of the auditory cue is misattributed to the same location as the visual cue (i.e. the puppet). The visual system plays a dominant role when navigating and interacting with the world around us.

1.2 Behavioural Aspects of Eye-hand Coordination in Goal-directed Action

As alluded to in the previous section, the available vision information enables us to interact with our surroundings. This is achieved through our ability to shift and control gaze location by maintaining and orienting eye and head positions (Guitton & Volle, 1987; Zangemeister & Stark, 1982). Despite our heavy reliance on continuous visual input to plan and execute actions, we often have to navigate the world in less-than-optimal conditions, for instance by storing the visual input in memory in the absence of visual feedback or across a saccadic eye movement. Because foveal vision provides the most detailed information for visually guided action, eye movements allow one to shift the target. Compared with peripheral vision, foveating on the target improves movement accuracy (Brown et al., 2005; Klostermann et al., 2020). In the absence of visual feedback, participants' reach is most accurate when gaze is directed toward the target (Henriques et al., 2003). Therefore, even in the dark, where we look matters and influences our action output. Indeed, gaze eccentricity provokes a systematic movement error the further one’s gaze is from the target (Bock, 1986; Bock & Eckmiller, 1986).

During a saccadic eye movement, the dynamic shift in gaze position triggers an oculocentric reframing, resulting in an overshoot error in the direction opposite the eye movement (Henriques et al., 1998; Medendorp & Crawford, 2002; Schütz et al., 2013). Most saccade studies investigating the influence of an update in the gaze-dependent overshoot effect have mainly used centrifugal saccades (saccades away from the target), and it is then assumed that other types of rapid eye movements behave similarly (e.g., Fiehler et al., 2011; Henriques et al., 1998; Khan, Pisella, Rossetti, et al., 2005). However, saccades can be used to move from one peripheral viewpoint to another; most often, centripetal saccades are used because they allow peripheral objects to be foveated. The earlier view held that this gaze-dependent overshoot error in saccades resulted from a misremembering of the target position. Later investigations challenged this perspective. As Dessing and colleagues (2012) suggested, the error resulted from a misestimation of hand position, and adding visual feedback of the hand eliminated the gaze-dependent overshoot effect. Interestingly, gaze location still produces a gaze-dependent overshoot effect in

reach even when a memory delay precedes movement onset (Fiehler et al., 2011). In other words, even without visual information, gaze location has a robust influence on movements, and the overshoot effect is not entirely dependent on visual feedback but on the internal representation of the target. Furthermore, the gaze-dependent error is not solely due to a shift in eye position; when reaching a somatosensory target, the same gaze-dependent error is observed after a shift in eye position or proprioceptive hand position before movement onset (Mueller & Fiehler, 2014, 2017). This reflects once again the importance of multisensory integration for proper motor planning (Burns & Blohm, 2010; Sober & Sabes, 2003, 2005).

1.3 Behavioural Dichotomy in Prehension

Thus far, we have explored movement control as an overall action in pointing tasks. However, voluntary goal-directed movements are composed of two phases: an initial ballistic phase, with a rapid movement to bring the limb close to the target, and a late adjustment phase with a slower movement where accuracy is increased as the hand approaches the target (Elliott et al., 2010; Woodworth, 1899). The distinction between these two phases of goal-directed action is also observable in prehension movements and is defined by the visuomotor channels hypothesis (Rizzolatti & Matelli, 2003). This theory distinguishes between the two stages of prehension as an initial transfer of the hand to the target object's location (reach component) and a subsequent grip of the target object (grasp component). When incorporating the dual phases of goal-directed movements within the visuomotor channels hypothesis, the initial ballistic phase could correspond to the reaching component of prehension, and the subsequent adjustment phase to the grasping component (Paulignan et al., 1991).

The component distinction in such visually guided action is also noticeable in how the two phases are affected by the absence of ongoing visual feedback, with the final phase being the most severely affected by visual sensory deprivation, as the movement refinement it requires benefits more from ongoing visual input. Compared with simple reach movements, final grasp movements require fine-tuning of the grip and digit positioning (Kamp et al., 2009; Monaco et al., 2015). Whereas the reach component might only incorporate information about the target location, the grasp component requires computing the target orientation and a specific finger-grip paradigm. Similar to the reach dependency on gaze location, the endpoints of the two digits' positions and orientations during grasping showed a gaze-centered pattern of grasping error

(Selen & Medendorp, 2011). Overall, prehension comprises two phases, whose respective errors are modulated by the presence or absence of visual information. In addition, they are influenced by the type of retinal information (foveal or peripheral) available to perform the action, reflecting the complexity of gathering the relevant ocular information to execute the targeted action while minimizing error.

Motor functions, such as prehension, have been evolutionarily conserved because they are important for interacting with our surroundings. This conservation is also observed in their homology across species (Fig. 1.1). However, Karl and Whishaw (2013) have proposed that they may have distinct evolutionary roots. By relying on haptic feedback and proprioceptive input, reach seems to have evolved from nonvisual stepping behaviour in quadrupeds, whereas grasp evolved from food-handling behaviour. This differentiation is also observed developmentally in infants, who tend to develop their reaching and grasping skills separately (Thomas et al., 2015). Eventually, as prehension skill advances, by two years of age, children can smoothly blend the reach-and-grasp components of movement, with a preshaping action visible during transport and before gripping the target (Kuhtz-Buschbeck et al., 1998).

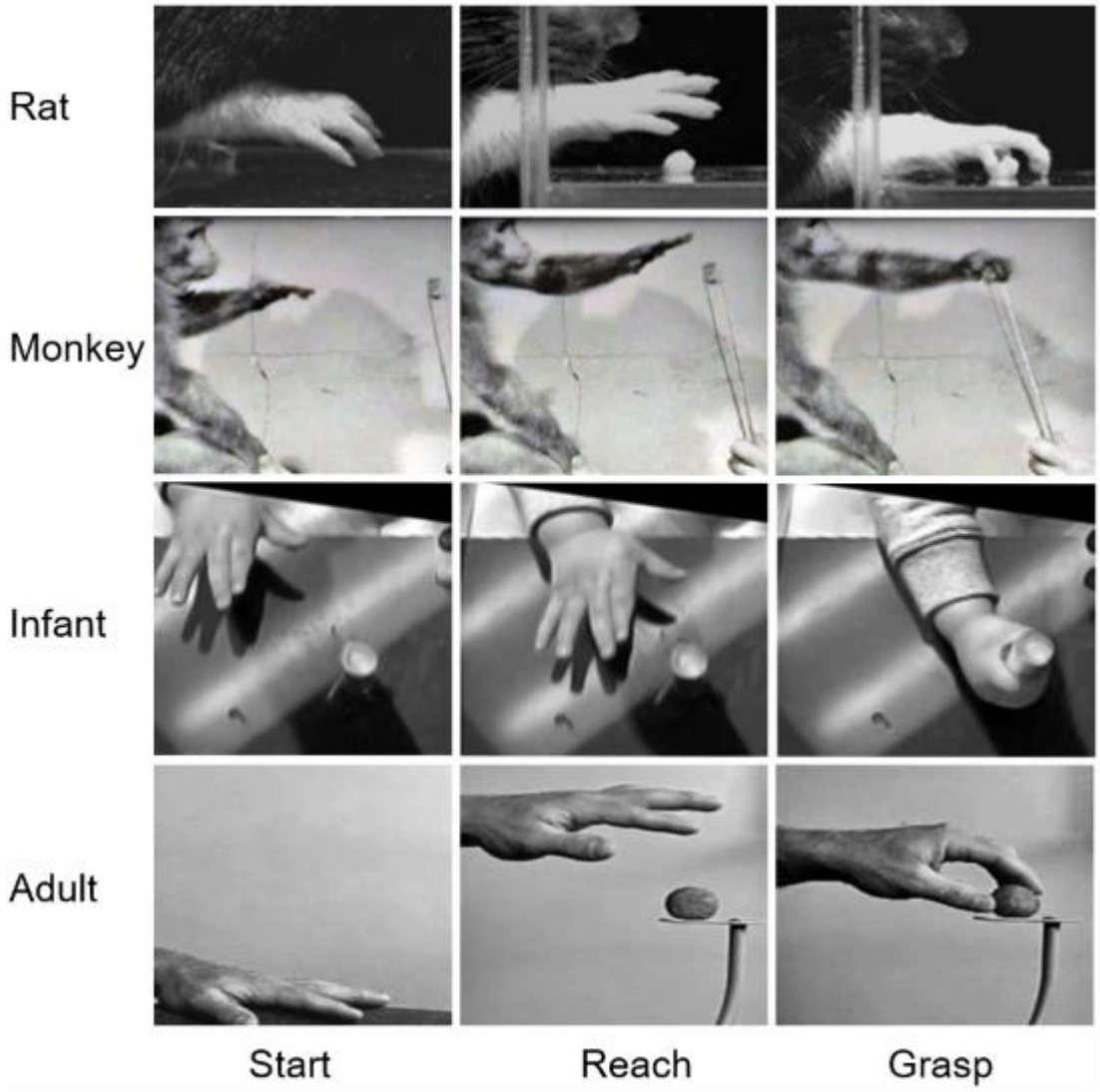


Figure 1.1. Frame illustration of upper-limb kinematic movement during visually guided reach and grasp of a target in a rat, a non-human primate, an infant, and an adult. Adapted from Karl & Whishaw (2013)

1.4 Functional Anatomy of the Reach and Grasp Systems

Electrophysiological animal research in rodents and non-human primates has helped us understand how the brain develops the dual components of prehension (Fig. 1.1). Starting from rodent work, the anterior motor cortex in the rat has a rostral forelimb area (RFA) and a caudal forelimb area (CFA). Their electrical stimulation elicits distinct movement outcomes. On the one hand, RFA stimulation produced hand-related movements such as grasping; on the other hand, CFA stimulation produced movement of the entire limb, akin to reaching (Bonazzi et al., 2013; Brown & Teskey, 2014).

With their opposable thumbs and high dexterity, non-human primates exhibit even greater similarity to humans in the types of movement they can achieve (Fig. 1.1). Early neurorecording studies show the posterior parietal cortex (PPC) as a singular hub for action integration (Fig. 1.2), as it is located at the intersection of visual input from the occipital cortex and sensory information from the somatosensory cortex (Mountcastle et al., 1975). The parietal cortex organization also reflects its regional proximity to these two regions, with neurons in the superior parietal lobule (SPL) increasing firing for somatosensory inputs and neurons in the inferior parietal lobule (IPL) having a particular increase in firing rate in the presence of visual information (Hyvärinen, 1982; Mountcastle et al., 1975). More medially in the PPC lies V6A, a visuomotor region that responds to both visual and somatosensory information and uses them to guide actions, particularly hand pre-shaping and grasping (Fattori et al., 2005, 2009; Galletti & Fattori, 2018). In addition, reach-related regions have been identified in MIP, area 5, and area 7A, whereas the grasp-related region was found in AIP (Galletti & Fattori, 2018). Reach- and grasp-related parietal clusters seem to follow a parallel pathway to frontal regions, with MIP connecting to ventral premotor cortex (PMv) and AIP connecting to dorsal premotor cortex (PMd).

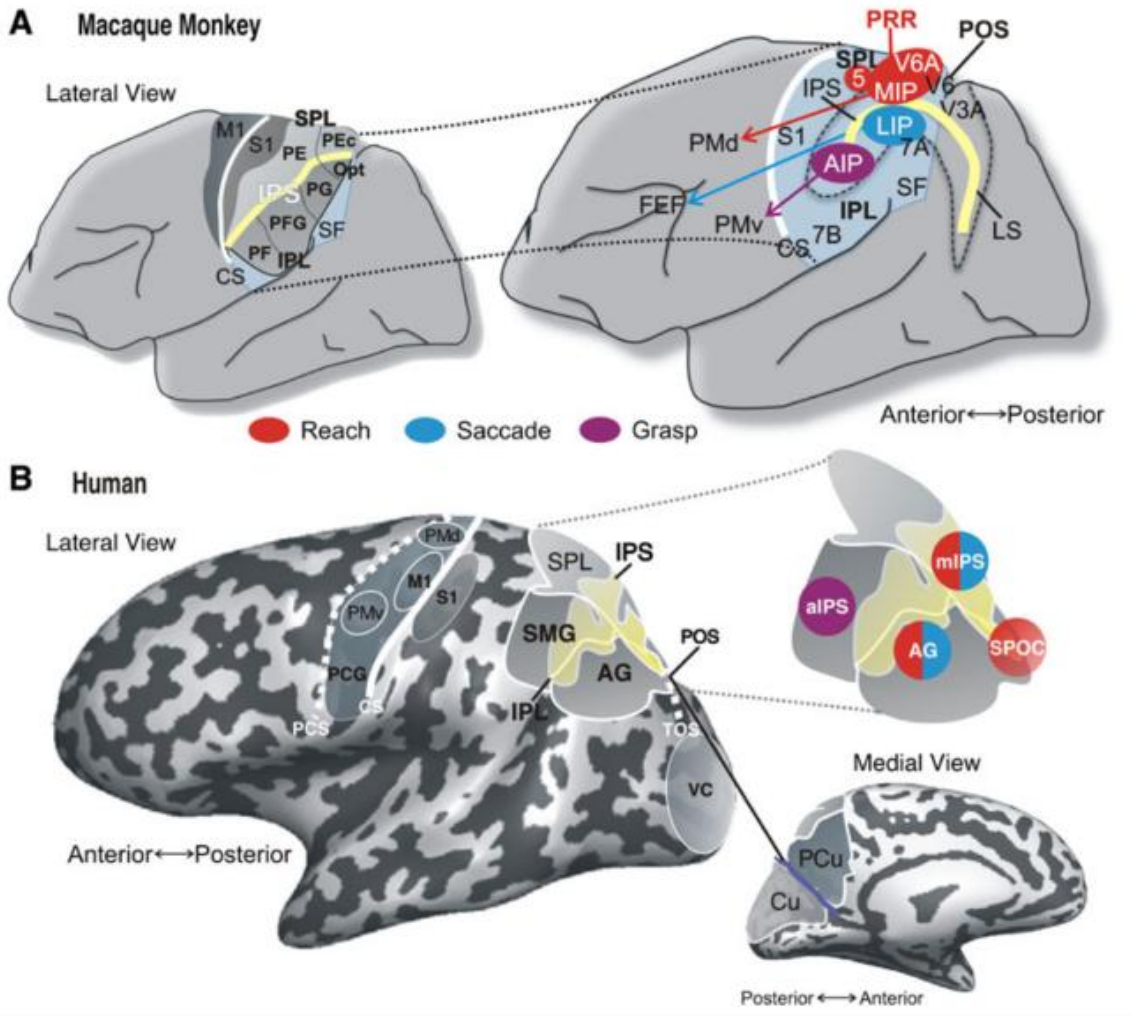


Figure 1.2. A contrast of the nonhuman primate and human parietal cortex. A) Macaque monkey brain showing basic anatomy and putative specialization of visuomotor function in the posterior parietal cortex for saccades, reaches, and grasps. In the rightmost panel of the monkey brain, the intraparietal sulcus (IPS) and lunate sulcus (LS) have been opened to reveal their fundi and banks. B) Human brain neuroanatomy differs substantially from that of monkeys. CS central sulcus, SF sylvian fissure, POS parieto-occipital sulcus, TOS transverse occipital sulcus, PCS postcentral sulcus, SPL superior parietal lobule (PE, PEc), IPL inferior parietal lobule (Opt, PG, PFG, PF), S1 primary somatosensory cortex, M1 primary motor cortex, Brodmann's areas 5, 7A and 7B, visual areas V3A, V6A, AIP anterior, MIP medial, LIP lateral sections of IPS, VC visual cortex, AG angular gyrus, aIPS anterior part of IPS, mIPS midposterior part of IPS, SPOC superior parieto-occipital cortex, PMd dorsal premotor cortex, PMv ventral premotor cortex, FEF frontal eye fields, SMG supramarginal gyrus, PCG postcentral gyrus, PCu precuneus, Cu cuneus (see text for details). Obtained from Vesia & Crawford (2012).

Studies of visuomotor deficits, for example, optic ataxia, have further implicated areas of the PPC in visuomotor action (Andersen et al., 2014; Cavina-Pratesi et al., 2013; Perenin & Vighetto, 1988). Optic ataxia is one of the three conditions observed in Balint's syndrome, a rare

neurological disorder caused by lesions of the posterior parietal cortex. The condition was first described by Balint, who defined optic ataxia as an inability to perform actions that rely on visual information (Andersen et al., 2014). On rare occasions, a unilateral lesion in the posterior parietal cortex results in pure optic ataxia, in the absence of the other symptoms of Balint's syndrome. In PPC, damage to the posterior intraparietal sulcus resulted in a visuomotor deficit in reach, whereas damage to the anterior intraparietal sulcus resulted in a visuomotor deficit in grasp (Binkofski et al., 1998; Kitadono & Humphreys, 2007; Medina et al., 2020). Neuropsychology experiments are a great tool for identifying the roles of different brain structures. However, their damage cannot be controlled, and it is extremely rare for a patient to exhibit clean damage limited to the brain area of interest.

Neuroimaging and neurostimulation research have been used to better understand the nervous system. For instance, a considerable portion of the cerebral cortex is dedicated to processing and regulating the constant flow of visual input. It is then carried through two cortical pathways. The ventral pathway uses vision to perceive, identify, and recognize objects, innervating the inferotemporal cortex, whereas the dorsal pathway uses vision to localize targets and guide actions, innervating the posterior parietal cortex (PPC) (Goodale & Milner, 1992). Furthermore, the multitude of fMRI studies on prehension has helped us establish a solid comprehension of its neural demands and, when combined with TMS, can provide causal evidence by linking brain activity to changes in movement outcomes (Haddadshargh et al., 2026; Hobot et al., 2021). fMRI studies provided evidence of partial separation between reach and grasp in the parietal cortex (Fig. 1.2). More specifically, there is a difference in activation during hand transportation related to the reach component from SPOC, SPL, and PMd reflecting a dorsomedial pathway (Cavina-Pratesi et al., 2007, 2010; Culham et al., 2003). In addition, there were activations related to the grasp component in aIPS and PMv. The posterior parietal cortex has been further differentiated between areas recruited during reaching, the posterior intraparietal cortex and superior parieto-occipital cortex, and the area recruited during grasping, the anterior intraparietal cortex (Begliomini et al., 2007; Murata et al., 2000; Vesia & Crawford, 2012). In addition, disruption in aIPS and PMv affected fast grasp and correction abilities during grip (Davare et al., 2006, 2008; Schettino et al., 2003).

However, these regions are not entirely isolated and appear to share connections. Movement correction in reach was disrupted by stimulation of the PPC and the medial PPC corresponding to hV6A (Brandolani et al., 2025; Desmurget et al., 1999). Indeed, Reichenbach and colleagues (2011) have shown that stimulation of aIPS also affects the motor correction of reach movements. Monaco and colleagues (2011) found a response in the dorsomedial pathway for wrist orientation, which should have been associated with the dorsolateral pathway as a component of grasp. The complexity of the movement outcome also influences the amplitude of activation: grasping shows less activation than manipulation, and even greater activation is observed during complex manipulation than during simple manipulation (Binkofski et al., 1999a; Rens et al., 2023).

Although cortical regions play a crucial role in motor control, the contribution of subcortical regions should not be overlooked (Fig. 1.3). These include, but are not limited to, the basal ganglia's role in overseeing voluntary movement, action selection and initiation, and the cerebellum's role in coordination, motor adaptation and correction (Manto et al., 2012; Nowak et al., 2007; Pierce & Péron, 2020). These subcortical regions are also involved in the planning and execution of reach-to-grasp movements. In the basal ganglia, recording from the subthalamic nucleus (STN) revealed task-related responses during prehension (Pötter-Nerger et al., 2017). In addition, neurodegeneration of the basal ganglia in Parkinson's disease causes deficits in reach and grasp, with greater variability in movement speed and an underscaled grip aperture during grasping (Fasano et al., 2022; Jackson et al., 2000). On the other hand, the cerebellum is important for prediction and correction during movement. Cerebellar patients exhibit greater variability in arm transport velocity, longer grip time, and an overestimation of the grip force used to compensate for their deficit (Brandauer et al., 2008; Manto et al., 2012; Rand et al., 2000; Rost et al., 2005). Single-cell recordings in monkeys revealed that the cerebellum is important for motor adaptability and flexibility after perturbations in reach-and-grasp tasks (Allan et al., 1993). In humans, the cerebellar hemispheres play a particular role in sensorimotor tasks, with the anterior lobe (lobules I-V) and part of the posterior lobe (lobules VI and VIII) being particularly recruited in action (Schmahmann, 2019). Furthermore, damage to the anterior lobe of the cerebellar hemisphere results in a deficit in motor control. In contrast, a milder deficit in motor control during reach-to-grasp is observed after damage to the posterior lobe (VI-XI),

specifically in VIII (Pierce & Péron, 2020). Overall, these findings demonstrate the distinct importance of subcortical regions in reach and grasp.

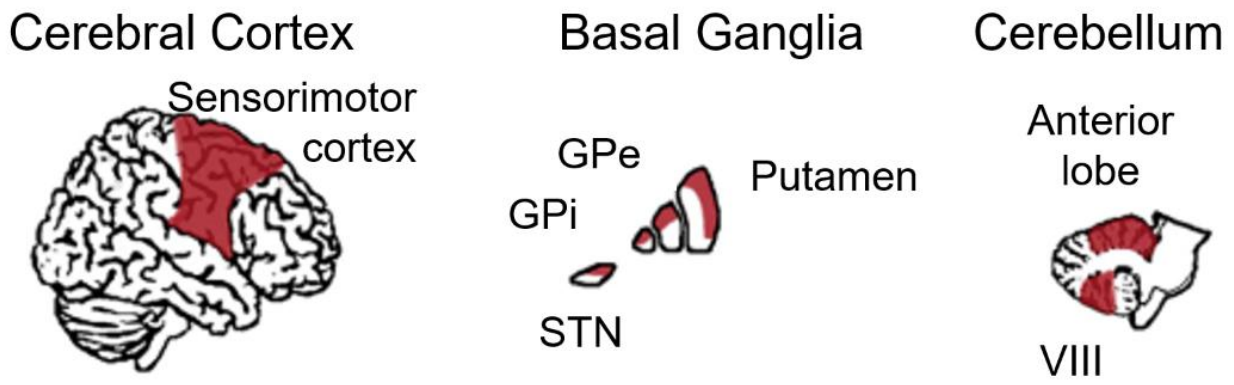


Figure 1.3. Schematic illustration of the cerebral cortex, the basal ganglia, and the cerebellum. The red highlights cortical and subcortical areas that share major structural and functional connections for motor control in a lateral view of the cortex, a coronal view of the basal ganglia, and a sagittal view of the cerebellum. Abbreviations: VIII: cerebellar hemispheric lobule VIII; GPe: external globus pallidus; GPi: internal globus pallidus; STN: subthalamic nucleus. Adapted from Pierce & Péron (2020).

The combination of neurophysiological, neuroimaging, and neuropsychological studies has allowed for a better understanding of the neural control of prehension (Grafton, 2010). Studies have demonstrated the importance of regions within the PPC in integrating visual and other sensory information to guide visuomotor planning and execution (Culham & Valyear, 2006). While great progress has been made in strengthening our understanding of the neural control of prehension and object manipulation, less effort has been devoted to understanding how we terminate our interaction with an object we have acquired. Because prehension and placement are two goal-directed actions, some knowledge from one should be transferable to the other. However, components of placement that differ from prehension still need exploration.

1.5 Behaviour and Neurophysiology of Object Placement

Our interaction with the desired object is not limited to aiming at and grasping it but also extends to carrying or disposing of it (Flindall & Gonzalez, 2019; Marteniuk et al., 1987). In general, every goal-directed prehension movement is associated with a placement movement to end the

interaction with the object. Because of their similarities as goal-directed actions, a portion of our understanding of goal-directed movement gained from prehension can be transferred to object placement. Indeed, like reach-to-grasp, reach-to-place (object placement) requires integrating relevant object features, such as location and orientation, to control actions. Similar to prehension, movement complexities in reach-to-place tasks increased reaction time and movement time (Hesse & Deubel, 2010). However, there are still many differences between the two goal-directed actions, which might result in a significant distinction in their neural control.

Grasping and placement movements might rely on similar object features; however, they differ in how they are influenced by visual information and the intention behind the action. Grasp starts with no haptic feedback from the target object and ends with physical contact, whereas object placement follows the opposite sequence. It begins with haptic feedback from the object in hand, which becomes irrelevant after the object is placed and released. While grasp relies on perceiving a physical object, object placement relies on an imagined image of the movement outcome. In visual input, object placement is influenced by binocular cues to a lesser extent than object grasping (Greenwald & Knill, 2009). The greater involvement of binocular vision in prehension might arise from a stronger reliance on 3D spatial information to orient and position the thumb and the index finger for a precision grip around the object. In addition, movement intentions – for example, between grasp-and-place an object and grasp-and-throw an object – influence movement kinematics during the initial prehension movement (Marteniuk et al., 1987; Naish et al., 2013; Schuboe et al., 2008). Overall, the information used to process and to initiate grasp and placement seems to differ.

Reach-and-grasp experiments largely dominate the study of neural control of goal-directed action, and only a few studies have examined brain activity beyond object acquisition. A few fMRI studies have investigated the level of object manipulation and used a grip-and-lift illusion with a discrepancy between the size and weight of objects to investigate the neural correlates of force correction and the dissociation between predicted and actual object weight (Chouinard et al., 2009; Jenmalm et al., 2006). Object manipulations such as these involve recruiting regions of the PPC, cerebellum, and motor cortex. Grasping and placement movements might both require integrating target properties, such as location and orientation (Greenwald & Knill, 2009; Hesse & Deubel, 2010). However, they differ in the information they rely on; grasp uses actual visual

information to guide action to the object, whereas placement relies on an imaginary representation of the movement outcome. Object properties relevant to grasp, such as shape and orientation, are known to be processed by the grasping network involving the intraparietal sulcus, the premotor cortex, and the motor cortex (Culham et al., 2003; Culham & Kanwisher, 2001; Davare et al., 2011; Di Bono et al., 2015).

By studying the behavioural deficits associated with visual agnosia and optic ataxia, Goodale and Milner (1992) used a "placement-like task" to differentiate between damage to the ventral pathway, which leads to visual agnosia, and damage to the dorsal pathway, which leads to optic ataxia. In their card letter-posting task, participants reached for and placed a card through a rectangular opening, with the opening oriented in various ways. Optic ataxic patients, who have an impaired dorsal stream, are unable to place the card in the slot accurately, whereas visual agnostic patients, who have an impaired ventral stream, perform the task with ease (Milner, 2017; Rossetti et al., 2003). Patients with occipitoparietal damage improve their object-placement accuracy when using an allocentric frame of reference and relate the target to elements in its surroundings (Berryhill et al., 2009). This means that the dorsal pathway relies on an egocentric reference frame, while the ventral pathway uses an allocentric reference frame; thus, including allocentric cues improves performance by recruiting the ventral stream (Chen & Crawford, 2020; Goodale, 1998). Despite these advancements, there are still gaps in our understanding of the neural modulation of reach-to-place, for example, how it differs from reach-to-grasp and the role of specific brain areas in executing object placement.

1.6 Neural Influence of Instructions on Action

In most goal-directed studies, researchers rely on participants' ability to comprehend and follow instructions, although the effect of this cognitive load is not directly tested. While it is rarely considered, this instruction also needs to be integrated with other available sensory information relevant to the task.

For instance, studies have shown that varying the action objective impacts the movement outcome. Indeed, the timing of eye and hand movement initiation is influenced by task instructions, with priority placed on action speed or accuracy (Fisk & Goodale, 1989). When the same visual input is provided, being instructed to use or ignore an available cue has also been shown to influence reach movement outcomes (Musa et al., 2024). Movement outcomes,

specifically accuracy, maximum force applied, and maintenance, are improved when participants are instructed to focus their attention outwardly by emphasizing the desired target, compared with focusing inwardly, for example, on the limb that needs to be moved (Marchant, 2011). In addition, receiving externally focused instruction has been shown to improve sports performance and balance (Lohse et al., 2014; Singh & Wulf, 2022). This external emphasis also offers an advantage in recovery from cerebrovascular accident (Fasoli et al., 2002). More specifically, the type of verbal instruction has been shown to elicit improvements in reach movements of the less-affected limb in stroke patients (Lin et al., 2008).

For auditory instructions to effectively influence motor outputs, the verbal information communicated must be integrated into the motor plan. Therefore, neural circuitry is required to facilitate this exchange (Fig. 1.4). Anatomically, a diffusion tractography study has found evidence that the arcuate fasciculus forms direct tracts connecting areas in the center for sound comprehension, the posterior superior temporal cortex, and the premotor cortex, which is important for action preparation (Frey et al., 2008). Similar to the visual system, the auditory system is believed to have ventral and dorsal streams for auditory perception and localization/action, respectively (Rauschecker, 2011; Rauschecker & Tian, 2000; Warren et al., 2005). From this finding, one could infer that the dorsal auditory stream's projection to the frontal region is necessary for planning and executing actions.

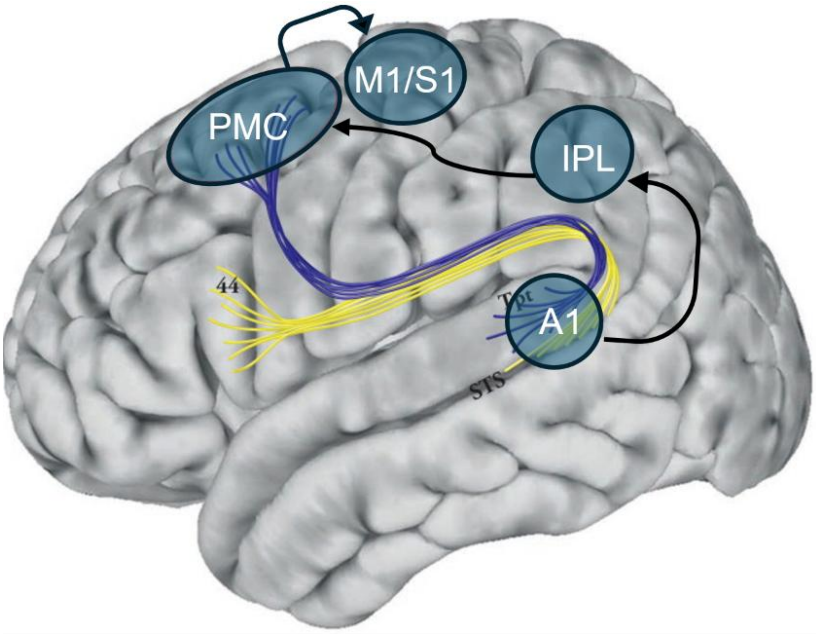


Figure 1.4. Illustration of the auditory-motor pathway, with direct connection to frontal regions via the arcuate fasciculus and indirect connection via the inferior parietal lobule (IPL). The tract connecting primary auditory cortex (A1) to Broca's area (Brodmann Area 44) in yellow and to premotor cortex (PMC) in blue. M1: primary motor cortex; S1: primary somatosensory cortex; STS: Superior Temporal Sulcus; Tpt: component of Wernicke's area. Adapted from Petrides (2014) and Rauschecker (2018).

1.7 Specific Aims and Hypotheses

Overall, goal-directed movements facilitate our interaction with elements in our surroundings. While the neural basis of prehension has been extensively studied in visuomotor experiments, alternative goal-directed movements, such as final object placement, and the integration of different sensory modalities into the motor plan are less well understood. To bridge this knowledge gap, I investigated goal-directed action using a single modality to compare reach-to-place and reach-to-grasp, and the integration of two modalities into the reach-to-grasp motor plan and execution. This project combined three studies investigating: 1) the influence of variable visual information on the psychophysics of placement, 2) the neural differentiation of placement from prehension movement, and 3) the neural impact of cue modality in prehension.

For the behavioural placement task in Chapter 2, participants placed and aligned a handheld object against a template displayed on a computer screen while varying their gaze direction. I used endpoint location error as a proxy for the reach-related component and endpoint orientation error as a proxy for the grasp/place-related outcome to investigate how these features are processed differently for grasp and placement. In terms of location, I expected to see a gaze-dependent overshoot effect based on the final gaze position, and that this overshoot would be accentuated in the absence of visual feedback, given the aforementioned similarity between prehension and reach-to-place actions. Furthermore, the study examined the three saccade types mentioned above to confirm that the gaze-dependent overshoot effect is present across these types. Regarding orientation in object placement, assuming that endpoint orientation relies on the same mechanism as grasping movements (Selen & Medendorp, 2011), I expected a gaze-dependent error in orientation with or without an intervening saccade, and despite changes in the level of visual feedback. While this study expanded our knowledge of prehension to placement, it did not include a direct comparison between the two.

For Chapter 3, I used an fMRI study to compare reach-to-place to reach-to-grasp movements while using similar cue modalities (visual and somatosensory). To have an overview of their

convergences and divergences, the analysis was conducted: 1) at the whole-brain activation level, 2) in preselected action-related regions identified by a data-driven approach, and 3) at the functional level, looking at their temporal fluctuation over time. Because object grasping and placement require integrating similar object features (location and orientation), I expected to observe an overlap in their cortico-cerebellar activation. However, differences in brain activity patterns and cortical functional connectivity are expected due to differences in their goals and the sensory information available to them. The results from the fMRI experiment will help elucidate the neural mechanism in a correlational approach and allow the investigation of motor control beyond typical prehension movements.

Chapters 2 and 3 examined how visual information shapes placement and how neural activity differs between placing and grasping, but in both studies, the action was specified solely by visual cues. In real-world motor control, however, instructions often arrive through other modalities (most commonly audition) and must be integrated with concurrent visual information about the target. How the brain combines auditory instruction on how to act with a visual cue on where to act remains unclear. Chapter 4, therefore, examined how different cue presentation modalities are integrated during prehension. For this purpose, I analyzed a previously collected fMRI dataset to investigate how visual cues and auditory instructions are combined to perform an action. In this task, participants received a visual cue indicating the target location and an auditory cue specifying how to grasp it. I investigated how multisensory cues for 'top-down' motor strategies and 'bottom-up' stimulus attributes are combined to achieve successful prehension of a physical target across varying presentation orders. As in the fMRI placement task, I used three approaches to investigate our question: whole-brain activation, responses in action-related areas, and functional connectivity. Therefore, they provided insight into the integration of various action cues through different analyses. I anticipated an order-dependent response in sensory-modality regions of the primary visual and auditory cortices. I reduced the order differentiation cue to the two cues being combined during preparation and action execution. Finally, functionally, I expected the two sensory cues to travel in parallel through different modules until they are merged in the motor output.

Together, these three studies trace the integration of sensory information across an expanding set of modalities, from vision alone in placement, to vision and somatosensory across grasp and

placement, to vision combined with auditory instruction in prehension, identifying the behavioural signatures and brain networks that support goal-directed action.

CHAPTER 2:

INFLUENCE OF GAZE, VISION, AND MEMORY ON HAND KINEMATICS IN A PLACEMENT TASK

Authors: Gaëlle N. Luabeya[1,2], Xiaogang Yan[1], Erez Freud[1-3] & J. Douglas Crawford[1-4]

Affiliations:

[1] Centre for Vision Research and Vision: Science to Applications Program, York University, Toronto, Ontario, Canada

[2] Department of Biology, York University, Toronto, Ontario, Canada

[3] Departments of Psychology, York University, Toronto, Ontario, Canada

[4] Kinesiology & Health Sciences, York University, Toronto, Ontario, Canada

Current Status: Chapter 2 is published in the Journal of Neurophysiology

Citation: Luabeya, G. N., Yan, X., Freud, E., & Crawford, J. D. (2024). Influence of gaze, vision, and memory on hand kinematics in a placement task. Journal of Neurophysiology, 132(1), 147-161.

2.1 Abstract

People usually reach for objects to *place* them in some position and orientation, but the placement component of this sequence is often ignored. For example, reaches are influenced by gaze position, visual feedback, and memory delays, but their influence on object placement is unclear. Here, we tested these factors in a task where participants placed and oriented a trapezoidal block against 2D visual templates displayed on a frontally located computer screen. In Experiment 1, participants matched the block to three possible orientations: 0° (horizontal), +45° and -45°, with gaze fixated 10° to the left/right. The hand and template either remained illuminated (closed-loop), or visual feedback was removed (open-loop). Here, hand location consistently overshot the template relative to gaze, especially in the open-loop task; likewise, orientation was influenced by gaze position (depending on template orientation and visual feedback). In Experiment 2, a memory delay was added, and participants sometimes performed saccades (towards, away from, or across the template). In this task, the influence of gaze on orientation vanished, but both template orientation and final gaze position influenced location errors. Contrary to our expectations, the previous saccade metrics also impacted placement overshoot. Overall, hand orientation was influenced by template orientation in a nonlinear fashion. These results demonstrate interactions between gaze and orientation signals in the planning and execution of hand placement and suggest different neural mechanisms for closed-loop, open-loop, and memory delay placement.

2.2 Introduction

Goal-directed hand movements facilitate a productive interaction with the world around us (Desmurget et al., 1998). In the case of prehension (reach-to-grasp movements), the influence of factors such as gaze position and levels of visual feedback is very well studied (e.g., Fiehler et al., 2011; Henriques et al., 1998; Schütz et al., 2013). However, the interaction with surrounding objects often does not end at object acquisition (Ballard et al., 1992; Johansson et al., 2001; Land, 2006). Take, for example, toasting a flat piece of bread. After acquiring the object, it must be transported, oriented, and correctly placed into a toaster slot. Despite their real-world importance, the determinants of placement performance have been relatively neglected compared to prehension. Here, we examined the influence of gaze position, saccades, and levels of visual feedback (open-loop, closed-loop, memory-guided) on hand location and orientation (and their interactions) in a simple visual / memory-guided placement task.

Grasp and placement share several common characteristics, e.g., they both use vision to determine object location and orientation; this visual location depends on internal knowledge of gaze position; they involve similar motor kinematics and proprioceptive feedback; somatosensory feedback is available at some points of both tasks; and they are influenced by task complexity (Hesse & Deubel, 2010; Parry et al., 2019; Scharoun et al., 2016; Tugac et al., 2019). For these reasons, one might expect them to share similar mechanisms and show similar gaze-dependencies. However, one cannot assume this to be true, because grasp and placement differ in their cognitive aspects (the intent to acquire as opposed to place), sensory aspects (different visual and somatosensory feedback), and sequential order (i.e., grasp typically precedes placement). Several studies examined sequential coordination between reach and placement (Flindall & Gonzalez, 2019; Quinlan & Culham, 2015) and how they influence each other (Seegelke et al., 2012). The final movement intentions of placement may influence movement kinematics during the grasping stage (Marteniuk et al., 1987; Naish et al., 2013; Schuboe et al., 2008). For instance, one might initiate an uncomfortable movement trajectory so long as it ends in a comfortable final position (Rosenbaum et al., 1996, 2006; Rosenbaum & Jorgensen, 1992). However, several fundamental aspects of eye-hand coordination that are well-studied in the reach system have not been studied in placement.

First, it is known that gaze direction strongly influences reaching and pointing. Gazing directly at the target increases our movement accuracy (Bock, 1986; Bock & Eckmiller, 1986). In some cases, the gaze remains locked onto the goal during reaching (Neggers & Bekkering, 2000), but in other real-world conditions, the gaze must remain focused on other tasks or anticipate future goals during the current reach (Fooken et al., 2021; Johansson et al., 2001; Land, 2006). When the gaze deviates from the target, people tend to make pointing / reaching errors that 'overshoot' in the opposite direction (Bock, 1986; Bock & Eckmiller, 1986; Henriques et al., 1998). This is clinically relevant because these gaze-dependent errors become more pronounced in the presence of parietal cortex damage (Khan, Pisella, Rossetti, et al., 2005). In the reach system, this overshoot is entirely determined by the final gaze position at the time of pointing (independent of previous saccades), consistent with the use of a gaze-centered updating mechanism for the reach goal (Fiehler et al., 2011; Henriques et al., 1998; Medendorp et al., 2003). It is noteworthy that these topics have mainly been studied using saccades away from the target (Fiehler et al., 2011; Henriques et al., 1998; Khan et al., 2007), so it is not clear whether the results extend to peripheral-to-peripheral

saccades or saccades towards the target (Shafer-Skelton & Golomb, 2018). To our knowledge, these basic eye-hand coordination issues have not been investigated in a placement task.

Second, several grasp studies have examined the kinematics of orienting the hand to the object (Monaco et al., 2015; Selen & Medendorp, 2011). Grasp orientation involves the coordination of the entire hand-arm system (Marotta et al., 2003) but can be dissociated from the reach location at both the behavioural and neural levels (Gallivan & Culham, 2015; Marotta et al., 2005; Vesia & Crawford, 2012). Place-to-match tasks (where typically the object is placed against a two-dimensional surface to match the location and orientation of a template stimulus) show an oblique effect, i.e., where oblique targets show an increase in orientation error in comparison to their cardinal counterparts (Gosselin-Kessiby et al., 2008; Hesse et al., 2021). In contrast to pantomiming movements, placement orientation is immune to damage to the ventral visual stream, suggesting a dorsal (parietal) mechanism (Goodale et al., 1994). Similar to pointing and reaching (Bock, 1986; Bock & Eckmiller, 1986; Henriques et al., 1998), grasp orientation is also dependent on current gaze position at movement onset (Selen & Medendorp, 2011), and this is reflected in gaze-grasp orientation interactions at the level of the parietal cortex (Baltaretu et al., 2020). Again, none of these factors have been studied in placement movements, so it is important to show how gaze and hand orientation interact in healthy participants, not only to understand the system, but to establish a normal baseline for patient studies.

Importantly, the preceding descriptions of behavioural errors are highly dependent on levels of visual feedback and memory. In the absence of allocentric cues (such as visual landmarks in the surroundings), movement errors generally increase as the delay between target presentation and movement onset increases (Chen et al., 2011; Krigolson & Heath, 2004; Steenhuis & Goodale, 1988). Visual feedback is particularly important for the final phase of action (Roberts et al., 2013), although orientation errors can also be improved by proprioceptive information about the target (Gosselin-Kessiby et al., 2008). Likewise, in the case of the gaze-dependent reach and orientation errors described above, these are normally overridden by visual feedback (Fiehler et al., 2011; Henriques et al., 1998; Selen & Medendorp, 2011). There are exceptions to these rules: for example, illusion-dependent grasp errors tend to dissipate with a memory delay (Goodale et al., 1994; Westwood & Goodale, 2003). The larger gaze-dependent errors seen in optic ataxia may dissipate over time, suggesting different spatial mechanisms for immediate versus delayed

reaching (Revol et al., 2003). The overall point is that reach and grasp errors may be highly sensitive to different levels of visual feedback, ranging from full visual feedback of the hand and desired goal (closed-loop) to the removal of this feedback (open-loop) to the addition of a memory delay.

The purpose of the current study was to investigate how hand location and orientation are influenced by gaze position, previous saccades, and various levels of visual feedback (closed-loop, open-loop, memory delay) in a placement task. Our hypothesis was that if the placement system shared similar mechanisms with the reach and grasp system (in the absence of proprioceptive feedback), we should see gaze-dependent overshoot errors in placement location that should be independent of previous saccades, and if placement behaves like grasp (Selen & Medendorp, 2011), the direction of gaze at movement onset may also influence orientation errors. We further expected these errors to grow with the progression from closed-loop to open-loop to memory delay, as the system increasingly relies on noisy internal models without the opportunity for visual feedback corrections.

To test this, we asked participants to place a trapezoidal shape against an oriented template in the center of a computer screen, with their gaze fixated on the template or deviated to the left or right. We divided this into two experiments, where 1) closed-loop and open-loop performances were compared, and 2) a memory delay was added to the open-loop condition, accompanied by sustained fixation or a saccade (which could be towards, away from, or across the template). We also tested interactions between hand location and orientation on these tasks. The results showed that our task yielded some of the predicted effects (such as an open-loop gaze-centered overshoot), but other results went contrary to expectation, such as reduced orientation errors after a delay.

2.3 Methods

2.3.1 Participants

A total of 36 young adults participated in this study, with 17 individuals taking part in Experiment 1 (8 females, 9 males, 14 right-handed, ages 22 - 34) and 19 in Experiment 2 (7 females, 12 males, all right-handed, ages 19 - 28). Notably, 5 participants completed both experiments. Of these, 16 (Experiment 1) and 14 (Experiment 2) participants, respectively, were included in our data analysis (see Data Analysis and Exclusion Criteria), providing sufficient power for our analysis (see

Statistical Analysis). Each participant self-reported normal or corrected-to-normal visual acuity with no reported neurological disorders. Written consent was collected from all participants, and they received monetary compensation for their time. All experimental procedures were approved by the York University Human Participants Review Committee.

2.3.2 Apparatus and Stimuli

A 70 cm × 40 cm Sony Television screen was used to present visual stimuli, which included gaze fixation points (a white dot to the right, left, or center of the screen) and rectangular target templates (a white rectangle displayed at the center of the screen in three possible orientations). This screen was mounted onto a stable table and connected to a computer for stimulus control (Fig. 2.1). The screen was covered with dark tints to decrease luminance (luminance = 0.000 cd/m^2 measured with Konica Minolta® Luminance Meters LS-100) and minimize extraneous allocentric cues. A chinrest, placed at the edge of the table, maintained the participant's head positioned 26 cm away from the screen and served to reduce body movements. The participant sat on an adjustable chair with their head on the chinrest and was positioned with their right eye directly in front of the center of the screen. A green LED light depicted the home position of the hand, halfway between the torso and the screen on the platform.

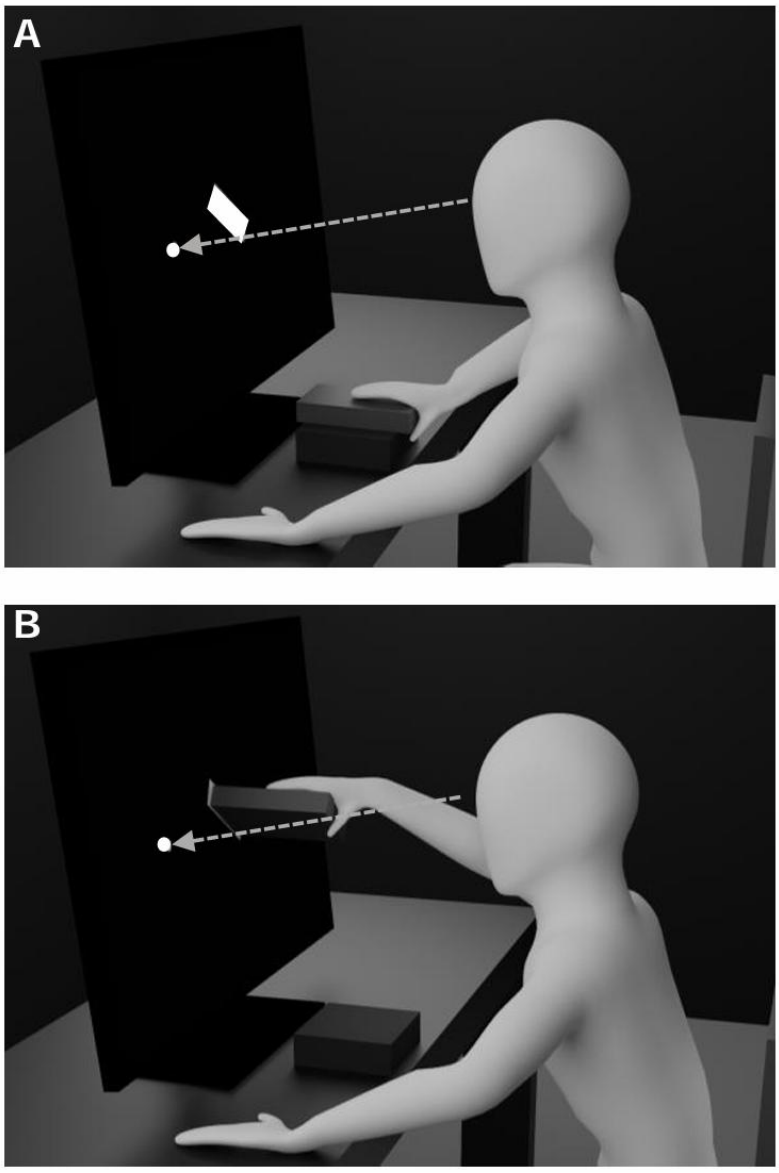


Figure 2.1. Experimental Task. A) Depicts the preparatory period before the go signal, with the hand at the resting position, gaze on the fixation (white dot to the left) and the target template (white rectangle) displayed at the screen center. B) Example of a final object placement against the template while gaze is maintained at the fixation point. The chinrest and eye-tracking device are not shown in this illustration.

The task involved placing a trapezoidal block against a template displayed on the computer screen (see next section for details). In its horizontal position, the trapezoidal block had a height of 2.0 cm, a width of 7.5 cm, with a depth of 10.0 cm on the left side and 8.0 cm on the right side. An elastic band passed through two openings and was tied around the participant's fingers. The object's real-time dynamic and kinetic motions were tracked and analyzed using the Optotrak 3020 motion

capture system (Northern Digital Inc, Waterloo, ON, Canada) at a sampling rate of 100 Hz; the system provided measurements of the hand position and motion during the experiment. The system monitored the position and motion of the block by collecting the location of six InfraRed Light Emitting Diodes (IREDs), which were affixed in groups of three onto two surfaces of the prism (the top surface and the left adjacent surface). They were used to create two three-dimensional virtual points that were averaged to calculate the central position of the front surface of the object and its orientation. The gaze location of the left eye was monitored using an ISCAN Eye Tracking system (ISCAN Inc, Woburn, Massachusetts, United States). The analog outputs of the gaze signals were sent to Optotrak Data Acquisition Units (ODAU). With a sampling rate of 1000 Hz, the digitized 2D gaze data was recorded toipogether with Optotrak IRED data during the experiment.

2.3.3 General Task Design

We conducted two psychophysical experiments to gain a fundamental understanding of how object placement is influenced by gaze location, target orientation, and level of visual feedback. The study investigated how varying levels of visual feedback (in Experiment 1) and the presence of saccades (in Experiment 2) affected the endpoint positioning of an object to match the location and orientation of the target. In the two tasks, the design included three gaze location / fixation points: either at the center of the screen, to the left, or to the right of the central location. The target, a rectangular object template, was always presented at the center of the screen and could have either horizontal (0°), +45°, or -45° orientation (Fig. 2.2A). These orientations were chosen based on the range that participants found comfortable in a preliminary testing session.

At the beginning of each trial, all room lights were extinguished, and participants held the trapezoidal block at the home position in a horizontal orientation with their right hand (four fingers above and thumb below the object). Participants then fixated their gaze on a point that appeared at one of the three positions (Fig. 2.2A). The rectangular target template (slightly larger than the block's forward 2 × 7.5 cm surface) then appeared at the center of the screen (aligned with the center fixation point). Participants were instructed to place the block orthogonal to the screen (with various levels of visual feedback) such that the forward-pointing section aligned with the location and orientation of the template (Fig. 2.1). Finally, they returned the hand / block to the home

position and prepared for the next trial (the detailed sequences of stimulus events are provided in the following two sections).

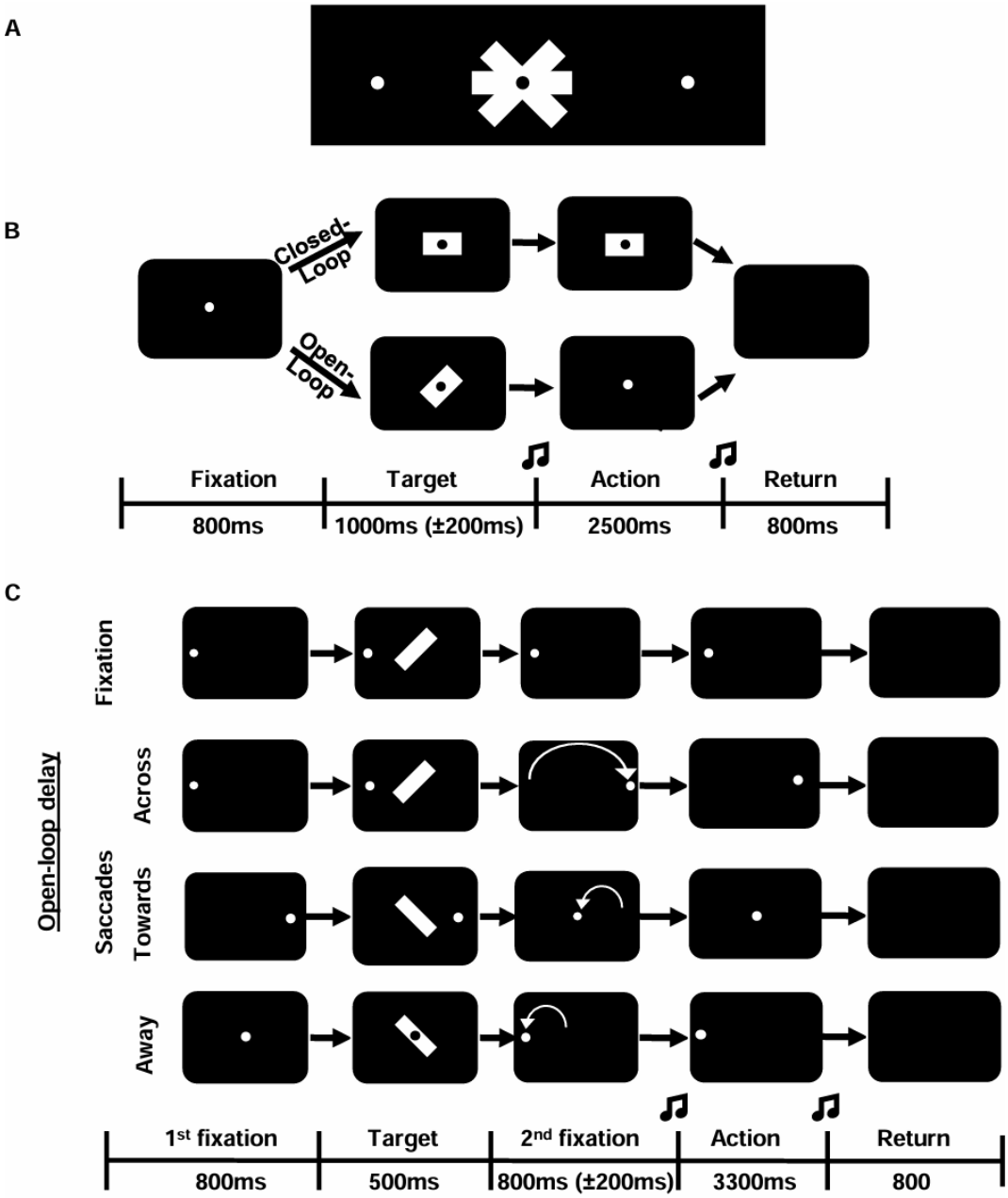


Figure 2.2. Experimental protocol. A) Illustrates the three possible fixation locations (left, center, and right) and target template orientation (-45°, 0°, and +45°) presented on a black LED screen; B) Schematic sequences of events for *Experiment 1*. Black rectangles represent the stimulus screen at different time points in a trial. Initially, the screen was black. Then, the gaze fixation stimulus appeared (in this case, at the center). In the *Closed-Loop Condition*, the target template (horizontal in this example) remained displayed, and an LED light illuminated the block and the participant's hand to provide visual feedback during the movement to the target. In the *Open-*

Loop Condition, the target template (+45° in this example) disappeared as the signal to initiate action. In both cases, the participant placed and maintained the object against the object template until an auditory signal indicated to return to the home position. C) Schematic sequence of events for memory and saccade conditions in *Experiment 2*. Participants first aimed their gaze toward the initial fixation point (left, right and center, depending on the condition). Then, a +45° or -45° target template is presented for 500 ms, followed by an 800 ms memory delay. Depending on the task, participants then either maintained fixation during the delay (*Fixation Condition*), made saccades across to the opposite fixation stimulus (*Saccade Across)*, toward the central fixation (*Saccade Towards*), or saccades away from center fixation (Saccade Away). Afterwards, an auditory 'go signal' instructed participants to place the object to the remembered target template orientation.

2.3.4 Experiment 1

The first experiment investigated the influence of gaze location and visual feedback on integrating a stimulus location and orientation during an object-placement task. The experiment was a within-subjects design involving 3×3×2 study parameters (three gaze positions, three orientations, and two visual conditions). The two visual feedback levels were either *closed-loop* with full visual feedback of the target template and the hand or *open-loop* with no visual feedback of the target template and the hand.

In all trial sequences (Fig. 2.2B), participants were allowed 800 ms with nothing on the screen to settle their hand position and prepare for the trial. Then, one of three fixation dots (center, 13° visual angle left or right) appeared and remained on for the entire duration of the trial. Participants maintained fixation on this dot throughout the trial. Following an initial 800 ms presentation of the fixation dot, a rectangular target template appeared at one of the three possible orientations. This target template was displayed for 1000 ± 200 ms before a beeping sound cued the placement movement. In the *closed-loop* condition, the target template remained visible, and a light illuminated the block and the hand for the duration of the movement; whereas in the *open-loop* condition, the target template was extinguished in an otherwise dark room (except for the fixation point), and participants had no visual feedback from the block and the hand during movement. In both cases, participants had 2500 ms to execute the movement and maintain the object placed against the screen until a return beeping signal was played. Then, the home LED was illuminated, and they had 800 ms to return to the home position. This was followed by a 2100 ms intertrial interval when two light bulbs behind the monitor were illuminated to prevent dark adaptation.

In each session, participants completed a total of 390 trials divided into five runs of 78 trials. Before starting a run, participants completed an eye calibration. Each run began and ended with three calibration (*closed-loop*) trials, which were only used offline to check the stability of the recording signals. The order of conditions was pseudorandomized so that each of the 18 possible trial types (three orientations × three gaze positions × two feedback conditions) was repeated 20 times across the entire experiment. Each run was 10.4 minutes long. Participants were given two minutes to rest after each run. Each experiment lasted approximately 72 minutes.

2.3.5 Experiment 2

The second experiment investigated the influence of saccade on placement location and orientation. The experiment was a within-subjects design involving 3 (Initial Gaze Locations) × 3 (Final Gaze Locations) × 2 (Orientations) study parameters. Here, there was always a memory delay (with no visual feedback of the target template or the hand) between seeing the target template and placing the object. The task design included three gaze locations (center screen, 10° visual angle left or right). Here, the fixation point could change (2/3 of the time) after the target template presentation, causing a saccade to occur after the target template disappeared and the change in fixation location prompted participants to do a saccadic eye movement. Combining the three gaze locations as initial and final fixation positions gave six types of saccadic eye movements (*away* from the central fixation to the left or right, *towards* the central fixation from left or right, or *across* the central fixation from left to right and vice versa, which involved a shift from one visual field to the other). The target template was presented in two possible orientations (+45° or -45°). Participants were presented with the target template and performed the placement movement after a brief memory delay.

Experiment 2 followed a similar sequence to Experiment 1 (Fig. 2.2C). The initial fixation point in the three possible locations (left, center, or right) appeared 500 ms after the trial started. After 800 ms, the rectangular target template was presented for 500 ms. As the target template was extinguished, the fixation point either remained in the same location (serving as *open-loop* delay) or moved to a new horizontal location for the saccade conditions. A beeping sound was played 800 ± 200 ms later and served as a cue to initiate the placement movement toward the TV monitor. Participants had 2500 ms to perform the movement and maintain the object placed against the screen until a return beeping signal was played. Then, they had 800 ms to return to their home

position, which was illuminated during that period. The return time was followed by a 1000 ms intertrial interval when two light bulbs behind the monitor were illuminated to prevent adaptation to the darkness.

In each session, participants completed a total of 432 trials divided among six runs of 72 trials. At the start of each run, participants completed an eye calibration. The order of conditions was pseudorandomized so that the 18 possible trial types (three initial gaze positions × three final gaze positions × two orientations) were repeated 24 times across the entire experiment. Each run was 8.28 minutes long. Participants were given two minutes to rest after each run. Each experiment lasted approximately 72 minutes.

2.3.6 Data Analysis and Exclusion Criteria

Eye-tracking and hand-tracking data were exported from the ISCAN and Optotrak Certus, respectively, and presented in a custom graphical user interface written in MATLAB (MathWorks Inc., Natick, MA). The data were preprocessed to ensure subjects' compliance with the procedure. The program automatically marked the onset of movement from the home position and recorded the movement endpoint when the object was placed in the target template location (Fig. 2.3 *Top Row*). The data were recorded in units of millimeters (Fig. 2.3 *Middle Row*). To derive location error, we calculated the difference between the center of the final object position and the center of the template (where negative values reflect leftward error). For orientation error, we compared the angle between the long axis of the object and the long axis of the template in polar coordinates (i.e., a positive value reflected a counterclockwise (CCW) rotation and a negative value represented a clockwise (CW) rotation relative to the template). Errors in location that are opposite to gaze location have been referred to as ‘gaze-centered overshoots’ (Henriques et al., 1998; Henriques & Crawford, 2000; Schütz et al., 2013). Likewise, when participants rotated the object too much for the 45° templates (relative to the horizontal template), we refer to this as ‘over-rotation.’

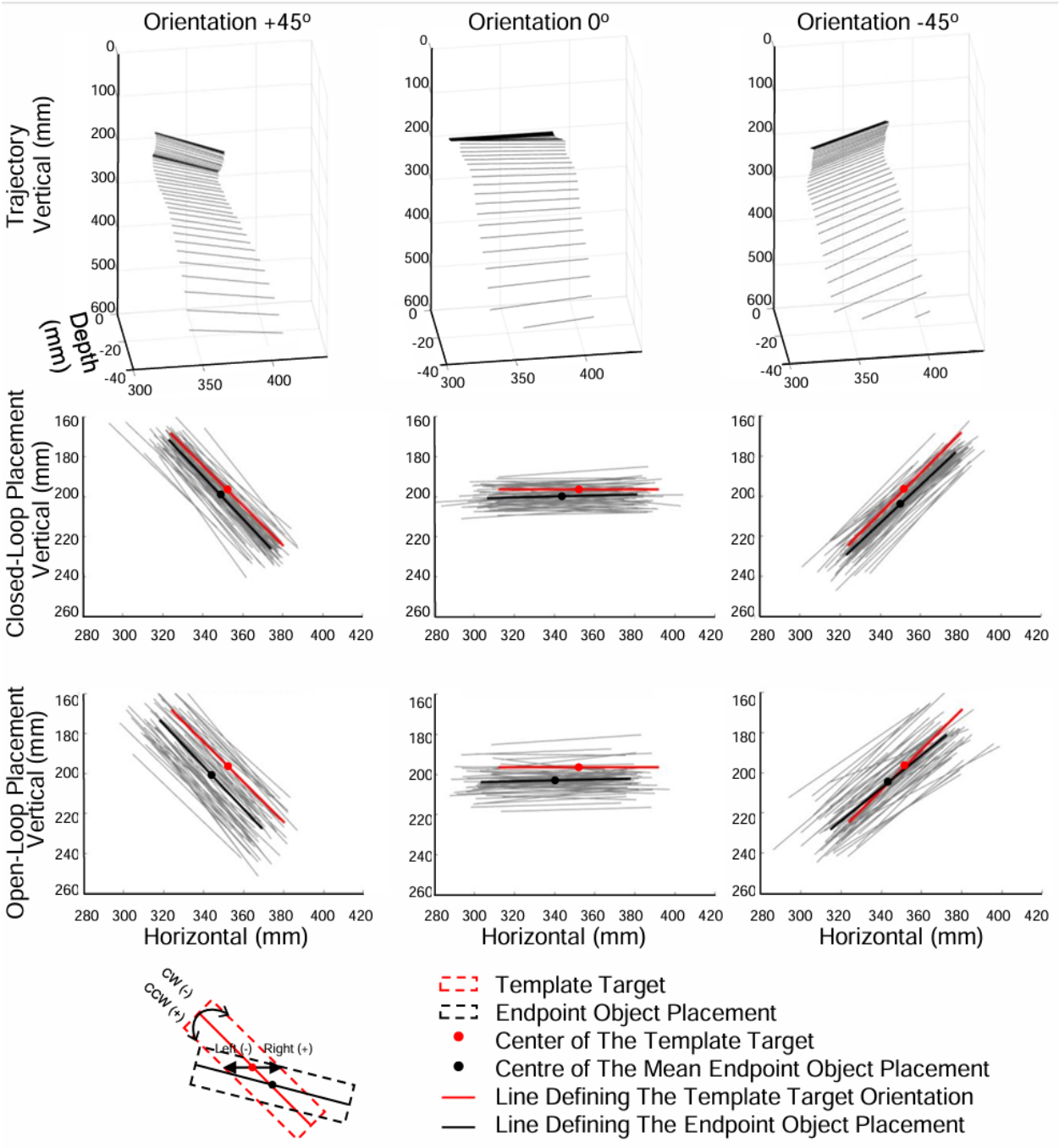


Figure 2.3. Typical placement kinematics for one participant in Experiment 1. The *top row* shows example trajectories of the forward-facing side of the object (black lines) towards three possible template orientations (from left to right: -45°, 0°, +45°) in 3D space. The *middle row* shows the 2D endpoint orientation and location of object placement (thin grey lines) for all trials for this participant and their average (thick black line) relative to the template location and orientation (red lines) in the *closed-loop* condition. The red and black dots represent the center of the template and the object placed, respectively. The *bottom row* shows the same for the *open-loop* condition. The legend at the bottom shows the rectangular template target in red, and the

black rectangle represents an example error in location (a negative value represents movement to the left and a positive value represents a movement to the right) and orientation (a negative value represents a clockwise rotation, CW, and a positive value represents a counterclockwise rotation, CCW)

Each trial went through a series of four exclusion criteria. The first exclusion criterion required that gaze was maintained on the fixation stimulus during the target template presentation and throughout the hand movement. The second exclusion criterion required that they reached their target template alignment before the return signal was played and the fixation point disappeared. The third criterion required that trials be discarded when the participant's movement onset occurred before the beep signal in memory-guided trials. The fourth criterion was enforced when the participant's orientation deviated by more than ±25° from the target templates. The inability to satisfy either one of these criteria resulted in the omission of the trial for further analysis. In Experiment 1, one participant's data were excluded because they failed to maintain fixation while performing hand movements in multiple trials. In Experiment 2, data from five participants were excluded because they did not attain the minimum number of valid trials for 1/3 of the conditions. For participants included in the analysis, 76.2% of the trials were used for Experiment 1 and 70.4% for Experiment 2.

2.3.7 Statistical Analysis

For each valid trial, the endpoint orientation and horizontal position were compared to the actual target template orientation and horizontal position (Fig. 2.3 *Middle Row*). Statistical analyses of each condition for each participant were conducted on the mean error to obtain placement movement accuracy in the endpoint horizontal location and in the endpoint orientation. In Experiment 1, to investigate how gaze location, target template orientation, and visual guidance affected movement accuracy, a three-way repeated-measures analysis of variance (RM ANOVA on three orientations (0°, -45°, and 45°) × three gaze locations (right, center, and left) × two visual guidance (visually or memory-guided actions)) was conducted on the accuracy of the endpoint orientation and the endpoint horizontal location. In Experiment 2, to investigate how adding a memory delay and different types of saccades influenced movement accuracy, a three-way repeated-measures analysis of variance (RM ANOVA on three presaccade gaze positions (right, center, and left) × three postsaccade gaze positions (right, center, and left) × two target template orientations (-45° and 45°)) was conducted on the accuracy of the endpoint orientation and the

endpoint horizontal position. All statistical analyses were conducted using RStudio software. A post-hoc power analysis was also conducted to confirm that our sample size was large enough to capture the effect for a two-tailed test with power at 0.8 and alpha of 0.05. We found that a sample size of 10 was determined to be sufficient for detecting the main effects. Mauchly's test was used to assess if sphericity was violated. In cases where sphericity was not assumed, Greenhouse-Geisser (GG) correction was used. If the RM ANOVA was significant with a $p < 0.05$, we conducted Bonferroni post-hoc tests to adjust for multiple comparisons. A follow-up interaction contrast test was conducted in cases where interaction was reported.

2.4 Results

2.4.1 Experiment 1

Experiment 1 tested how object placement is influenced by gaze location, target template orientation, and level of visual feedback. The study investigated how *closed-loop* and *open-loop* conditions during a placement movement influenced the endpoint positioning of an object to match the location and orientation of the central target template. Two sets of data from the same movement were studied: the endpoint error in location (relative to the center point of the target template) and the endpoint error in orientation (relative to the orientation of the template). These two values were defined by comparing the discrepancy of the final object position and orientation (after placement) relative to the target template's actual position and orientation (Fig. 2.3 *Middle and Bottom Rows*).

Location error. Error in final object position was measured and analyzed to study the influence of visual feedback, gaze position, and target template orientation on horizontal object placement position. The violin plots in Fig. 2.4 A and *B* summarize the distribution of placement location errors in each condition. Because the physical variation in gaze was in the horizontal plane, we exclusively considered the error in the endpoint position in the horizontal dimension, where a negative value indicates movement to the left and a positive value indicates movement to the right.

The data (Fig. 2.4 A and B) revealed a general error bias to the right, i.e., when looking straight ahead and placing the object to the central target template. There was also a greater spread in location error in the *open-loop* conditions in comparison to *closed-loop* guided movements. When comparing the average position error across participants, we could observe a tendency to overshoot

location relative to gaze, i.e., they made placement errors to the left when looking to the right and errors to the right when looking to the left (Fig. 2.4C). In addition, this pattern became stronger in the absence of visual feedback.

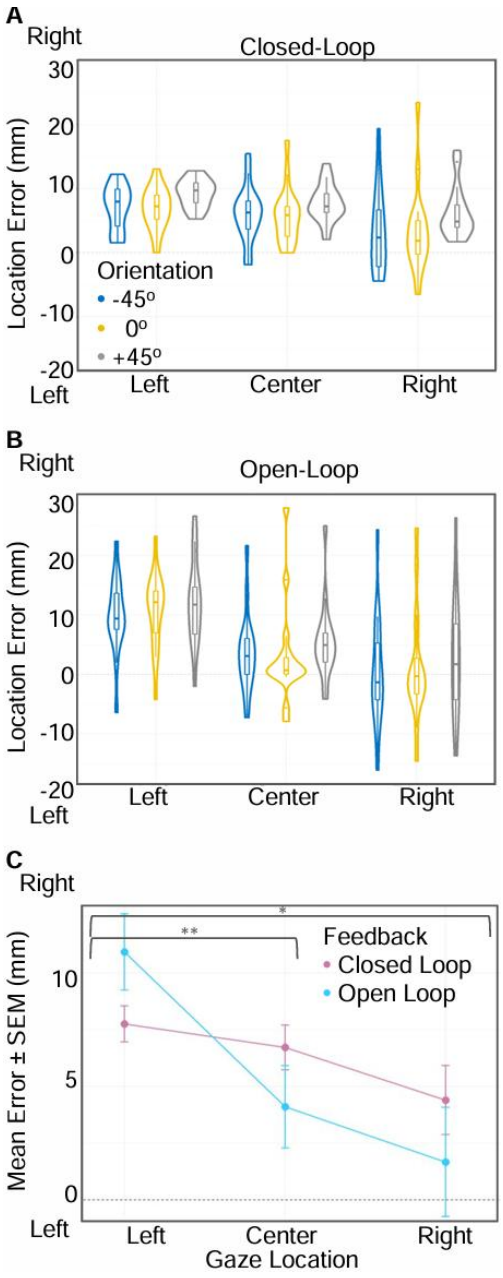


Figure 2.4. Graph of Location Errors in *Experiment 1*. A-B) Violin plots representing placement location errors for the left, center, and right gaze fixation locations in the *Closed-Loop* (A) and *Open-Loop* (B) conditions. Violin plots show the distribution of the participant's average location error and include the median (as the dot) and the interquartile range (as the bar in the center of the violin). Location error was quantified as the horizontal difference between the

object center and template center, where the mean of participants' endpoint position is compared to the target template position, and the error is used to compute the accuracy in the horizontal position. The values from the y-axis provide information regarding the direction of the error: a positive value indicates movement errors toward the right, and a negative value indicates movement errors to the left. C) Mean horizontal endpoint error (± SEM) across participants in endpoint horizontal location plotted as a function of gaze position. The graph displays the mean error and standard error of participants' endpoint position on the screen in comparison to the actual target template position on the screen. The x-axis represents the three possible gaze locations (left, center, or right). Asterisks indicate significant gaze-dependent errors, and there was a statistically significant 2-way interaction between gaze location and level of visual feedback.

We conducted a three-way repeated-measures analysis of variance (ANOVA) composed of 3 (Gaze Locations) × 3 (Orientations) × 2 (Levels of Feedback). The results showed main effects of Gaze Location ($F_{2,30} = 8.068$, $P_{GG} = 0.007$, $\eta^2 = 0.35$) and Orientation ($F_{2,30} = 7.334$, $P = 0.002$, $\eta^2 = 0.33$) on object location, as well as a significant interaction effect of Location and Levels of Feedback ($F_{2,30} = 7.620$, $P_{GG} = 0.006$, $\eta^2 = 0.34$). There was no significant interaction effect between gaze location and orientation ($F_{4,60} = 1.033$, $P = 0.397$, $\eta^2 = 0.06$) and between level of visual feedback and the orientation ($F_{2,30} = 0.305$, $P = 0.738$, $\eta^2 = 0.02$) and no significant three-way interaction effect was found for the endpoint location error ($F_{4,60} = 0.672$, $P = 0.613$, $\eta^2 = 0.04$). While there was a bias toward placing the object to the right, the main effect of gaze location showed a significantly greater location error toward the right for leftward gaze locations compared to central and right gaze locations. In addition, there was a greater error toward the left in the +45° orientation in comparison to the 0° orientation and the -45° orientation.

A post-hoc test investigating the interaction contrasts between Gaze Location and Level of Visual Feedback revealed a difference in the slope pattern of placement location as a function of gaze location. Bonferroni's adjustment was employed to control for family-wise error. Because of the overall shift of these placement location errors to the right, the increased gaze-dependent effect (with no visual feedback) caused pointing errors to increase at the left gaze position (mean difference = 3.16mm, d = 0.60) but decrease at the center (mean difference = -2.46mm, d = 0.42) and right fixations (mean difference = -2.73mm, d = 0.34).

Overall, participants showed a bias in object placement to the right, and tended to overshoot the central target template relative to gaze position, especially in the absence of visual feedback. Furthermore, the standard deviations showed more variability in the data in the absence of visual

feedback. These results tend to agree with observations made in pointing and reaching studies (.e.g., 2, 3).

Orientation error. Errors in final object orientation were measured and analyzed to study the influence of visual feedback, gaze position, and target template orientation on placement orientation. The violin plots in Fig. 2.5 (*upper row*) summarize the distribution of orientation errors in the closed loop (5A) and open loop (5B) conditions, where a negative value indicates a clockwise error in orientation and a positive value indicates a counterclockwise error in orientation. Based on visual inspection of the figure, performance was variable across participants, but there was an overall trend to make CW errors (over-rotation) at the CW template (blue), CCW errors at the horizontal template (yellow), whereas mean error at the CCW template (gray) was smaller and more variable across conditions and gaze positions. Additionally, error distributions tended to be larger in the *open-loop* condition compared to *closed-loop* visual feedback.

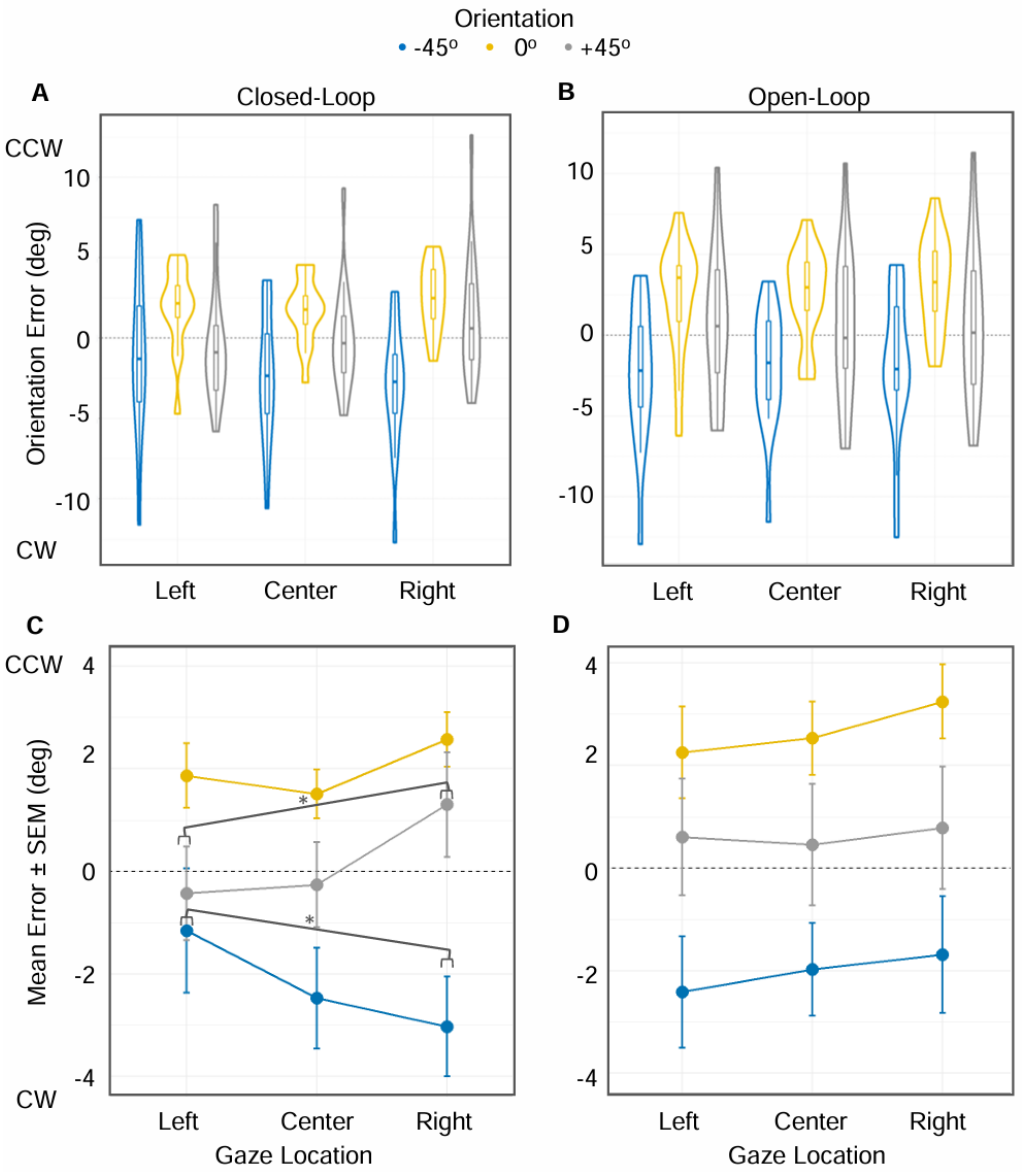


Figure 2.5. Orientation Errors in *Experiment 1*. A-B) Violin plots illustrating placement orientation errors for the left, center, and right locations in the *Closed-Loop* (A) and *Open-Loop* (B) conditions. Violin plots show the distribution of the participant's average orientation errors, including the median (as the dot) and the interquartile range (as the bar in the center of the violin). Errors were the angular difference between object and template orientation, where a positive value indicates a counterclockwise rotation and a negative value indicates a clockwise rotation. C-D) Error in endpoint orientation (mean ± SEM across participants) plotted as a function of gaze location. There was a statistically significant 3-way interaction between gaze location, level of visual feedback, and target template orientation. There was a statistically significant 2-way interaction between gaze location and target orientation (C). Asterisks indicate significant gaze-dependent errors in orientation for +45° and -45° in the *closed-loop* condition. However, the interaction was not significant in the *open-loop* condition (D).

A second three-way ANOVA was conducted to investigate the influence of gaze location, target template orientation, and visual feedback on final object orientation during placement movements. The ANOVA revealed a significant main effect of Orientation ($F_{2,30} = 7.017$, $P_{GG} = 0.009$, $\eta^2 = 0.32$), a significant two-way interaction effect between Orientation and Gaze Location ($F_{4,60} = 3.522$, $P = 0.012$, $\eta^2 = 0.19$) and a three-way interaction between Orientation, Gaze Location, and Visual Feedback ($F_{4,60} = 9.48$, $P = 0.000$, $\eta^2 = 0.39$).

Post-hoc tests were conducted to investigate the three-way interaction contrasts between gaze location, target template orientation, and visual feedback levels. After correction for multiple comparisons, there was a significant difference in the slopes when comparing the error in orientation for the +45° and – 45° degree angles in the two levels of visual feedback when the gaze location was to the left or the right ($P < 0.05$). A 2-way interaction Orientation x Gaze Location was observed only in the *closed-loop* condition.

The latter two-way interaction is visually evident in Fig. 2.5C, where CW orientation errors increased from left to right gaze for the CW (-45°) template, whereas errors became more CCW for other templates. In contrast, all three templates showed similar gaze dependencies (more CCW for left-to-right gaze) in the closed loop condition (Fig. 2.5 D). This condition-dependent difference likely reflects the three-way interaction between orientation, gaze, and condition mentioned above. Thus, all three factors (target orientation, gaze location, and visual feedback) affected the orientation error, especially at the oblique (±45°) template orientations.

2.4.2 Experiment 2

The main purpose of Experiment 2 was to 1) assess object placement location and orientation errors when a memory delay was added to the task, and 2) examine how these errors are influenced by the occurrence of different types of horizontal saccades (*towards*, *away* from, or *across* the template stimulus) during this memory interval. Once again, we analyzed the endpoint accuracy error in location (relative to the center point of the visual template) and the endpoint accuracy error in orientation (relative to the orientation of the template) (Fig. 2.3 *Middle Row*). We begin with an analysis of the data based only on the final gaze position (next two sub-sections) and then test if the errors were also influenced by the initial gaze position / saccade vector.

Location Error. The violin plots in Fig. 2.6A/B show the distributions of error in placement relative to the target template for each template orientation and final gaze position. Based on visual inspection of the data, the errors appear to overshoot the target relative to gaze; for instance, they lean more to the right (positive) for leftward gaze. Visual inspection also suggests that location errors were modulated by template orientation, i.e., there appears to be a modest tendency to place the object more to the right for the +45° (CCW) template compared to the -45° (CW) template.

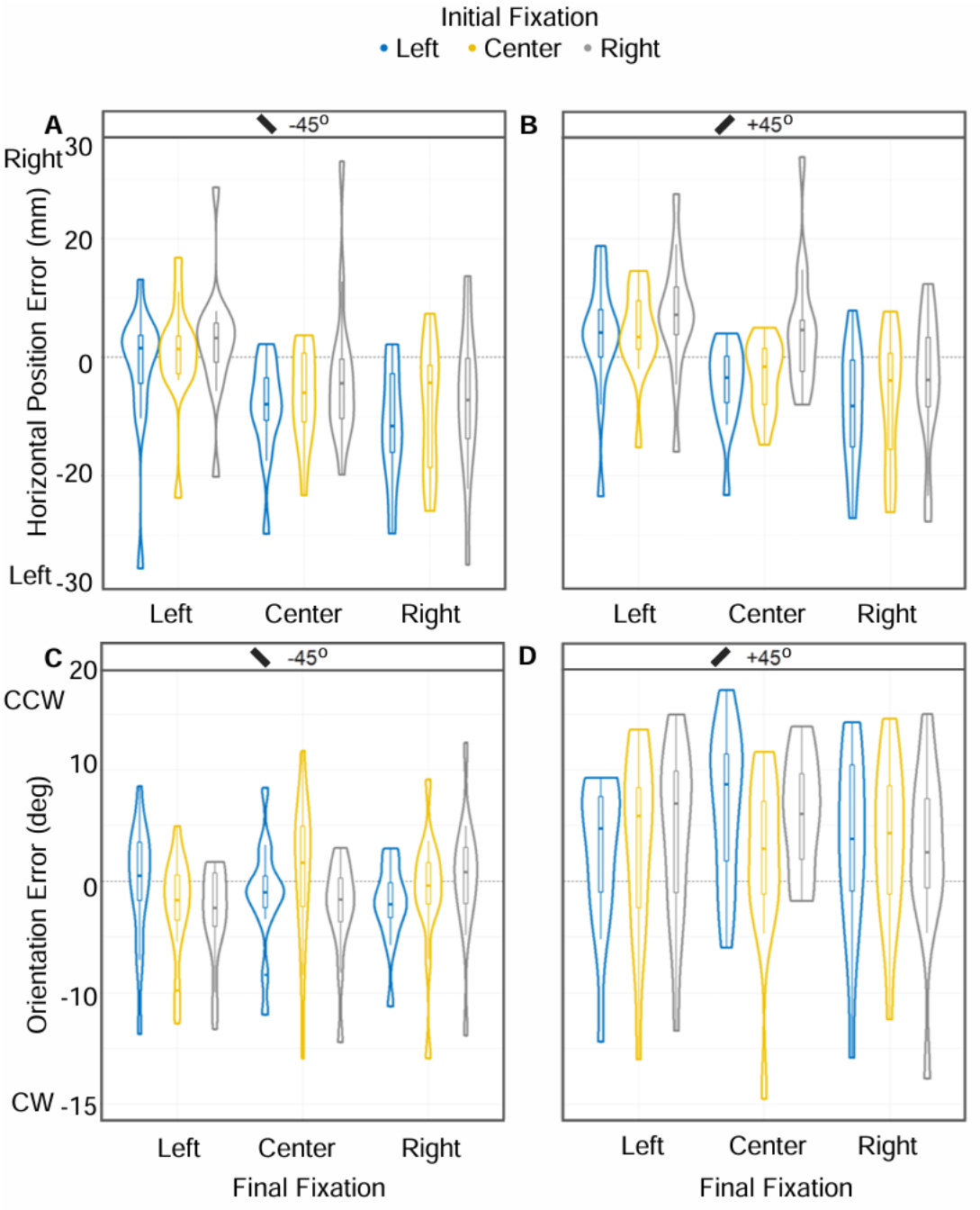


Figure 2.6. Distribution of Location and Orientation Errors for *Experiment 2*. Violin plots show the distribution of the participant's average errors, including the median (depicted as the dot) and the interquartile range (as the bar in the center of the violin). Top panels: Violin plots representing placement location errors for (A) -45° target orientation and (B) +45° target template orientation. The data are grouped according to the final gaze locations and color-coded according to initial gaze locations. A positive value indicates movement towards the right, and a negative value indicates movement to the left. Bottom panels: Violin plots illustrating placement orientation for (C) -45° target template orientation and (D) +45° target template orientation. The values from the y-axis provide information regarding the direction of the error: a positive value indicates a counterclockwise rotation and a negative value indicates a clockwise rotation. Other plotting conventions are the same as those for the upper row.

To quantify these trends, we conducted a repeated measure 3 × 3 × 2 ANOVA analysis, with three initial gaze locations (left, center, or right), three final gaze locations (left, center, or right), and two orientations (+45° or -45°) as the variables. A three-way ANOVA revealed a significant main effect of Final Gaze Location ($F_{2,26} = 10.317$, $P = 0.000$, $\eta 2 = 0.44$) related to the gaze overshoot described above. There was also a significant main effect of Orientation on Placement Location ($F_{1,13} = 20.16$, $P = 0.000$, $\eta^2 = 0.61$).

There was no significant main effect of Initial Gaze Location ($F_{2,26} = 2.817$, $P_{GG} = 0.109$, $\eta^2 = 0.18$), but Initial Gaze Location × Orientation showed a significant two-way interaction ($F_{2,26} = 4.059$, $P = 0.029$, $\eta^2 = 0.24$). Post-hoc tests showed that (compared to saccades from center gaze), saccades from leftward gaze (but not the rightward gaze) showed a stronger influence of both counterclockwise (mean difference = 4.55mm, d = 0.43) and clockwise (mean difference = 2.32mm, d = 0.20) orientation on placement location. There was no significant three-way interaction (Orientation × Initial Gaze Location × Final Gaze Location: $F_{4,52} = 1.436$, $P = 0.235$, $\eta^2 = 0.10$).

Orientation Error. A second ANOVA was conducted on the average difference between participants' performed endpoint orientation and the actual target template orientation (again, based only on the final gaze position). Looking at the violin plot to see a summary statistic of the distribution of error, there is a greater variation and relative positive (counterclockwise) shift in the block final orientation for the +45° in comparison to the -45° (Fig. 2.6 C and D). A repeated measure 3 × 3 × 2 ANOVA analysis was conducted, with three Initial Gaze Locations (left, center, or right), three Final Gaze Locations (left, center, or right), and two Orientations (+45° or

-45°) as the variables. The three-way repeated measure ANOVA was conducted to investigate the influence of saccade types and target template orientation on endpoint orientation error.

2.4.3 Influence of Initial Gaze Position During Saccades

Fig. 2.7 A, C and E show endpoint location errors as a function of final gaze, but now the data are separated according to initial gaze position. Initial gaze positions are indicated by the symbols (left ▲, center ●, right ■), and template orientation is indicated by the color (pink rotated clockwise, blue rotated counterclockwise). The top row shows fixation data, the middle row shows saccade data *towards* / *away* from the target, and the bottom row shows *across* saccade data. Fixation data show the typical 'overshoot' pattern, as do the saccade *away* data and saccade *across* data.

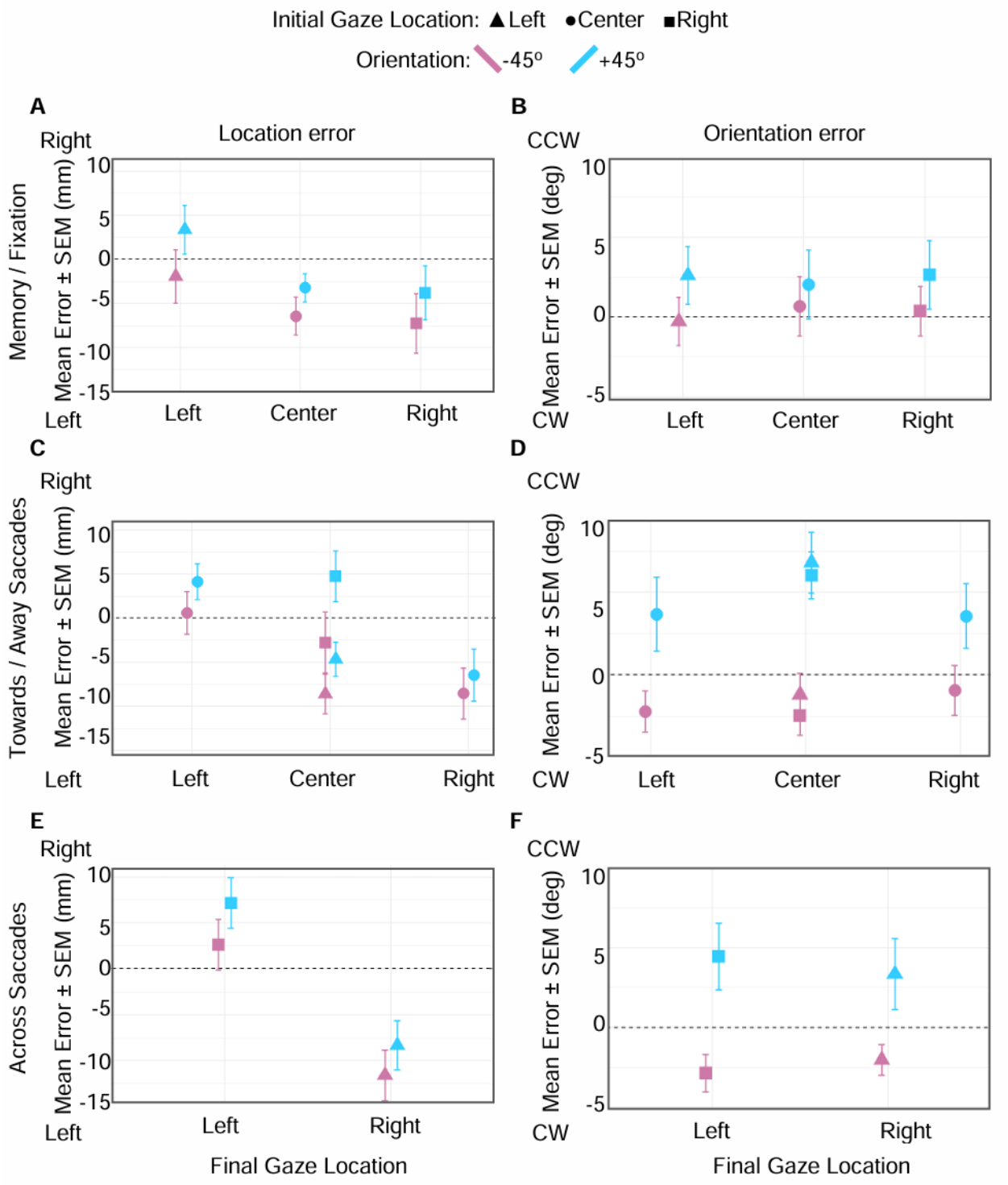


Figure 2.7. Mean Location Error (*left column*) and Orientation Errors (*right column*) in *Experiment 2*, plotted as a function of final gaze position and coded according to template orientation (-45° pink / +45° blue) and initial gaze location (left ▲, center ●, right ■). *Top row*: *Fixation* data (where initial and final gaze location are identical); *Middle row*: saccade *towards / away* data; *Bottom row: Saccade across data*.

The exception is the saccade *towards* data, i.e., the saccades that end at center in Fig. 2.7C. Here, placements with leftward saccades / clockwise templates and rightward saccades / counterclockwise templates had small errors, as expected, but the opposite pairs (leftward / counterclockwise, rightward / clockwise) ended with large errors in opposite directions, as though overcorrecting for the placement overshoots observed at the original gaze position (in the fixation task). This accounts for the saccade / orientation interaction that emerged in our statistical analysis and contradicts the normal rule that final gaze determines hand position errors.

The results revealed a significant main effect of template Orientation on hand orientation errors ($F_{1,13} = 8.544$, $P = 0.012$, $\eta^2 = 0.40$). There was no significant main effect of initial gaze ($F_{2,26} = 0.488$, $P = 0.062$, $\eta^2 = 0.04$) or final gaze location ($F_{2,26} = 2.988$, $P = 0.0685$, $\eta^2 = 0.19$) on the endpoint orientation, but there was a significant two-way interaction between Initial Gaze Location and Orientation ($F_{2,26} = 5.534$, $P = 0.009$, $\eta^2 = 0.30$) and a three-way interaction for Orientation, Initial and Final Gaze Location ($F_{4,52} = 10.437$, $P = 0.000$, $\eta^2 = 0.45$). Follow-up tests showed no significant interaction between Initial Gaze Location, Final Gaze Location, and Orientation (all $P > 0.05$). In short, hand orientation errors were primarily influenced by template orientation, but this interacted with initial gaze location.

Fig. 2.7 B, D and F illustrate the influence of final gaze, initial gaze, and template orientation on object orientation using the same conventions as the left column, showing fixation data (top row), saccades *towards* / *away* data (middle row) and saccades *across* (bottom row). A relative positive counterclockwise rotation was always seen for the +45° angle in the saccade conditions and a relative negative clockwise rotation for the -45° angle. This effect was small in the memory-fixation condition (Fig. 2.7 B) but became stronger in the saccade condition data shown here (Fig. 2.7 D and F). These subtle differences likely correspond to the interactions mentioned earlier. After the correction for multiple comparisons, there was no clear main effect of gaze endpoint on orientation, i.e., the plots in Figure 2.7 B, D, F did not consistently slope upwards to the left or right.

2.5 Discussion

Whereas the influence of vision and gaze position on reach / pointing location is well studied, their influence on object placement (in both the location and orientation domains) has largely been

ignored. In this study, we investigated the influence of gaze location, level of visual feedback, saccades, and target template orientation on the accuracy of orientation and horizontal position in an object placement task. In Experiment 1, we assessed the accuracy in fixation gaze conditions, with and without visual feedback of the target template and hand location during the placing movement. As in reaching and pointing movements (Fiehler et al., 2011; Henriques et al., 1998; Schütz et al., 2013), there was a systematic overshoot of endpoint location in the direction opposite to the gaze location that increased in the *open-loop* (no visual feedback) condition. Participants sometimes overestimated rotations of the placement template from horizontal, and this pattern was influenced by gaze location and visual feedback. We also tested (Experiment 2) how an increased memory delay and various saccade patterns would affect placement accuracy. While a consistent effect of gaze location could be observed in endpoint location during placement, it was not observed in orientation for all conditions. However, endpoint orientation errors were influenced more by the target template orientation than by the gaze location.

2.5.1 General Bias in Placement Location

Our results showed a general bias in placement endpoint location, most easily observed when participants looked straight ahead at the horizontal template. It is possible that this was a visual strategy to allow participants to see the edge of the template as the block approached its final destination. Alternatively, this could be linked to a proprioceptive motor bias. Similar proprioceptive bias in the endpoint reach has been shown to have a gaze-independent component (Mueller & Fiehler, 2014). In either case, one might expect this bias to reverse for the left hand (this was not tested).

2.5.2 Influence of Template Orientation on Placement Orientation

A consistent observation in both experiments is that target orientation influences the placement orientation error. Since we only used template orientations that participants reported to be comfortable with, and the pattern depended on visual conditions, these errors were unlikely to be due to biomechanical constraints. In experiment 1 (*closed* and *open-loop*), there was a nonlinear relationship such that the -45° CW template had a more CW bias, the 0° orientation template had a more CCW bias, and the +45° CCW template had a small CCW bias. The pattern was simpler in experiment 2 (over-rotation for both +/- 45° templates), but the absence of a horizontal template

in experiment 2 precludes one from judging whether that effect was linear. Overall, the type of error seen in placement orientation depended on the template orientation.

The influence of target orientation on movement has also been shown in grasping studies, such that the grasp angle depends on the object orientation (Desmurget et al., 1996; Fan et al., 2006). In addition, Mason & Bryden (2007) reported an over-rotation in a grasp, which was more pronounced for the oblique orientation. While this is consistent with our experiment 2 results and our experiment 1 results for the CCW template, we did not see this in all of our experiment 1 conditions. It is possible that this is because participants developed different strategies depending on visual feedback (i.e., to avoid obscuring the template). However, the current study cannot discriminate whether this was a learned strategy or some miscalibration in the 'dorsal stream' transformations for action.

2.5.3 Influence of Gaze Position on Placement Location

Reaching and pointing studies have shown a gaze-dependent overshoot effect in the direction opposite to the gaze location before movement onset (Bock, 1986; Bock & Eckmiller, 1986; Enright, 1995; Henriques et al., 1998; Henriques & Crawford, 2000). These original findings have been extended across different memory delays, with egocentric and allocentric frames of reference (Fiehler et al., 2011; Lewald & Ehrenstein, 2000; Schütz et al., 2013, 2015; Vaziri et al., 2006). Finally, such gaze-dependent errors interact with the errors related to initial hand position and may be magnified by damage to the parietal cortex (Khan et al., 2007; Khan, Pisella, Rossetti, et al., 2005).

Regarding object placement, we observed similar gaze-centered patterns of reach error during placement. This suggests that the overshoot effect is present across various types of goal-directed movement and is not exclusive to a simple reach movement. Presumably, these errors result from miscalibrations in the gaze-dependent transformation from visual coordinates to motor coordinates for hand motion (Beurze et al., 2006; Blohm & Crawford, 2007). Two specific explanations for this phenomenon are that the target direction is overestimated relative to gaze (Henriques et al., 1998) or that gaze direction is underestimated relative to the target (McGuire & Sabes, 2009). An alternative theory, supported by some evidence, is that the error does not occur in the reach transformation, but rather in the transformation of hand position signals into gaze-centered coordinates when compared to vision for computation of the reach plan (Dessing et al., 2012;

Sober & Sabes, 2003; Vesia et al., 2008, 2010). In any case, the observation that this effect generalizes to different behaviours (pointing, reach, placement) suggests a common computational mechanism.

2.5.4 Influence of Gaze Position on Placement Orientation

In the current study, we observed orienting errors that changed direction based on the retinal location and orientation of the target template. This suggests that gaze location and target template orientation are two elements that interact and influence the final orienting error observed in object placement. Similar to the oblique effect observed in grasping studies (Gosselin-Kessiby et al., 2008; Hesse et al., 2021), the gaze-dependent orienting error in placement was only significant for the oblique orientations. This might reflect a tendency to process reach information along coordinate system-like channels (Soechting & Flanders, 1992), although little physiological evidence supports this idea (Blohm et al., 2009). Another possibility is that gaze-dependent location errors could produce gaze-dependent orientation errors if the perceived distance of the near end of the template is magnified more / less than that of the far corner. This would tend to rotate the perceived orientation of our oblique (but not horizontal) templates. Overestimation of the near corner would lead to an over-rotation, whereas overestimation of the corner further from the gaze location would lead to an under-rotation. This would result in V-like patterns (or inverted V) in the gaze-dependent orientation plots shown in Figure 2.5. However, such patterns were inconsistent in the *closed-loop* condition and absent in the *open-loop* condition.

It has been shown that gaze direction interacts with 2D wrist pointing direction for grasp orientation (Selen & Medendorp, 2011), but it is less clear why gaze direction would interact with 3D orientation of the hand about the axis of the wrist (as in the current task). Object location and orientation are spatially independent variables that do not tend to cross-correlate in visuomotor adaptation studies (Marotta et al., 2005). Further, orienting objects in this dimension involves coordinated movements of the fingers, wrist, and upper arm (Marotta et al., 2003). These factors again suggest a high-level but non-specific gaze-orientation interaction, perhaps in the dorsal visual stream. We will speculate about such mechanisms in a later section below.

2.5.5 Influence of Visual Feedback and Memory Delay

Previous studies have shown that having visual feedback of the target and/or hand position during reach influences accuracy in the movement, presumably by aiding the online calculation of the reach vector (Sober & Sabes, 2005; Vesia et al., 2008, 2010). Conversely, prolonging the delay period following a transient visual stimulus beyond 250 ms decreases movement accuracy, presumably due to degradation in the egocentric visual memory of the target stimulus (Chen et al., 2011; Glover, 2004; Heath, 2005).

To determine if these factors held during placement movement, we investigated how changes in the presence of visual feedback influence participants' accuracy in their final placement of an object. We first looked at the influence of visual feedback on gaze-dependent errors in Experiment 1. Consistent with previous studies (Fiehler et al., 2011; Henriques et al., 1998; Thompson & Henriques, 2011), we found a significant increase in gaze-dependent location overshoots in the absence of visual feedback. In contrast, visual feedback did not mitigate the significant gaze-dependent orientation errors found in the oblique orientations. This suggests that these orientation errors were not due to a visual strategy but rather some internal visuomotor miscalibration, perhaps related to gaze-dependent transformations in the 'dorsal stream.'

As expected, gaze-dependent location errors persisted with the addition of a memory delay in Experiment 2. This remains consistent with the notion of dorsal stream errors that appear in the absence of visual feedback, which then requires a shift to ventral stream processing (Schenk & Hesse, 2018). If one compares the data in Figure 2.5 B, D in Experiment 1 to Figure 2.7 B in Experiment 2, it appears that gaze-dependent orientation errors were reduced in the Memory / Fixation condition, although we did not directly compare this within the same experiment. It has been suggested that the addition of a memory delay to reach tasks engages 'ventral stream' visual processes (Khan, Pisella, Vighetto, et al., 2005; Milner et al., 2003). If the ventral stream is better at processing orientation information than the dorsal stream, this might explain why gaze location did not influence orientation errors in this condition. This functional anatomy is highly speculative, but our behavioural results highlight that memory-guided reach may rely on different neural mechanisms, and this does not always lead to inferior performance.

2.5.6 Influence of Saccades

Previous studies have shown that in the presence of saccades, the final gaze position determines memory-guided reach errors, and this has been used to support the notion of gaze-centered updating (Beurze et al., 2006; Henriques et al., 1998; Medendorp & Crawford, 2002; Schütz et al., 2013). However, those studies consistently relied on saccades *away* (from the target toward some peripheral fixation position). In the real world, saccades may follow a variety of different repertoires. The present study examined three of these repertoires (*away*, *towards*, and *across* the target template) to see if memory-guided placement shows the same pattern (i.e., dependence only on final gaze), and if those results generalized to different saccade amplitudes, directions, and positions.

Our overall statistical analysis confirmed that final gaze position, rather than initial gaze position, determined the influence of saccades on memory-guided placement. However, there were more nuances when we examined specific types of saccades. Saccades *away* and saccades *across* the target template followed the expected pattern, supporting the notion that gaze-centered updating for memory-guided reaching also generalizes to placement tasks. The main difference was in saccades *towards*, which appeared to 'overcorrect' the influence of initial gaze position, i.e., produce overshoots opposite to the initial gaze position, depending on the saccade direction and the orientation of the template. In general, final gaze positions tended to produce an opposite overshoot in reach location (similar to Experiment 1), with the largest influence observed in the *across* condition.

2.5.7 Caveats and limitations

As in any such experiments, the results in this study are specific to the task and can only be generalized to other tasks with further experimentation. Clearly, this was a visually impoverished environment with artificially fixed gaze positions; thus, the errors reported here might be suppressed during gaze fixation in a richer environment containing allocentric cues (Byrne et al., 2010; Chen et al., 2011). However, gaze is not always locked to placement targets in real-world circumstances (Johansson & Flanagan, 2009), and peripheral vision does not have the same acuity. Another caveat is that, although our participants interacted with a real 3D object, they placed it toward a 2D surface that did not have depth or somatosensory cues. In our increasingly technology-dominated lives, people often interact with 2D touch screens, but it is possible that additional gaze-

dependencies and brain mechanisms are engaged in a complete 3D environment (Blohm et al., 2008; Konen & Kastner, 2008; Kourtzi, 2003; Kourtzi & Kanwisher, 2001; Snow et al., 2011; Van Pelt & Medendorp, 2008). Finally, although this study was inspired by the literature on eye-hand coordination during reaching / pointing, we did not directly compare reach and placement in the current experiment, so we could only provide qualitative comparisons based on the literature.

2.5.8 Possible Neural substrates

The literature on neural control of goal-directed action is dominated by reach and grasp experiments, whereas relatively few studies have examined brain activity beyond goal acquisition. Several functional Magnetic Resonance Imaging studies have investigated the neural mechanisms of object manipulation. For example, the size-weight illusion has been used to investigate the neural correlates of force correction and weight prediction (Chouinard et al., 2009). Object manipulations such as these involve the recruitment of regions in the posterior parietal cortex (PPC), the cerebellum, and the motor cortex.

Thus, at this time, one must speculate on the neural mechanisms of placement based on what is known about the reach / grasp system. As noted above, the dorsal visual stream, corresponding dorsal occipital and posterior parietal cortex, is the likely site for the integration of visual and other sensory information to guide visuomotor planning (Culham & Valyear, 2006; Orban et al., 2021; Vesia & Crawford, 2012). The mid-posterior intraparietal cortex (mIPS) is involved in calculating the hand-target vector for reach transport (Orban et al., 2021; Pitzalis et al., 2013) and thus might likewise be engaged in our match-to-template task. Anterior IPS is involved in grasp formation (Culham & Valyear, 2006), and thus might be involved in the 'inverse grasp' for placement: letting go of the object at the end. The superior parietal occipital cortex (SPOC) has been shown to have both transport and grasp signals (e.g., Pitzalis et al., 2013; Prado et al., 2005), and is specifically involved in orienting the hand (Monaco et al., 2011); so again, it might be engaged in a task like this. Of course, PPC does not operate in isolation but rather communicates extensively with frontal reach areas such as the dorsal and ventral premotor cortex and primary motor cortex (Turella & Lingnau, 2014; Vesia & Crawford, 2012; Vingerhoets, 2014).

Although the dorsal stream is associated with the use of online visual control, lateral and superior occipital cortex and PPC have been implicated in memory and planning for reaching in a delay

task (Cappadocia et al., 2017; Chen et al., 2014; Vesia et al., 2010). These areas are also implicated in the gaze-dependent transformations for reach (Andersen & Buneo, 2002; Blohm et al., 2009; Chang et al., 2009; Galletti et al., 1995). However, as noted above, it has been argued that the ventral stream becomes engaged in memory-guided reaches, especially as the delay increases (Schenk & Hesse, 2018; Schenk & McIntosh, 2010). Our observations show that gaze-centered updating is involved in placement, a phenomenon associated with PPC (Culham & Valyear, 2006; Medendorp et al., 2003). Specifically, we recently implicated a cortical network involving frontal eye fields, inferior parietal cortex (specifically supramarginal gyrus), aIPS, and dorsal PPC in updating grasp orientation during saccades, which may have played a similar role here (Baltaretu et al., 2020).

2.5.9 Conclusions

Prehension and placement are both goal-directed movements that require identifying the target location and its orientation in order to successfully perform the desired movement. However, they differ greatly in intention, as one (reach) is generally used to acquire an object, and the other (placement) is used to dispose of it. It does, however, appear that they follow certain similar kinematic rules of eye-hand coordination. As in reach movements, placement movements (in our task) showed degraded performance in the absence of vision and a trend to overestimate direction relative to gaze. The influence of gaze on orientation was less systematic, but we observed orientation overshoots in our task as well as various subtle interactions between gaze and orientation, depending on different levels of visual feedback and memory delay.

These observations suggest that at least some aspects of the acquisitional reach system (such as early gaze-centered processing) are shared by the placement system and provide other details that need to be accounted for in modelling the system. They also have practical implications. If our observations generalize to other conditions, this would have consequences for any technology or task that requires highly accurate placement in both the location and orientation on a two-dimensional plane. For example, our results might translate to the use of tools, as tool-assisted grasp resembles object placement in some respects but also leads to its perception as an extension of the hand (e.g., Cardinali et al., 2009; Farnè & Làdavas, 2000). Future studies could also investigate the similarity between place and tool-assisted grasp. Further, this study provides a baseline of healthy behaviour for further studies in patients. For example, based on previous reach

and pointing studies, one might expect these errors to increase in any pathology that impairs parietal cortex function (Khan et al., 2007; Khan, Pisella, Rossetti, et al., 2005).

CHAPTER 3:

BEYOND REACH I: NEUROIMAGING REVEALS DIFFERENT CORTICO-CEREBELLAR NETWORKS FOR GRASP VS. OBJECT PLACEMENT

Authors: Gaëlle N. Luabeya[1-4], Erez Freud[1-5] & J. Douglas Crawford[1-6]

Affiliations:

[1]Centre for Integrative and Applied Neuroscience, York University, Canada

[2]Centre for Vision Research, York University, Canada

[3]VISTA and Connected Minds Programs, York University, Canada

[4]Department of Biology, York University, Canada

[5]Department of Psychology, York University, Canada

[6]Department of Kinesiology & Health Sciences, York University, Canada

Current Status: Chapter 3 is submitted and a preprint is available on bioRxiv

Citation: Luabeya, G. N., Freud, E., & Crawford, J. D. (2026). Beyond Reach I: Neuroimaging Reveals Different Cortico-cerebellar Networks for Grasp vs. Object Placement. bioRxiv, 2026-04.

3.1 Abstract

Object manipulation usually involves both acquisition and placement, but neuroimaging studies tend to focus on its initial reach-to-grasp component. To understand how grasp and placement are represented in the brain, we designed an event-related fMRI study in which 20 participants alternated between grasping / placing a rectangular object from / toward templates presented at variable locations and orientations on an inclined plane. Despite the similarity in target information (i.e., location and orientation), we expected to see sensory and intentional task differences, as the grasp relied on matching the hand to the object, whereas placement relied on matching the object to the template. For our analysis, we examined BOLD activation across two epochs (planning phase before movement onset and execution phase during the movement), and applied graph-theoretical analysis (GTA) of whole-brain functional connectivity based on the joint time series from these two epochs. In both tasks, we found that common activation was predominantly in prefrontal regions during planning and in sensorimotor regions during execution, with a specific increase in cerebellar activation during placement. Furthermore, the greater placement activation was also found in action-related regions of interest during the planning phase, and they could accurately decode between our two tasks. GTA categorized the two networks into three identical modules (prefrontal, cerebellar-occipito-parietal, and sensorimotor) and found task-based differences in modularity scores in the prefrontal and cerebellar-occipito-parietal modules. Overall, these data show that although reach-to-grasp and reach-to-place movements share extensive neural circuitry, they also exhibit task-specific differences, likely related to differences in intentionality during planning and in sensory feedback during movement execution.

3.2 Introduction

Goal-directed actions, such as prehension, often begin with an initial reach-to-grasp movement, but this is usually just the prelude toward the ultimate intention: to manipulate and/or place the object somewhere. For example, when loading a dishwasher, although one first grasps a dirty plate, the real objective of the full movement is to place and orient the dish correctly in the lower rack and run a successful cleaning cycle. Such actions underscore the importance of considering not only movement initiation but also its termination. It is perhaps surprising then that nearly all studies of hand control tend to focus on the initial reaching and grasping component (Castiello, 2005; Castiello & Begliomini, 2008; Grafton, 2010; Turella & Lingnau, 2014), and only a 'handful' have examined the placement movements that often follow (Flindall & Gonzalez, 2019; Luabeya et al., 2024). Reach-to-grasp and reach-to-place share many similarities (e.g., eye-hand coordination, goal coding, transport kinematics, hand-object integration) but also differ in terms of intention and sensory feedback (Greenwald & Knill, 2009; Hesse & Deubel, 2010; Luabeya et al., 2024). However, at this time, it is unclear how these commonalities and differences influence the underlying cortical and subcortical networks for action.

Given the commonalities between grasp and placement, one might expect many of the neural mechanisms involved in reach-to-grasp to be relevant to placement as well. In terms of the transport component as part of the dorsomedial pathway, this might include the primary visual cortex (V1), superior parietal occipital cortex (SPOC), middle/posterior intraparietal sulcus (mIPS/pIPS), dorsal premotor cortex (PMd), primary sensory cortex (S1), and primary motor cortex (M1) (Chinellato et al., 2011; Galletti & Fattori, 2018; Karl & Whishaw, 2013; Rizzolatti & Matelli, 2003). In contrast, grasp aspects might be processed by the dorsolateral pathway and involve V1, anterior intraparietal sulcus (aIPS), ventral premotor cortex (PMv), S1, and M1 (Culham et al., 2003; Culham & Kanwisher, 2001; Vesia et al., 2017). Finally, although neuroimaging studies tend to focus on the cerebral cortex, it is well known that subcortical structures, including the cerebellum, are involved in supporting reach and grasp (Becker & Person, 2019; Izawa et al., 2012; Nowak et al., 2007; Shirinbayan et al., 2019; Thach, 2014).

The intentional differences between grasping and placing (i.e., acquiring vs. disposing of an object) might be reflected in the higher-level signals of the 'reach' network. In contrast, the sensory differences might evoke more specific differences in sensory regions. Indeed, grasp planning tends

to be feed-forward driven, with the intention to match the hand to the object (Blohm & Crawford, 2007; Johansson & Edin, 1993), whereas placement involves different intentions (to match the object to the desired location) and additional sensory feedback at the planning and execution phases (Luabeya et al., 2026). Thus, during grasp planning and execution, vision needs to only focus on the desired object to acquire, whereas placement may require higher-level cognitive comparisons between the object and a seen or visualized target. Further, grasp starts without haptic feedback and ends with physical contact with the object, whereas place begins with haptic feedback that ends when the object is released. Each of these factors should influence cortical and subcortical sensory signals.

Further discussion of specific neural mechanisms requires speculation because direct experimental evidence is currently lacking. Neuroimaging studies have examined post-grasp actions such as object manipulation and size-weight perceptual discrepancies (Chouinard et al., 2009; Jenmalm et al., 2006), but to our knowledge, no previous imaging study has directly contrasted the mechanisms for grasping versus placing an object, either at the level of activation or at the level of functional network topology and dynamics.

To address this question, we designed an fMRI study in which participants alternated between grasping and placing a real object from / toward templates at varying locations and orientations. For a comprehensive understanding of their difference, we completed four types of analysis: 1) univariate voxelwise contrasts to establish whole-brain differences, 2) region-of-interest (ROI) analyses based on conventional reach / grasp coordinates, 3) a multivoxel-based classification analysis of our ROIs to confirm their task-dependency, and 4) a graph theoretical analysis (GTA) of functional connectivity to investigate how the whole-brain distribution of signals differs between these tasks. For this analysis, we also removed global trends (the general rise in Blood-Oxygen-Level-Dependent (BOLD) activation before action), which have been suggested to reflect long-range signal correlations (Musa et al., 2025).

Given the literature and theoretical considerations provided above, we expected to find common activation across the known reach-to-grasp system, as well as local and network-level differences related to higher-level planning and sensory feedback. We found that *grasp* and *placement* share similar cortical activation patterns during the *planning* and *execution* phases, but exhibit local differences in activation, particularly in the cerebellum, that support accurate task decoding.

Further, our functional connectivity analysis revealed three modules spanning the occipital, parietal, and frontal cortex, as well as the cerebellum. Overall, our results indicate that grasp and place share many similarities but differ in higher-order planning and sensory integration.

3.3 Methods

3.3.1 Participants

Twenty-two participants passed our initial screening process in the MRI simulator suite; however, two were excluded due to discomfort in the actual MRI scanner. A total of 20 subjects (11 females, 9 males; average age, 25; SD, 4.82) participated in this study. An a priori power analysis was conducted using G*Power 3.1.9.7 (Faul et al., 2007) to determine the required sample size. Based on an effect size of 0.67 (derived from a previous task-based functional connectivity analysis; Luabeya et al., 2026), an alpha level of 0.05, and a desired power of 0.80, the analysis indicated that a total sample size of 20 participants would be required to achieve the targeted statistical significance. All participants self-reported normal or corrected-to-normal visual acuity with no reported neurological disorders and were right-handed. They provided informed consent prior to the experiment and received monetary compensation for their time. The experimental procedures were approved by the York University Human Participants Review Committee (Certificate #: e2023-336).

3.3.2 Apparatus and Stimuli

An inclined platform placed on the participant's pelvis was used to present the stimuli (Fig. 3.1A). The platform was positioned approximately 22 cm from the participant to facilitate a natural view and comfortable hand movements to the left and right. Participants used a black cuboid object that could be picked up and placed in a hollowed rectangular template on the platform (Fig. 3.1B). The template could be positioned in two locations (the top-right or the bottom-left of the platform) and could be displayed in two possible orientations: clockwise (+30°) or counterclockwise (-30°). An experimenter in the scanner wore headphones with instructions on how to change the location and

orientation of the hollowed template during the intertrial interval. Two light-emitting diode (LED) lights would illuminate the target during the trial.

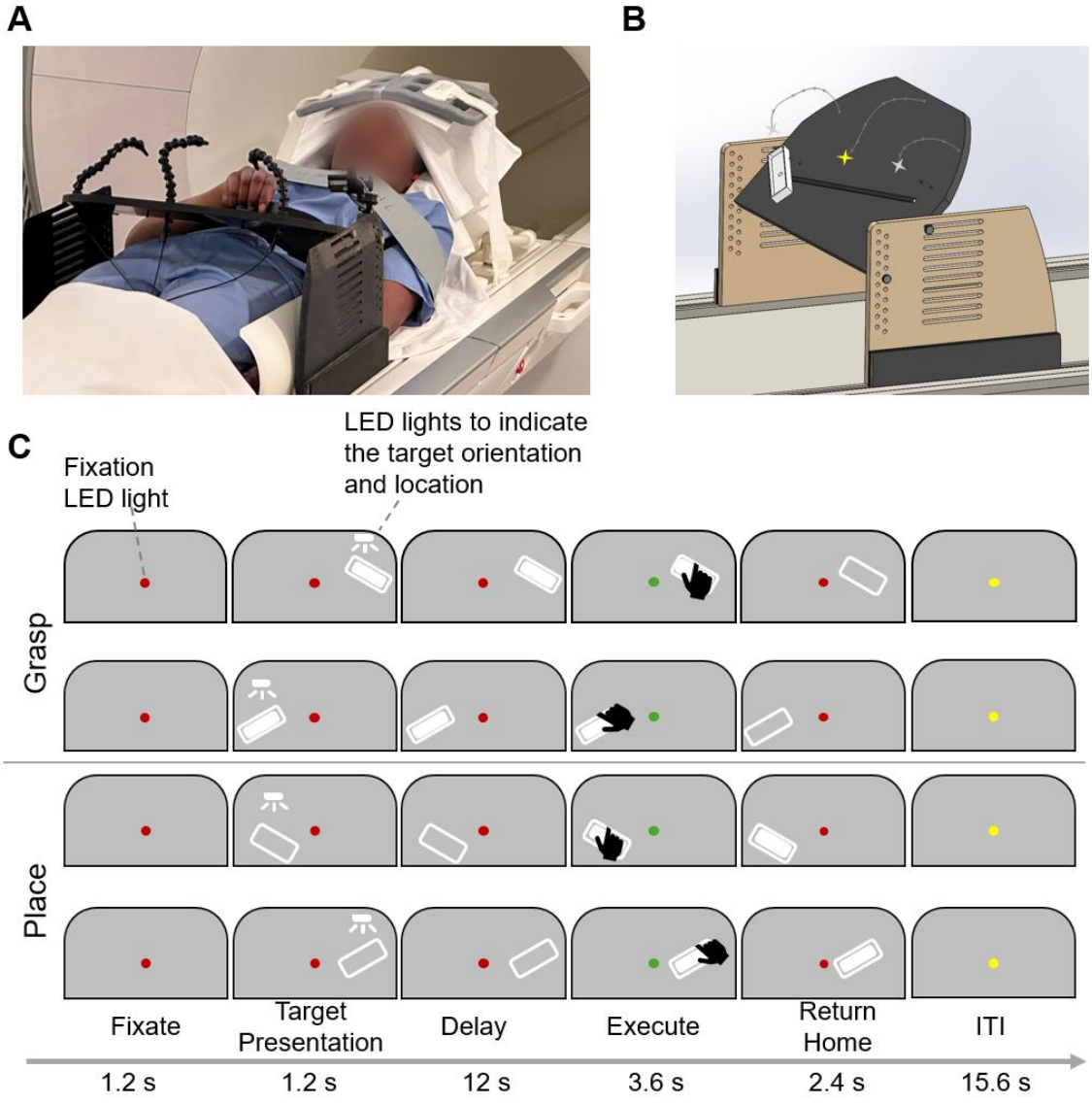


Figure 3.1. A) Experimental setup. Participants were instructed to maintain fixation on the LED light at the center, and they could grasp / place the object to the left or the right. B) View of the inclined platform with the template presented to the left, with the fixation light as a yellow star and the left and right LED lights as white stars. C) The time sequence shows four possible movement types: left or right grasp and left or right place with the target presented in a clockwise or counterclockwise orientation. In a trial, participants began by fixating on a red light, and a target was illuminated on the platform for 1.2 s. They waited an additional 12 s until the light turned green to perform the grasp or the place. They had 3.6 s to perform the movement and 2.4 s to return to their home position when the light turned red again. Finally, there was a 15.6 s inter-trial period before the next trial.

Participants laid in the scanner with their heads tilted (20 °) to facilitate a direct view of the objects. Foam cushions immobilized their head and upper arms to reduce motion artifacts. A belt was placed around the participant's waist to serve as the home position, from which they started and returned after performing the movements required in the trial. To maintain similar haptic feedback between the two tasks during the intertrial interval, the belt featured a cuboid object that participants could hold in preparation for a *grasp* trial or rest the object on it in preparation for a *place* trial. Additionally, movement of the upper arms was restricted by a strap.

All lights on the platform and the audio to the experimenter were controlled by a custom program on a laptop PC that received signals from the MRI scanner at the start of each trial. The windows in the scanner room were blocked with black curtains, and the room's lights remained off to improve visibility of the dimmed fixation light and the lights illuminating the target. The platform featured an infrared camera that recorded the participants' hand movements to monitor their performance during the experiment (MRC 12M with a custom Infrared illuminator).

3.3.3 Experimental Task Design

In this slow event-related fMRI task (Fig. 3.1B), participants grasped or placed a real 3D object to the left or right of their body midline, in clockwise or counterclockwise orientation. Participants grasped and picked up the object or placed and left it on a template on the platform. A trial consisted of three epochs: a *planning* phase after target presentation, an *execution* phase when the participant moved to place or grasp the object and returned to their home position with (after *grasp* movement) or without it (after *placing* the object on the platform), and finally an intertrial period in preparation for the subsequent trial. Henceforth, the two task-relevant phases of the trial will be referred to as the *planning* and *execution*, and the two actions will be referred to as *grasp* and *place*.

Each trial began with a red fixation point, which remained visible throughout the *planning* phase. After 1.2 seconds, the target was illuminated for another 1.2 seconds, appearing on either the left or the right. This cue was followed by a 12-second delay period during which only the red fixation point was shown, allowing participants to prepare their movement without additional visual information. At the end of the *planning* phase, the fixation point turned green, serving as the go signal. Participants then had 3.6 seconds to perform either a *grasp* or a *place* movement and to hold the object at the target location until the fixation turned red again. Following this, they had 2.4 seconds to return to their home position. In the *grasp* condition, they returned with the object

in hand; whereas, in the *place* condition, they returned without the object and instead held a mock block at their home position. Therefore, within a run, a *place* trial always followed a *grasp* trial, and vice versa. Each trial concluded with a 15.6-second intertrial interval, during which a yellow fixation light was displayed.

Overall, this paradigm formed a 2 (location instruction: left, right) × 2 (orientation instruction: clockwise, counterclockwise) × 2 (movement: *grasp*, *place*) design, resulting in 8 conditions. Each run consisted of 16 trials; therefore, each experimental condition was repeated twice in a pseudo-randomized order. A 14.4-second and a 13.2-second fixation point were added at the beginning and the end of each run, respectively, yielding a run time of 9.74 minutes. Each participant completed eight runs; however, for half of the participants, the odd runs began with a *place* trial, and the even runs began with a *grasp* trial, whereas the other half followed the reverse order. The sequence of conditions (*place* vs. *grasp*) was counterbalanced this way to reduce systematic bias. Additionally, an anatomical scan and a gradient echo field map were collected midway through the data collection session. Combined with setup time and a practice run, an entire session was approximately 2.5 hours.

3.3.4 Imaging Parameters

Our data were collected at York University (Toronto, Canada) using a 3-T whole-body MRI system (Siemens Magnetom TIM Trio, Erlangen, Germany). To facilitate the visibility of the stimuli in the head-titled setup, the 12-channel coil of the anterior part of the 32-channel coil was replaced with a 4-channel flex coil while its 20-channel coil's posterior portion was maintained (Fig. 3.1A).

The T2*-weighted functional data were acquired using a single-shot gradient echo-planar imaging (EPI) sequence with the following parameters: a repetition time (TR) of 1200 ms, echo time (TE) of 30 ms, a flip angle of 66°, a 240 mm field of view (FOV) and a 96 × 96 matrix, yielding a resolution of 2.5 × 2.5 × 3.0 mm^3. Fifty-four axial slices were acquired with no inter-slice gap using an interleaved multi-slice mode. Slice acceleration (multiband) and GRAPPA in-plane acceleration (factor 2) were employed to accelerate acquisition. A total of 490 volumes were collected per run. A high-resolution T1-weighted anatomical image was also acquired using a 3D MPRAGE sequence (TR = 2300 ms, TE = 2.26 ms, inversion time = 900 ms, flip angle = 8°, total acquisition time = 5 min 21 s) with a 256 × 256 matrix over a 256 mm FOV, yielding a 1.0 mm^3 isotropic resolution across 192 sagittal slices. To correct for B0 field inhomogeneities, a gradient

echo field map was acquired using a dual-echo sequence with TR = 566 ms, TE1 = 4.92 ms, TE2 = 7.38 ms, flip angle = 60°, and total acquisition time = 1 min 51 s with the same geometry and resolution as the functional images (2.5 × 2.5 × 3.0 mm^3 voxels, 54 axial slices, FOV = 240 mm). The field map was used during preprocessing to improve spatial accuracy and reduce distortion in the EPI data.

3.3.5 Preprocessing

Data were converted to NIFTI format using NITRC MRIcroGL, then they were preprocessed and analyzed using the FMRIB Software Library (FSL) (Jenkinson et al., 2012). The first three volumes of each scan were omitted to avoid T1 saturation effects. We used high-pass temporal filtering to remove low-frequency artifacts, applied spatial smoothing with a kernel size of 6.0 mm, and performed an interleaved slice scan time correction. We motion-corrected each functional run using MCFLIRT, which applied a rigid-body transformation to correct for motion artifacts (Jenkinson et al., 2002). Volumes that showed abrupt head movements over 0.9 mm were marked as outliers and regressed out (Siegel et al., 2014). Runs with 10% of volumes marked as outliers were excluded from further analysis. Functional acquisitions were coregistered to anatomical images using the Brain-Boundary Registration in the Montreal Neurological Institute (MNI152) standard space (Mazziotta et al., 1995). To confirm their compliance with the task and ensure that they were comfortable in a tight space, participants performed practice trials in an MRI simulator before the data collection session. Participants' movements and adherence to the instructions were monitored offline. Trials were excluded from further analysis if participants did not move on time, skipped a trial, or if the experimenter's hand was visible during the trial.

3.3.6 Graph Theoretical Analysis

Since the brain is fundamentally relational, it can therefore be viewed as a network that shares information to achieve various goals and can even be considered beyond its physical connections, based on its functionality (Biswal et al., 1995; Friston, 1994). These considerations have led to the development of functional connectivity analysis and the use of mathematical approaches such as graph theoretical analysis (GTA), which represent the brain as a graph with a set of nodes (vertices) that are linked (edges) (Fig. 3.2 A, E) (Bullmore & Sporns, 2009; Farahani et al., 2019).

To achieve this graph representation of our network, we created 6 mm diameter spheres on FSLeyes for our 200 cortical regions of interest (ROIs) and 32 cerebellar ROIs. These coordinates

were identified using Yeo's 17-network atlas with a 200-node cortical parcellation and a 32-node cerebellar parcellation (Nettekoven et al., 2024; Schaefer et al., 2018). Considering both cortical and subcortical regions provides a comprehensive assessment of their implications in motor control, as the cerebellum is important for timing, prediction, and coordination (Bastian, 2006; Salman, 2002; Sokolov et al., 2017). The raw BOLD signals from these 232 spheres, for each run across all participants included in our analysis, were extracted to conduct graph-theoretical functional connectivity analysis (Fig. 3.2B). For these runs, we also obtained the event files, parameter estimates, and residuals for each region of interest to compute the contrast-reduced time series of our data. This approach was taken to remove elements irrelevant to our task (for example, the color of the fixation point), which might otherwise obscure our results (Musa et al., 2025; Luabeya et al., 2026). Because we intended to understand the difference between grasp and place, we extracted 17 volumes representing our events of interest for each trial in a run (Fig. 3.2C). During a trial, our 17 datapoints included the two volumes before the start of the trial and ran until the initial movement to the platform to grasp or place the object. Then, we correlated the extracted contrast-reduced time series of the nodes against each other for all the trials (Fig. 3.2D). The correlation outputs yielded 232 × 232 adjacency matrices. We computed their absolute values to confirm that we were limiting our analysis to the amplitude of the correlations, not their directionality (Ran et al., 2020). We calculated the grand average across all trials to create one undirected weighted adjacency matrix per condition. Each value in the matrix represents the strength of the functional connection 'edge' between two nodes (Fig. 3.2E).

Network analysis using GTA can be understood at three different levels: 1) a macro/global scale, which views the entire network as one conglomerate system, 2) a meso/intermediate scale, which looks at the subnetwork that forms communities in the system, 3) a micro/local scale, which identifies the individual nodes leading the communication in the network. At the global level, the *clustering coefficient* assesses the network's ability to facilitate the formation of highly connected subnetwork cliques to optimize information sharing; the *global efficiency* quantifies how effectively the network exchanges information; and the *energy* estimates the stability of network synchronization (Demaine et al., 2006; Ghaderi et al., 2020; Latora & Marchiori, 2001; Rubinov & Sporns, 2010). Overall, these measures allow one to evaluate the integration and segregation of the network as a whole unit. At the meso-scale, to maximize communication efficiency and reduce the effort required to share information, the brain uses a small-world organization, where nodes

are grouped into smaller communities with greater communication (Newman, 2006; Sporns & Betzel, 2016). The modularity analysis allows the identification of these communities (modules) with high connectivity within the subnetwork rather than across subnetworks (Fig. 3.2F). These communities reveal how our network segregates functionally to achieve a more effective information flow (Latora & Marchiori, 2001). At the local scale, to identify which nodes are particularly important for communication within and between modules, we computed two centrality measures (eigenvector centrality and betweenness centrality; Fig 3.2G). For this purpose, and to quantify the quality of our module, we combined the trial-by-trial adjacency matrices for each participant, yielding a unique averaged adjacency matrix for each condition. We then computed eigenvector centrality to identify local hubs within modules and betweenness centrality to identify global hubs driving communication across modules (Bonacich, 2007; Freeman, 1977).

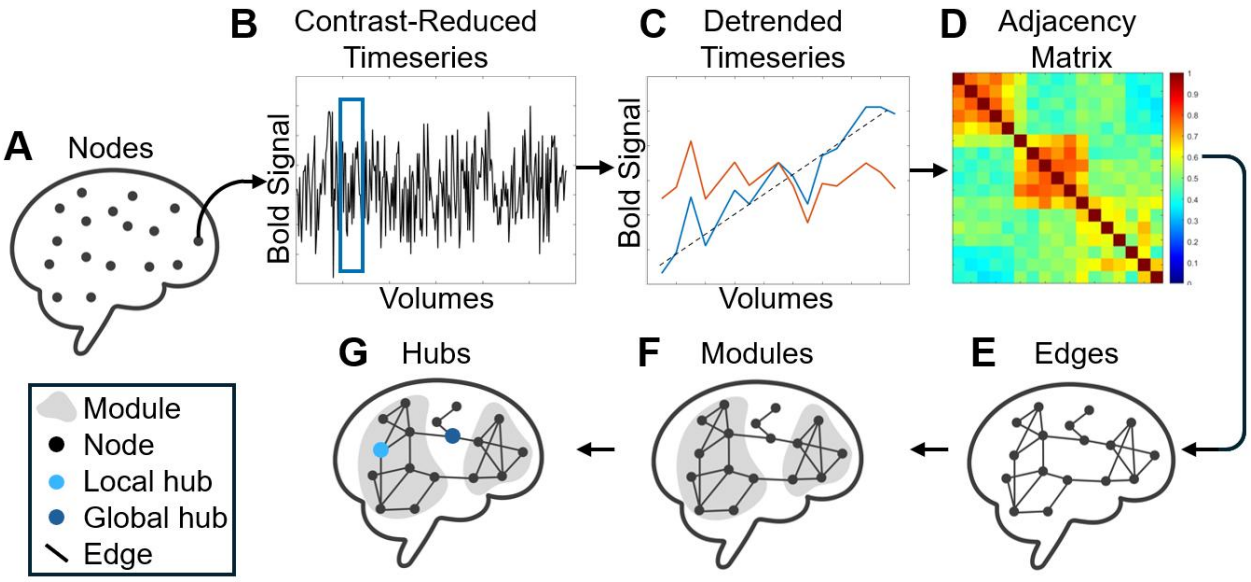


Figure 3.2. Illustration of the graph theoretical pipeline. A) Sagittal view of the brain with its set of nodes representing the different regions of interest (ROIs) from where functional data are collected. B) BOLD signal contrast-reduced timeseries is computed from an entire run for each node. Blue box corresponds to one trial extracted. C) The blue line depicts the contrast-reduced timeseries from each trial (spanning from the end of the intertrial period prior to the trial to the end of the *execution* phase); the dashed line represents its line trend, which is removed by applying a detrending algorithm. The detrended timeseries is presented in red. D) Adjacency matrix comprising the absolute value of the correlation of all the nodes in our network. These matrices are used to compute GTA measures. Blue shows nodes of low correlation, and red shows nodes of high correlation. E) The connection between the different nodes is represented by 'edges', the lines linking the different nodes. F) Grey areas represent the modules formed in

the network. They are groups of nodes with stronger connectivity within the modules than outside the modules. G) Represents nodes of particular importance. There are eigenvector centrality hubs, which have a node with a strong connection to other highly connected nodes in blue, and betweenness centrality hubs, which serve as bridges connecting different clusters of nodes in red.

Then, centrality measurements were computed on these matrices using the Brain Connectivity Toolbox (Rubinov & Sporns, 2010). We assessed the modularity score of each module by calculating Newman's Modularity (Q) using an open-access 'MODU' function (Ghaderi et al., 2020, 2025; Newman, 2006).

Sensorimotor studies have often reported a "buildup" or ramping of BOLD activation over time during a trial. Musa and colleagues (2025) have shown that detrending (removing the linear trend present in the data) reduces long-range communication and focuses more on local processes (Fig. 3.2C). We wanted to use a similar approach to investigate how the formation of modules might be impacted by the absence of 'global communication'. Therefore, we also computed the modularity analysis in this detrended time series.

3.3.7 Statistical Analyses

3.3.7.1 Univariate Analysis

Data analyses were performed using the general linear model conducted on FSL FEAT (version 6.00). Each run was modeled using a voxelwise GLM, with each predictor derived from a boxcar wave function convolved with FSL's canonical double-gamma hemodynamic response function, and temporal derivatives included to account for variability in response timing. For runs that were not completely excluded from further analysis but contained behavioural errors (e.g., hand movement during the *planning* phase), we included a predictor to regress out these trials (corresponding to 36 trials in total). We modeled our predictors using these two time periods (*planning* and *execution* phases) based on movement type (*grasp* or *place*), resulting in a total of four predictors of interest: Planning-Grasp, Planning-Place, Execution-Grasp, and Execution-Place. We then used a fixed-effect model to combine the valid runs within subjects. Finally, we used a non-parametric permutation test with 5000 permutations to conduct group analysis. We applied FSL randomise with a Threshold-Free Cluster Enhanced (TFCE) approach to correct for multiple comparisons and produced a Family-Wise Error corrected p-value < 0.05 (Worsley, 2001). We compared them to the intertrial interval, which served as the baseline for identifying brain areas that showed increased activation during the *planning* and *execution* phases. After performing the

permutation test for our two conditions to specify areas with conjoined increases in activity, we identified the minimum significant cluster size and used the largest cluster size to define significant joint activation in their intersection map for *planning* and *execution* phases. We also contrasted *grasp* and *place* during the two phases to identify regions that showed increased activity specific to the movement type.

3.3.7.2 Regions-of-Interest and Classification Analyses

Region-of-interest (ROI) analysis was conducted across seven action-related areas in the left hemisphere, as all movements were performed with the right hand, using RStudio 2024.12.1. These regions included the primary visual cortex (V1), posterior intraparietal cortex (pIPS), anterior intraparietal cortex (aIPS), primary sensory cortex (S1), primary motor cortex (M1), ventral premotor cortex (PMv), and dorsal premotor cortex (PMd). Their coordinates were identified from the neurosynth.org meta-analysis using the keywords grasping and reaching, and V1 coordinates were defined from previous grasping work (Monaco et al., 2020), which were converted to MNI space using seed-based d mapping (smproject.com) according to Lancaster and colleagues (2007). For each ROI, the parameter estimate values were extracted and averaged from a 6 mm radius sphere around the centroid coordinates. We extracted parameter estimates for the four predictors (Planning Grasp, Planning Place, Execution Grasp, and Execution Place) across the 7 ROIs to assess their ability to dissociate between grasp and place in a classification analysis. We conducted t-tests to compare the beta weight in our two conditions (*grasp* vs *place*) and used false discovery rate (FDR: q) to correct for multiple comparisons.

Afterward, we attempted to identify how well these regions can dissociate between our two main conditions. We conducted trial-by-trial extraction of the beta weight for each ROI after z-normalizing its 3D image to remove run-specific amplitude differences. We removed outliers relative to the mean, resulting in a total of 122 voxels per ROI per trial to feed the same number of voxels to our classifier. We applied them in a supervised classification analysis using MATLAB's Classifier Learner app, which evaluates different algorithms to identify the most efficient approach for distinguishing between our two conditions. To confirm that the trained classifier could generalize to an untrained dataset, we used 10-fold cross-validation (Valente et al., 2021; Varoquaux et al., 2017; Weaverdyck et al., 2020). This machine learning approach is a robust resampling technique where the data is divided into 10 parts ('folds'), then trained on 9 folds and

tested on the last one. The step is repeated in 10 iterations so that each fold is tested at least once. Then, we used the Kruskal-Wallis algorithm to rank the importance of each feature introduced to the model in their classification effort, therefore providing a way to identify which ROIs and phases carried meaningful information to represent the movement type.

3.3.7.3 GTA Statistics

To understand how grasp and place information is shared functionally, we used the modularity function in the BCT toolbox at the standard resolution of 1 and assigned each node to a module. To statistically confirm that subnetworks are nonrandom modules whose modularity exceeds that expected under a null model, we created a randomized subnetwork of the same size. We then computed the mean log-transformed value of the normalized modularity score and applied it to a one-sample sign-flip permutation test (right-tailed with 50000 permutations). To compare our two conditions, we also conducted a nonparametric permutation t-test with 10000 randomizations for our modularity score and corrected for multiple comparisons using a false discovery rate (FDR: q) (Luabeya et al., 2026; Tomou et al., 2025). We calculated our centrality measures for the unmodified *grasp* and *place* conditions to determine which nodes serve as hubs that lead intra- (eigenvector centrality) and inter-module (betweenness centrality) communication. To identify reliable hubs and avoid circular analysis, the centrality data were split into two groups. The first subset selected candidate hubs, defined as nodes with centrality measures at or above the 95th percentile. The second subset was tested for significance by conducting a one-sample sign-flip permutation test, comparing the real centrality dataset to null models and generating centrality scores. To increase stability in our analysis, we applied split-half validation with 100 iterations and defined hubs as nodes that were reliably selected as part of the 95th percentile and identified as statistically significant compared to null in at least 60 of the 100 validation iterations.

3.4 Results

The aim of this study was to compare and contrast brain activity and functional connectivity during *grasping* versus *placing* movements. We first performed a voxelwise univariate analysis to identify brain regions that showed overlapping or different activation between conditions at the whole-brain level. Next, we conducted a region-of-interest (ROI) analysis to focus on specific cortical areas previously implicated in object-directed actions, providing more targeted insights into task-related activity patterns. We then applied a decoding classifier to determine whether the observed activity patterns could reliably distinguish between *grasp* and *place* movements, providing a data-

driven validation of task-specific neural signatures. Finally, we performed a GTA functional connectivity analysis to investigate how the brain organizes itself functionally to execute our two action types, using both original and detrended datasets (Fig. 3.2C). All brain networks were visualized using BrainNet Viewer (Xia et al., 2013).

3.4.1 Univariate Analysis

General Activation during Planning Phase. To identify general *planning* activity across our two tasks, we computed increases in BOLD activation relative to baseline for *grasp* (Fig. 3.3 A), for *place* (Fig. 3.3 B) and their conjunction (Fig. 3.3 C) with $P_{FWE} < 0.05$. We observed a widespread bilateral increase in activity for both *Grasp* and *Place* tasks, as confirmed in the conjunction analysis (Fig. 3.3 C). This included Prefrontal Cortex (PFC), Superior Frontal Gyrus (SFG), insula, cingulate cortex, Supplementary Motor Area (SMA), Superior Temporal Gyrus (STG), Inferior Parietal Lobule (IPL), Middle Temporal Gyrus (MTG), and Early Visual Cortex (EVC). However, left PMd, M1, and S1 showed a significant increase in activity for *Place* that was not observed in *Grasp* or conjunction analysis. During *planning,* the cerebellar vermis (VI-X) and the left cerebellar lobules (I-VI, VIIb, IX, Crus I, Crus II) showed increased activation for both *Grasp* and *Place*; whereas the right cerebellum showed a smaller overlapping activation in the right lobules (VI and Crus I). Overall, our two conditions shared many similarities across the cortex and cerebellum, but also hinted at differences that we will focus on further below.

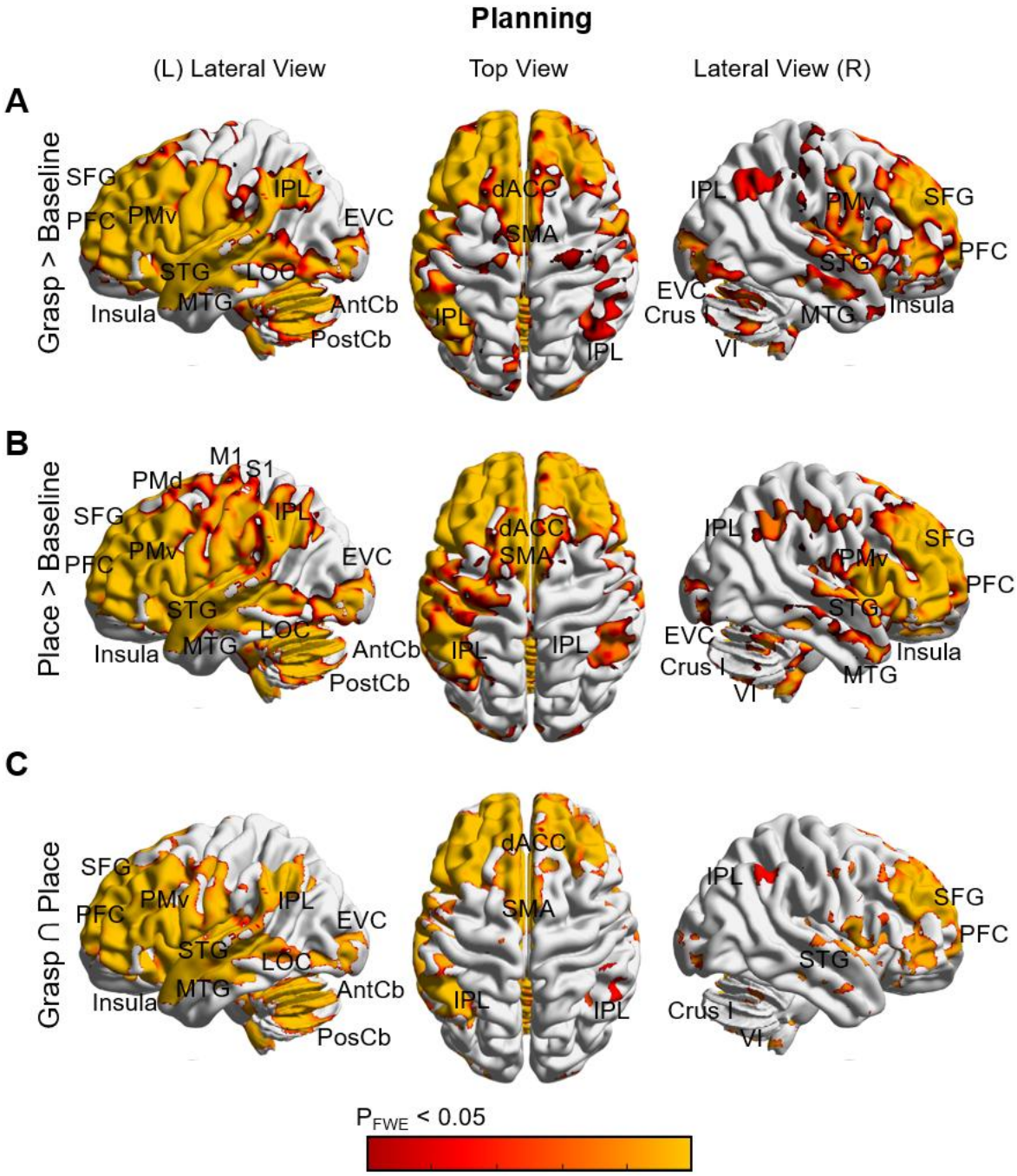


Figure 3.3. Cortical activation maps for the *Grasp* (A), *Place (B) conditions, and their conjunction* (C) during the *planning* phase. Color bars indicate statistical intensity from a non-parametric permutation test with 5000 permutations (with a $P_{FWE} < 0.05$). Warmer colors indicate greater activation than baseline. Lateral and medial views of both hemispheres are shown for each condition. Abbreviations: dACC: dorsal anterior cingulate cortex, EVC: Early visual cortex, LOC: Lateral occipital cortex, M1: Primary motor cortex, MTG: Middle temporal gyrus, PFC: Prefrontal cortex, PMd: Dorsal premotor cortex, PMv: Ventral premotor cortex, IPL: Inferior parietal lobule, S1: Primary somatosensory cortex, SFG: Superior frontal gyrus, SMA:

Supplementary motor area, SPOC: Superior parieto-occipital cortex, STG: Superior temporal gyrus, AntCb: Anterior cerebellar lobe, PostCb: Posterior cerebellar lobe.

General Activation during Execution Phase. Again, we computed increases in activity relative to baseline for *Grasp* (Fig. 3.4 A), *Place* (Fig. 3.4 B) and their conjunction (Fig. 3.4 C) (for $P_{FWE} < 0.05$) to identify similarities and differences during *execution* phase. We observed a widespread bilateral increase in activity for *grasp* and *place* (confirmed in the conjunction) in the S1, PMd, PMv, SMA, Superior Parietal Lobule (SPL), SPOC, LOC, insula, and cingulate cortex. In addition, we found lateralization with greater activity in left M1 (i.e., opposite hemisphere to the hand used). In the cerebellum, there were wide bilateral activations in the anterior lobules (I-V), the posterior lobules (VI-X, Crus I and II) for both *grasp* and *place*. Overall, outside of the sensorimotor cortex, activation was more lateralized during the *planning* phase and bilateral during the *execution*. Furthermore, there was less frontal activation but more sensorimotor activation during the *execution* phase.

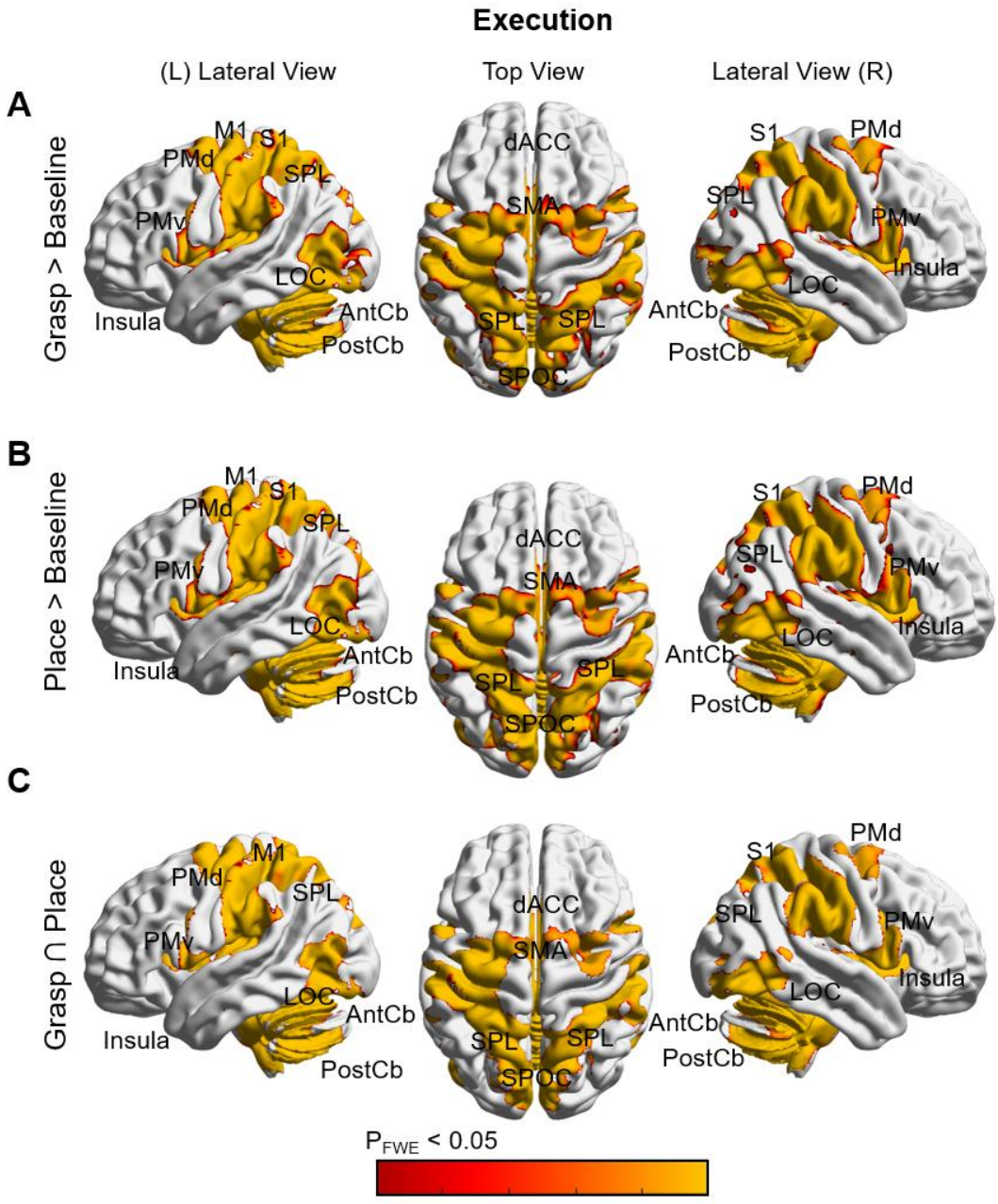


Figure 3.4. Cortical activation maps for the Grasp (A), *Place (B) conditions, and their conjunction* (C) during the *execution* phase. Color bars indicate statistical intensity from a non-parametric permutation test with 5000 permutations (with a $P_{FWE} < 0.05$). Warmer colors indicate greater activation than baseline. Lateral and medial views of both hemispheres are shown for each condition. Abbreviations: dACC: dorsal anterior cingulate cortex, EVC: Early visual cortex, LOC: Lateral occipital cortex, M1: Primary motor cortex, MTG: Middle temporal gyrus, PMd: Dorsal premotor cortex, PMv: Ventral premotor cortex, SPL: Superior parietal lobule, S1: Primary somatosensory cortex, SMA: Supplementary motor area, SPOC: Superior parieto-occipital cortex, AntCb: Anterior cerebellar lobe, PostCb: Posterior cerebellar lobe.

Differences Between Reach and Place Activity. To directly distinguish task-specific activity, we performed a Grasp vs Place contrast across the two task epochs. During the *planning* phase, there was a significant increase in the left lingual gyrus for the *grasp* condition, and two cerebellar locations for *place*: Right lobule VIIIa and Right lobule V (Fig. 3.5A). During the *execution* phase, there were task-specific increases in activation for *placement* in the left and right occipital cuneus, occipital fusiform gyrus and lingual gyrus (Fig. 3.5B). The cerebellum showed bilateral *place*-related preference in the spinocerebellum (lobules I-X and Crus II) and the cerebrocerebellum (lobules I-IX). These findings suggest that grasp and place exhibit regional specialization, which we explore further in the next section.

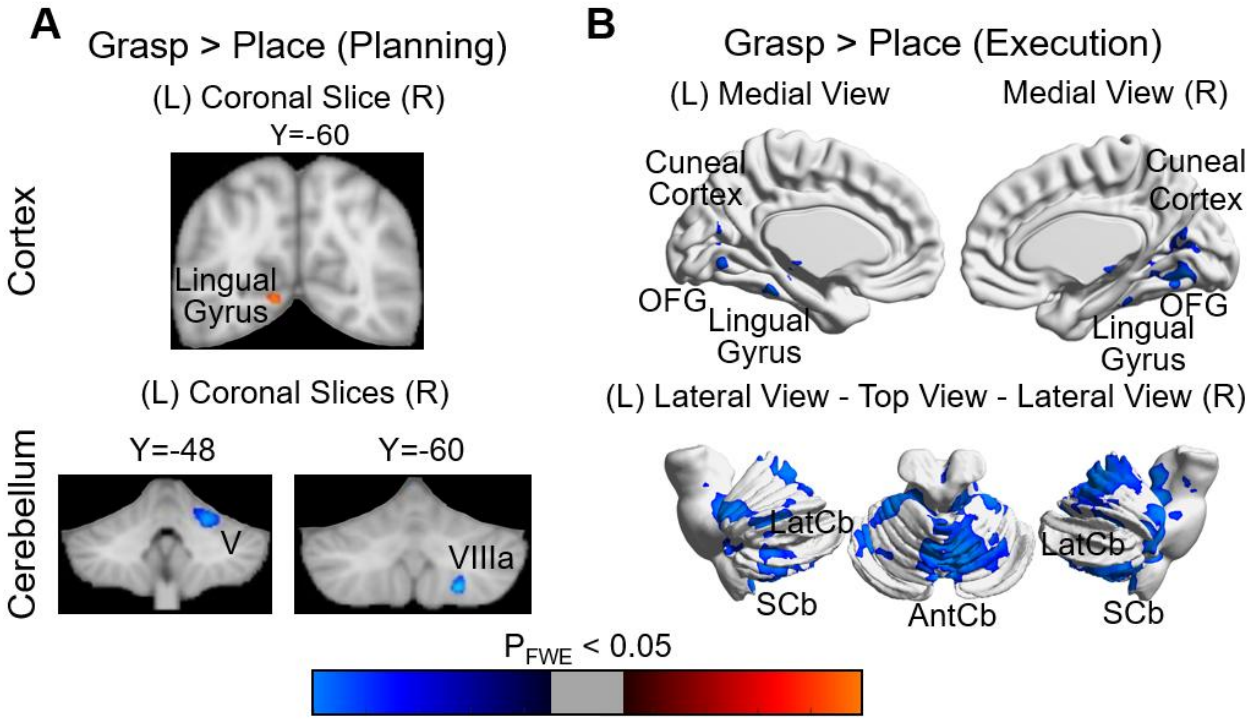


Figure 3.5. Cortical activation maps for the *Grasp* vs *Place* comparison during the *planning* phase (A) and the *execution* phase (B). Color bars indicate statistical intensity. Color bars indicate statistical intensity from a non-parametric permutation test with 5000 permutations (with a $P_{FWE} < 0.05$). Cool colors represent a significantly greater activation for *Place*, and warm colors depict a significantly greater activation for *Grasp*. The top row shows cortical activation from a coronal slice ($Y_{MNI} = -60$) during *planning* and the bilateral medial views during *execution*. The bottom row shows cerebellar activation from two coronal slices ($Y_{MNI} = -48$ and $Y_{MNI} = -60$) during *planning* and the lateral and top views during the *execution*. Abbreviations: OFG: Occipital Fusiform Gyrus, AntCb: Anterior lobe of cerebellum, V: Cerebellar Lobule V, VIIIa: Cerebellar Lobule VIIIa, LatCb: Lateral cerebellum (cerebrocerebellum), SCb: Spinocerebellum.

3.4.2 Region of Interest Analysis

To examine task-related brain activity within known action-related areas, we conducted paired-sample t-tests on β weights extracted from 7 ROIs in the left hemisphere to compare *grasp* and *place*. During the *planning* phase (Fig. 3.6A), *placement* showed a significant increase compared to *grasp* in aIPS (mean difference = 0.071, t(19) = 2.400, q = 0.026), S1 (mean difference = 0.044, t(19) = 3.129, q = 0.005), M1 (mean difference = 0.049, t = 2.427, q = 0.025), and PMd (mean difference = 0.077, t(19) = 2.749, q = 0.013), but not in V1 (mean difference = 0.028, t(19) = 0.854, q = 0.434), pIPS (mean difference = 0.013, t(19) = 0.925, q = 0.434), and PMv (mean difference = 0.015, t(19) = 0.798, q = 0.434). None of the seven ROIs showed significant task modulations during the *execution* phase (Fig. 3.6B) after false discovery rate (q > 0.05).

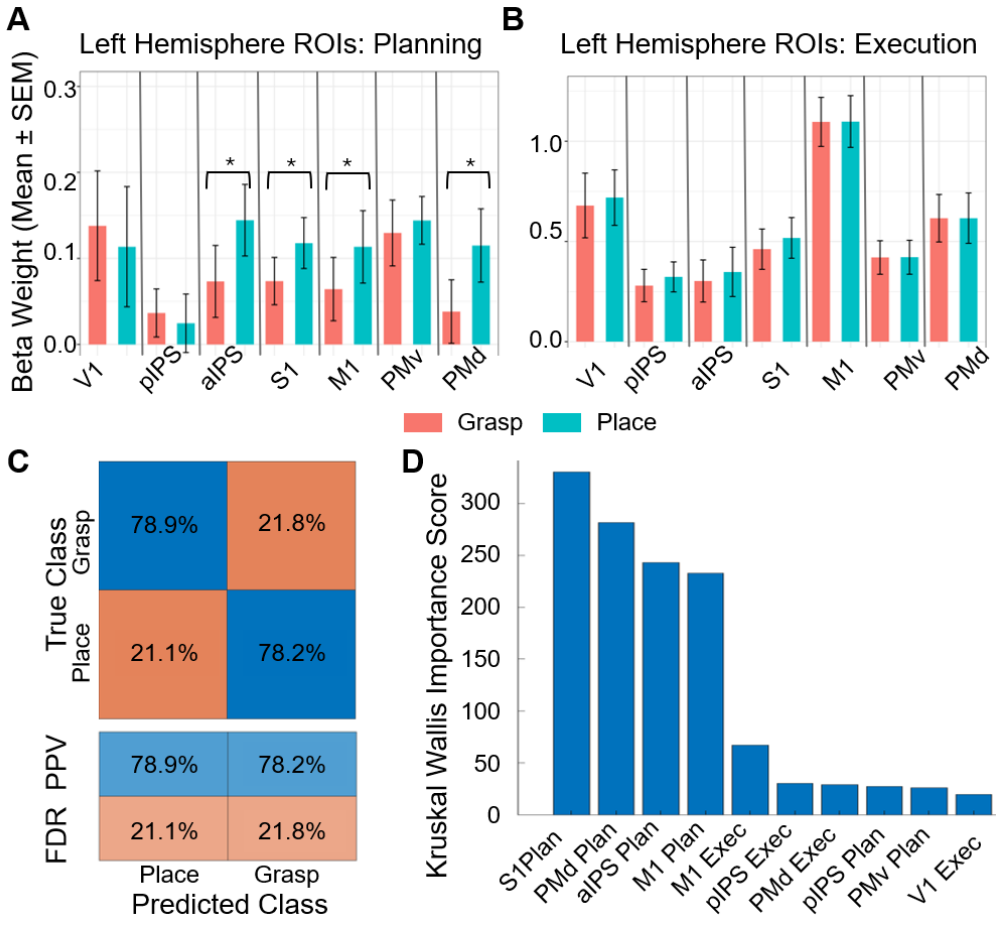


Figure 3.6. Bar graphs of the beta weights from 7 ROIs in the left hemisphere during the *planning* phase (A) and the *execution* phase (B). Asterisks show the significant difference between *grasp* and *place* at p < 0.05 after FDR correction. C) Multivoxel Classifier Analysis represents the performance of the k-Nearest Neighbor algorithm to differentiate between *Grasp* and *Place*. The top table panel displays the confusion matrix, comparing the predicted data point

identity (*grasp* or *place*) with its true identity. The bottom panel table shows the positive predictive values (PPV) and false discovery rates (FDR) of the *Grasp* data (left column) and the *Place* data (right column). D) The Kruskal-Wallis importance scores of the ROIs and time period (Plan = *planning* phase, Exec = *execution* phase) to classify between *grasp* and *place*.

3.4.3 Classification Analysis

We used classifier models to see whether these action-related regions of interest (Fig. 3.6A) could differentiate between *grasp* and *place*. Among the models tested, the weighted K-Nearest Neighbors (KNN) achieved the highest accuracy of 78.53% in distinguishing between *grasp* and *place* during 10-fold cross-validation. KNN is a supervised algorithm that classifies based on its proximal neighbors, placing greater emphasis (weight) on the closest neighbors (Ghaderi et al., 2023). Outperforming the traditional Support Vector Machine (SVM) algorithm, as weighted KNN is less affected by outliers, and is more suitable for complex, flexible data. The classification performance was summarized in our confusion matrix, which shows the distribution of true and predicted class labels (Fig. 3.6C). The true class reflects class-specific sensitivity, and the predicted class reports the positive predictive value (PPV) and the false discovery rate (FDR). The model achieved a PPV of 78.9% (95% Confidence interval (CI) [78.3 – 79.5]) with an FDR of 21.1% (CI [20.5 – 21.7]) for the *Grasp* movement, and a PPV of 78.25% (CI [77.6 – 78.8]) with an FDR of 21.8% (CI [21.3 – 22.4]) for the *Place* movement. The Kruskal-Wallis (KW) feature selection analysis revealed that the information obtained during the *planning* phase from S1 (KW score = 330.67), PMd (KW score = 281.70), aIPS (KW score = 243.10), and M1 (KW score = 232.68) ranked as the most informative in order to distinguish between *grasp* and *place* at an Importance Score greater than 100 (Fig. 3.6D).

3.4.4 Graph Theory Analysis

To compare functional connectivity in our two tasks at the whole brain level, we used a graph-theoretical analysis (GTA) approach and correlated the contrast-reduced time series of our 232 cortico-cerebellar nodes (Fig. 3.2). We did not find any significant difference between commonly used global parameters (Clustering Coefficient, Global Efficiency and Energy) for the reach vs. placement networks (Supplementary Fig. 3.1), so we instead focused on the mesoscale and local aspects of functional network organization. We also examined the influence of detrending the data (Fig. 3.2C), which has been shown to reduce large-scale signal correlations (Musa et al., 2025).

Modularity Analysis: Original Data. To understand the mesoscale properties of these networks, we conducted a modularity analysis, which grouped our nodes into modules/subnetworks, with higher connectivity within modules than across modules (Fig. 3.7A-B). We identified three modules in the original *grasp* and *place* conditions: a Cerebello-Occipito-Parietal Module (Module 1: red), a Prefrontal Module (Module 2: blue), and a Sensorimotor Module (Module 3: purple). For the original (unmodified) time series, the node assignments were identical between *grasp* and *place*.

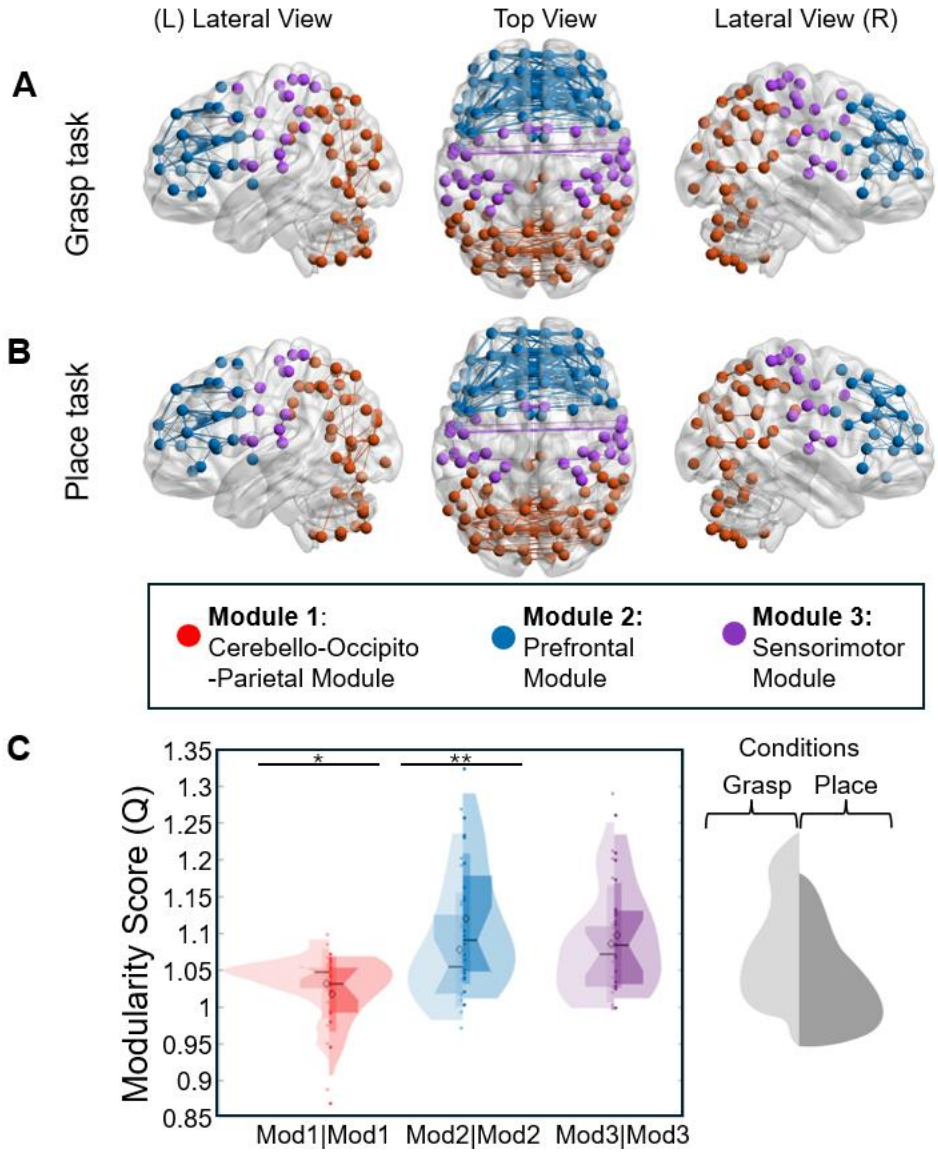


Figure 3.7. Trend unmodified network modularity analysis. A) represents the three module groupings for the *grasp* task. B) represents the three module groupings for the *place* task. C) Violin plots of the Modularity score of each module from the networks. The *Grasp*'s modules are

presented in the lighter colors to the left and the *Place*'s modules are presented in the darker colors to the right (Mod = Module). Modules are color-coded: Cerebello-Occipito-Parietal Module (Module 1) in red, the Prefrontal Module (Module 2) in blue and Sensorimotor (Module 3) in purple. The FDR-corrected significant differences between conditions are indicated by asterisks with *: $p < 0.05$, **: $p < 0.01$, and ***: $p < 0.001$.

We then used the modularity score to quantify how strong the communities were compared to a random subnetwork of the same size and whether their community strengths differed depending on the task executed (Fig. 3.7C). We found that all three modules performed better than a null model for the *grasp* condition (Module 1 q = 0.0062, Module 2 q = 5.90E-5, Module 3 q = 5.90E-5). However, only two of the three modules had scores significantly greater than the null model for the *place* condition (Module 1: q = 0.0866; Module 2: q = 2.99E-5; Module 3: q = 2.99E-5).

When the modules are compared based on condition (Fig. 3.7C), we found that Module 1 and Module 2 showed a significant difference, with *grasp* having a higher modularity score than *place* for Module 1 ($t(19) = 2.7395$, q = 0.0139) and inversely, *place* having a higher modularity score than *grasp* in Module 2 ($t(19) = -3.6379$, q = 0.0045), whereas Module 3 did not show a significant difference in modularity score ($t(19) = -0.9754$, q = 0.3447). Overall, the data suggest that *grasp* and *place* are grouped into three similar 'real' nonrandom modules in the network, where the sensorimotor module was task-independent, the Cerebello-Occipito-Parietal module showed a higher modularity score for *grasp*, and the Prefrontal module showed a higher score for *placement*.

Modularity Analysis: Detrended Data. To assess how the general increase in BOLD response influences modularity, we computed the modularity score in datasets with detrended contrast-reduced time series. After detrending, the nodes were grouped into three modules for the *grasp* condition (Fig. 3.8A), similar to those for the original dataset. When tested against a null model, their modularity scores remained significantly higher than chance (Module 1 q = 0.0069, Module 2 q = 1.20E-4, Module 3 q = 5.99E-5).

In contrast, the nodes in the *place* condition were grouped into four modules (Fig. 3.8B): an Occipito-Parietal Module (Module 1A in dark red), a Cerebellar Module (Module 1B in yellow), a Prefrontal Module (Module 2 in blue), and a Sensorimotor Module (Module 3 in red). When tested against a null model, only three of these modules were considered to be nonrandom (Module 1A q = 2.666E-5, Module 1B q = 0.9625, Module 2 q = 2.666E-5, Module 3 q = 2.666E-5). These

data suggest that, after detrending, the network's integrative behaviour decreases in the *place* condition relative to the *grasp* condition.

To quantify these differences, we again computed modularity scores (Fig. 3.8C). Compared to Module 1 (*Grasp*), Module 1A (*Place*) showed a significant increase in modularity for the *place* condition ($t(19) = -6.7144$, $q = 1.998E\text{-}4$), whereas Module 1 (*Grasp*) compared with Module 1 B showed a lower modularity score ($t(19) = 5.294$, $q = 1.998E\text{-}4$). Module 2 still showed a significant increase in its modularity strength for *place* in comparison to *grasp* ($t(19) = -3.4168$, $q = 0.0027$), and Module 3 did not have a significant difference between *grasp* and *place* ($t(19) = -1.387$, $q = 0.1871$). These results suggest that removing the global trend amplifies the differences between the *grasp* and *place* networks.

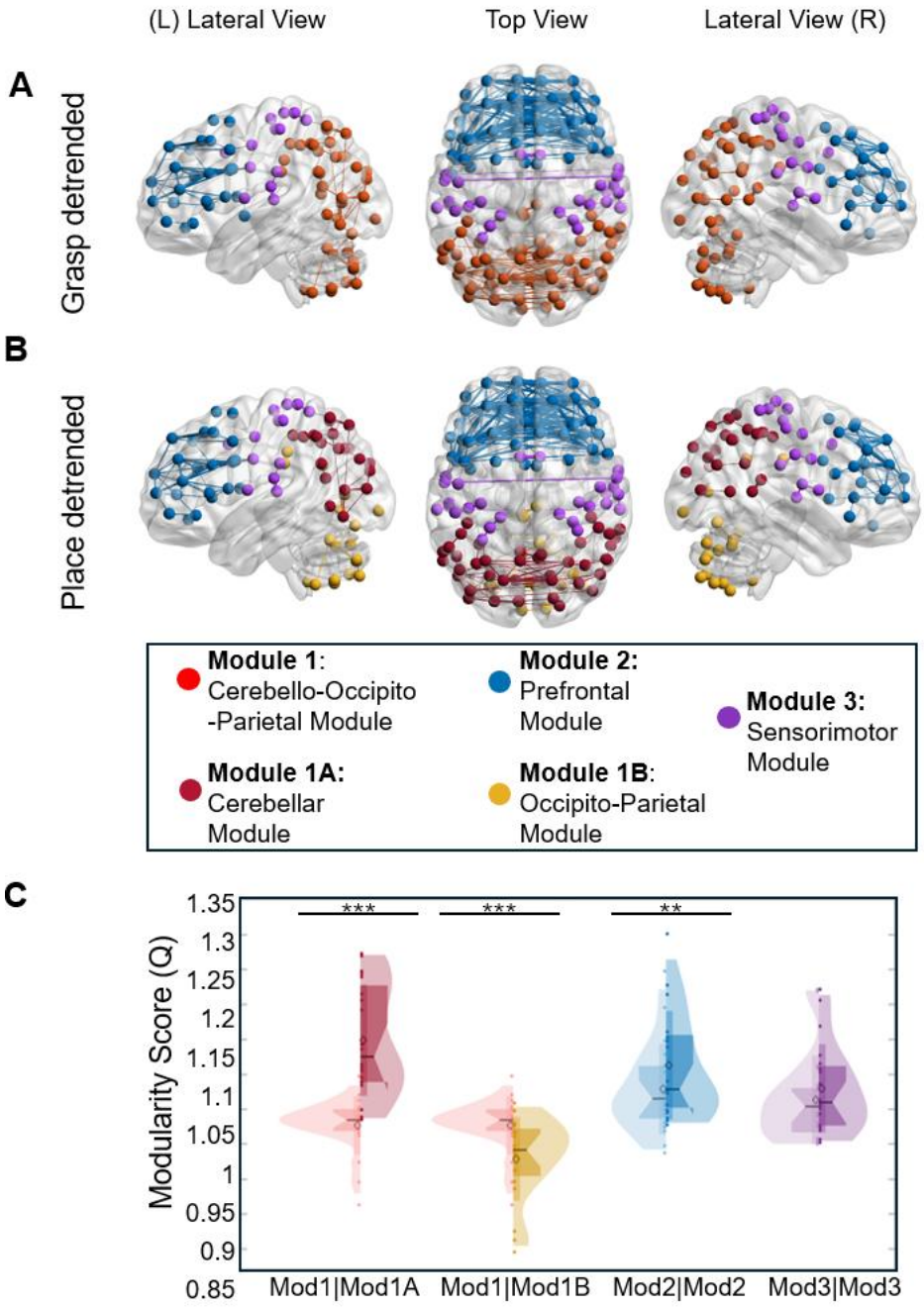


Figure 3.8. Detrended Network modularity analysis for the *Grasp* and *Place* conditions. A) represents the three module groupings for the *grasp* task. B) represents the four module groupings for the place *grasp* task. C) Violin plots of the Modularity score of each module from the networks. The *Grasp* modules are presented in the lighter colors to the left and the *Place* modules are presented in the darker colors to the right (Mod = Module). Modules are color-coded: Cerebello-Occipito-Parietal Module (Module 1) in red, Prefrontal Module (Module 2) in blue and Sensorimotor (Module 3) in purple for the *grasp* side, and Cerebellum Module (Module 1A) in burgundy, Occipito-Parietal Module (Module 1B) in yellow, Prefrontal Module (Module 2) in blue and Sensorimotor (Module 3) in purple for the *place* side. The FDR-corrected

significant differences between conditions are indicated by asterisks with *: $p < 0.05$, **: $p < 0.01$, and ***: $p < 0.001$.

Network Hubs: Local vs. Global Connectivity. We used two centrality measures (eigenvector and betweenness) to identify hubs: nodes that are highly correlated with other highly correlated nodes, and nodes that served as important bridges connecting other pairs of nodes, respectively. To be qualified as hubs, our nodes had to 1) fall within the top 95th percentile of centrality measures among all nodes, and 2) show statistically significant higher centrality compared to the corresponding node in a null model. Therefore, the hubs are not derived from a direct comparison between our conditions but by contrasting them with randomized network configurations.

Eigenvector centrality was used to identify nodes that were highly correlated within a module (Fig. 3.9A-B). In the Grasp condition (Fig. 3.9A), we identified eight eigenvector hubs, with three hubs located in the Cerebello-Occipito-Parietal Module in the left hemisphere (Temporal Occipital Cortex (TempOcc), Extrastriate Visual Cortex (ExStr), and Cerebellum lobule VI), four nodes in the Prefrontal Module (two hubs in the right Dorsal Prefrontal Cortex (PFCd) and Lateral Prefrontal Cortex (PFCl) from both hemispheres), and one hub in the Sensorimotor Module (left dorsal anterior cingulate cortex (dACC)). The *Place* condition produced seven eigenvector hubs (Fig. 3.9B), located primarily in the Prefrontal Module (PFCd, PFCl, and medial posterior Prefrontal Cortex (PFCmp) in both hemispheres, and one left Occipital hub in the Cerebello-Occipito-Parietal Module (TempOcc). Overall, the Grasp and *Place* networks shared several hubs (TempOcc, PFCd, and PFCl), but the rest were distinct. Specifically, the grasp network had more occipital and cerebellar hubs (from Module 1), and the place network had more frontal hubs (from Module 2).

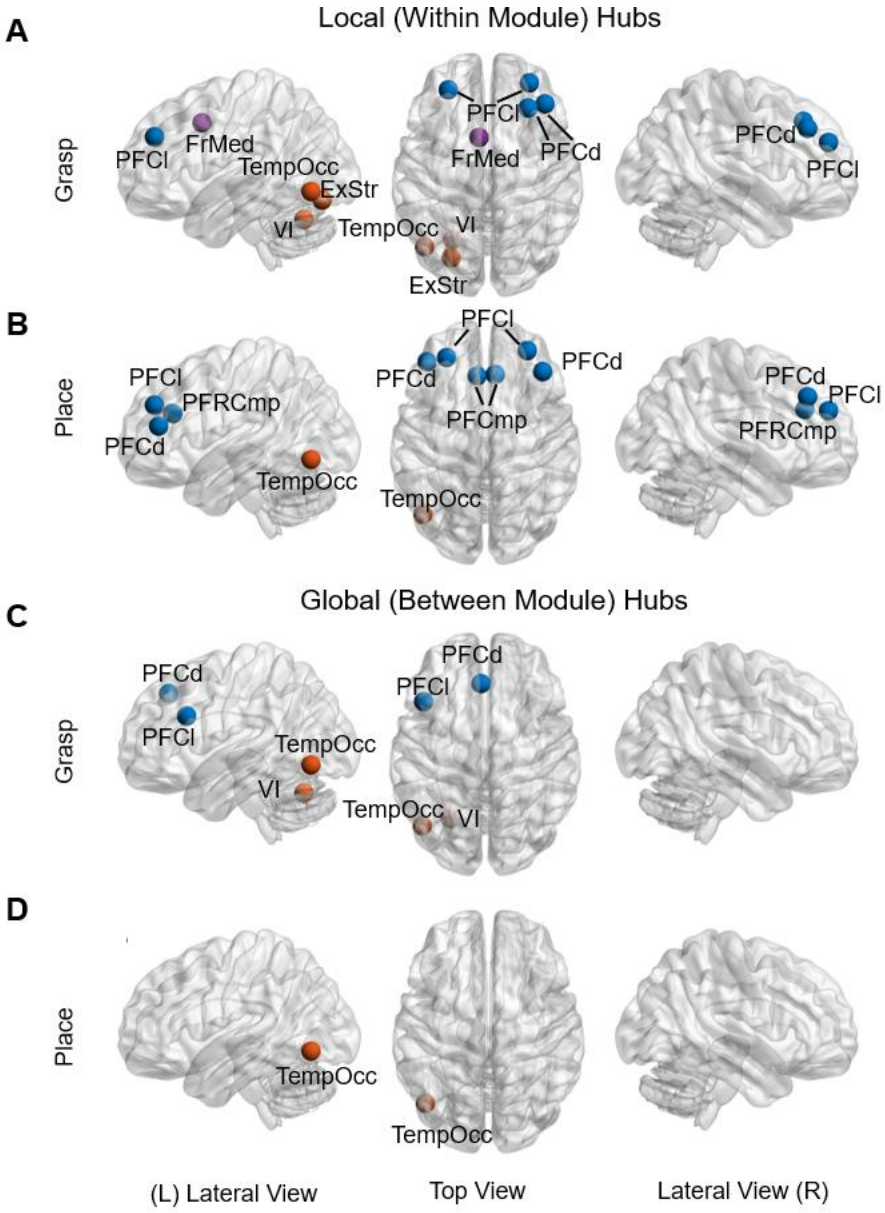


Figure 3.9. Brain maps showing local and global hubs for the *Grasp* and *Place* conditions. Hubs were defined as nodes at the 95th percentile or higher and were significantly different from null models at alpha < 0.05 FDR-corrected. Local hubs are calculated using the eigenvector centrality for *Grasp* (A) and for *Place* (B). Global hubs are calculated using the betweenness centrality for *Grasp* (C) and for *Place* (D). Blue nodes are part of the Prefrontal Module, and red nodes are part of the Cerebello-Occipito-Parietal Module. Abbreviations: ExStr: Extrastriate Visual Cortex, ParOcc: Parietal Occipital Cortex, PFCd: Dorsal Prefrontal Cortex, PFCl: Lateral Prefrontal Cortex, PFClv: Ventrolateral Prefrontal Cortex, PFCmp: medial posterior Prefrontal Cortex, TempOcc: Temporal Occipital Cortex, TempPole: Temporal Pole, VI: left Cerebellum, VIII: Left lobule VIII Cerebellum, Crus I: Left Crus I Cerebellum.

We used *betweenness* centrality to identify nodes that were highly correlated across modules. In the grasp network (Fig. 3.9C), we identified 2 global hubs in the Prefrontal Module (PFCd and PFCl in the left hemisphere) and 2 global hubs in the Cerebello-Occipito-Parietal Module (TempOcc and Cerebellum lobule VI in the left hemisphere). In contrast, the place network only had a global hub in left TempOcc, which is part of the Cerebello-Occipito-Parietal Module (Fig. 3.9D). Overall, *grasp* and *place* share a unique global hub in the temporal occipital cortex, but *grasp* had a greater number of nodes identified as hubs.

3.5 Discussion

Previous studies of movement control have largely focused on the initial act of prehension (i.e., Desmurget et al., 1996; Grafton, 2010; Karl & Whishaw, 2013), but less is known about the object placement that is often the ultimate goal of the interaction. In particular, it is not known how the intention to reach or place, and the resulting differences in sensory feedback, influence cerebello-cortical activation and functional networks. To address these questions, we conducted an alternating reach-to-grasp and reach-to-place experiment, compared the associated BOLD activation at the whole brain and ROI levels, used the latter to decode task type, and investigated functional connectivity metrics using GTA. Given that both actions involved the same objects and transport kinematics, we expected to see an overlap in the brain regions activated, but hypothesized that differences in the pattern of brain activity and cerebello-cortical functional connectivity would emerge due to the differences in intention and sensory feedback. Our results confirm that different structures were recruited (especially in the cerebellum), that action-related ROIs were modulated by task, and that functional network modularity was task-dependent.

3.5.1 Univariate BOLD Analysis during Planning and Execution

To understand the relationship between grasp and placement control, we first performed a whole-brain analysis across movement preparation and execution. In the following sections, we consider first their commonalities, then their differences.

3.5.1.1 Common (Task-independent) Cortical and Subcortical Activation

Planning Phase. Our data show that *grasp* and *place* elicit a similar widespread increase in brain activation in preparation for action, primarily in the bilateral frontal, temporal, and occipital cortices, as well as in the left cerebellum, and in a specific parietal activation in the inferior parietal lobule. While extensive cortical activation during action planning has been reported in previous

work (Baltaretu et al., 2020; Cappadocia et al., 2017), we also observed extensive cerebellar activation. Consistent with ipsilateral (to the right hand) lateralization (Grodd et al., 2001; Mottolese et al., 2013), we observed activation in the right Crus I and lobule VI, which have been implicated in bridging higher-order planning and motor control (Chabrol et al., 2019; Gao et al., 2018; Koziol et al., 2014; Park et al., 2018; Sokolov et al., 2017; Wagner et al., 2019; Zhu et al., 2023). We also saw widespread left cerebellar activation linked to visuospatial processing (Starowicz-Filip et al., 2021), which was generally similar in both tasks.

Execution Phase. During movement, premotor cortex, SMA, SPL, SPOC, and LOC were recruited in both tasks, presumably to maintain movement goals and correct movement errors (Cappadocia et al., 2017; Filimon, 2010). Finally, there was extensive bilateral cerebellar involvement. This bilateral action could support communication between the left and right cerebellum, as visuospatial information is shared with the right hemisphere, which is then recruited for ipsilateral motor control. These findings represent general reach transport-driven commands, feedback, and adjustments that do not dissociate the specific movement type.

Furthermore, there is a general shift in activation between these two phases as one progresses from planning the action to its execution, with planning showing greater involvement of PFC and IPL, and execution showing greater recruitment of sensorimotor regions and SPL. This reflects a transition from conscious motor intention preparation, as the movement goals are taken into account, to the integration of somatosensory cues to achieve the motor output (Castiello et al., 2000; Desmurget & Sirigu, 2012; Gamberini et al., 2021). This temporal distinction could hint at a processing differentiation in the parietal cortex as the action is planned and executed.

3.5.1.2 Selective (Task-dependent) Cortical and Subcortical Activation

Planning Phase. A whole brain voxelwise '*grasp* vs *place'* contrast revealed an increase in activation in the left (occipital) lingual gyrus for *grasp* and two cerebellum regions (right lobule V and VIIIa) for *placement*. As part of the ventral stream, the lingual gyrus is thought to be involved in identifying objects' features required to perform the *grasp* (Kumral et al., 2025; Palejwala et al., 2021; Valyear & Culham, 2010). Respectively, cerebellar lobules V and VIIIa have been shown to implement visual working memory and the processing of proprioceptive information for motor control (Bhanpuri et al., 2013; Boisgontier & Swinnen, 2014; Brissenden et al., 2021; Rondi-Reig et al., 2014).

These placement-specific activations suggest a role of the cerebellum in processing visual information to compare the object to the template target's features for a placement-specific motor plan, also taking into account the body's position when holding the object (Boisgontier & Swinnen, 2014; Therrien & Bastian, 2015). Presumably, this involves thalamic connections linking the ipsilateral cerebellum to contralateral cortex (Spampinato et al., 2024; Therrien & Bastian, 2015).

Finally, we observed greater preparatory activation in primary motor and somatosensory cortex during placement (Fig. 3.6A). Previous studies have shown that somatomotor cortex activity can predict planned action (Ariani et al., 2022; Gale et al., 2021). Our work shows that this activity also predicts the action type. Participants held a block at the start of both tasks (see METHODS), so these differences cannot be due to passive sensory feedback, but reflect the attentional gating of that feedback (since the initial block was only relevant in the *place* task) and/or different movement intentions.

Execution Phase. During action, we observed a relative increase in BOLD response in occipital regions (cuneal cortex, lingual cortex, and occipital fusiform gyrus) and the cerebellum during *placement*. Increased occipital activation could reflect the more complex visual feedback required to exactly match block location and orientation to the template (Luabeya et al., 2024). This can also be viewed as comparing a target to a landmark, which is known to engage ventral occipital cortex (Chen et al., 2014; Musa et al., 2025). In contrast, our *grasp* task was more forgiving, i.e., grip variations could be corrected after contact with the object (Lederman & Wing, 2003; Lukos et al., 2007; Paulun et al., 2014; Rearick & Santello, 2002).

3.5.1.3 Region of Interest Analysis and Classification

Although our voxelwise analysis suggested task overlap across large areas of cortex, this does not preclude the possibility of more subtle modulations within this activation. To test this possibility, we performed an ROI analysis of several well-established areas for visually-guided action (Castiello & Begliomini, 2008; Culham et al., 2003; Culham & Kanwisher, 2001; Monaco et al., 2024). We did not find any differences during *execution*, but we found several significant task differences during the *planning* phase, with placement showing greater activation in aIPS, M1, S1, and PMd. Again, these differences might be accounted for by both the need to process somatosensory information from the block and more complex visuospatial relations in the *Place*

task. Finally, our classification analysis confirmed that activity in these regions differentiated between our *Grasp* vs. *Place* tasks, a result that may be relevant for the application of brain-machine interfaces for real-world reach-place sequences (Lebedev & Nicolelis, 2017; Nicolas-Alonso & Gomez-Gil, 2012).

Canonically, aIPS has been described as important for computing object features relevant to grasping (Frey et al., 2005; Rice et al., 2006). Indeed, compared with less fine-tuned actions, such as reaching or pointing, grasp exhibits greater activation in this parietal region. However, when it is contrasted with another action requiring a comparable level of motor precision, we found greater recruitment of aIPS for placement, demonstrating that aIPS is not an exclusively grasp-related region but carries object features relevant for dexterous motor control. Its greater activation during placement could reflect an increased need for fine-tuning, given its reduced tolerance for movement errors. Perhaps placing an object in a wider space, which does not require a highly precise movement, would not elicit such an increase in aIPS involvement, similar to the difference observed between performing a precision grasp on a small object and a power grasp on a larger object, which does not need the same intricacy in the movement (Cavina-Pratesi et al., 2018; Ehrsson et al., 2000). Therefore, aIPS involvement goes beyond a finger configuration for grasping; instead, it gathers object features relevant to precise maneuvering for successful object interactions.

3.5.2 Graph Theoretical Functional Connectivity Analysis

To understand the similarities and differences between grasp and placement at a functional network level, we used a graph theoretical approach. This allowed us to assess the distribution of correlated BOLD time series at three levels: global (macro-level), intermediate (meso-level), and local (micro-level). This analysis again revealed both functional similarities and differences between our two motor tasks, as discussed below.

3.5.2.1 Macro-scale Network Features: Equivalence of Global Parameters

At the macro-scale, global GTA parameters suggest that grasping and placing mechanisms share similar levels of information transfer efficiency, overall segregation, and synchrony. This may reflect the fact that in both cases the brain was in a similar 'motor control' state (Madole et al., 2023), related to the shared transport mechanisms discussed above. However, it could also be the

case that global measures are simply not sufficiently specific to distinguish between very similar behaviours (Di et al., 2013; Ghaderi et al., 2023; Luabeya et al., 2026; Musa et al., 2025).

3.5.2.2 Meso-scale Network Features: Similar Modules, Different Community Strengths

Our modularity analysis revealed the same subnetworks in both tasks: a cerebello-occipito-parietal module, a prefrontal module, and a sensorimotor module. This segregation likely reflects three major processes: 1) higher-order cognitive processes (such as the assimilation of the instruction into the motor plan in the prefrontal module), 2) incorporation of visuospatial cues into the motor plan through the cerebello-occipito-parietal module, and 3) action control in the sensorimotor module (Luabeya et al., 2026). We did not observe segregation of dorsal-ventral visual streams previously documented in a simple pointing task (Musa et al., 2025), possibly because the current tasks require greater processing of both object location and orientation information (Monaco et al., 2011, 2020; Velji-Ibrahim et al., 2022). Finally, the modularity scores of the sensorimotor module were similar in both tasks, likely because they both place high demands on somatomotor cortex.

However, the modularity scores of the other two modules showed significant task differences (Fig. 3.7). G*rasp* showed higher modularity in the cerebello-occipital-parietal module, whereas *place* showed higher modularity in the prefrontal module. This suggests that the prefrontal module had less functional connectivity with other modules in the place task. This shift in neural topology demonstrates selective task-specific intra-module strengthening (Finc et al., 2026) and is consistent with the lack of prefrontal 'betweenness hubs' in this task (see the next section). Conversely, this suggests that the cerebello-occipital-parietal module functioned more independently in the grasp task.

Finally, omitting the overall trend in the data (the general rising trend of BOLD activation across the entire brain during movement planning and execution) affected the *place* condition more than the *grasp* condition (Fig. 3.8). Specifically, this resulted in a division of the cerebello-occipito-parietal module into two submodules: a highly modular occipito-parietal module and a less modular cerebellar module. Previous work has suggested that global trends in the data sustain distal communication, such that trend removal highlights more local processes (Musa et al., 2025). This is consistent with the notion that the cerebello-occipito-parieto module is involved in the integration of multimodal information in both our tasks.

3.5.2.3 Micro-scale Network Features: Local vs. Global Hubs

Because GTA measures are based on correlations between nodes, important hubs may not necessarily correspond to the nodes with the highest activation (Tomasi et al., 2014). However, our hubs (Fig. 3.9) fell within regions that showed increased activation (Figs. 3.3 and 3.4), suggesting that highly activated areas tend to also share signals broadly with other regions. Once again, at this scale, we found both commonalities and differences between tasks.

Both tasks shared a temporal occipital hub associated with the dorsal attention network (Schaefer et al., 2018) that served as both a local (within-module) and a global (between-module) hub. Multi-centrality hubs, which are important for both local and global connectivity, are particularly robust and essential in the network topology (Bertolero et al., 2017; Oldham et al., 2019). Temporal occipital cortex, part of the ventral visual stream (Goodale & Milner, 1992), is involved in both object recognition and object-object spatial relations (Avanzini et al., 2013; Chen et al., 2014), which play a role in both tasks (i.e., hand-object / object-template recognition and matching). It is thus expected that this region would show both internal and global connectivity for both tasks.

In addition, *grasp* and *place* shared local hubs in the lateral and dorsal prefrontal cortex, parts of the ventral attention network, and the fronto-parietal control network (Schaefer et al., 2018). These regions are associated with motor control inhibition, information value processing, and response selection during tasks (Dixon & Christoff, 2014; Krämer et al., 2013; Rowe et al., 2000). Overall, these hubs reflect the general cognitive, sensory, and motor demands of both tasks

Finally, we also found task-specific differences in both local and global hubs. In terms of significant local hubs, the *place* task had more eigenvector hubs in the prefrontal cortex than the *grasp* task (6 vs. 4), re-emphasizing the internal computations in areas such as PFCmp and PFCd, which are involved in motor correction after error (Danielmeier et al., 2011). This might reflect a greater need for accuracy in the place task. In contrast, the grasp task showed an additional hub in the sensorimotor module, specifically, in dorsal anterior cingulate cortex ('FrMed'), an area associated with error prediction (Modirrousta & Fellows, 2008; Schulz et al., 2011). Grasp also showed more hubs in the cerebello-occipito-parietal module. Together, these might reflect the need for more local computations for feed-forward control in the *grasp* condition.

In terms of global connectivity, *grasp* showed betweenness hubs in prefrontal cortex (PFCd and PFCl), the temporal occipital region, and cerebellar lobule VI, being involved in long-range communication. These might reflect stable connections underlying well-established internal models of the world required for feed-forward control (McNamee & Wolpert, 2019; Wolpert et al., 1995). In contrast, *placement* showed fewer betweenness hubs overall, indicating a less integrated system, perhaps reflecting less reliance on internal models and more reliance on sensory feedback. In particular, placement showed no significant prefrontal hubs, consistent with the increase in modularity discussed above. However, it maintained the temporal occipital hub, perhaps reflecting communication of visual object-template relationship with the sensorimotor module (Musa et al., 2025).

3.5.2.4 Limitations and Future Direction

We acknowledge several limitations that may influence the interpretation of our results. First, even though the runs in the study were pseudorandomized, there could be an order-related variable, as the experimental design required alternating between grasp and place. Whereas this was partially mitigated by our counterbalanced order of runs, within a run, a grasp was still followed by a placement, and a placement by a grasp. Therefore, residual activity might be carried over from one trial to the next and obscure the differentiation between our conditions (Aguirre, 2007; Buckner, 1998). While a long intertrial interval was used to give sufficient time for the hemodynamic response to return to baseline, it is still possible that some residual noise was carried from the previous trial. Therefore, the differentiation between our tasks may not have been fully captured; however, we were still successful in demonstrating a noticeable difference between grasp and placement. Since placement required the presence of an object held in hand and grasp does not, even without order-dependency, participants would still be aware of the action they will perform in the upcoming trial. To address some aspects of the task predictability, we varied the extrinsic object features (orientation and location). Future work could also include incongruent tasks in which the action is planned but not executed.

Second, looking more specifically at the GTA analysis, because of the nature of an event-related task, our analysis was executed on a relatively short window from which the correlation was extracted. This could result in unstable trial-by-trial edge estimates. Therefore, we avoided making assumptions based on individual trials, aggregated their outputs within subjects, and conducted

network-wide analysis to understand the system as a whole. Furthermore, we compared our GTA measures to a null model and conducted cross-validation to substantiate the robustness of our findings. Other neuroimaging studies have successfully applied GTA and functional connectivity analyses on shorter event-related studies (Luabeya et al., 2026; Musa et al., 2025; Shirer et al., 2012; Tomou et al., 2025). For future directions, one could address temporal constraints in a more naturalistic setting by repeating these experiments with electroencephalography (EEG), magnetoencephalography (MEG), or Near-Infrared Spectroscopy (fNIRS).

Finally, another limitation of the GTA modularity analysis stems from the implementation of its standard resolution parameter (Bassett et al., 2013), which limits the ability to identify more stringent communities in the network. Indeed, small modules may be less affected by detrending, as they might already account for the drift in the trial. Therefore, they would be less influenced by trend removal and better represent local communications. Future applications of GTA to sensorimotor control could optimize the resolution parameters used and improve module detection sensitivity.

3.5.2.5 General Implications for Sensorimotor Imaging Studies

Manual control supports most of our interactions with the external world. Although the field of sensorimotor neuroscience has grown immeasurably through the study of simple reach-to-grasp movements, it is equally important to go 'beyond reach' to study how objects are used once they are grasped (Binkofski et al., 1999; Talati et al., 2005; Turesky et al., 2018). This particular study demonstrates that reach-to-grasp and reach-to-place movements, while superficially similar, evoke different neural mechanisms, likely due to the different computational requirements of these tasks (Luabeya et al., 2024; Lukos et al., 2007; Naish et al., 2013; Paulun et al., 2014; Rearick & Santello, 2002). A second outcome of this experiment was that neuroimaging studies tend to emphasize cerebral cortex, but in this study, the cerebellum proved important for distinguishing between our tasks. It is well known that this and other subcortical regions are crucial components in movement control (De La Peña et al., 2020; Ji et al., 2019), and their damage can result in drastic impairments (i.e., Schucht et al., 2013; Wong et al., 2013), so these areas should be considered more in neuroimaging studies. Finally, we hope that this and similar studies (Luabeya et al., 2026; Musa et al., 2025) demonstrate the utility and importance of applying tools like GTA (often employed for the study of resting-state data in block designs) to event-related, behavioural

paradigms. This approach provides a direct way to quantify global signal distributions, network modularity, and local network hubs in the context of the behaviour that they have evolved to produce.

3.5.2.6 Conclusion

This study addresses fundamental differences in whole brain activation and functional connectivity between reach-to-grasp and reach-to-place movements. Our results suggest that these behaviours share substantial commonality in their patterns of brain activation. However, they show meaningful differentiation in the importance of the cerebellum in processing and maintaining the sensory information during the planning and execution of placement movements, in the decoding capacity of signals from action-related regions (aIPS, PMd, M1, and S1) during movement planning, and in the differentiating modularity between grasp and place. These differences could have real-world applications for understanding how brain damage affects the different components of manual interaction, and for brain-machine applications in realistic behavioural situations.

CHAPTER 4:

MODULAR INTEGRATION OF AUDITORY INSTRUCTIONS AND VISUAL CUES INTO THE CORTICAL REACH NETWORK

Authors: Gaëlle N. Luabeya[1,2,3,4], Ada Le[2], Amir Hossein Ghaderi[2,7], Lina Musa[1,2,3,5], Simona Monaco[2,8], Erez Freud[1,2,3,4,5] & J. Douglas Crawford[1,2,3,4,5,6]

Affiliations:

[1]Centre for Integrative and Applied Neuroscience, York University, Canada
[2]Centre for Vision Research, and Vision: Science to Applications Program, York University, Canada
[3]Connected Minds Program, York University, Canada
[4]Department of Biology, York University, Canada
[5]Department of Psychology, York University, Canada
[6]Department of Kinesiology & Health Sciences, York University, Canada
[7]Center for Affective Neuroscience, Development, Learning and Education (CANDLE), University of Southern California, Los Angeles, CA, USA
[8]Center for Mind/Brain Sciences, University of Trento, Italy

Current Status: Chapter 4 is submitted and a preprint is available on bioRxiv

Citation: Luabeya, G. N., Le, A., Ghaderi, A., Musa, L., Monaco, S., Freud, E., & Crawford, J. D. (2026). Modular Integration of Auditory Instructions and Visual Cues into the Cortical Reach Network. bioRxiv, 2026-01

4.1 Abstract

Humans often need to integrate 'bottom-up' stimulus attributes (e.g., object shape) with 'top-down' instructions (e.g., how to pick it up) for adaptive behaviour. To investigate how such cues are integrated into the cortical reach network, we employed an fMRI paradigm where participants viewed a cube to their left or right (visual cue) and were verbally instructed to use a horizontal or vertical grip (auditory cue), in varying order. Univariate voxel-wise and region-of-interest analysis confirmed the expected order-dependent activation of sensory regions, followed by robust parietofrontal activation. Graph-theory analysis revealed two significant subnetworks (modules): an Occipital-Parietal module (likely integrating the visual cue into the reach plan) and a Temporal-Frontal module (likely integrating the auditory cue into the grasp plan), both converging in somatomotor cortex. Cue-order influenced modularity, i.e., the module corresponding to the first cue tended to dominate contralateral motor cortex, and conversely a classification model decoded cue-order based on modularity. Local network hubs were order-independent and occupied traditional reach areas, whereas global (between module) hubs were order-dependent and more distributed. Overall, these results suggest that multisensory integration of top-down and bottom-up cues for action is a network phenomenon that relies on both lateral and serial communication between parallel sensorimotor modules.

4.2 Introduction

Voluntary actions are driven by both 'bottom-up' sensory cues and 'top-down' cognitive cues for motor planning (Ariani et al., 2015; Fried et al., 2017; Virameteekul & Bhidayasiri, 2022). For example, the first time one uses a fork, the visual system provides information about its shape, size, orientation, and location, but a caregiver likely provides instructions on how to grasp it correctly. In such cases, the brain must thus integrate both bottom-up visual cues and top-down instructions to form the optimal motor plan. Although numerous studies have considered that cortical regions support various aspects of action planning and execution (e.g., Glover, 2004; Majdandžić et al., 2007; Gallivan et al., 2011), most such studies did not consider the multisensory-motor integration processes required to integrate their top-down task instructions with their bottom-up sensory stimuli.

Prehension can be broken down into the transport component, which moves the hand to the correct location, and the grasp component, which shapes the hand to the object (Desmurget et al., 1998;

Jeannerod, 1984). The bottom-up source of visual information for such movements, e.g., location, shape, size, and orientation of the fork described above, can be reliably attributed to well-studied processes in the visual system and involved in the ‘dorsal stream’ parietofrontal circuits for reach (i.e., Goodale and Milner, 1992; Henriques et al., 1998; Crawford et al., 2011; Chen et al., 2023; Luabeya et al., 2024). In monkeys and humans, location information appears to be processed through the 'dorsal visual stream', including connections spanning early visual cortex (V1), dorsal occipital cortex, superior parietal-occipital cortex (SPOC), posterior intraparietal cortex (pIPS), and dorsal premotor cortex (PMd) (Baltaretu et al., 2020; Gallivan & Culham, 2015; Mishkin & Ungerleider, 1982; Rizzolatti & Matelli, 2003; Vesia & Crawford, 2012). In contrast, grasp involves both ventral and dorsal stream processes, including lateral occipital cortex (LOC), anterior intraparietal cortex (aIPS), and ventral premotor cortex (PMv) (Begliomini et al., 2008; Jacobs et al., 2010; Klein et al., 2023). Ultimately, these high-level planning areas are thought to activate neurons in primary somatosensory (S1) and primary motor (M1) areas, leading to the activation of specific muscle groups for action (Ariani et al., 2022; Schieber, 2001; Umeda et al., 2019).

The influence of top-down verbal instructions, although often used in laboratory paradigms, is less understood, perhaps because it involves aspects of cognition traditionally considered outside the realm of sensorimotor control. As noted above, this often involves instructions on how and what to do, especially when learning new tasks. Once learned, this may evolve into an affordance: the implicit knowledge of the various ways an object can be handled (Gibson & Maunsell, 1997; Osiurak et al., 2017), but instruction, whether through imitation, signage, or language, continues to play a role in many activities. In the case of verbal instruction, auditory information is thought to be relayed from the primary auditory cortex (A1) through Wernicke's area to eventually reach frontal regions, facilitating comprehension of the sound (Binder, 2000; Friederici, 2011; Hickok & Poeppel, 2007; Price, 2012). A recent resting-state Magnetoencephalography study reported stronger phase coupling between the primary auditory cortex (A1) and the ventral premotor cortex (Bedford et al., 2025), suggesting that sensorimotor networks have a modality-specific organization.

The question remains: how are these two sources of information (top-down verbal instructions for motor strategy and bottom-up sensory features) integrated for planning and execution of reach

movements? One possibility is that specific regions of interest (ROIs) in the parietal or frontal cortex perform this function (Andersen & Cui, 2009; Miller & Cohen, 2001). An alternative approach is to consider this question from a whole-brain network perspective (Musa et al., 2025). Specifically, how are these two types of signals distributed through the cortex during reach-to-grasp planning? A whole-brain network approach also has considerable medical relevance, since stroke and other forms of brain damage can impair cue integration for motor control (Edwards et al., 2019; Guggisberg et al., 2019).

One way to address this question is to phrase it in terms of 'functional connectivity,' i.e., correlations between signals across different brain areas (Damoiseaux & Greicius, 2009; Honey et al., 2009; Stam et al., 2016). By extracting time series from multiple ROIs as 'nodes', and correlating them to construct 'adjacency matrices' from all these areas, one can apply network science tools in graph theoretical analysis (GTA) to characterize various properties of their functional network (Bassett & Sporns, 2017; Bullmore & Sporns, 2009; Rubinov & Sporns, 2010). In the field of cognitive neuroscience, GTA has gained popularity in resting-state fMRI (functional Magnetic Resonance Imaging) and EEG (Electroencephalography) studies (Medaglia, 2017; Smitha et al., 2017; Sun et al., 2019), but in recent years, it has also been applied to event-related EEG and fMRI data (Ghaderi et al., 2023; Musa et al., 2025; Tomou et al., 2025). With this, one can investigate and compare the global network properties (e.g., energy, efficiency, clustering), intermediate properties (i.e., modularity), and local properties (i.e., hubness) of various functional networks (Bullmore & Sporns, 2009; Ghaderi et al., 2018; Newman, 2006; Rubinov & Sporns, 2010). Task instruction has been shown to alter network properties in the visual system (Musa et al., 2025), but to our knowledge, its influence on multimodal integration in the motor system has not been investigated.

To understand how the brain integrates bottom-up visual cues with top-down verbal instructions for grasp rotation, we employed a cue-separation fMRI task in which participants were visually cued to the object attributes (e.g., location, shape, size, orientation), and verbally instructed on which way to orient the hand (vertical or horizontal grip). In addition, we alternated the order of cue presentation to assess whether the timing of cue presentation influences brain activity and connectivity. From our whole-brain univariate analysis, we expected to see order-dependent activation of the sensory cortex since these responses tend to be transient (Hasson et al., 2008;

Jäncke et al., 2002), whereas preparatory motor activity tends to ramp up toward execution (Cappadocia et al., 2017). Alongside voxelwise analyses, we conducted ROI-based analyses to test a priori hypotheses in reach-and-grasp regions, and then a comprehensive GTA network analysis based on the functional connectivity of the BOLD time series.

Based on the literature cited above, we expected that sensory areas (primary visual and auditory cortex) would show order-dependent activation, depending on the order of stimulus cue presentation, but that this order-dependence would successfully decrease as this information was integrated in higher-level parietofrontal areas, progressing to motor cortex. In terms of network analysis, one would expect 1) visual activation to correlate with dorsal stream parietal activation, 2) auditory signals in temporal cortex might correlate with activity in higher-level frontal planning areas, and 3) for these two parallel sensorimotor 'modules' to converge somehow in somatomotor cortex. One would expect local hubs to emerge within these modules, whereas global 'between module' hubs should reveal additional lateral integrative mechanisms. Finally, we used a machine-learning classification technique to assess which network features encode cue order.

4.3 Methods

4.3.1 Participants

This study was a secondary analysis of a dataset that was only published in abstract form (Le et al., 2015). Twelve right-handed individuals (8 females, 4 males; age range, 21-37 years; median, 27 years) participated in the original study, based on the numbers used in contemporaneous sensorimotor imaging studies (Cappadocia et al., 2017; Chen et al., 2014; Fabbri et al., 2016; Gallivan et al., 2013). We acknowledge that these participant numbers are low compared to the current standards for perceptual / cognitive tasks, but reach planning and execution produce highly reliable and robust BOLD activation (Bennett & Miller, 2010; Poldrack et al., 2017), such that even modest participant numbers have been shown to provide sufficient power for functional network analysis (Musa et al., 2025). Further, we conducted a post hoc power analysis to confirm that we had sufficient statistical power for analysis of even our least robust region-of-interest results, and used permutation testing and cross-validation to establish the reliability of our GTA findings (see *Statistical Analysis* section, below). Participants self-reported normal or corrected-to-normal visual acuity with no reported neurological disorders and were all right-handed. Participants provided informed consent before the experiment and received monetary

compensation for their time. All experimental procedures were approved by the York University Human Participants Review Committee (Certificate #: 2015-219; protocol renewed November 22, 2021).

4.3.2 Apparatus and Stimuli

Data were collected at York University (Toronto, Canada) using a 3-T whole-body MRI system (Siemens Magnetom TIM Trio, Erlangen, Germany). Participants lay on the MRI bed with a platform over their pelvis, where the stimuli were presented. Headphones were worn to hear auditory instructions. To reduce motion artifacts, the head was immobilized using foam cushions, and a strap further restricted their upper arms. To facilitate the view of the stimuli in the head-tilted setup, the anterior part of the 12-channel coil was removed and replaced by a 4-channel flex coil, while the posterior portion of the 12-channel coil was maintained (Fig. 4.1A).

During experiments, two grasp stimuli were fixed to an inclined platform placed above the participants' pelvis (Fig. 4.1A). Grasp stimuli consisted of two square-shaped (5 cm × 5 cm × 1.8 cm) plexiglass objects fixed to the left and right sides of the platform, at a relative height / distance chosen to optimize the biomechanical comfort of forearm motion. The objects were illuminated via underlying optic fibers to indicate which object needed to be grasped. The specific platform distance and height were adjusted for each participant so that they could comfortably reach both objects. Object orientation was fixed so that objects could be grasped with either a horizontal or

vertical grip. An adjustable 'snake' was used to place a dim, fibre-controlled LED between the two objects for visual fixation.

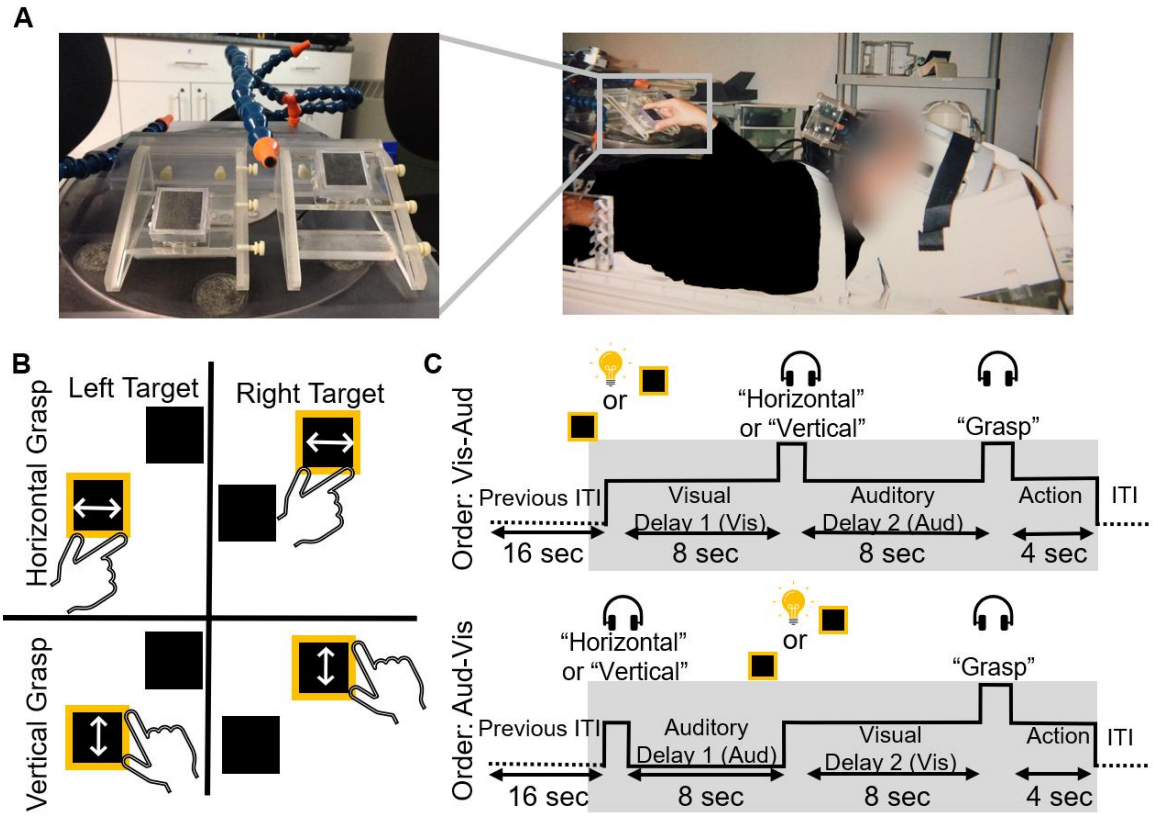


Figure 4.1. A) Experimental setup. Participants were instructed to maintain fixation on the LED light in the center, and they could grasp the object to the left or right. B) Presentation of the four possible orientations and location combinations for the grasp. C) Timeline of a single trial for each of the two trial types (Visual-Auditory and Auditory-Visual). For the Visual-Auditory trials, participants were first visually cued about the reach location, followed by an 8-second delay (Vis-Aud-D1). Then, participants were given auditory instructions about the grasp orientation, which was also followed by an 8-second delay (Vis-Aud-D2). For Auditory-Visual trials, the instructions were given in the reverse order: participants were first given auditory instructions on the grasp orientation. After an 8-second delay (Aud-Vis-D1), participants were then visually cued about the grasp location. This was followed by another 8-second delay (Aud-Vis-D2). Then, participants had 4 seconds to reach and grasp the object. Note that the auditory cues were transient and that the visual cues were sustained until the end of the task, such that participants performed a visually guided action. The inter-trial time was 16 seconds.

All lights and audio were controlled by a custom program on a laptop PC that received signals from the MRI scanner at the start of each trial. The windows in the scanner room were blocked

with black curtains, and the room lights remained off so that, except for the fixation light, nothing on the platform was visible to the participant when the object illuminator was off. Outside the scanner room, we monitored the participant's compliance with the task using an infrared camera (MRC 12M) to record hand movements and an eye tracker (iViewX with an MRI-compatible Avotec Silent Vision system).

4.3.3 Experimental Task Design

To investigate the brain areas involved in integrating reach location and grasp orientation, we employed a cue-separation paradigm that temporally separates auditory and visual cue presentations (Baumann et al., 2009; Cappadocia et al., 2017; Chen et al., 2014). At the start of each trial (Fig. 4.1B), the central fixation light was illuminated, and participants maintained their gaze on it. Participants were then provided with a visual cue of the object's location to the left or right (Visual Cue: Vis). Participants were then provided with a verbal instruction ('Horizontal' or 'Vertical') telling them to grasp the object with a horizontal or vertical grip posture (Auditory Cue: Aud).

The order of these two cues (Vis-Aud vs. Aud-Vis) varied randomly, with an 8-second delay period (D1) after the first cue presentation, a second 8-second delay period (D2) after the second cue presentation, and a final 4-second period to grasp the object (Fig. 4.1C). After each trial, participants were required to return to the starting position on the pelvis and remain still during a 16-second intertrial interval before the subsequent trial. Therefore, a complete trial was 36 seconds long.

Overall, this paradigm formed a 2 (location instruction: left, right) × 2 (orientation instruction: horizontal, vertical) × 2 (order: Vis-Aud, Aud-Vis) study, resulting in 8 conditions. Each run consisted of 16 trials; therefore, each experimental condition was repeated twice in a random order. A baseline of 8 seconds was added to the end of each run, yielding a run time of 9.73 minutes. Each participant completed 8 runs presented in a randomized order and repeated each experimental condition 16 times. Additionally, an anatomical scan for each subject was collected halfway through the data collection session. Combined with setup time, practice trials to become familiar with the task, and brief breaks between runs, an entire session lasted approximately 2.5 hours.

4.3.4 Imaging Parameters

The T2*-weighted functional experimental data were recorded using a single-shot gradient echo-planar imaging (including repetition time (TR) of 2 seconds, echo time (TE) of 30 ms, and flip angle of 90° in a 192 mm field of view (FOV), a 64 × 64 matrix size, yielding a resolution of 3.0 mm × 3.0 mm and a 3.5 mm slice thickness with no gap). Each volume contained 35 slices, which were sampled in an ascending and interleaved order. With the functional data, a T1-weighted anatomical scan was acquired in the same orientation as the functional imaging data using a 3D acquisition sequence (192 × 256 × 256 mm FOV with repeated matrix size yielding a resolution of 1.0-mm isovoxel, inversion time of 900 ms, TR of 1900 ms, TE of 2.52 ms, and flip angle of 9°).

4.3.5 Preprocessing

Data were cleaned and analyzed using the FMRIB Software Library 6.0.7.17 (Jenkinson et al., 2012) before moving to RStudio 2024.12.1 for Region of Interest Analysis and MATLAB R2024b for Graph Theory Analysis. The first two volumes of each scan were omitted to avoid T1 saturation effects. We used high-pass temporal filtering to remove low-frequency artifacts, applied spatial smoothing with a kernel size of 6.0 mm, and performed a slice scan time correction. We motion-corrected each functional run using MCFLIRT, which applied a rigid-body transformation. Runs that showed head displacements over 1 mm were excluded from further analysis. However, one participant displayed a large head motion in the first trial during two runs; therefore, only the initial trial was excluded. Functional acquisitions were coregistered to anatomical images using the Brain-Boundary Registration in the Montreal Neurological Institute (MNI152) 1 mm standard space (Mazziotta et al., 1995). Participants' hand movements and gaze fixations were assessed offline to confirm their compliance with the instructions. Combining all exclusion criteria across participants, fewer than 5% of trials needed to be removed from further analysis.

4.3.6 Graph Theoretical Analysis

For our functional connectivity analysis, we created 200 spheres of 3 mm radius on FSLeyes using the 200 nodes' coordinates from the Schaefer-200 Atlas (Schaefer et al., 2018; Fig. 4.2A). The raw BOLD signals from each sphere for each run across all participants included in our analysis were extracted to conduct the functional connectivity analysis (Fig. 4.2B). For these runs, we also obtained the event files, the parameter estimates, and the residuals for each region of interest to

compute the contrast-reduced time series of our data. Contrast-reduced time series is a partial model fit of the voxel time course that computes contrast-related signals and residual errors while removing condition-irrelevant regressors, following the implementation described in FSL FEAT Model (McCarthy, 2025). Thus, yielding a cleaner signal that reflects condition-specific neural dynamics (Musa et al., 2025). Data from all the trials used in our analysis were extracted from the run prior to further analysis (Fig. 4.2C).

To construct functional networks, we calculated correlations of the contrast-reduced timeseries obtained across the 200 nodes for each trial (Musa et al., 2025; Tomou et al., 2025). Our data points started with the last two volumes of the intertrial period preceding the first cue presentation and continued until the end of the grasp period (grey box in Fig. 4.1C). The absolute values of the correlation outputs were placed in 200 × 200 adjacency matrices (Fig. 4.2D). These matrices were averaged across all trials, so that each participant had one matrix per condition. Then, the graph theoretical measures were calculated for each participant (i.e., for each matrix), and statistical comparisons were performed between conditions. However, for modularity analysis, averaging across participants yielded a single matrix per condition, which was then used to identify modules.

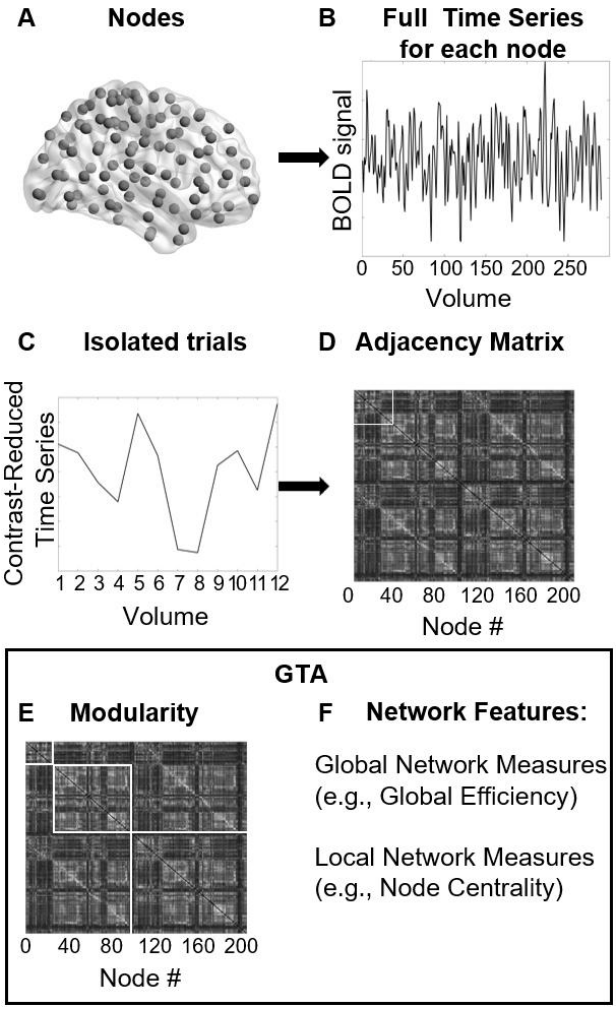


Figure 4.2. Schematic representation of graph theoretical analysis (GTA) applied to fMRI data. A) A cortical surface model illustrating the brain, with 200 regions of interest (ROIs) / nodes used for network analysis. B) The blood-oxygen-level-dependent (BOLD) signal extracted from the entire run for each ROI. C) Isolation of the contrast-reduced time series for individual trials. D) Construction of an adjacency matrix representing functional connectivity between brain nodes. E) Application of GTA to examine network properties, such as modularity, where each square delimits a module. F) Extraction of global and local network measures, including global efficiency and node centrality, to quantify brain network organization.

Then, GTA measurements were computed on these matrices using the Brain Connectivity Toolbox (Rubinov & Sporns, 2010). In addition, self-developed functions for the energy and modularity scores were used (Ghaderi et al., 2020, 2025). Definitions of the GTA measures used are provided in Table 1. First, we divided our whole-brain network from the grand average into modules, smaller dense communities of non-overlapping nodes, which were identified by maximizing Newman-

Girvan modularity for undirected networks. We maximized the number of communications within the subnetwork and minimized the number of connections (edges) across subnetworks. All brain networks were visualized using BrainNet Viewer (Xia et al., 2013). Second, we computed Newman's *Modularity* Algorithm (Q), a measure of the quality of the division into subcommunities, by comparing the number of within-community edges to the expected number of edges in a random subnetwork of the same number of nodes (Ghaderi et al., 2025; Newman, 2006). More details on the approach used can be found in Tomou and colleagues (2025).

To better understand how information flows through the brain and which nodes are influential for the functional connectivity, we computed the eigenvector centrality and the betweenness centrality. The first centrality measure identified the major *eigenvector hubs,* which are well-connected nodes with high functional connectivity to other highly connected nodes, and the second centrality measure highlighted the major betw*eenness hubs,* which are regions that act as bridges between separate parts of the network (such as two different modules). These values were selected by identifying the nodes that represented the top 1% and the top 5% of the measured centrality values (Tomou et al., 2025). To capture core aspects of brain network organization, we computed the clustering coefficient, a measure of the functional segregation of the brain as the tendency of neighbour nodes to be strongly connected, the global efficiency, a measure of the functional integration which represents how efficiently information is exchanged across the whole network, and finally the energy, a measure of the dynamics and stability of synchronization in the network. All of these measures were normalized to a null model (Váša & Mišić, 2022). We created these randomized datasets using a self-developed MATLAB code available for open access at https://github.com/AHGhaderi/Null-model. We computed the GTA measures using all trials combined, regardless of trial type, to assess the overall results. They were also computed separately for each trial condition (Vis-Aud or Aud-Vis) to compare differences across trial types.

Finally, we employed a machine learning approach to assess how well these graph theory features can dissociate between the two orders of cue presentation. Therefore, a supervised classification analysis was conducted using MATLAB's *Classifier Learner* app based on each trial for all the participants. We then used the Kruskal-Wallis algorithm to rank the importance of each input in its attempt to distinguish between our two conditions.

Table 4.1. Glossary of Graph Theory Measures used for our weighted networks

Term	Definition	Interpretation	Scale	Key Reference
Clustering Coefficient	Assesses the tendency of nodes in the network to form tightly interconnected groups ('cliquiness') and is averaged across nodes to investigate it globally.	A high clustering coefficient indicates that neighboring brain regions are strongly interconnected, supporting local specialization and segregated processing.	Global	(Demaine et al., 2006)
Global Efficiency	Represents how connected the nodes in the network are by quantifying the average inverse shortest path length between all pairs of nodes to determine how easily information can be transferred across the network.	High global efficiency indicates that information can be rapidly exchanged across the entire network, supporting integration. Lower global efficiency reflects longer paths and a more segregated network, which may favor specialized processing.	Global	(Latora & Marchiori, 2001; Rubinov & Sporns, 2010)
Energy	Reflects the overall connectivity strength and synchronization stability across the network. This assesses the metabolic or wiring cost of maintaining a connection.	High energy indicates a stable, synchronized dynamical state in the network.	Global	(Ghaderi et al., 2020)
Modularity	Measures how well a network can be subdivided into communities (modules) characterized by dense connections within modules and sparse connections between modules.	Higher modularity reflects stronger segregation, meaning the network is organized into specialized subsystems; lower modularity reflects a more	Meso	(Newman, 2006; Sporns & Betzel, 2016)

		integrated or globally mixed network.		
Eigenvector Centrality	Identify influential nodes in a network by considering not only the number of connections, but also the importance of the nodes they connect to.	Nodes with high eigenvector centrality can be considered as local network hubs because they are embedded in well-connected neighborhoods. High values indicate nodes that can efficiently spread or integrate information across the network.	Local	(Bonacich, 2007)
Betweenness Centrality	Identifies important hubs that serve as intermediate steps between a pair of other nodes by measuring how often a node lies on the shortest paths between pairs of other nodes. These nodes often link different modules, supporting global integration.	Nodes with high betweenness centrality act as bridges or bottlenecks, facilitating communication between different parts of the network and serving as connector hubs.	Local	(Freeman, 1977; Van Den Heuvel & Sporns, 2013)

4.3.7 Statistical Analysis

Univariate Data Analysis: Functional MRI data were analyzed using FSL FEAT (version 6.00). At the individual run level, we used a voxelwise general linear model (GLM). Each predictor was derived from a boxcar wave function convolved with FSL's canonical double-gamma hemodynamic response function, with temporal derivatives included to account for variability in response timing. We defined the delay phases and the action as the period of interest. We modelled our predictors using these three time periods (Delay 1, Delay 2, and Action) based on cue presentation (Vis-Aud or Aud-Vis), resulting in a total of 6 predictors of interest: Delay 1 Vis-Aud,

Delay 1 Aud-Vis, Delay 2 Vis-Aud, Delay 2 Aud-Vis, Grasp Vis-Aud, and Grasp Aud-Vis. We combined all conditions (left/right and vertical/horizontal) for each order of cue presentation within each period and compared them to baseline to investigate their general response to the task. For each subject, their run-level results were combined using a fixed-effects model. Finally, group-level analyses were performed using a mixed-effects model (FLAME 1), with statistical maps cluster-corrected using a z-normalized threshold of 2.3 and a corrected cluster significance threshold of P = 0.05 (Worsley, 2001). The threshold was selected in accordance with previous action-related fMRI studies (Gertz et al., 2017; Marangon et al., 2016). Surface plots were generated using Nilearn functions in Python (Abraham et al., 2014).

Region of Interest Analysis: We hypothesized that cortical areas known to be involved in motor control would exhibit a specific increase in activity and carry information regarding the order of cue presentation. For this effort, we extracted beta weights from 7 regions of interest (V1, SPOC, pIPS, aIPS, PMv, PMd, and M1), and their values were averaged from a 6 mm radius sphere created around centroid coordinates. For early visual cortex, the coordinates were identified by converting Talairach values reported in a visually guided grasping task (Monaco et al., 2024) to MNI coordinates using seed-based d mapping according to Lancaster and colleagues (2007). In contrast, the other regions were identified from Neurosynth data terms based on meta-analyses using the terms: "reaching" and "grasping" (Yarkoni et al., 2011). The ROIs were then used to extract β-weight values for each participant in the Vis-Aud and Aud-Vis conditions during the three phases (Delay 1, Delay 2, and Action). We computed paired t-tests on their β-weights to identify regions that differ significantly from zero, and compared them across conditions (Vis-Aud vs Aud-Vis). We used the false-discovery rate based on the number of ROIs assessed to correct for multiple comparisons. Following the approach reported by Baltaretu and colleagues (2020), we conducted a post hoc power analysis to verify that our sample was sufficient to detect a difference in the order of cue presentation. Using the β-weight, which shows the smallest difference between the two conditions (at pIPS) in delay 1, we found that at our sample size, the region has an effect size (d(repeated) = 1.05) and provides power = 0.91.

GTA analysis: Using a community-assignment algorithm, all nodes in our network were grouped into modules. To confirm that modules exceeded the modularity expected under a null model, they were normalized to the modularity of a randomized subnetwork. A modularity score greater than

1 indicates that the connectivity within the selected group of nodes (subnetwork) is more organized than would be expected by chance. Because the normalized modularity score is strictly positive and interpreted as a relative measure, it was log-transformed, and a non-parametric one-sample sign-flip permutation test (right-tailed with 50000 permutations) was applied to statistically confirm that the results are not due to a random network. Modules with non-significant modularity scores were also reported for completeness. In addition, nonparametric permutation t-tests with 10000 randomizations were computed to compare graph theoretic features (Modularity, Cluster Coefficient, Global Efficiency, and Energy) between the two orders of cue presentation (Tomou et al., 2025). A false discovery rate (FDR: q) was calculated to obtain an adjusted p-value, controlling for multiple comparisons. Furthermore, using nonparametric permutation testing allowed us to account for the small sample size, as it avoids distributional assumptions required in parametric tests and creates a randomized dataset by reassigning condition labels. We can then assess whether our original data differs significantly from the null distribution. For our classification, we employed a 10-fold cross-validation procedure to assess the model's performance and prevent overfitting. This approach validated the stability of our classification by dividing the data into 10 groups (folds), with the model being trained on 9 folds and tested on the remaining fold. This was repeated for 10 iterations, so that each fold served as the test fold at least once.

4.4 Results

The goal of this study was to employ GTA network analysis to determine how our sensory cues (i.e., visual for object, auditory for grip strategy) were integrated for action. To justify this analysis, we first used univariate voxelwise and ROI analyses to confirm that our task produced the expected order-dependent sensory activation during cue presentation, followed by robust parietofrontal activation during reach planning and action.

4.4.1 Whole-Brain Univariate Analyses

For this analysis, we examined activation during Delay 1, Delay 2, and Action versus the baseline. Based on previous neuroimaging studies (i.e., Nelson & Mayhew, 2025; Straube et al., 2017), one might expect BOLD activation in the two delay periods to be dominated by the type and order of the sensory stimulus, i.e., visual followed by auditory cortex activation in the Vis-Aud order, and the reverse in the Aud-Vis order. During the Action phase, we expected additional activation of the fronto-parietal cortex and other areas associated with reach execution. We first computed the order-

combined increase in activity relative to baseline (Vis-Aud + Aud-Vis > baseline) across the three epochs (Fig. 4.3, *Left Column*). During Delay 1 (Fig. 4.3A), we observed an increase in activity in the bilateral Early Visual Cortex (z = 5.85), the left Supramarginal Gyrus (z = 3.35), the left Precentral Gyrus (z = 3.24), and the left Postcentral Gyrus (z = 4.0). Delay 2 (Fig. 4.3B) showed a greater activation in the same regions: the bilateral Early Visual Cortex (z = 5.47), the left Supramarginal Gyrus (z = 3.52), the left Precentral Gyrus (z = 2.95), the left Postcentral Gyrus (z = 3.19), as well as in the Superior Temporal Gyrus (auditory cortex: A1; z = 3.98) and the Lateral Occipital Cortex (z = 2.94).

During the execution phase (Fig. 4.3C), both tasks resulted in widespread activity in the insula, the middle and posterior cingulate cortex, the superior temporal gyrus, and the striate cortex, pre- and postcentral gyrus, with highest increase in activation in visually-guided action such as the bilateral Lingual Gyrus (z = 6.1), Cuneus (z = 6.0), Lateral Occipital Cortex (z = 6.1), Superior Parietal Lobule (z = 5.87), Supramarginal Gyrus (z = 5.8), Precentral Gyrus (z = 6.0), and Postcentral Gyrus (z = 5.8). In addition to continued activation (or reactivation) of visual and auditory sensory areas, we observed a broad swath of activation spanning all four cortical lobes during the Action Phase, including most of the well-known reach and grasp-related brain areas (Cavina-Pratesi et al., 2010; Turella & Lingnau, 2014; Vingerhoets, 2014).

4.4.2 Region of Interest Analysis: Visual and Motor Components of the Reach Network

To test the influence of cue order on brain activation within regions of interest (ROIs), we isolated the β weights from seven reach and grasp-related brain areas in visual and motor cortex (V1, SPOC, pIPS, aIPS, PMv, PMd, and M1 in the left hemisphere; see Table 4.2). To complement whole-brain analyses, we performed ROI-based analyses to test a priori hypotheses in regions implicated in motor control. Their event-related responses were evaluated relative to zero, corresponding to the implicit baseline in the inter-trial interval, before extending our analysis to examine the effect of the order of cue presentation. During Delay 1, we found a significant increase in β values for V1, SPOC, pIPS, and M1 in the Vis-Aud Order as well as M1 in the Aud-Vis Order. During Delay 2, we found a significant increase in β weights in the two orders for V1, SPOC, pIPS, aIPS, and M1, whereas PMv showed a decrease in β weight. Finally, during the grasp, we observed increased activation across all regions investigated: V1, SPOC, pIPS, aIPS, PMv, PMd, and M1. When comparing the two orders, we only found a significant difference during Delay 1

in V1 ($q = 8.65 \times 10^{-5}$), SPOC ($q = 8.017 \times 10^{-3}$), and pIPS ($p = 0.026$); however, the difference in pIPS did not survive the correction for multiple comparisons ($q = 6.085 \times 10^{-2}$). Overall, these findings suggest a decrease in cue-order-dependence and an increase in overall brain activity as cue information accumulated toward the final grasp performance.

Table 4.2. Summary of Means, Standard Errors, and FDR-corrected q-values for the significant difference in β weight

	ROI	Order	Mean	SE	FDR q-value
Delay 1	V1	Vis-Aud	0.929	0.126	1.905×10^{-4}
	SPOC	Vis-Aud	0.289	0.067	6.808×10^{-3}
	pIPS	Vis-Aud	0.160	0.047	0.024
	M1	Vis-Aud	0.140	0.042	0.024
		Aud-Vis	0.132	0.043	0.029
Delay 2	V1	Vis-Aud	0.984	0.136	2.375×10^{-4}
		Aud-Vis	1.033	0.170	5.360×10^{-4}
	SPOC	Vis-Aud	0.390	0.075	1.367×10^{-3}
		Aud-Vis	0.371	0.086	2.181×10^{-3}
	pIPS	Vis-Aud	0.255	0.054	2.181×10^{-3}
		Aud-Vis	0.248	0.058	2.983×10^{-3}
	aIPS	Vis-Aud	0.131	0.032	3.172×10^{-3}
		Aud-Vis	0.109	0.048	0.050
	PMv	Vis-Aud	-0.112	0.042	0.029
		Aud-Vis	-0.120	0.042	0.026
	M1	Vis-Aud	0.286	0.084	0.010
		Aud-Vis	0.218	0.081	0.029
Grasp	V1	Vis-Aud	1.649	0.315	3.242×10^{-4}
		Aud-Vis	1.843	0.234	1.432×10^{-5}
	SPOC	Vis-Aud	1.240	0.105	1.013×10^{-6}
		Aud-Vis	1.242	0.099	1.013×10^{-6}
	pIPS	Vis-Aud	1.217	0.152	1.090×10^{-5}
		Aud-Vis	1.218	0.140	1.090×10^{-5}

	aIPS	Vis-Aud	0.938	0.275	5.881×10^{-3}
		Aud-Vis	0.917	0.260	5.131×10^{-3}
	PMv	Vis-Aud	0.750	0.101	1.876×10^{-5}
		Aud-Vis	0.647	0.078	1.090×10^{-5}
	PMd	Vis-Aud	1.306	0.169	1.432×10^{-5}
		Aud-Vis	1.264	0.150	1.090×10^{-5}
	M1	Vis-Aud	2.509	0.365	3.375×10^{-5}
		Aud-Vis	2.430	0.313	1.432×10^{-5}

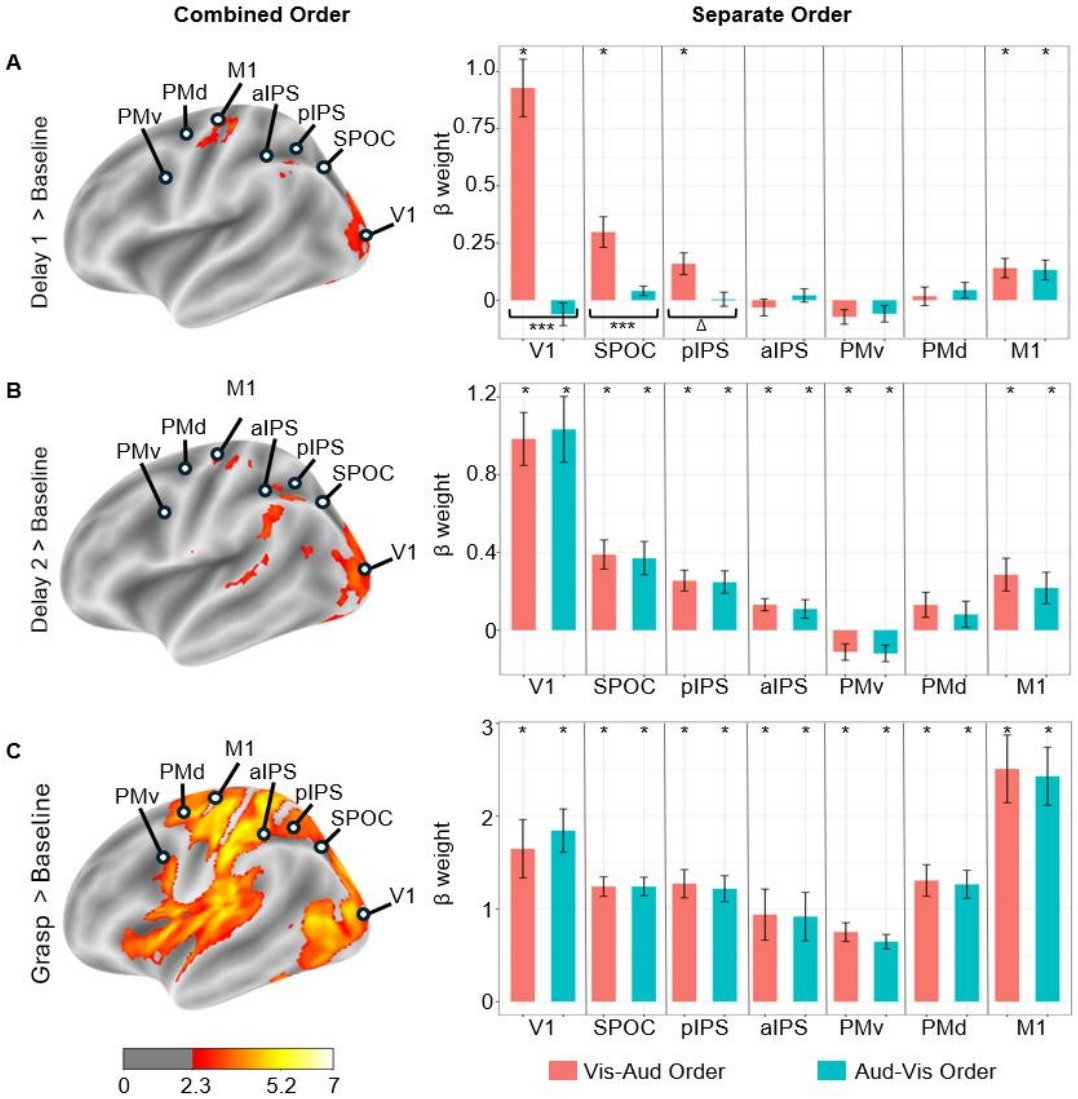


Figure 4.3. Left panel presents the lateral views of the cortical activation maps in the left hemisphere for the combined order during the three epochs, with colour bars indicating statistical intensity (z threshold = 2.3). Highlighted in circles are seven regions of interest used to plot the bar graphs. Right panel presents the average β weight (± standard error) for Visual Cortex (V1), Superior Parietal Occipital Cortex (SPOC), posterior Intraparietal Sulcus (pIPS), anterior Intraparietal Sulcus (aIPS), ventral Premotor Cortex (PMv), dorsal Premotor Cortex (PMd), and Primary Motor Cortex (M1) for the Visual-Auditory Order (in pink) and the Auditory-Visual Order (in blue). Asterisks above the bars indicate regions with β weights significantly different from zero. Asterisks below the graphs indicate that the β weights differ significantly by cue presentation order, and Δ shows that the β weights differ significantly by order, but this difference did not survive correction for multiple comparisons. FDR was applied to correct for multiple comparisons. A) shows the results during the first delay period, B) shows the results during the second delay period, whereas C) shows the results during the grasp/action phase.

4.4.3 Functional Network Analysis

Having confirmed that our task generally produced the patterns of sensory and motor activation that one would expect from the literature, we proceeded to our main questions: how are our two cues (visual for object properties, and auditory for the grip plan) integrated into the cortical reach network, and to what degree are the resulting functional networks dependent on the order of cue presentation? For this purpose, we performed a functional network analysis using *graph theory*, based on correlations between the contrast-reduced time series of our various cortical nodes (Fig. 4.2). In this analysis, we examined the time period from the end of the previous intertrial period of each trial up to the end of the grasp period, both for the combined and separate cue orders.

4.4.3.1 Global Network Properties.

We computed the global network features (clustering coefficient, global efficiency, energy) normalized with a null distribution to ensure that our data formed a 'real' (not random) network and compared their values for the two cue presentation orders (Fig. 4.4). A clustering coefficient value equal to or above 1 represents a non-random network, which is evident in the combined clustering coefficient (mean = 1.002, SE = 1.855×10^{-4}, p = 9.998×10^{-5}) as well as the separate order clustering coefficient (Vis-Aud: mean = 1.002, SE = 1.765×10^{-4}, p = 2.00×10^{-4} and Aud-Vis: mean = 1.002, SE = 2.011×10^{-4}, p = 2.40×10^{-4}; Fig. 4.4 A-B). A global efficiency value smaller than 1 represents a non-random network, as observed in both the combined global efficiency of the combined condition (mean = 0.9918, SE = 0.0012, p = 3.199×10^{-4}) and the separate order global efficiency (Vis-Aud: mean = 0.990, SE = 0.0015, p = 2.799×10^{-4} and Aud-Vis: mean =

0.9905, SE = 9.437×10^{-4}, p = 2.20×10^{-4}; Fig. 4.4 C-D). Similarly, an Energy value smaller than 1 represents a non-random network, as found in both the combined energy (mean = 0.8434, SE = 0.0085, p = 2.00×10^{-4}) and the separate orders (Vis-Aud: mean = 0.8440, SE = 0.0075, p = 3.199×10^{-4} and Aud-Vis: mean = 0.8438, SE = 0.0084, p = 2.40×10^{-4}; Fig. 4.4 E-F). However, our permutation t-tests comparing the global measures between the Vis-Aud and Aud-Vis conditions were not significant: clustering coefficient (t(11) = -0.188, p = 0.858), global efficiency (t(11) = -0.181, p = 0.859), and energy (t(11) = 0.044, p = 0.964). Overall, these analyses supported the notion that these are 'real' networks, even when separated into the two order conditions, but a more detailed analysis at the mesoscale (modular) and local (hub) layers was required to test our hypotheses.

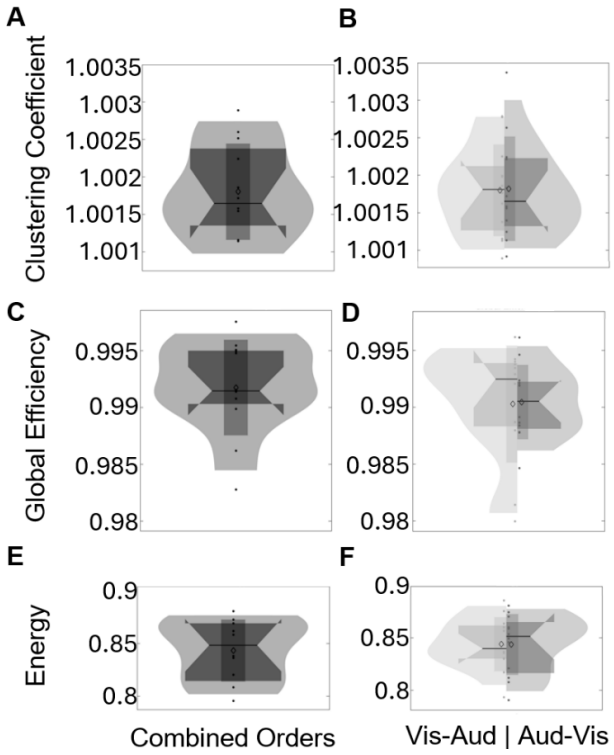


Figure 4.4. Violin plots displaying distributions of normalized global network parameters: clustering coefficient (A, B), global efficiency (C, D), and energy (E, F). The left column (A, C, E) plots the distributions of the whole dataset (combined orders). The right column (B, D, F) plots the distributions of the Vis-Aud order vs. Aud-Vis order.

4.4.3.2 Correlated Time Series Suggest Parallel Processing Streams

Our hypothesis was that sensorimotor integration in this task would be modular, i.e., visual signals should be integrated into the motor system via the parietal cortex, whereas auditory signals could be integrated via frontal centres. If this is correct, then the BOLD time series in the visual cortex should tend to correlate with parietal signals, whereas those in the auditory cortex should correlate with frontal signals.

To illustrate this, we selected example regions from the Schaeffer atlas whose locations overlapped with areas of peak cortical activity (Fig. 4.5). The time series for primary visual cortex (A) resembled and significantly correlated with the time course for superior parietal lobule (B) in both presentation orders (overall $r = 0.762$, $t(10) = 3.72$, $q = 0.008$ for Vis-Aud order and $r = 0.932$, $t(10) = 8.13$, $q = 4.083\times10^{-5}$ for Aud-Vis order). Likewise, the time course for the peak voxel within primary auditory cortex (C) resembled and significantly correlated with the time course for the peak voxel in dorsal premotor cortex (D) (overall $r = 0.962$, $t(10) = 11.12$, $q = 4.763\times10^{-6}$ for Vis-Aud order and $r = 0.845$, $t(10) = 5.00$, $q = 0.003$ for Aud-Vis order). In contrast, the opposite correlations (V1-premotor, A1-SPL) were lower and non-significant ($r = 0.490$, $q = 0.141$ and $r = 0.619$, $q = 0.051$ for Vis-Aud order; $r = -0.025$, $q = 0.939$ and $r = 0.080$, $q = 0.9188$ for Aud-Vis order). These specific examples appear to support our hypothesis. The next section employs GTA analysis to quantitatively test this hypothesis for 200 nodes distributed across the entire cortex.

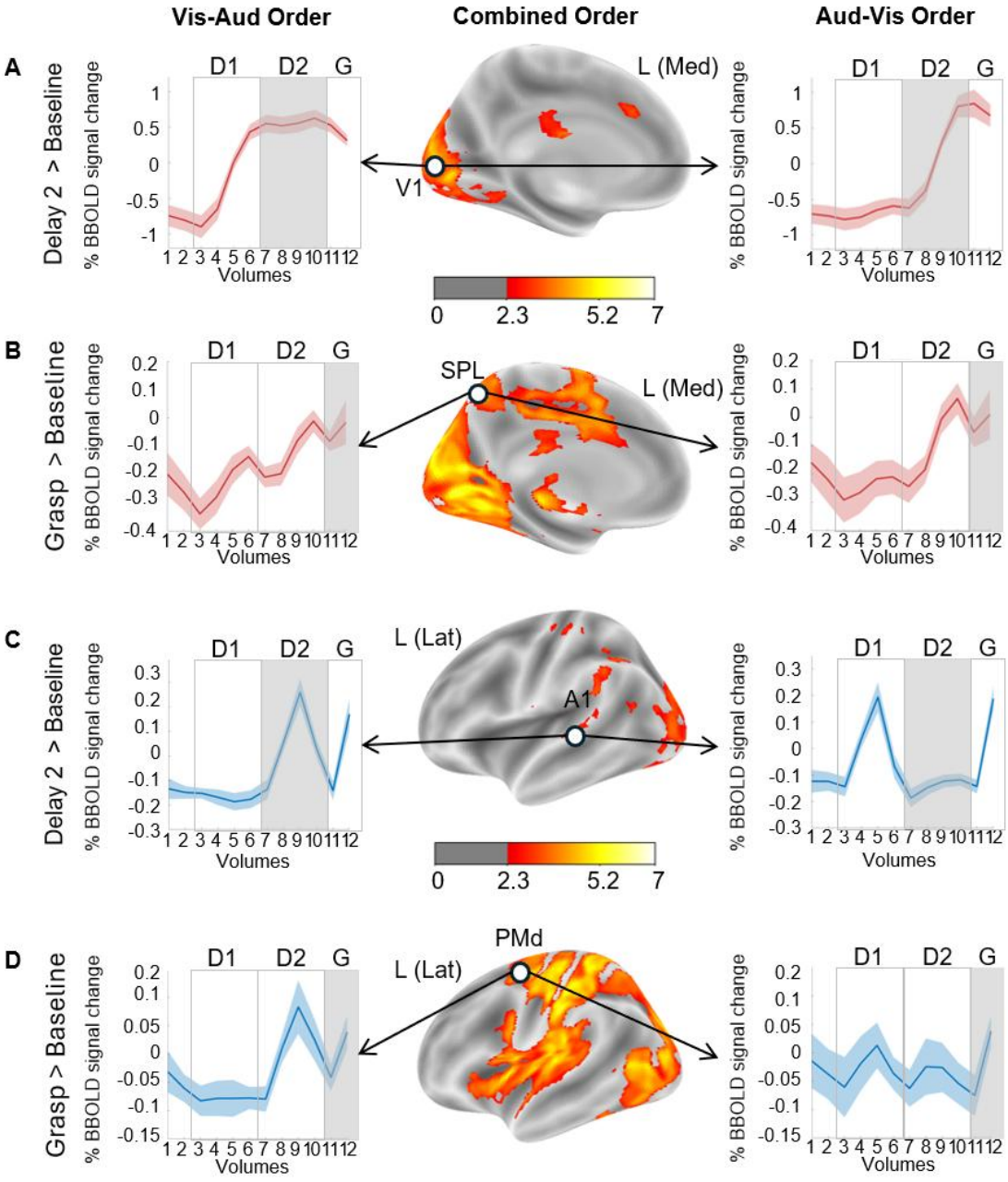


Figure 4.5. Medial and lateral views of the cortical activation maps for the Vis-Aud and Aud-Vis conditions during the Delay 2 and Grasp epochs are presented in the left hemisphere, with colour bars indicating statistical intensity (z threshold = 2.3). Highlighted in circles are two cue-acquisition regions (Primary Visual Cortex [V1; MNI: -5, -93, -4] and Primary Auditory Cortex [A1; MNI: -51, -4, -2]) and two regions involved in preparation for action (dorsal Premotor Cortex [PMd; MNI: -43, 6, 43], Superior Parietal Lobule [SPL; MNI: -17, -53, 68]) from which the average percentage change in BOLD signal was extracted (± standard error). On the left, these data are presented for the Visual-Auditory (Vis-Aud) condition; on the right, for the Auditory-Visual (Aud-Vis) condition. A & C) show the results during the second delay period; B & D) show the results during the grasp/action phase. These regions are highlighted in a grey-

shaded square in the time series. The 12 data points represent time in terms of volumes within a trial (D1: Delay 1, D2: Delay 2, G: Grasp). Shaded regions indicate variability across participants. Time-course data are color-coded red for V1 (in A and B) and SPL, and blue for A1 and PMd (in C and D).

4.4.3.3 Modularity Analysis: Occipital-Parietal vs. Temporal-Frontal Modules

A formal modularity analysis provides the means to extend and quantify the examples shown in Figure 4.5 by identifying clusters of highly correlated BOLD time series (Fig. 4.2E) between our 200 nodes (Fig. 4.2A). Figure 4.6A shows the results of such an analysis in our complete, order-combined dataset. This analysis subdivided our nodes into three putative modules: a Temporal-Frontal-Somatomotor module spanning the central sulcus (Module 1, blue), another module spanning Occipital-Parietal-Somatomotor cortex (Module 2, red), and a third module (Module 3, yellow) spanning the remaining nodes. We will summarize the functional anatomy of these putative modules qualitatively and then quantify / test their significance in the following paragraphs.

Module 1 (blue) was largely bilateral and appears to be involved in relaying the auditory instruction for the grip strategy. This module included areas in the Superior Temporal Gyrus that were activated during auditory cue presentation, as well as regions involved in preparation and execution of action, including Lateral Prefrontal Cortex, Dorsal and Ventral Premotor Cortex, and most portions of primary somatomotor cortex (preparation and execution of action) (Monaco et al., 2024; Rizzolatti & Luppino, 2001).

Module 2 (red) appears to relay visual information about the stimulus to the motor system. This module included bilateral occipital areas (such as the Striate Cortex and Extrastriate Cortex) that were activated by the visual stimulus during the Delay periods, and bilateral posterior parietal areas (including the Superior Parietal Lobule and Intraparietal Sulcus) implicated in visually guided reach and grasp (Buneo & Andersen, 2006; Culham & Valyear, 2006; Gallivan & Culham, 2015; Grefkes & Fink, 2005). This module also 'invaded' portions of the left somatomotor cortex that were likely related to right-hand motion (Kim et al., 1993; Penfield & Boldrey, 1937).

Module 3 (yellow) spans prefrontal cortex and portions of inferior parietal and temporal cortex; however, this module did not reach significance.

Order-Dependence. When the data were divided by order (Fig. 4.6B-C), the same basic modular organization persisted (i.e., a Temporal-Frontal-Somatomotor module and an Occipital-Parietal-Somatomotor module), but with some subtle differences. For example, when the visual cue was presented first (Fig. 4.6B), there was a continued invasion of connectivity of the Occipital-Parietal-Somatomotor module into the left somatomotor cortex. In contrast, when the auditory cue was presented first (Fig. 4.6C), the Occipital-Parietal-Somatomotor module was more restricted, and the blue module fully spanned both sides of the Somatomotor cortex, decreasing lateralization in both modules.

Overall, these results suggest that 1) information from the visual cue dominated the 'dorsal stream' visual areas involved in visually guided movement, 2) the auditory cue (for the grip plan) was incorporated into more frontal mechanisms, and 3) these modules were largely independent of cue order, except that the initial cue (auditory or visual) tended to dominate signals in the hand-related portion of left somatomotor cortex.

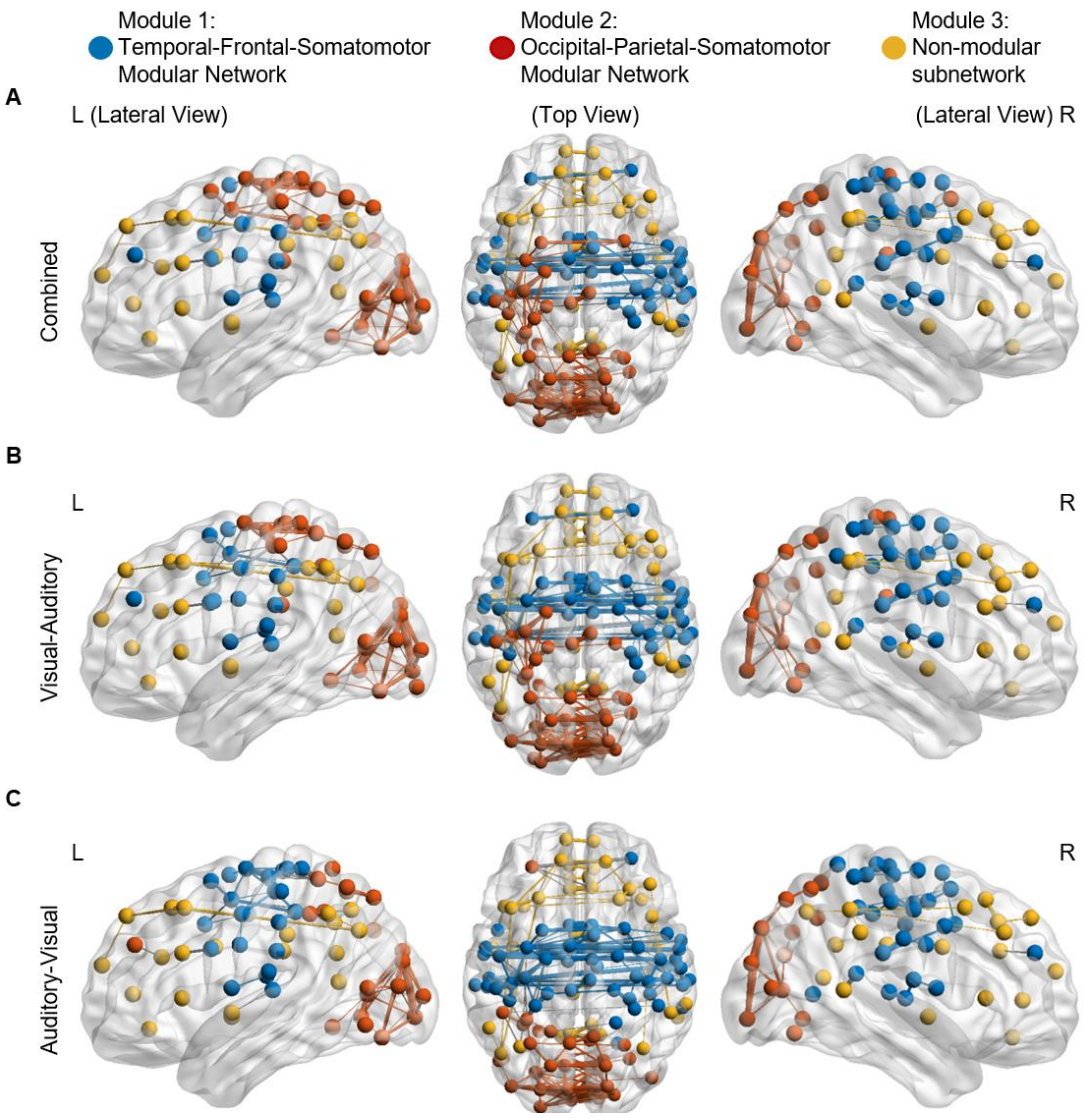


Figure 4.6. Network modularity analysis for the Visual-Auditory and Auditory-Visual conditions. A) Combined network modularity across both conditions. B) Modular structure of functional brain networks during the Visual-Auditory condition. C) Modular structure during the Auditory-Visual condition. Nodes represent brain regions, and edges represent the functional connections between them. Modules are color-coded: the Occipital-Parietal-Somatomotor Module (red), the Temporal-Frontal-Somatomotor Module (blue), and the non-significant module (yellow). Three views of the brain are shown: right hemisphere (R), top-down, and left hemisphere (L). This analysis highlights distinct modular organization patterns associated with each condition.

To quantify these results, we computed the modularity score (Q) for each sub-network, first in the combined dataset (Fig. 4.7A). Out of the three communities, modularity was significantly higher

than the null model for two modules: Module 1 (mean log value = 0.163; $q = 4.799\times10^{-4}$) and Module 2 (mean log value = 0.195, $q = 4.799\times10^{-4}$), but not for Module 3 (mean log value = -0.032, q = 0.998). There was a significant difference ($t(11) = -8.637$, $q = 4.693\times10^{-6}$) in modularity between Module 1 (mean = 1.179, SE = 0.022) and Module 3 (mean = 0.9684, SE = 0.007). There was also a significant difference ($t(11) = -9.280$, $q = 4.650\times10^{-6}$) between Module 2 (mean = 1.218, SE = 0.024) and Module 3. However, there was no significant difference in modularity between Module 1 and Module 2 ($t(11) = 0.913$, q = 0.379).

We then did the same for the order-separated networks (Fig. 4.7B-C). In both cases, the normalized modularity values were significantly greater than expected from a null model for Module 1 (mean log $value_{Vis\text{-}Aud} = 0.160$, $q = 4.499\times10^{-4}$; mean log $value_{Aud\text{-}Vis} = 0.146$, $q = 2.999\times10^{-4}$) and Module 2 (mean log $value_{Vis\text{-}Aud} = 0.198$, $q = 4.999\times10^{-4}$; mean log $value_{Aud\text{-}Vis} = 0.237$, $q = 2.999\times10^{-4}$). In the Vis-Aud condition, there was a significant difference between Module 1 (mean = 1.175, SE = 0.019) and Module 3 (mean = 0.971, SE = 0.009; $t(11) = -9.421$, $q = 4.011\times10^{-6}$) and between Module 2 (mean = 1.222, SE = 0.027) and Module 3 ($t(11) = -7.469$, $q = 1.872\times10^{-5}$). There was no significant difference between Module 1 and Module 2 ($t(11) = 1.163$, q = 0.276). However, there was a significant difference among all three modules in the Aud-Vis order (Fig. 4.7C): between Module 2 (mean = 1.273, SE = 0.035) and Module 3 (mean = 0.969, SE = 0.007; $t(11) = -7.917$, $q = 1.082\times10^{-5}$), Module 1 (mean = 1.158, SE = 0.017) and Module 2 ($t(11) = 2.333$, q = 0.040), Module 1 and Module 3 ($t(11) = -9.590$, $q = 3.362\times10^{-6}$). This pattern indicates that cue order does not induce a uniform network-wide change, but instead differentially affects subnetworks, likely reflecting their respective roles in processing recent versus previously integrated information.

Finally, there was a significant order-dependent difference in modularity for Module 2 ($t(11) = -3.036$, q = 0.035), but not in the other modules ($t(11) = 0.143$, q = 0.263 for Module 1; $t(11) = 0.215$, q = 0.832 for Module 3). These comparisons were performed at the standard modularity resolution parameter (γ) of 1, but modularity showed fairly consistent increases in all three datasets as the γ values were changed from 0.9 to 1.2 (Fig. 4.7D).

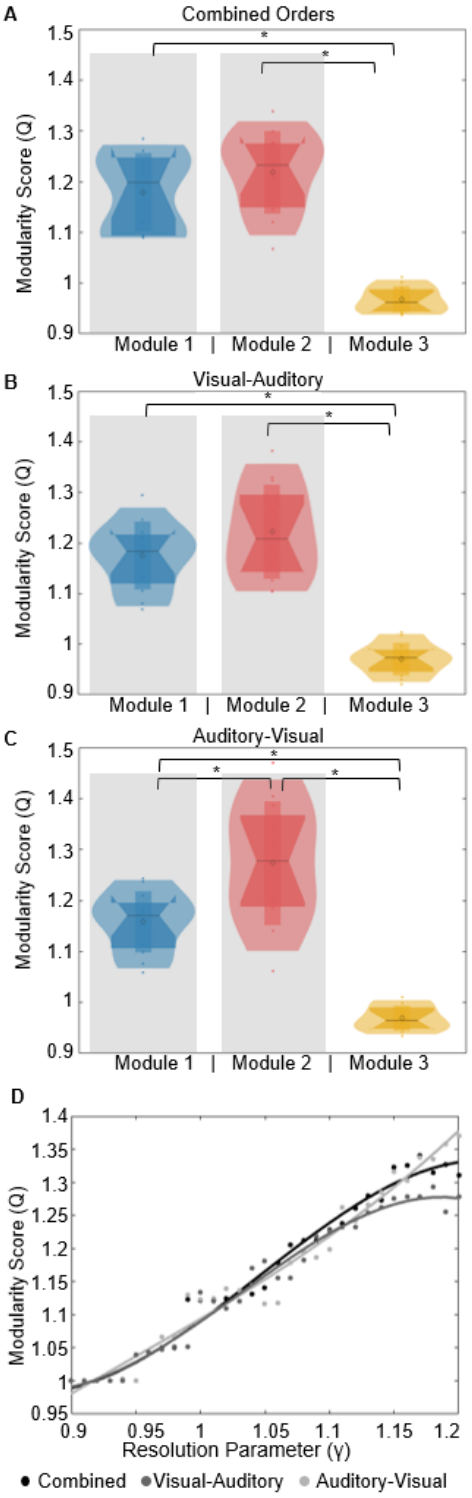


Figure 4.7. Modularity comparisons across experimental conditions and gamma values. A-C) Violin plots of modularity values for identified network modules when the orders are combined (A), in the Visual-Auditory condition (B), and the Auditory-Visual condition (C). Modules are color-coded: Module 1 (blue), Module 2 (red), and Module 3 (yellow). Asterisks (*) indicate significant differences between modules with $q<0.05$, and the grey boxes indicate modules with

modularity significantly greater than a random network. D) Modularity values as a function of resolution parameter for the Combined Order (black), Visual-Auditory Order (dark gray), and Auditory-Visual Order (light gray). Points represent data, and lines indicate best-fit curves. This analysis highlights differences in network modularity across task conditions and tuning parameters.

4.4.3.4 Classification Analysis: Cue Order-Dependence.

The analysis provided above suggests that global network parameters did not distinguish cue order-dependence, whereas the modularity parameter was modestly successful at distinguishing order. To confirm this objectively, we applied a classifier algorithm to identify which of our GTA measurements (Modularity, Clustering Coefficient, Global Efficiency, and Energy) could best distinguish between the order of cue presentation. Decoding was performed using a Narrow Neural Network classification algorithm.

The model achieved a positive predictive value (PPV) of 59.8% (95% Confidence Interval (CI): 55.5% to 62.3%) with a false discovery rate (FDR) of 40.2% (95% CI: 37.7% to 44.5%) for the Vis-Aud order, and a PPV of 59.9% (95% CI: 55.9% to 63.1%) with an FDR of 40.1% (95% CI: 36.9% to 44.1%) for the Aud-Vis order. The Kruskal-Wallis feature selection analysis showed that the Modularity scores from Module 2 (Occipital-Parietal-Somatomotor Modular Network), followed by Module 1 (Temporal-Frontal-Somatomotor Modular Network), were the most meaningful in differentiating between the two orders of cue presentation. This demonstrates that although overall classification accuracy was modest, the model was able to distinguish between the orders above chance level and confirms that modularity was the most important parameter.

4.4.3.5 Eigenvector Centrality Hubs.

Finally, we considered which nodes in our network acted as important 'hubs'. Eigenvector centrality was used to compute local (i.e., within-module) hubs. Fig. 4.8A shows the top 95th- and 99th-percentile eigenvector hubs in our modules when the orders are combined, as well as for the two cue presentation orders (Table 4.3). Hubs in Module 1 (blue) included nodes in bilateral dorsal anterior Cingulate Cortex (ROI47 & ROI146). Hubs for Module 2 (red) included Somatomotor Area (ROI78) and multiple occipital regions (in the left hemisphere – ROI37, ROI41, ROI46, ROI91, and ROI92 – and in the right hemisphere – ROI145 and ROI190). Overall, these hubs

corresponded to known components of the 'salience/attention' network (Schaefer et al., 2018; Seeley, 2019; Seeley et al., 2007) and occipito-parieto-frontal reach system.

When the cue orders were separated into Vis-Aud (Fig. 4.8B) and Aud-Vis (Fig. 4.8C), there was an overall decrease in the number of hubs in Module 2 (ROI91 – Left Striate Cortex and ROI37 – Left Extrastriate) and an increase in the number of hubs in Module 1 (ROI32 – Left Frontal Eye Field and ROI87 – Left Precentral Gyrus). Comparing the two orders, ROI78 (Left Precentral Gyrus) switched between modules, tending to join the module dominated by the first sensory cue (i.e., Module 1 for Aud-Vis, Module 2 for Vis-Aud). Otherwise, the hubs for the two cue orders were nearly identical, i.e., the same ROIs were identified as important hubs, and they showed the same module assignments.

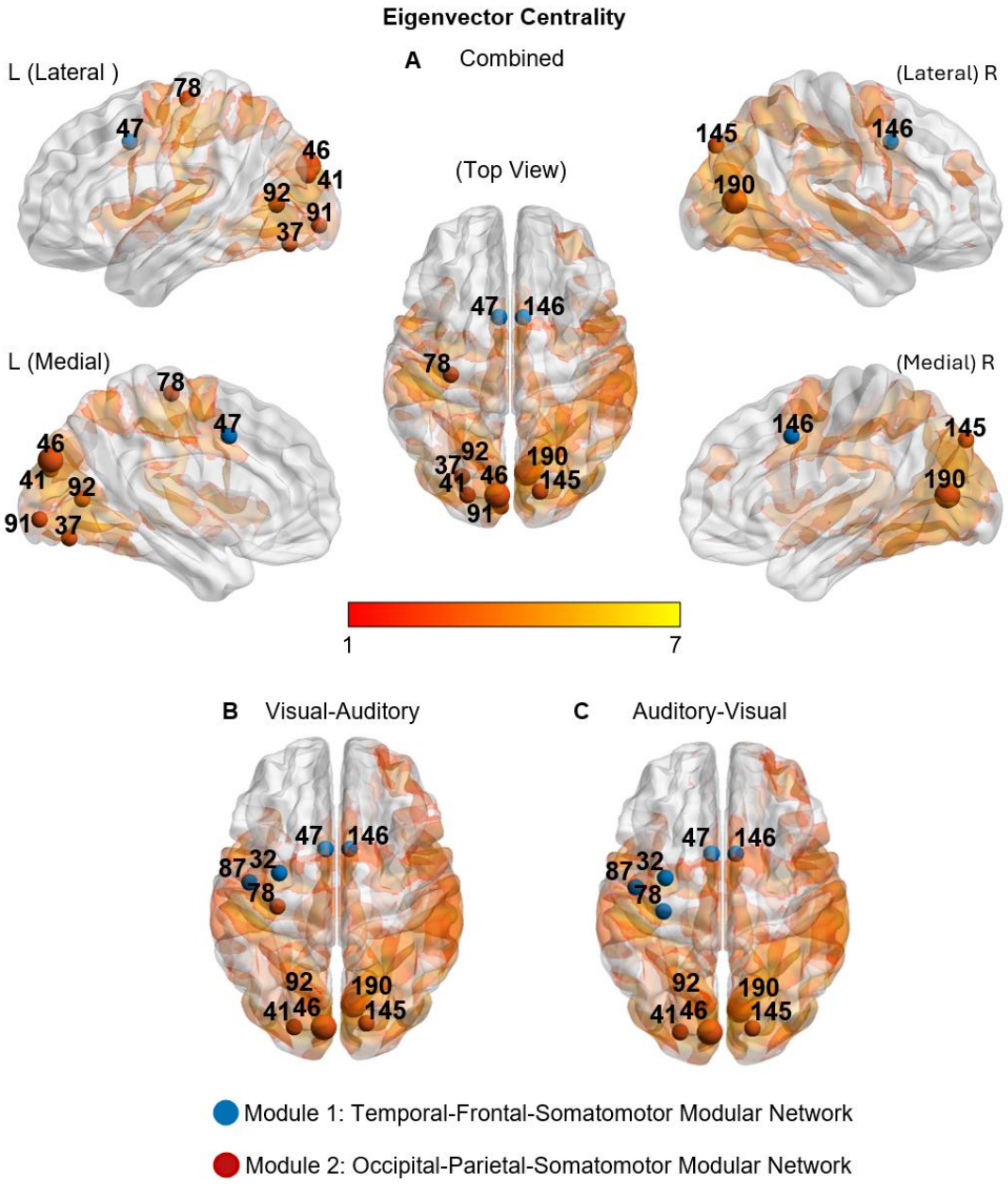


Figure 4.8. Eigenvector centrality hubs presented on brain maps overlaid with activation in the action phase for (A) the combined order, (B) the Visual-Auditory Order, and (C) the Auditory-Visual Order. Smaller hubs correspond to nodes with an eigenvector centrality above 95%, and larger hubs correspond to those with an eigenvector centrality above 99%. Blue nodes are part of the Module 1 – Temporal-Frontal-Somatomotor Module, and red nodes are part of the Module 2 – Occipital-Parietal-Somatomotor Module.

Table 4.3. Eigenvector Centrality Hubs

ROI #	ROI Name	Network	X	Y	Z	Module
32	Left Hemisphere Frontal Eye Fields parcel 1	Dorsal Attention Network B	-31	-4	53	1
37	Left Hemisphere Visual Central Extrastriate parcel 1	Visual Central Network	-26	-77	-14	2
41	Left Hemisphere Extrastriate parcel 5	Visual Central Network	-23	-87	23	2
46	Left Hemisphere Superior Extrastriate parcel 2	Visual Peripheral Network	-7	-87	28	2
47	Left Hemisphere Frontal Medial parcel 1	Salience/Ventral Attention Network A	-6	9	41	1
78	Left Hemisphere Somatomotor A parcel 4	Somatomotor Network A	-32	-22	64	1,2
87	Left Hemisphere Central parcel 2	Somatomotor Network B	-47	-9	46	1
91	Left Hemisphere Striate parcel 1	Visual Central Network	-5	-93	-4	2
92	Left Hemisphere Striate Calcarine parcel 1	Visual Peripheral Network	-11	-70	7	2
145	Right Hemisphere Superior Extrastriate parcel 3	Visual Peripheral Network	16	-85	39	2
146	Right Hemisphere Frontal Medial parcel 1	Salience/Ventral Attention Network A	7	9	41	1
190	Right Hemisphere Striate Calcarine parcel 1	Visual Peripheral Network	9	-75	9	2

Note: Col 1: ROI Numbers, Col 3-5 MNI coordinates, Col 6: Module associated with these hubs. ROIs derived from the 200 parcellation from the Schaefer 17 Networks Atlas (Schaefer et al., 2018).

4.4.3.6 Betweenness Centrality Hubs.

Betweenness centrality hubs represent nodes with broader 'connections', i.e., correlations that tend to cross between modules. Fig. 4.9 (Table 4.4) shows nodes with the top 95th and 99th percentiles of betweenness centrality, color-coded by module. When the orders were combined, the majority of the hubs were part of Module 1 (blue) and were located in the bilateral Frontal regions (ROI47, ROI86, ROI146, and ROI148), the bilateral Auditory Cortex (ROI84 and ROI182), and the Parietal Operculum Cortex (ROI160). In addition, there was one hub from Module 2 (red) in the right Occipital Cortex (ROI137) and two hubs from Module 3 (yellow) in the right Insula (ROI192) and Frontal Operculum Cortex (ROI148).

When the two orders were investigated separately, hubness was more distributed throughout the cortex, included more occipital nodes, and showed greater variability between the two conditions (compared to Eigenvector Hubs). Specifically, the two orders had four order-independent hubs, two of which are part of Module 1 (ROI47 in the left Frontal Cortex and ROI85 in the left Auditory Cortex), and three of which are part of Module 2 (ROI91 and ROI92 in the bilateral Occipital Cortex and ROI137 in the right Occipital Cortex). In addition, the Visual-Auditory condition had distinct hubs including four regions in the right Frontal Cortex from Module 1 (ROI165, ROI148, ROI164, and ROI184), three hubs part of the Occipital Cortex in Module 2 (in the left hemisphere: ROI41, ROI91 and in the right hemisphere: ROI141), and bilateral Temporal region as part of the Module 3 (ROI83 and ROI192). As for the Auditory-Visual Order, the hubs in Module 1 also included the right Frontal region (ROI146), the left Somatomotor area (ROI86), the right Auditory Cortex (ROI182), and the right Parietal Operculum Cortex (ROI160). Module 2 included hubs from the right Occipital regions (ROI190) and the left Lateral Prefrontal Cortex (ROI66). Finally, the non-significant module included hubs in the left Cingulate Cortex (ROI10). In short, compared to eigenvector hubs, betweenness centrality hubs tended to occupy more sensory nodes and were more cue order-dependent.

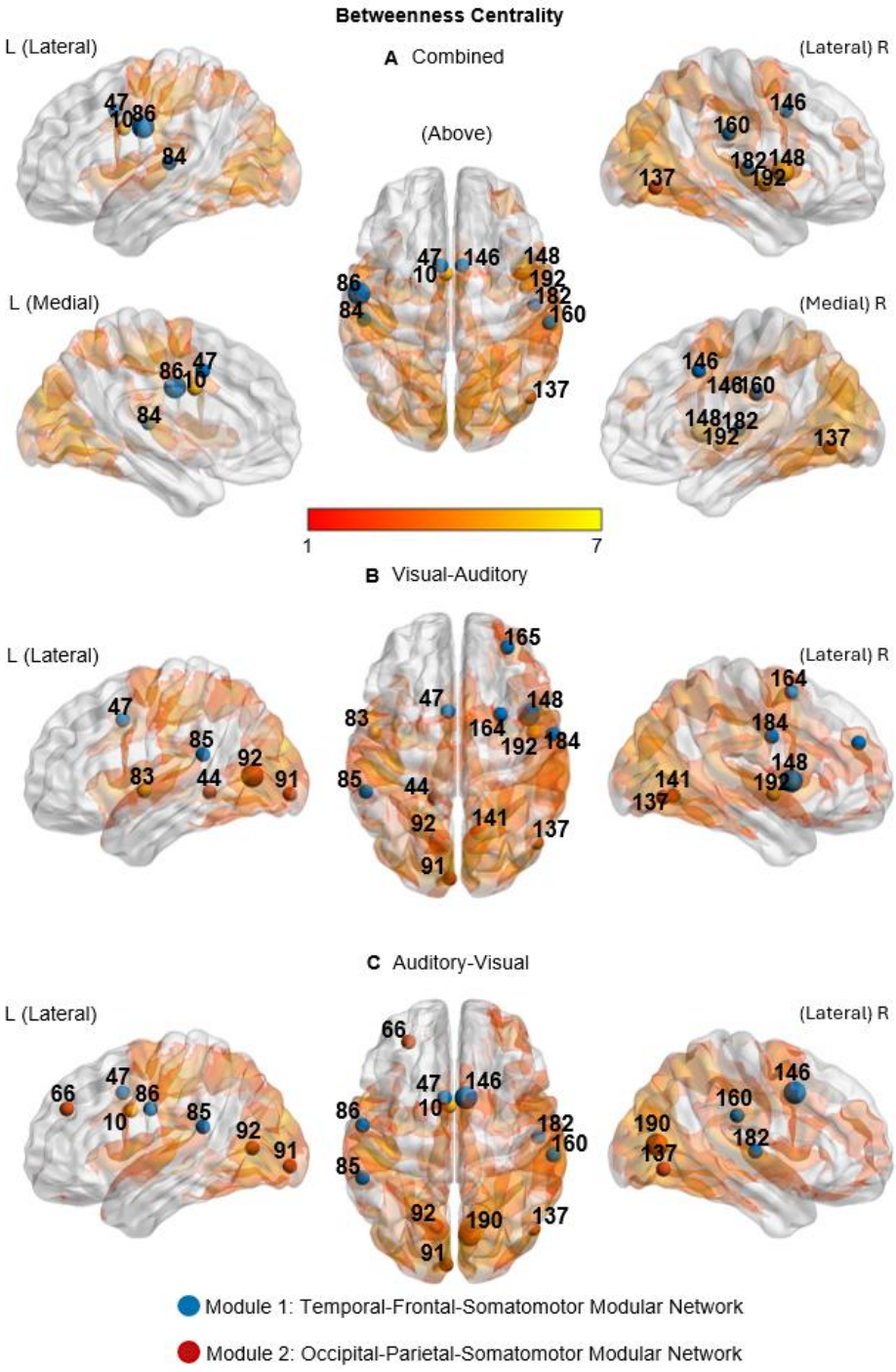


Figure 4.9. Betweenness centrality hubs are presented on brain maps overlaid with activation in the action phase for (A) the combined order, (B) the Visual-Auditory Order, and (C) the Auditory-Visual Order. Smaller hubs correspond to nodes with betweenness centrality above 95%, and larger hubs correspond to nodes with betweenness centrality above 99%. Blue nodes are part of the Module 1 – Temporal-Frontal-Somatomotor Module. Red nodes are part of the Module 2 – Occipital-Parietal-Somatomotor Module.

Table 4.4. Betweenness Centrality Hubs

ROI #	Name	Network	X	Y	Z	Module
10	Left Hemisphere Middle Cingulate parcel 1	Control Network A	-3	4	30	3
44	Left Hemisphere Inferior Extrastriate parcel 3	Visual Peripheral Network	-14	-44	-3	2
47	Left Hemisphere Frontal Medial parcel 1	Salience/Ventral Attention Network A	-6	9	41	1
66	Left Hemisphere Lateral Prefrontal Cortex parcel 1	Salience/Ventral Attention Network B	-28	43	31	2
83	Left Hemisphere Auditory parcel 1	Somatomotor Network B	-51	-4	-2	3
84	Left Hemisphere Auditory parcel 2	Somatomotor Network B	-53	-24	9	1
85	Left Hemisphere Auditory parcel 3	Somatomotor Network B	-56	-40	20	1
86	Left Hemisphere Central parcel 1	Somatomotor Network B	-56	-8	31	1
91	Left Hemisphere Striate parcel 1	Visual Central Network	-5	-93	-4	2
92	Left Hemisphere Striate Calcarine parcel 1	Visual Peripheral Network	-11	-70	7	2
137	Right Hemisphere Extrastriate parcel 2	Visual Central Network	48	-71	-6	2
141	Right Hemisphere Inferior Extrastriate parcel 1	Visual Peripheral Network	12	-65	-5	2
146	Right Hemisphere Frontal Medial parcel 1	Salience/Ventral Attention Network A	7	9	41	1
148	Right Hemisphere Frontal Operculum parcel 1	Salience/Ventral Attention Network A	43	7	4	1
160	Right Hemisphere Parietal Operculum parcel 1	Salience/Ventral Attention Network A	60	-26	27	1
164	Right Hemisphere Dorsal Prefrontal Cortex parcel 1	Control Network A	26	7	58	1

165	Right Hemisphere Lateral Prefrontal Cortex parcel 1	Salience/Ventral Attention Network B	30	48	27	1
182	Right Hemisphere Auditory parcel 1	Somatomotor Network B	51	-15	5	1
184	Right Hemisphere Central parcel 1	Somatomotor Network B	58	-5	31	1
190	Right Hemisphere Striate Calcarine parcel 1	Visual Peripheral Network	9	-75	9	2
192	Right Hemisphere Insula parcel 2	Salience/Ventral Attention Network A	46	-4	-4	3

Note: Col 1: ROI Numbers, Col 3-5 MNI coordinates, Col 6: Module associated with these hubs. ROIs derived from the 200 parcellation from the Schaefer 17 Networks Atlas (Schaefer et al., 2018).

4.5 Discussion

Movement can be initiated by multisensory top-down and bottom-up signals, which are integrated to achieve the desired action. In this study, we explored 1) how such cues (verbal instruction for grip orientation and visual cues for object attributes) are integrated into the motor system, and 2) whether this is influenced by the order of presentation. Overall, we found that cue integration is not undertaken by a single region or evenly distributed across all cortical areas. Instead, we found that cue-related information was processed through cortical sub-modules that progressed from the sensory cortex, communicated laterally, and finally converged in the somatomotor cortex.

Specifically, our univariate analysis revealed order-dependent responses in the sensory cortex, followed by widespread order-independent activation during the planning and execution phases. The analysis of global network properties showed that we were dealing with a non-random network with order-independent global parameters. Mesoscale analysis revealed that the data can be divided into three modules, with two significantly modular subnetworks: the temporal-frontal-somatomotor and occipital-parietal-somatomotor modules. These modules included hubs in the frontal and occipital cortex, respectively, whereas 'betweenness' hubs (thought to be involved in intermodular communication) were found in the auditory / frontal cortex, and the occipital cortex, respectively, with additional hubs in the non-significant module. In our classification analysis, we found that the modularity index values for these two modules were the most effective parameter

for distinguishing between the order of cue presentation. We will discuss each of these results, in particular their relation to cue integration and its order-dependence, below.

4.5.1 Univariate Analysis: Activation and Order Dependence

During cue presentation phases, activation was primarily observed in sensory-related regions (Fig. 4.3), with a transient response in A1 during the verbal instruction and a more sustained response in V1 once the grasp target was illuminated. As expected, these responses were order-dependent, most clearly arising first in the sensory area corresponding to the modality of the first cue. In addition, we observed activation in restricted premotor and sensorimotor regions during cue presentation, consistent with advanced processing of visual and auditory information and preparation for the upcoming action (Hall et al., 2000; Singhal et al., 2013; Vannest et al., 2009).

As participants transitioned through the different phases of our task, we observed a typical increase in brain activity, culminating in widespread, order-independent cortical activation during the action execution phase (Begliomini et al., 2008; Brandi et al., 2014; Cappadocia et al., 2017; Klein et al., 2023). This included occipital-parietal-frontal areas, which are required to accomplish visually-guided movement (Gallivan & Culham, 2015; Vesia & Crawford, 2012). In addition, we observed activation within the 'action mode' network, including cingulo-opercular areas thought to support the integration of bottom-up visual information with task-relevant information (Dosenbach et al., 2025; Yu et al., 2023). These data suggest that cue integration is occurring, but do not show how.

None of these results were surprising, and indeed that was the point of this analysis: to show that our task showed the expected order-dependent sensory activation and robust sensorimotor activation required for our network analysis.

4.5.2 Graph Theory Analysis of Functional Network Properties

The main assumption behind this study is that multimodal cue integration for action is accomplished through functional network properties, rather than specific sites. The basic concept behind functional network analysis is that signal correlations reflect the propagation of information through a network (Sporns, 2002). This is illustrated in Figure 4.5, where all four example regions of interest show a general rising trend in activation, which has been associated with global integration (Musa et al., 2025), but some pairs (notably A1 and PMC, and V1 and SPL) show higher degrees of correlation. Graph Theory analysis provides a means to formally quantify these

relationships across many nodes. The insights gained from this analysis are described in the following sub-sections.

4.5.3 Order-Independent Integration at the Global Level

We used global network measures and normalized them to a random network model to assess whether they differed significantly from the null model (Ghaderi et al., 2023; Musa et al., 2025; Váša & Mišić, 2022). Both the combined and order-dependent networks were shown to be 'true', i.e., non-random networks (Fig. 4.7). Specifically, these networks showed 1) significantly lower Global Efficiency, consistent with the greater constraints in information processing present in a real brain network (Bullmore & Sporns, 2009; Latora & Marchiori, 2001), 2) significantly higher clustering coefficients, a measure of how well the network formed clusters of highly correlated nodes, (Achard & Bullmore, 2007; Tomasi et al., 2013), and 3) significantly lower Energy reflecting the effort used to maintain organization in the network (Rubinov & Sporns, 2010; Watts & Strogatz, 1998).

4.5.4 Network Integration: Modules and their Local Hubs

We next examined modularity, a mesoscale measure of how well a network can be divided into communities (modules), to understand how top-down auditory and bottom-up visual cues were integrated into the reach network. We also considered local 'eigenvector centrality' hubs within these modules, which generally aligned well with activation maps from the execution phase (Fig. 4.8-9).

Module 1. As shown in Figure 4.6A, the temporal-frontal-somatomotor module contained nodes in the primary auditory cortex and areas involved in reach planning execution, including premotor regions, SMA, and most of the bilateral somatomotor cortex (Gallivan et al., 2011; Hanakawa et al., 2008; Pilacinski et al., 2018). Local 'Eigenvector' hubs in this module included bilateral anterior cingulate cortex, implicated in the 'action-mode network' (Dosenbach et al., 2025). Although one cannot infer anatomy or causality from this data, based on previous anatomic and physiological studies, our results strongly suggest that the auditory instruction for the motor strategy (horizontal vs. vertical grip) was incorporated into motor planning and execution through this module. In particular, these components of this module are consistent with previous studies suggesting that the auditory-verbal-motor processing stream travels from the superior temporal

cortex to the inferior frontal cortex and reaches the premotor cortex (Hickok & Poeppel, 2015; Rauschecker, 2011).

Module 2. The occipital-parietal-somatomotor module included much of the visual cortex, as well as parietofrontal areas involved in visuomotor transformation, including SPOC, IPS, superior parietal cortex, and portions of the left somatomotor cortex contralateral to the hand used. Hubs for this network were mainly found in the visual cortex, with one in the left somatomotor cortex. Again, based on the known physiology of these areas, our network data strongly suggest that the visual aspects of the task (location, shape, size, orientation of the object) were communicated through this module (Cavina-Pratesi et al., 2010; Gallivan et al., 2009; Gallivan & Culham, 2015; Singhal et al., 2013). Overall, the components of this module are consistent with the classic notion of a dorsal (occipital-parietal-frontal) visual stream for visually guided action (Goodale et al., 1994; Goodale & Milner, 1992)

Module 3. While its modularity was not statistically significant, this community is worth noting because it contains many high-level temporal and frontal areas implicated in non-sensorimotor functions such as attention, salience, task selection, and decision-making (Moerel et al., 2024; Rens et al., 2017; Rossi et al., 2009).

Order-Dependence. Interestingly, more hubs appeared when we separated our data by cue order, including the frontal eye fields (FEF) within the dorsal attention network, the dorsal anterior cingulate cortex (ACC) within the ventral attention network, and nodes of both the dorsal and ventral somatomotor networks. These regions may be more strongly engaged in the later phases of integration, as frontal and motor regions are recruited for action execution. In particular, the dorsal ACC has been linked to action planning, decision making, and behavioural adaptation (Kurkela & Ritchey, 2024; Srinivasan et al., 2013). However, local hubs were virtually identical in the two orders (Fig. 4.8B-C). This supports the notion that local hubs are relatively stable in their membership to specific modules.

The exception is that Modules 1 and 2 seemed to 'compete' for the left somatomotor hub, depending on which came first. This is reflected more broadly in the pattern that either Module 1 or 2 invaded the left somatomotor cortex (as if competing for right-hand dominance), depending on which cue appeared first. This seems to underlie our finding that Modules 1 and 2 were most important for decoding task order from these data.

4.5.5 Lateral Integration: Betweenness Centrality

Is cue integration only achieved through feedforward processing? Another measure, Betweenness Centrality, provides the potential to identify putative hubs for lateral communication between modules. As shown in Figure 4.9, betweenness centrality hubs appeared in broader areas, including more sensory areas, especially when the data were separated by cue order. Important hubs were found within the control network and somatomotor network for Module 1, within the visual central and visual peripheral networks for Module 2, and within the salience/attention and action-mode networks for the two modules (Dosenbach et al., 2025; Seeley, 2019). These findings suggest that our two cue-dependent modules (one and two) communicate with each other before information converges in the somatomotor cortex. If so, integration is an ongoing process involving both lateral and feedforward converging projections.

4.5.6 Caveats and Limitations

Our findings suggest that (at the level of the BOLD signal) cue integration is distributed between communicating modules rather than concentrated in a few distinct areas, a pattern that has also been reported in previous studies (Bertolero et al., 2015; Cavina-Pratesi et al., 2010; Gordon et al., 2018; Vossel et al., 2014). However, several caveats are worth considering. First, we again acknowledge that our number of participants was low by current standards, although this is offset by the robust and reliable activation produced in our task (Fig. 4.3), and our statistical analyses suggest that even the more modest effects (i.e. the order-dependence) were sufficiently reliable for univariate and GTA analysis, and ultimately the results made sense in terms of the previous literature.

Second, our attempts to derive specific sites for integration *within* ROIs have consistently failed, but it is always important to replicate results using other tasks and recording techniques. Third, a recent study suggested that the directionality and linearity of the BOLD response may not correlate with neural activity as well as previously thought (Epp et al., 2025). To some degree, functional connectivity is less sensitive to this problem, since it relies on the absolute value of BOLD-to-BOLD correlations. But still, all such results are correlative, so any discussion of causation, direct communication, or directionality is speculative. Fourth, the BOLD response likely represents the 'democratic vote' of large populations of neurons, so there is likely far more diversity and intermingling of cue signals within regions of interest revealed by our data. Finally, we only

examined cortical networks; however, subcortical regions, the basal ganglia, cerebellum, and thalamus, likely also contribute to these networks (Battaglia-Mayer & Caminiti, 2019).

4.5.7 Possible Clinical Implications

It is well established that damage to the dorsal visual stream (corresponding to our Module 2) interrupts the visually guided movement (Goodale & Milner, 1992; Khan et al., 2007; Khan et al., 2005; Pisella et al., 2000) and based on our data, one would expect damage to our Modules to degrade the ability to use verbal commands for action (Wheaton & Hallett, 2007). This does not mean that these modules are fixed; indeed, we expect that specific cues are flexibly integrated via distinct modular streams, depending on both the sensory modality and the cue's relevance to the task. For example, one might speculate that switching the meaning of our cues (i.e., visual for motor strategy and auditory for location) or pairing a completely different sensory modality (e.g., somatosensory) with a different outcome (e.g., to make an eye movement) would result in an entirely different network (Groh & Werner-Reiss, 2002; Rens et al., 2017).

This combination of network distribution and modular specificity could explain why some patients retain partial function after focal damage, as alternative routes are used to maintain communication across the network. And again, these alternative networks might include subcortical pathways (Battaglia-Mayer & Caminiti, 2019; Grefkes & Fink, 2011; Guggisberg et al., 2019). Extending our task-related functional network approach could lead to a better understanding of how plasticity contributes to brain injury recovery and how degeneration in brain diseases like dementia and Parkinson's disease can be delayed (Bedford et al., 2025; Hao & Zou, 2025; Jahan et al., 2026).

4.5.8 Conclusion

Overall, these analyses suggest that multimodal integration of visuospatial cues and verbal instructions for reach is a network phenomenon, involving two separate (occipital-parietal and temporal-frontal) modules that communicate via lateral connections and converge in the somatomotor cortex. Within these modules, local network hubs may participate in this process through relatively fixed sensorimotor roles for a given task, whereas more distributed sensory and motor 'betweenness' hubs may underlie the lateral communication. Finally, in our task, varying cue order had relatively little effect on cortical networks at the global level, but produced subtle, decodable effects at the mesoscale (modular) and local levels. This approach, combining event-related recordings, univariate analysis, and whole-brain functional connectivity, may also

be useful for understanding cortical networks for rehabilitation following damage. Overall, this study shows that multisensory-motor integration of top-down instructions and bottom-up sensory cues is achieved through parallel but laterally communicating and serially converging modules.

CHAPTER 5:

GENERAL DISCUSSION

5.1 General Summary of Results

Our nervous system is continuously flooded with sensory stimuli that need to be processed, combined, and/or contrasted to form a unified experience of the world and to execute an intended action. The principal goal of this thesis project was to deepen our understanding of the multitude of cognitive processes involved in motor control planning and execution. To this end, I completed three experiments: 1) looking at how variation in visual input results in a change in object placement error in contrast to what is known from reach-to-grasp literature, 2) expanding the subject by investigating the cortical-cerebellar juxtaposition between grasp and placement, and 3) exploring how cross-modality integration of sensory information through bottom-up visual cues and top-down auditory instructions is achieved in grasp planning and execution.

Chapter 2 took a behavioural approach to question how visual information and its updates influence the endpoint reach location and placement orientation. In Experiment 1, similar to reach, placement exhibited the standard endpoint overshoot error in location and showed a greater error amplitude after a memory delay in Experiment 2. In contrast, endpoint orientation error was more affected by the template orientation than the gaze location. In Experiment 2, a longer memory delay increased the amplitude of endpoint overshoot errors. Furthermore, the type of saccade affected the direction and eccentricity of the observed reach error, increasing variability in orientation error. This demonstrates that reach-to-grasp and reach-to-place, while they share some similarity in overshoot effect, remain distinct actions that can be reflected in their error type.

Broadening the comparison between initiating and terminating an interaction with an object, Chapter 3 showed that grasp and placement, both visuomotor actions, share highly similar brain activity patterns and functional connectivity features. However, placement required a substantial recruitment of sensorimotor regions and the cerebellum, reflecting its greater motor complexity and a pronounced need for coordination to achieve the required movement. Furthermore, movement intentions were more readily deciphered during the preparatory state and were

indistinguishable during the execution phase. Therefore, it unveils a seemingly generic, methodical process during execution. Surprisingly, during planning, there was a noticeable difference between grasping and placing in S1 despite the region receiving identical haptic input, indicating that movement intention affects perception and that stakes rise with the complexity of the upcoming task. This shows that it is not only the type of sensory information available but also its importance for the movement that influences the neural response.

Expanding this sensory modality reality, a subsequent fMRI study was analyzed to consider the multimodal integration of visual cues and auditory verbal instruction (Chapter 4). The graph-theoretic analysis demonstrated that the two information types communicate via two functional connectivity modules (the Occipital-Parietal-Somatomotor Module and the Temporal-Frontal-Somatomotor Module), thereby integrating in sensorimotor regions. Putatively, they originate in their respective encoding regions in the auditory and visual cortices and interact with frontal and parietal cortices, while they are processed for integration. While I could infer the cue order from the GTA modularity scores, it had only a marginal influence on brain activity and global connectivity features.

Collectively, these studies converge on a single principle: goal-directed actions are not dictated by a fixed motor program driven by stimulus parameters, but by a complex, dynamic network that combines bottom-up sensory information, top-down comprehension, and one's intention. This flexibility is implemented across distributed, partially segregated cortico-cerebellar networks rather than in a focal integrative locus. Grasping and placing share a common scaffold as goal-directed actions, yet placing is not simply grasping in reverse. It showed greater variability in endpoint orientation and depended more heavily on the cerebellum and action-related sensorimotor regions. Placement intention elicits a distinct somatosensory response during grasping, even when presented with identical haptic information. A similar intention-driven flexibility appears at the level of sensory input: top-down auditory instructions and bottom-up visual cues are integrated through coordinated communication across multiple cortical network modules. Taken together, the thesis reframes reaching, grasping, and placing not as a catalogue of distinct motor behaviours but as a family of intention-dependent operations implemented across a distributed cortico-cerebellar network.

5.2 Scientific Implications

The results have a tangible impact on the field. Here, I would like to explore three implications of the findings and methodology for motor control research. Firstly, in goal-directed movement, action termination is not just the biomechanical reverse of action initiation. My results show that placement has a distinct visuomotor processing effect, influenced by its intention, and necessitates greater recruitment of sensorimotor-cerebellar regions. Whereas grasp orientation error is gaze-dependent, with or without an intervening saccade (Selen & Medendorp, 2011), placement orientation was more strongly governed by the template than by gaze, indicating that the two actions draw on object features differently. Placement is not simply the reverse of grasping, but a distinct visuomotor operation that depends on action intention, haptic state, orientation constraints, and sensorimotor/cerebellar coordination. Broadly put, the kinematic and neural similarities of the two movements cannot be inferred from their apparent symmetry; they need to be investigated to reveal their uniqueness.

Secondly, the plethora of information integrated to perform an action, including but not limited to movement intention, somatosensory information, visual contributions, and auditory instruction, is not simply achieved by their recruitment into a distinct brain area. Instead, a distributed set of subnetworks is employed to integrate higher-order processes with sensory information and to converge the motor command for executing the action. This argues against a single-locus account of multisensory integration for action and reframes integration as a property of coordinated, partially segregated networks.

Finally, this dynamic change demonstrates the value of combining task-based fMRI with a graph theoretical model of functional connectivity. Functional connectivity analysis is well established in resting-state studies, in which changes in functional connectivity before and after an intervention are investigated (Van Den Heuvel & Hulshoff Pol, 2010). Resting-state designs, however, cannot capture the online reconfiguration of networks that occurs as a task unfolds. Therefore, using task-based fMRI remains essential, and when combined with graph-theoretical analysis, it allows one to examine the network from multiple angles at the global, meso-, and local scales. This approach offers the field a means of asking not only which regions change their activity during an action, but also how the network is reorganized to drive the interaction.

5.3 Potential Applications

Because grasp and placement engage partially distinguishable neural resources, and verbal instruction can impact the motor plan, the results of these studies warrant practical consideration for how motor disorders are assessed and treated. The distinction observed in S1, M1, PMd, and aIPS indicated that the two actions are processed differently and could have consequences at three stages of clinical care.

In the diagnostic realm, grasp and placement could be impaired independently. Therefore, assessing the two actions separately may reveal grasp-only or place-only deficits, which are missed when the action is tested as a broad concept, because the approach used to compensate for the movement might obscure their differences. A patient could successfully grasp an object but fail to maintain grip strength, use haptic feedback, or display additional coordination to transport and place it in a tight space. Evaluating placement as a distinct ability could sharpen the detection of specific sensorimotor deficits.

In targeted cerebral treatment, this work revealed that movement intention matters, and that the involvement of sensorimotor areas depends on the action's goal and complexity rather than on muscle responses alone. These elements should be considered when exploring a possible site for stimulation or neuromodulation. Framing interventions around the action goal, rather than only the affected effector, may improve their precision. For example, sensory loss after stroke can impair manipulation even if motor function is largely unaffected (Kita et al., 2013). In addition, bradykinesia in Parkinson's patients describes a deficit in movement initiation that may result from an impairment of the basal ganglia-thalamocortical circuitry (Fasano et al., 2022). In these two cases, targeted intervention would need to be assessed to help diminish or reverse the affected motor defect.

In the rehabilitation domain, improvement in one skill does not necessarily mean that its extension will improve over time. Moreover, the way an action goal is presented in verbal instruction and the focus of attention (the effector vs the action goal) can shape the movement outcome. Therefore, instruction design becomes an important vehicle for success in rehabilitation, as the same action, but framed differently, can generate differences in

performance. These could have implications for both patients' recovery and even athletes seeking to reach their full potential.

The differentiation we observed in S1, M1, PMd, and aIPS demonstrates that not all movements are achieved using the same processes, indicating a contrast in how grasp and placement are processed. The greater activation of S1 and M1 during placement could reflect their specific involvement in movement preparation and execution. This could have implications for rehabilitation, where failure in haptic feedback or motor processing could cause a greater deficit in the transport and disposal of an object, even when the ability to perform the initial grasp to acquire the object is intact. Therefore, work on the action goal and complexity is essential in rehabilitation efforts and tentative stimulation location.

5.4 Limitations

For practical and methodological reasons, the three studies presented were conducted in a highly controlled environment. This control provides an essential condition for isolating and identifying the effect of each variable tested. However, it constrains how well the findings can be extended to natural behaviour. In this section, I will discuss four of these limitations: the unnatural constraints imposed on participants, the existing gap between laboratory-controlled tasks and real-world action, demographic restrictions in the tasks, and the fundamental limitations of the neuroimaging methods used.

The experimental settings restricted movements that are normally free. In both the behavioural task and the MRI scanner, participants' head and eye movements were constrained. These were chosen to minimize motion artifact in the scanner and to control gaze shifts in the behavioural task, thereby requiring participants to perform actions that are not as fluid and dynamic as natural action. In addition, participants performed the task in the scanner in an atypical supine position with their head tilted. The actions were also realized in the dark or in dim light to control visual feedback. This reduced visibility results in decreased visual acuity and degrades foveal vision relative to everyday viewing. Each of these constraints improves experimental control at the cost of mimicking natural reach, grasp, and placement movements.

The tasks executed were simplified versions of natural behaviour, which are generally not done in isolation and carry a lot of context and meaning. In the behavioural task, the placement was

completed against a screen, and the return to the home position was used instead of place and let go, as one would do when returning a book to a bookshelf, for example. As a result, the action lacked purpose and a meaningful goal. Thus, it is not clear how these findings generalize to real object interaction, to the richness of everyday tasks, and to how purposeful object manipulations impact motor planning and execution.

The findings are also constrained by the demographics of the sample. All participants were healthy young adults, yet visuomotor processing, central to this work, changes across the lifespan and is precisely what is disrupted by motor-related neurological conditions. Young adults are important to study, as they can help establish a baseline for comparing behavioural changes. Yet, this restriction limits how well the findings can be applied to the entire population. The specificity of motor control development in early childhood and the deficits in old age remain to be explored, especially if we intend to use similar findings to influence diagnostic and rehabilitation initiatives. It is, therefore, important to assess how these features change throughout the life span. Furthermore, another demographic limitation was applied by focusing on right-handed individuals, especially for the fMRI studies. Although they represent approximately 10.6% of the population (Papadatou-Pastou et al., 2020), left-handed participants are often excluded from studies of visuomotor action, particularly in neuroimaging, because they display a unique pattern of hemisphere specialization (Hervé et al., 2013). However, it is important to consider how the results can generalize to the rest of the population.

In addition to the constraints mentioned above, the fMRI neuroimaging approach carries intrinsic limitations in its data acquisition, which cannot be ignored. fMRI measures the hemodynamic response, a slow, indirect indicator of neural activity. Therefore, its limited temporal resolution cannot fully capture the rapid changes present in motor control. Furthermore, it is very sensitive to motion in the scanner and creates a dichotomy, as participants are required to remain still while performing hand and lower-arm movements to the target.

5.5 Future Directions

While the studies conducted offer valuable insights into how goal-directed actions are planned and executed, there remain multiple avenues for future consideration to understand how they can

generalize to the entire population. This could be achieved through four initiatives to address the limitations reported above.

The behavioural constraints used in the task could be relaxed in future work to offer a more naturalistic setting. Using a head-free, gaze-unrestrained, full view of the objects would allow participants to optimize their movements as they see fit. Much is known about naturalistic grasping, but comparable work directly contrasting grasping and placement, under head-free, gaze-unrestrained conditions with the target fully visible, is still lacking. By tracking posture, head, and eye locations, we could better understand the contribution of these features to a productive action.

The actions studied in these experiments were deliberately simple. Future research could vary movement complexity and include purposeful object manipulation, for instance, contrasting writing with a pen to writing using finger tracing on a touchscreen. In this simple case, the movement intention – to write – remains the same, but the effort's complexity increases. Milner and colleagues (Milner et al., 2006) have reported an increase in cerebro-cerebellar response as object-manipulation complexity increases. However, more research is needed to understand how changes in dexterity requirements affect motor output during object manipulation.

Since all participants were healthy young adults, the next essential step is to test how these processes vary across demographics. Developmentally, it is unclear whether placement matures alongside grasp or follows its own trajectory. There is evidence that infants grasp early in development by three to four months, but only begin stacking and placing by ten months (Marcinowski et al., 2019). At the other end of the lifespan, declining motor control in healthy aging, as well as its further disruption after neurodegeneration, may affect the stages of object interaction unequally. Another component would be to expand the comparison to include left-handed individuals and to take into account their uniqueness. Including these groups is necessary both to reflect the population and to develop rehabilitation tools that apply beyond healthy, right-handed young adults.

The temporal limits and challenges of handling movement artifacts in fMRI invite the consideration of neuroimaging methods. With EEG, MEG, and fNIRS, neural activity can be

measured directly at higher temporal resolution. Furthermore, fNIRS has a greater tolerance for movement and would be ideal for a more naturalistic investigation of the neural basis of motor control planning and execution. Pairing these recordings with motion capture of the head, eye, and limb could help link rapid neural dynamics to movement kinematics. In addition, perturbation methods such as transcranial magnetic stimulation could test whether the regions implicated here are causally necessary, moving beyond the correlational picture that functional connectivity alone can provide.

5.6 Conclusion

Our countless daily interactions with the world, with all its intricacies, are only possible through the effortless performance of goal-directed movements. Whether to initiate or terminate the interaction with an object, the brain relies on an elaborate process to decipher among multiple sensory inputs, integrate the desired motor output, process the instruction provided, and adapt through feedback loops. The work presented in this thesis examined that process across its full arc, exploring the behavioural and neural similarities and differences between reach-to-grasp and reach-to-place, and considering the verbal instructions received during prehension. Its central contribution is to show that placement is not simply grasping in reverse, but a distinct visuomotor operation shaped by action intention, haptic state, orientation constraints, and sensorimotor–cerebellar coordination. More broadly, the findings argue that object-directed actions are not fixed motor programs read from the stimulus. Still, flexible operations shaped by intention and task instructions are implemented across distributed, partially segregated networks rather than any single region. By characterizing these processes from their behavioural signatures to their network organization, this thesis advances our understanding of the fundamental components of action and points toward applications for diagnosing and rehabilitating movement after brain injury and disease.

REFERENCES

Abraham, A., Pedregosa, F., Eickenberg, M., Gervais, P., Mueller, A., Kossaifi, J., Gramfort, A., Thirion, B., & Varoquaux, G. (2014). Machine learning for neuroimaging with scikit-learn. *Frontiers in Neuroinformatics*, *8*. https://doi.org/10.3389/fninf.2014.00014

Achard, S., & Bullmore, E. (2007). Efficiency and Cost of Economical Brain Functional Networks. *PLoS Computational Biology*, *3*(2), e17. https://doi.org/10.1371/journal.pcbi.0030017

Aguirre, G. K. (2007). Continuous carry-over designs for fMRI. *NeuroImage*, *35*(4), 1480–1494. https://doi.org/10.1016/j.neuroimage.2007.02.005

Allan, M. S., Clause, D., Pierre, F., John, K., & Nathalie, P. (1993). Comparing Cerebellar and Motor Cortical Activity in Reaching and Grasping. *Canadian Journal of Neurological Sciences / Journal Canadien Des Sciences Neurologiques*, *20*(S3), S53–S61. https://doi.org/10.1017/S0317167100048538

Andersen, R. A., Andersen, K. N., Hwang, E. J., & Hauschild, M. (2014). Optic Ataxia: From Balint's Syndrome to the Parietal Reach Region. *Neuron*, *81*(5), 967–983. https://doi.org/10.1016/j.neuron.2014.02.025

Andersen, R. A., & Buneo, C. A. (2002). Intentional Maps in Posterior Parietal Cortex. *Annual Review of Neuroscience*, *25*(1), 189–220. https://doi.org/10.1146/annurev.neuro.25.112701.142922

Andersen, R. A., & Cui, H. (2009). Intention, Action Planning, and Decision Making in Parietal-Frontal Circuits. *Neuron*, *63*(5), 568–583. https://doi.org/10.1016/j.neuron.2009.08.028

Ariani, G., Pruszynski, J. A., & Diedrichsen, J. (2022). Motor planning brings human primary somatosensory cortex into action-specific preparatory states. *eLife*, *11*, e69517. https://doi.org/10.7554/eLife.69517

Ariani, G., Wurm, M. F., & Lingnau, A. (2015). Decoding Internally and Externally Driven Movement Plans. *The Journal of Neuroscience*, *35*(42), 14160–14171. https://doi.org/10.1523/JNEUROSCI.0596-15.2015

Avanzini, P., Fabbri-Destro, M., Campi, C., Pascarella, A., Barchiesi, G., Cattaneo, L., & Rizzolatti, G. (2013). Spatiotemporal dynamics in understanding hand—Object interactions. *Proceedings of the National Academy of Sciences*, *110*(40), 15878–15885. https://doi.org/10.1073/pnas.1314420110

Ballard, D. H., Hayhoe, M. M., Li, F., & Whitehead, S. D. (1992). Hand-eye coordination during sequential tasks. *Philosophical Transactions of the Royal Society of London. Series B: Biological Sciences*, *337*(1281), 331–339.

Baltaretu, B. R., Monaco, S., Velji-Ibrahim, J., Luabeya, G. N., & Crawford, J. D. (2020). Parietal Cortex Integrates Saccade and Object Orientation Signals to Update Grasp Plans. *The Journal of Neuroscience*, *40*(23), 4525–4535. https://doi.org/10.1523/JNEUROSCI.0300-20.2020

Bassett, D. S., Porter, M. A., Wymbs, N. F., Grafton, S. T., Carlson, J. M., & Mucha, P. J. (2013). Robust detection of dynamic community structure in networks. *Chaos: An Interdisciplinary Journal of Nonlinear Science*, *23*(1), 013142. https://doi.org/10.1063/1.4790830

Bassett, D. S., & Sporns, O. (2017). Network neuroscience. *Nature Neuroscience*, *20*(3), 353–364. https://doi.org/10.1038/nn.4502

Bastian, A. J. (2006). Learning to predict the future: The cerebellum adapts feedforward movement control. *Current Opinion in Neurobiology*, *16*(6), 645–649. https://doi.org/10.1016/j.conb.2006.08.016

Battaglia-Mayer, A., & Caminiti, R. (2019). Corticocortical Systems Underlying High-Order Motor Control. *The Journal of Neuroscience*, *39*(23), 4404–4421. https://doi.org/10.1523/JNEUROSCI.2094-18.2019

Baumann, M. A., Fluet, M.-C., & Scherberger, H. (2009). Context-Specific Grasp Movement Representation in the Macaque Anterior Intraparietal Area. *The Journal of Neuroscience*, *29*(20), 6436–6448. https://doi.org/10.1523/JNEUROSCI.5479-08.2009

Becker, M. I., & Person, A. L. (2019). Cerebellar Control of Reach Kinematics for Endpoint Precision. *Neuron*, *103*(2), 335-348.e5. https://doi.org/10.1016/j.neuron.2019.05.007

Bedford, O., Noly-Gandon, A., Ara, A., Wiesman, A. I., Albouy, P., Baillet, S., Penhune, V., & Zatorre, R. J. (2025). Human Auditory–Motor Networks Show Frequency-Specific Phase-Based Coupling in Resting-State MEG. *Human Brain Mapping*, *46*(1), e70045. https://doi.org/10.1002/hbm.70045

Begliomini, C., Nelini, C., Caria, A., Grodd, W., & Castiello, U. (2008). Cortical Activations in Humans Grasp-Related Areas Depend on Hand Used and Handedness. *PLoS ONE*, *3*(10), e3388. https://doi.org/10.1371/journal.pone.0003388

Begliomini, C., Wall, M. B., Smith, A. T., & Castiello, U. (2007). Differential cortical activity for precision and whole-hand visually guided grasping in humans. *European Journal of Neuroscience*, *25*(4), 1245–1252. https://doi.org/10.1111/j.1460-9568.2007.05365.x

Bennett, C. M., & Miller, M. B. (2010). How reliable are the results from functional magnetic resonance imaging? *Annals of the New York Academy of Sciences*, *1191*(1), 133–155. https://doi.org/10.1111/j.1749-6632.2010.05446.x

Berryhill, M. E., Fendrich, R., & Olson, I. R. (2009). Impaired distance perception and size constancy following bilateral occipitoparietal damage. *Experimental Brain Research*, *194*(3), 381–393. https://doi.org/10.1007/s00221-009-1707-7

Bertolero, M. A., Yeo, B. T. T., & D'Esposito, M. (2015). The modular and integrative functional architecture of the human brain. *Proceedings of the National Academy of Sciences*, *112*(49). https://doi.org/10.1073/pnas.1510619112

Bertolero, M. A., Yeo, B. T. T., & D'Esposito, M. (2017). The diverse club. *Nature Communications*, *8*(1), 1277. https://doi.org/10.1038/s41467-017-01189-w

Beurze, S. M., Van Pelt, S., & Medendorp, W. P. (2006). Behavioral Reference Frames for Planning Human Reaching Movements. *Journal of Neurophysiology*, *96*(1), 352–362. https://doi.org/10.1152/jn.01362.2005

Bhanpuri, N. H., Okamura, A. M., & Bastian, A. J. (2013). Predictive Modeling by the Cerebellum Improves Proprioception. *The Journal of Neuroscience*, *33*(36), 14301–14306. https://doi.org/10.1523/JNEUROSCI.0784-13.2013

Binder, J. R. (2000). Human Temporal Lobe Activation by Speech and Nonspeech Sounds. *Cerebral Cortex*, *10*(5), 512–528. https://doi.org/10.1093/cercor/10.5.512

Binkofski, F., Buccino, G., Posse, S., Seitz, R. J., Rizzolatti, G., & Freund, H. -J. (1999). A fronto-parietal circuit for object manipulation in man: Evidence from an fMRI-study. *European Journal of Neuroscience*, *11*(9), 3276–3286. https://doi.org/10.1046/j.1460-9568.1999.00753.x

Binkofski, F., Dohle, C., Posse, S., Stephan, K. M., Hefter, H., Seitz, R. J., & Freund, H. J. (1998). Human anterior intraparietal area subserves prehension: A combined lesion and functional MRI activation study. *Neurology*, *50*(5), 1253–1259. https://doi.org/10.1212/WNL.50.5.1253

Biswal, B., Zerrin Yetkin, F., Haughton, V. M., & Hyde, J. S. (1995). Functional connectivity in the motor cortex of resting human brain using echo-planar mri. *Magnetic Resonance in Medicine*, *34*(4), 537–541. https://doi.org/10.1002/mrm.1910340409

Blohm, G., & Crawford, J. D. (2007). Computations for geometrically accurate visually guided reaching in 3-D space. *Journal of Vision*, *7*(5), 4. https://doi.org/10.1167/7.5.4

Blohm, G., Keith, G. P., & Crawford, J. D. (2009). Decoding the Cortical Transformations for Visually Guided Reaching in 3D Space. *Cerebral Cortex*, *19*(6), 1372–1393. https://doi.org/10.1093/cercor/bhn177

Blohm, G., Khan, A. Z., Ren, L., Schreiber, K. M., & Crawford, J. D. (2008). Depth estimation from retinal disparity requires eye and head orientation signals. *Journal of Vision*, *8*(16), 1–23. https://doi.org/10.1167/8.16.3

Bock, O. (1986). Contribution of retinal versus extraretinal signals towards visual localization in goal-directed movements. *Experimental Brain Research*, *64*(3), 476–482. https://doi.org/10.1007/BF00340484

Bock, O., & Eckmiller, R. (1986). Goal-directed arm movements in absence of visual guidance: Evidence for amplitude rather than position control. *Experimental Brain Research*, *62*(3), 451–458. https://doi.org/10.1007/BF00236023

Boisgontier, M. P., & Swinnen, S. P. (2014). Proprioception in the cerebellum. *Frontiers in Human Neuroscience*, *8*. https://doi.org/10.3389/fnhum.2014.00212

Bonacich, P. (2007). Some unique properties of eigenvector centrality. *Social Networks*, *29*(4), 555–564. https://doi.org/10.1016/j.socnet.2007.04.002

Bonazzi, L., Viaro, R., Lodi, E., Canto, R., Bonifazzi, C., & Franchi, G. (2013). Complex Movement Topography and Extrinsic Space Representation in the Rat Forelimb Motor Cortex as Defined by Long-Duration Intracortical Microstimulation. *The Journal of Neuroscience*, *33*(5), 2097–2107. https://doi.org/10.1523/JNEUROSCI.3454-12.2013

Bosen, A. K., Fleming, J. T., Allen, P. D., O'Neill, W. E., & Paige, G. D. (2017). Accumulation and decay of visual capture and the ventriloquism aftereffect caused by brief audio-visual disparities. *Experimental Brain Research*, *235*(2), 585–595. https://doi.org/10.1007/s00221-016-4820-4

Brandauer, B., Hermsdörfer, J., Beck, A., Aurich, V., Gizewski, E. R., Marquardt, C., & Timmann, D. (2008). Impairments of prehension kinematics and grasping forces in patients with cerebellar degeneration and the relationship to cerebellar atrophy. *Clinical Neurophysiology*, *119*(11), 2528–2537. https://doi.org/10.1016/j.clinph.2008.07.280

Brandi, M.-L., Wohlschläger, A., Sorg, C., & Hermsdörfer, J. (2014). The Neural Correlates of Planning and Executing Actual Tool Use. *The Journal of Neuroscience*, *34*(39), 13183–13194. https://doi.org/10.1523/JNEUROSCI.0597-14.2014

Brandolani, R., Galletti, C., Di Gloria, D., Fattori, P., & Breveglieri, R. (2025). Functional specialization of the human posterior parietal cortex in visually and proprioceptively driven reaching corrections. *Communications Biology*, *8*(1), 1658. https://doi.org/10.1038/s42003-025-09040-5

Brissenden, J. A., Tobyne, S. M., Halko, M. A., & Somers, D. C. (2021). Stimulus-Specific Visual Working Memory Representations in Human Cerebellar Lobule VIIb/VIIIa. *The Journal of Neuroscience*, *41*(5), 1033–1045. https://doi.org/10.1523/JNEUROSCI.1253-20.2020

Brown, A. R., & Teskey, G. C. (2014). Motor Cortex Is Functionally Organized as a Set of Spatially Distinct Representations for Complex Movements. *The Journal of Neuroscience*, *34*(41), 13574–13585. https://doi.org/10.1523/JNEUROSCI.2500-14.2014

Brown, L. E., Halpert, B. A., & Goodale, M. A. (2005). Peripheral vision for perception and action. *Experimental Brain Research*, *165*(1), 97–106. https://doi.org/10.1007/s00221-005-2285-y

Buckner, R. L. (1998). Event-related fMRI and the hemodynamic response. *Human Brain Mapping*, *6*(5–6), 373–377. https://doi.org/10.1002/(SICI)1097-0193(1998)6:5/6%3C373::AID-HBM8%3E3.0.CO;2-P

Bullmore, E., & Sporns, O. (2009). Complex brain networks: Graph theoretical analysis of structural and functional systems. *Nature Reviews Neuroscience*, *10*(3), 186–198. https://doi.org/10.1038/nrn2575

Buneo, C. A., & Andersen, R. A. (2006). The posterior parietal cortex: Sensorimotor interface for the planning and online control of visually guided movements. *Neuropsychologia*, *44*(13), 2594–2606. https://doi.org/10.1016/j.neuropsychologia.2005.10.011

Burns, J. K., & Blohm, G. (2010). Multi-Sensory Weights Depend on Contextual Noise in Reference Frame Transformations. *Frontiers in Human Neuroscience*, *4*. https://doi.org/10.3389/fnhum.2010.00221

Byrne, P. A., Cappadocia, D. C., & Crawford, J. D. (2010). Interactions between gaze-centered and allocentric representations of reach target location in the presence of spatial updating. *Vision Research*, *50*(24), 2661–2670. https://doi.org/10.1016/j.visres.2010.08.038

Cappadocia, D. C., Monaco, S., Chen, Y., Blohm, G., & Crawford, J. D. (2017). Temporal Evolution of Target Representation, Movement Direction Planning, and Reach Execution in Occipital–

Parietal–Frontal Cortex: An fMRI Study. *Cerebral Cortex*, *27*(11), 5242–5260. https://doi.org/10.1093/cercor/bhw304

Cardinali, L., Frassinetti, F., Brozzoli, C., Urquizar, C., Roy, A. C., & Farnè, A. (2009). Tool-use induces morphological updating of the body schema. *Current Biology*, *19*(13), 1157. https://doi.org/10.1016/j.cub.2009.06.048

Castiello, U. (2005). The neuroscience of grasping. *Nature Reviews Neuroscience*, *6*(9), 726–736. https://doi.org/10.1038/nrn1744

Castiello, U., & Begliomini, C. (2008). The Cortical Control of Visually Guided Grasping. *The Neuroscientist*, *14*(2), 157–170. https://doi.org/10.1177/1073858407312080

Castiello, U., Bennett, K. M., Egan, G. F., Tochon-Danguy, H. J., Kritikos, A., & Dunai, J. (2000). Human inferior parietal cortex 'programs' the action class of grasping. *Cognitive Systems Research*, *1*(2), 89–97. https://doi.org/10.1016/S1389-0417(99)00011-X

Cavina-Pratesi, C., Connolly, J. D., & Milner, A. D. (2013). Optic ataxia as a model to investigate the role of the posterior parietal cortex in visually guided action: Evidence from studies of patient M.H. *Frontiers in Human Neuroscience*, *7*. https://doi.org/10.3389/fnhum.2013.00336

Cavina-Pratesi, C., Connolly, J. D., Monaco, S., Figley, T. D., Milner, A. D., Schenk, T., & Culham, J. C. (2018). Human neuroimaging reveals the subcomponents of grasping, reaching and pointing actions. *Cortex*, *98*, 128–148. https://doi.org/10.1016/j.cortex.2017.05.018

Cavina-Pratesi, C., Goodale, M. A., & Culham, J. C. (2007). FMRI Reveals a Dissociation between Grasping and Perceiving the Size of Real 3D Objects. *PLoS ONE*, *2*(5), e424. https://doi.org/10.1371/journal.pone.0000424

Cavina-Pratesi, C., Monaco, S., Fattori, P., Galletti, C., McAdam, T. D., Quinlan, D. J., Goodale, M. A., & Culham, J. C. (2010). Functional Magnetic Resonance Imaging Reveals the Neural Substrates of Arm Transport and Grip Formation in Reach-to-Grasp Actions in Humans. *The Journal of Neuroscience*, *30*(31), 10306–10323. https://doi.org/10.1523/JNEUROSCI.2023-10.2010

Chabrol, F. P., Blot, A., & Mrsic-Flogel, T. D. (2019). Cerebellar Contribution to Preparatory Activity in Motor Neocortex. *Neuron*, *103*(3), 506-519.e4. https://doi.org/10.1016/j.neuron.2019.05.022

Chang, S. W. C., Papadimitriou, C., & Snyder, L. H. (2009). Using a Compound Gain Field to Compute a Reach Plan. *Neuron*, *64*(5), 744–755. https://doi.org/10.1016/j.neuron.2009.11.005

Chen, J., Paciocco, J. U., Deng, Z., & Culham, J. C. (2023). Human Neuroimaging Reveals Differences in Activation and Connectivity between Real and Pantomimed Tool Use. *The Journal of Neuroscience*, *43*(46), 7853–7867. https://doi.org/10.1523/JNEUROSCI.0068-23.2023

Chen, Y., Byrne, P., & Crawford, J. D. (2011). Time course of allocentric decay, egocentric decay, and allocentric-to-egocentric conversion in memory-guided reach. *Neuropsychologia*, *49*(1), 49–60. https://doi.org/10.1016/j.neuropsychologia.2010.10.031

Chen, Y., & Crawford, J. D. (2020). Allocentric representations for target memory and reaching in human cortex. *Annals of the New York Academy of Sciences*, *1464*(1), 142–155. https://doi.org/10.1111/nyas.14261

Chen, Y., Monaco, S., Byrne, P., Yan, X., Henriques, D. Y. P., & Crawford, J. D. (2014). Allocentric versus Egocentric Representation of Remembered Reach Targets in Human Cortex. *The Journal of Neuroscience*, *34*(37), 12515–12526. https://doi.org/10.1523/JNEUROSCI.1445-14.2014

Chinellato, E., Grzyb, B. J., Marzocchi, N., Bosco, A., Fattori, P., & Del Pobil, A. P. (2011). The Dorso-medial visual stream: From neural activation to sensorimotor interaction. *Neurocomputing*, *74*(8), 1203–1212. https://doi.org/10.1016/j.neucom.2010.07.029

Chouinard, P., Large, M., Chang, E., & Goodale, M. (2009). Dissociable neural mechanisms for determining the perceived heaviness of objects and the predicted weight of objects during lifting: An fMRI investigation of the size–weight illusion. *NeuroImage*, *44*(1), 200–212. https://doi.org/10.1016/j.neuroimage.2008.08.023

Crawford, J. D., Henriques, D. Y. P., & Medendorp, W. P. (2011). Three-Dimensional Transformations for Goal-Directed Action. *Annual Review of Neuroscience*, *34*(1), 309–331. https://doi.org/10.1146/annurev-neuro-061010-113749

Culham, J. C., Danckert, S. L., Souza, J. F. X. D., Gati, J. S., Menon, R. S., & Goodale, M. A. (2003). Visually guided grasping produces fMRI activation in dorsal but not ventral stream brain areas. *Experimental Brain Research*, *153*(2), 180–189. https://doi.org/10.1007/s00221-003-1591-5

Culham, J. C., & Kanwisher, N. G. (2001). Neuroimaging of cognitive functions in human parietal cortex. *Current Opinion in Neurobiology*, *11*(2), 157–163. https://doi.org/10.1016/S0959-4388(00)00191-4

Culham, J. C., & Valyear, K. F. (2006). Human parietal cortex in action. *Current Opinion in Neurobiology*, *16*(2), 205–212. https://doi.org/10.1016/j.conb.2006.03.005

Damoiseaux, J. S., & Greicius, M. D. (2009). Greater than the sum of its parts: A review of studies combining structural connectivity and resting-state functional connectivity. *Brain Structure and Function*, *213*(6), 525–533. https://doi.org/10.1007/s00429-009-0208-6

Danielmeier, C., Eichele, T., Forstmann, B. U., Tittgemeyer, M., & Ullsperger, M. (2011). Posterior Medial Frontal Cortex Activity Predicts Post-Error Adaptations in Task-Related Visual and Motor Areas. *The Journal of Neuroscience*, *31*(5), 1780–1789. https://doi.org/10.1523/JNEUROSCI.4299-10.2011

Davare, M., Andres, M., Cosnard, G., Thonnard, J.-L., & Olivier, E. (2006). Dissociating the Role of Ventral and Dorsal Premotor Cortex in Precision Grasping. *The Journal of Neuroscience*, *26*(8), 2260–2268. https://doi.org/10.1523/JNEUROSCI.3386-05.2006

Davare, M., Kraskov, A., Rothwell, J. C., & Lemon, R. N. (2011). Interactions between areas of the cortical grasping network. *Current Opinion in Neurobiology*, *21*(4), 565–570. https://doi.org/10.1016/j.conb.2011.05.021

Davare, M., Lemon, R., & Olivier, E. (2008). Selective modulation of interactions between ventral premotor cortex and primary motor cortex during precision grasping in humans. *The Journal of Physiology*, *586*(11), 2735–2742. https://doi.org/10.1113/jphysiol.2008.152603

De La Peña, M. J., Gil-Robles, S., De Vega, V. M., Aracil, C., Acevedo, A., & Rodríguez, M. R. (2020). A Practical Approach to Imaging of the Supplementary Motor Area and Its Subcortical

Connections. *Current Neurology and Neuroscience Reports*, *20*(11), 50. https://doi.org/10.1007/s11910-020-01070-2

Demaine, E. D., Emanuel, D., Fiat, A., & Immorlica, N. (2006). Correlation clustering in general weighted graphs. *Theoretical Computer Science*, *361*(2–3), 172–187. https://doi.org/10.1016/j.tcs.2006.05.008

Desmurget, M., Epstein, C. M., Turner, R. S., Prablanc, C., Alexander, G. E., & Grafton, S. T. (1999). Role of the posterior parietal cortex in updating reaching movements to a visual target. *Nature Neuroscience*, *2*(6), 563–567. https://doi.org/10.1038/9219

Desmurget, M., Gréa, H., & Prablanc, C. (1998). Final posture of the upper limb depends on the initial position of the hand during prehension movements. *Experimental Brain Research*, *119*(4), 511–516. https://doi.org/10.1007/s002210050367

Desmurget, M., Prablanc, C., Arzi, M., Rossetti, Y., Paulignan, Y., & Urquizar, C. (1996). Integrated control of hand transport and orientation during prehension movements. *Experimental Brain Research*, *110*(2), 265–278. https://doi.org/10.1007/BF00228557

Desmurget, M., & Sirigu, A. (2012). Conscious motor intention emerges in the inferior parietal lobule. *Current Opinion in Neurobiology*, *22*(6), 1004–1011. https://doi.org/10.1016/j.conb.2012.06.006

Dessing, J. C., Byrne, P. A., Abadeh, A., & Crawford, J. D. (2012). Hand-related rather than goal-related source of gaze-dependent errors in memory-guided reaching. *Journal of Vision*, *12*(11), 17–17. https://doi.org/10.1167/12.11.17

Di Bono, M. G., Begliomini, C., Castiello, U., & Zorzi, M. (2015). Probing the reaching–grasping network in humans through multivoxel pattern decoding. *Brain and Behavior*, *5*(11), e00412. https://doi.org/10.1002/brb3.412

Di, X., Gohel, S., Kim, E. H., & Biswal, B. B. (2013). Task vs. Rest—Different network configurations between the coactivation and the resting-state brain networks. *Frontiers in Human Neuroscience*, *7*. https://doi.org/10.3389/fnhum.2013.00493

Dixon, M. L., & Christoff, K. (2014). The lateral prefrontal cortex and complex value-based learning and decision making. *Neuroscience & Biobehavioral Reviews*, *45*, 9–18. https://doi.org/10.1016/j.neubiorev.2014.04.011

Dosenbach, N. U. F., Raichle, M. E., & Gordon, E. M. (2025). The brain's action-mode network. *Nature Reviews Neuroscience*, *26*(3), 158–168. https://doi.org/10.1038/s41583-024-00895-x

Edwards, L. L., King, E. M., Buetefisch, C. M., & Borich, M. R. (2019). Putting the "Sensory" Into Sensorimotor Control: The Role of Sensorimotor Integration in Goal-Directed Hand Movements After Stroke. *Frontiers in Integrative Neuroscience*, *13*, 16. https://doi.org/10.3389/fnint.2019.00016

Ehrsson, H. H., Fagergren, A., Jonsson, T., Westling, G., Johansson, R. S., & Forssberg, H. (2000). Cortical Activity in Precision- Versus Power-Grip Tasks: An fMRI Study. *Journal of Neurophysiology*, *83*(1), 528–536. https://doi.org/10.1152/jn.2000.83.1.528

Elliott, D., Hansen, S., Grierson, L. E. M., Lyons, J., Bennett, S. J., & Hayes, S. J. (2010). Goal-directed aiming: Two components but multiple processes. *Psychological Bulletin*, *136*(6), 1023–1044. https://doi.org/10.1037/a0020958

Enright, J. T. (1995). The Non-visual Impact of Eye Orientation on Eye-Hand Coordination. *Vision Research*, *35*(11), 1611–1618. https://doi.org/10.1016/0042-6989(94)00260-S

Epp, S. M., Castrillón, G., Yuan, B., Andrews-Hanna, J., Preibisch, C., & Riedl, V. (2025). BOLD signal changes can oppose oxygen metabolism across the human cortex. *Nature Neuroscience*. https://doi.org/10.1038/s41593-025-02132-9

Fabbri, S., Stubbs, K. M., Cusack, R., & Culham, J. C. (2016). Disentangling Representations of Object and Grasp Properties in the Human Brain. *Journal of Neuroscience*, *36*(29), 7648–7662. https://doi.org/10.1523/JNEUROSCI.0313-16.2016

Fan, J., He, J., & Tillery, S. I. H. (2006). Control of hand orientation and arm movement during reach and grasp. *Experimental Brain Research*, *171*(3), 283–296. https://doi.org/10.1007/s00221-005-0277-6

Farahani, F. V., Karwowski, W., & Lighthall, N. R. (2019). Application of Graph Theory for Identifying Connectivity Patterns in Human Brain Networks: A Systematic Review. *Frontiers in Neuroscience*, *13*, 585. https://doi.org/10.3389/fnins.2019.00585

Farnè, A., & Làdavas, E. (2000). Dynamic size-change of hand peripersonal space following tool use: *NeuroReport*, *11*(8), 1645–1649. https://doi.org/10.1097/00001756-200006050-00010

Fasano, A., Mazzoni, A., & Falotico, E. (2022). Reaching and Grasping Movements in Parkinson's Disease: A Review. *Journal of Parkinson's Disease*, *12*(4), 1083–1113. https://doi.org/10.3233/JPD-213082

Fasoli, S. E., Trombly, C. A., Tickle-Degnen, L., & Verfaellie, M. H. (2002). Effect of Instructions on Functional Reach in Persons With and Without Cerebrovascular Accident. *The American Journal of Occupational Therapy*, *56*(4), 380–390. https://doi.org/10.5014/ajot.56.4.380

Fattori, P., Breveglieri, R., Marzocchi, N., Filippini, D., Bosco, A., & Galletti, C. (2009). Hand Orientation during Reach-to-Grasp Movements Modulates Neuronal Activity in the Medial Posterior Parietal Area V6A. *The Journal of Neuroscience*, *29*(6), 1928–1936. https://doi.org/10.1523/JNEUROSCI.4998-08.2009

Fattori, P., Kutz, D. F., Breveglieri, R., Marzocchi, N., & Galletti, C. (2005). Spatial tuning of reaching activity in the medial parieto-occipital cortex (area V6A) of macaque monkey. *European Journal of Neuroscience*, *22*(4), 956–972. https://doi.org/10.1111/j.1460-9568.2005.04288.x

Faul, F., Erdfelder, E., Lang, A.-G., & Buchner, A. (2007). G*Power 3: A flexible statistical power analysis program for the social, behavioral, and biomedical sciences. *Behavior Research Methods*, *39*(2), 175–191. https://doi.org/10.3758/BF03193146

Fiehler, K., Schütz, I., & Henriques, D. Y. P. (2011). Gaze-centered spatial updating of reach targets across different memory delays. *Vision Research*, *51*(8), 890–897. https://doi.org/10.1016/j.visres.2010.12.015

Filimon, F. (2010). Human Cortical Control of Hand Movements: Parietofrontal Networks for Reaching, Grasping, and Pointing. *The Neuroscientist*, *16*(4), 388–407. https://doi.org/10.1177/1073858410375468

Finc, K., Adamska-Stolarczyk, I., & Bassett, D. S. (2026). Flexible Modularity in the Human Brain: How Network Architecture Reconfigures Over Time. *PsyArXiv*. osf.io/preprints/psyarxiv/6pzgm_v1

Fisk, J. D., & Goodale, M. A. (1989). The Effects of Instructions to Subjects on the Programming of Visually Directed Reaching Movements. *Journal of Motor Behavior*, *21*(1), 5–19. https://doi.org/10.1080/00222895.1989.10735461

Flindall, J. W., & Gonzalez, C. L. R. (2019). Wait wait, don't tell me: Handedness questionnaires do not predict hand preference for grasping. *Laterality: Asymmetries of Body, Brain and Cognition*, *24*(2), 176–196. https://doi.org/10.1080/1357650X.2018.1494184

Fooken, J., Kreyenmeier, P., & Spering, M. (2021). The role of eye movements in manual interception: A mini-review. *Vision Research*, *183*, 81–90. https://doi.org/10.1016/j.visres.2021.02.007

Freeman, L. C. (1977). A Set of Measures of Centrality Based on Betweenness. *Sociometry*, *40*(1), 35. https://doi.org/10.2307/3033543

Frey, S., Campbell, J. S. W., Pike, G. B., & Petrides, M. (2008). Dissociating the Human Language Pathways with High Angular Resolution Diffusion Fiber Tractography. *The Journal of Neuroscience*, *28*(45), 11435–11444. https://doi.org/10.1523/JNEUROSCI.2388-08.2008

Frey, S. H., Vinton, D., Norlund, R., & Grafton, S. T. (2005). Cortical topography of human anterior intraparietal cortex active during visually guided grasping. *Cognitive Brain Research*, *23*(2–3), 397–405. https://doi.org/10.1016/j.cogbrainres.2004.11.010

Fried, I., Haggard, P., He, B. J., & Schurger, A. (2017). Volition and Action in the Human Brain: Processes, Pathologies, and Reasons. *The Journal of Neuroscience*, *37*(45), 10842–10847. https://doi.org/10.1523/JNEUROSCI.2584-17.2017

Friederici, A. D. (2011). The Brain Basis of Language Processing: From Structure to Function. *Physiological Reviews*, *91*(4), 1357–1392. https://doi.org/10.1152/physrev.00006.2011

Friston, K. J. (1994). Functional and effective connectivity in neuroimaging: A synthesis. *Human Brain Mapping*, *2*(1–2), 56–78. https://doi.org/10.1002/hbm.460020107

Gale, D. J., Flanagan, J. R., & Gallivan, J. P. (2021). Human Somatosensory Cortex Is Modulated during Motor Planning. *The Journal of Neuroscience*, *41*(27), 5909–5922. https://doi.org/10.1523/JNEUROSCI.0342-21.2021

Galletti, C., Battaglini, P. P., & Fattori, P. (1995). Eye Position Influence on the Parieto-occipital Area PO (V6) of the Macaque Monkey. *European Journal of Neuroscience*, *7*(12), 2486–2501. https://doi.org/10.1111/j.1460-9568.1995.tb01047.x

Galletti, C., & Fattori, P. (2018). The dorsal visual stream revisited: Stable circuits or dynamic pathways? *Cortex*, *98*, 203–217. https://doi.org/10.1016/j.cortex.2017.01.009

Gallivan, J. P., Cavina-Pratesi, C., & Culham, J. C. (2009). Is That within Reach? fMRI Reveals That the Human Superior Parieto-Occipital Cortex Encodes Objects Reachable by the Hand. *The Journal of Neuroscience*, *29*(14), 4381–4391. https://doi.org/10.1523/JNEUROSCI.0377-09.2009

Gallivan, J. P., & Culham, J. C. (2015). Neural coding within human brain areas involved in actions. *Current Opinion in Neurobiology*, *33*, 141–149. https://doi.org/10.1016/j.conb.2015.03.012

Gallivan, J. P., McLean, D. A., Valyear, K. F., & Culham, J. C. (2013). Decoding the neural mechanisms of human tool use. *eLife*, *2*, e00425. https://doi.org/10.7554/eLife.00425

Gallivan, J. P., McLean, D. A., Valyear, K. F., Pettypiece, C. E., & Culham, J. C. (2011). Decoding Action Intentions from Preparatory Brain Activity in Human Parieto-Frontal Networks. *Journal of Neuroscience*, *31*(26), 9599–9610. https://doi.org/10.1523/JNEUROSCI.0080-11.2011

Gamberini, M., Passarelli, L., Filippini, M., Fattori, P., & Galletti, C. (2021). Vision for action: Thalamic and cortical inputs to the macaque superior parietal lobule. *Brain Structure and Function*, *226*(9), 2951–2966. https://doi.org/10.1007/s00429-021-02377-7

Gao, Z., Davis, C., Thomas, A. M., Economo, M. N., Abrego, A. M., Svoboda, K., De Zeeuw, C. I., & Li, N. (2018). A cortico-cerebellar loop for motor planning. *Nature*, *563*(7729), 113–116. https://doi.org/10.1038/s41586-018-0633-x

Gertz, H., Lingnau, A., & Fiehler, K. (2017). Decoding Movement Goals from the Fronto-Parietal Reach Network. *Frontiers in Human Neuroscience*, *11*. https://doi.org/10.3389/fnhum.2017.00084

Ghaderi, A. H., Baltaretu, B. R., Andevari, M. N., Bharmauria, V., & Balci, F. (2020). Synchrony and Complexity in State-Related EEG Networks: An Application of Spectral Graph Theory. *Neural Computation*, *32*(12), 2422–2454. https://doi.org/10.1162/neco_a_01327

Ghaderi, A. H., Brown, E. C., Clark, D. L., Ramasubbu, R., Kiss, Z. H. T., & Protzner, A. B. (2023). Functional brain network features specify DBS outcome for patients with treatment resistant depression. *Molecular Psychiatry*, *28*(9), 3888–3899. https://doi.org/10.1038/s41380-023-02181-1

Ghaderi, A. H., Moradkhani, S., Haghighatfard, A., Akrami, F., Khayyer, Z., & Balcı, F. (2018). Time estimation and beta segregation: An EEG study and graph theoretical approach. *PLOS ONE*, *13*(4), e0195380. https://doi.org/10.1371/journal.pone.0195380

Ghaderi, A. H., Taghizadeh, S., & Nazari, M. A. (2025). Altered visual network modularity and communication in ADHD subtypes: Classification via source-localized EEG modules. *Biomedical Signal Processing and Control*, *106*, 107755. https://doi.org/10.1016/j.bspc.2025.107755

Gibson, J. R., & Maunsell, J. H. R. (1997). Sensory Modality Specificity of Neural Activity Related to Memory in Visual Cortex. *Journal of Neurophysiology*, *78*(3), 1263–1275. https://doi.org/10.1152/jn.1997.78.3.1263

Glover, S. (2004). Separate visual representations in the planning and control of action. *Behavioral and Brain Sciences*, *27*(1), 3–24. https://doi.org/10.1017/S0140525X04000020

Goodale, M. (1998). Frames of Reference for Perception and Action in the Human Visual System. *Neuroscience & Biobehavioral Reviews*, *22*(2), 161–172. https://doi.org/10.1016/S0149-7634(97)00007-9

Goodale, M. A., Jakobson, L. S., & Keillor, J. M. (1994). Differences in the visual control of pantomimed and natural grasping movements. *Neuropsychologia*, *32*(10), 1159–1178. https://doi.org/10.1016/0028-3932(94)90100-7

Goodale, M. A., & Milner, A. D. (1992). Separate visual pathways for perception and action. *Trends in Neurosciences*, *15*(1), 20–25. https://doi.org/10.1016/0166-2236(92)90344-8

Gordon, E. M., Lynch, C. J., Gratton, C., Laumann, T. O., Gilmore, A. W., Greene, D. J., Ortega, M., Nguyen, A. L., Schlaggar, B. L., Petersen, S. E., Dosenbach, N. U. F., & Nelson, S. M. (2018). Three Distinct Sets of Connector Hubs Integrate Human Brain Function. *Cell Reports*, *24*(7), 1687-1695.e4. https://doi.org/10.1016/j.celrep.2018.07.050

Gosselin-Kessiby, N., Messier, J., & Kalaska, J. F. (2008). Evidence for Automatic On-Line Adjustments of Hand Orientation During Natural Reaching Movements to Stationary Targets. *Journal of Neurophysiology*, *99*(4), 1653–1671. https://doi.org/10.1152/jn.00980.2007

Grafton, S. T. (2010). The cognitive neuroscience of prehension: Recent developments. *Experimental Brain Research*, *204*(4), 475–491. https://doi.org/10.1007/s00221-010-2315-2

Greenwald, H. S., & Knill, D. C. (2009). A comparison of visuomotor cue integration strategies for object placement and prehension. *Visual Neuroscience*, *26*(1), 63–72. https://doi.org/10.1017/S0952523808080668

Grefkes, C., & Fink, G. R. (2005). The functional organization of the intraparietal sulcus in humans and monkeys: Intraparietal sulcus in monkeys and humans. *Journal of Anatomy*, *207*(1), 3–17. https://doi.org/10.1111/j.1469-7580.2005.00426.x

Grefkes, C., & Fink, G. R. (2011). Reorganization of cerebral networks after stroke: New insights from neuroimaging with connectivity approaches. *Brain*, *134*(5), 1264–1276. https://doi.org/10.1093/brain/awr033

Grodd, W., Hülsmann, E., Lotze, M., Wildgruber, D., & Erb, M. (2001). Sensorimotor mapping of the human cerebellum: fMRI evidence of somatotopic organization. *Human Brain Mapping*, *13*(2), 55–73. https://doi.org/10.1002/hbm.1025

Groh, J. M., & Werner-Reiss, U. (2002). Visual and Auditory Integration. In *Encyclopedia of the Human Brain* (pp. 739–752). Elsevier. https://doi.org/10.1016/B0-12-227210-2/00363-0

Guggisberg, A. G., Koch, P. J., Hummel, F. C., & Buetefisch, C. M. (2019). Brain networks and their relevance for stroke rehabilitation. *Clinical Neurophysiology*, *130*(7), 1098–1124. https://doi.org/10.1016/j.clinph.2019.04.004

Guitton, D., & Volle, M. (1987). Gaze control in humans: Eye-head coordination during orienting movements to targets within and beyond the oculomotor range. *Journal of Neurophysiology*, *58*(3), 427–459. https://doi.org/10.1152/jn.1987.58.3.427

Haddadshargh, G., De Freitas, R. M., Mak, J., Boos, A., Fang, X., Collinger, J. L., McKernan, G., Zhan, L., Liu, F., & Wittenberg, G. F. (2026). Mapping the Causal Roles of Non-Primary Motor Areas in Human Reach Planning and Execution. *Human Brain Mapping*, *47*(2), e70465. https://doi.org/10.1002/hbm.70465

Hall, D. A., Haggard, M. P., Akeroyd, M. A., Summerfield, A. Q., Palmer, A. R., Elliott, M. R., & Bowtell, R. W. (2000). Modulation and task effects in auditory processing measured using fMRI. *Human Brain Mapping*, *10*(3), 107–119. https://doi.org/10.1002/1097-0193(200007)10:3%3C107::AID-HBM20%3E3.0.CO;2-8

Hanakawa, T., Dimyan, M. A., & Hallett, M. (2008). Motor Planning, Imagery, and Execution in the Distributed Motor Network: A Time-Course Study with Functional MRI. *Cerebral Cortex*, *18*(12), 2775–2788. https://doi.org/10.1093/cercor/bhn036

Hao, S., & Zou, J. (2025). Targeting neuroplasticity: A viewpoint on a future research direction with Parkinson's disease-related fatigue. *Frontiers in Aging Neuroscience*, *17*, 1503296. https://doi.org/10.3389/fnagi.2025.1503296

Hasson, U., Yang, E., Vallines, I., Heeger, D. J., & Rubin, N. (2008). A Hierarchy of Temporal Receptive Windows in Human Cortex. *The Journal of Neuroscience*, *28*(10), 2539–2550. https://doi.org/10.1523/JNEUROSCI.5487-07.2008

Heath, M. (2005). Role of Limb and Target Vision in the Online Control of Memory-Guided Reaches. *Motor Control*, *9*(3), 281–309. https://doi.org/10.1123/mcj.9.3.281

Henriques, D. Y. P., & Crawford, J. D. (2000). Direction-dependent distortions of retinocentric space in the visuomotor transformation for pointing. *Experimental Brain Research*, *132*(2), 179–194. https://doi.org/10.1007/s002210000340

Henriques, D. Y. P., Klier, E. M., Smith, M. A., Lowy, D., & Crawford, J. D. (1998). Gaze-Centered Remapping of Remembered Visual Space in an Open-Loop Pointing Task. *The Journal of Neuroscience*, *18*(4), 1583–1594. https://doi.org/10.1523/JNEUROSCI.18-04-01583.1998

Henriques, D. Y. P., Medendorp, W. P., Gielen, C. C. A. M., & Crawford, J. D. (2003). Geometric computations underlying eye-hand coordination: Orientations of the two eyes and the head. *Experimental Brain Research*, *152*(1), 70–78. https://doi.org/10.1007/s00221-003-1523-4

Hermann, T., Höner, O., & Ritter, H. (2006). AcouMotion – An Interactive Sonification System for Acoustic Motion Control. In S. Gibet, N. Courty, & J.-F. Kamp (Eds.), *Gesture in Human-Computer Interaction and Simulation* (Vol. 3881, pp. 312–323). Springer Berlin Heidelberg. https://doi.org/10.1007/11678816_35

Hervé, P.-Y., Zago, L., Petit, L., Mazoyer, B., & Tzourio-Mazoyer, N. (2013). Revisiting human hemispheric specialization with neuroimaging. *Trends in Cognitive Sciences*, *17*(2), 69–80. https://doi.org/10.1016/j.tics.2012.12.004

Hesse, C., Bonnesen, K., Franz, V. H., & Schenk, T. (2021). Card posting does not rely on visual orientation: A challenge to past neuropsychological dissociations. *Neuropsychologia*, *159*, 107920. https://doi.org/10.1016/j.neuropsychologia.2021.107920

Hesse, C., & Deubel, H. (2010). Advance Planning in Sequential Pick–and–Place Tasks. *Journal of Neurophysiology*, *104*(1), 508–516. https://doi.org/10.1152/jn.00097.2010

Hickok, G., & Poeppel, D. (2007). The cortical organization of speech processing. *Nature Reviews Neuroscience*, *8*(5), 393–402. https://doi.org/10.1038/nrn2113

Hickok, G., & Poeppel, D. (2015). Neural basis of speech perception. In *Handbook of Clinical Neurology* (Vol. 129, pp. 149–160). Elsevier. https://doi.org/10.1016/B978-0-444-62630-1.00008-1

Hobot, J., Klincewicz, M., Sandberg, K., & Wierzchoń, M. (2021). Causal Inferences in Repetitive Transcranial Magnetic Stimulation Research: Challenges and Perspectives. *Frontiers in Human Neuroscience*, *14*, 586448. https://doi.org/10.3389/fnhum.2020.586448

Honey, C. J., Sporns, O., Cammoun, L., Gigandet, X., Thiran, J. P., Meuli, R., & Hagmann, P. (2009). Predicting human resting-state functional connectivity from structural connectivity. *Proceedings of the National Academy of Sciences*, *106*(6), 2035–2040. https://doi.org/10.1073/pnas.0811168106

Hutmacher, F. (2019). Why Is There So Much More Research on Vision Than on Any Other Sensory Modality? *Frontiers in Psychology*, *10*, 2246. https://doi.org/10.3389/fpsyg.2019.02246

Hyvärinen, J. (1982). Posterior parietal lobe of the primate brain. *Psysiological Reviews*, *62*(3), 1060–1129.

Izawa, J., Criscimagna-Hemminger, S. E., & Shadmehr, R. (2012). Cerebellar Contributions to Reach Adaptation and Learning Sensory Consequences of Action. *The Journal of Neuroscience*, *32*(12), 4230–4239. https://doi.org/10.1523/JNEUROSCI.6353-11.2012

Jackson, G. M., Jackson, S. R., & Hindle, J. V. (2000). The control of bimanual reach-to-grasp movements in hemiparkinsonian patients. *Experimental Brain Research*, *132*(3), 390–398. https://doi.org/10.1007/s002210000354

Jacobs, S., Danielmeier, C., & Frey, S. H. (2010). Human Anterior Intraparietal and Ventral Premotor Cortices Support Representations of Grasping with the Hand or a Novel Tool. *Journal of Cognitive Neuroscience*, *22*(11), 2594–2608. https://doi.org/10.1162/jocn.2009.21372

Jahan, I., Harun-Ur-Rashid, M., Islam, Md. A., Sharmin, F., Al Jaouni, S. K., Kaki, A. M., & Selim, S. (2026). Neuronal plasticity and its role in Alzheimer's disease and Parkinson's disease. *Neural Regeneration Research*, *21*(1), 107–125. https://doi.org/10.4103/NRR.NRR-D-24-01019

Jäncke, L., Wüstenberg, T., Scheich, H., & Heinze, H.-J. (2002). Phonetic Perception and the Temporal Cortex. *NeuroImage*, *15*(4), 733–746. https://doi.org/10.1006/nimg.2001.1027

Jeannerod, M. (1984). The Timing of Natural Prehension Movements. *Journal of Motor Behavior*, *16*(3), 235–254. https://doi.org/10.1080/00222895.1984.10735319

Jenkinson, M., Bannister, P., Brady, M., & Smith, S. (2002). Improved Optimization for the Robust and Accurate Linear Registration and Motion Correction of Brain Images. *NeuroImage*, *17*(2), 825–841. https://doi.org/10.1006/nimg.2002.1132

Jenkinson, M., Beckmann, C. F., Behrens, T. E. J., Woolrich, M. W., & Smith, S. M. (2012). FSL. *NeuroImage*, *62*(2), 782–790. https://doi.org/10.1016/j.neuroimage.2011.09.015

Jenmalm, P., Schmitz, C., Forssberg, H., & Ehrsson, H. H. (2006). Lighter or Heavier Than Predicted: Neural Correlates of Corrective Mechanisms during Erroneously Programmed Lifts. *The Journal of Neuroscience*, *26*(35), 9015–9021. https://doi.org/10.1523/JNEUROSCI.5045-05.2006

Ji, J. L., Spronk, M., Kulkarni, K., Repovš, G., Anticevic, A., & Cole, M. W. (2019). Mapping the human brain's cortical-subcortical functional network organization. *NeuroImage*, *185*, 35–57. https://doi.org/10.1016/j.neuroimage.2018.10.006

Johansson, R. S., & Edin, B. B. (1993). Predictive Feed-Forward Sensory Control During Grasping and Manipulation in Man. *Biomedical Research*, *14*(4), 95–106.

Johansson, R. S., & Flanagan, J. R. (2009). Coding and use of tactile signals from the fingertips in object manipulation tasks. *Nature Reviews Neuroscience*, *10*(5), 345–359. https://doi.org/10.1038/nrn2621

Johansson, R. S., Westling, G., Bäckström, A., & Flanagan, J. R. (2001). Eye–Hand Coordination in Object Manipulation. *The Journal of Neuroscience*, *21*(17), 6917–6932. https://doi.org/10.1523/JNEUROSCI.21-17-06917.2001

Kamp, C. V. D., Bongers, R. M., & Zaal, F. T. J. M. (2009). Effects of Changing Object Size During Prehension. *Journal of Motor Behavior*, *41*(5), 427–435. https://doi.org/10.3200/35-08-033

Karl, J. M., & Whishaw, I. Q. (2013). Different Evolutionary Origins for the Reach and the Grasp: An Explanation for Dual Visuomotor Channels in Primate Parietofrontal Cortex. *Frontiers in Neurology*, *4*. https://doi.org/10.3389/fneur.2013.00208

Kawato, M., Furukawa, K., & Suzuki, R. (1987). A hierarchical neural-network model for control and learning of voluntary movement. *Biological Cybernetics*, *57*(3), 169–185. https://doi.org/10.1007/BF00364149

Kenessy, J. (2021). Functional Outcomes of Auditory and Visual Integration. *Optometry & Visual Performance*, *9*(4).

Khan, A. Z., Crawford, J. D., Blohm, G., Urquizar, C., Rossetti, Y., & Pisella, L. (2007). Influence of initial hand and target position on reach errors in optic ataxic and normal subjects. *Journal of Vision*, *7*(5), 1–16. https://doi.org/10.1167/7.5.8

Khan, A. Z., Pisella, L., Rossetti, Y., Vighetto, A., & Crawford, J. D. (2005). Impairment of Gaze-centered Updating of Reach Targets in Bilateral Parietal–Occipital Damaged Patients. *Cerebral Cortex*, *15*(10), 1547–1560. https://doi.org/10.1093/cercor/bhi033

Khan, A. Z., Pisella, L., Vighetto, A., Cotton, F., Luauté, J., Boisson, D., Salemme, R., Crawford, J. D., & Rossetti, Y. (2005). Optic ataxia errors depend on remapped, not viewed, target location. *Nature Neuroscience*, *8*(4), 418–420. https://doi.org/10.1038/nn1425

Kim, S. G., Ashe, J., Georgopoulos, A. P., Merkle, H., Ellermann, J. M., Menon, R. S., Ogawa, S., & Ugurbil, K. (1993). Functional imaging of human motor cortex at high magnetic field. *Journal of Neurophysiology*, *69*(1), 297–302. https://doi.org/10.1152/jn.1993.69.1.297

Kita, K., Otaka, Y., Takeda, K., Sakata, S., Ushiba, J., Kondo, K., Liu, M., & Osu, R. (2013). A pilot study of sensory feedback by transcutaneous electrical nerve stimulation to improve manipulation deficit caused by severe sensory loss after stroke. *Journal of NeuroEngineering and Rehabilitation*, *10*(1), 55. https://doi.org/10.1186/1743-0003-10-55

Kitadono, K., & Humphreys, G. W. (2007). Interactions between perception and action programming: Evidence from visual extinction and optic ataxia. *Cognitive Neuropsychology*, *24*(7), 731–754. https://doi.org/10.1080/02643290701734721

Klein, L. K., Maiello, G., Stubbs, K., Proklova, D., Chen, J., Paulun, V. C., Culham, J. C., & Fleming, R. W. (2023). Distinct Neural Components of Visually Guided Grasping during Planning and Execution. *The Journal of Neuroscience*, *43*(49), 8504–8514. https://doi.org/10.1523/JNEUROSCI.0335-23.2023

Klostermann, A., Vater, C., Kredel, R., & Hossner, E.-J. (2020). Perception and Action in Sports. On the Functionality of Foveal and Peripheral Vision. *Frontiers in Sports and Active Living*, *1*, 66. https://doi.org/10.3389/fspor.2019.00066

Konen, C. S., & Kastner, S. (2008). Two hierarchically organized neural systems for object information in human visual cortex. *Nature Neuroscience*, *11*(2), 224–231. https://doi.org/10.1038/nn2036

Kourtzi, Z. (2003). Representation of the Perceived 3-D Object Shape in the Human Lateral Occipital Complex. *Cerebral Cortex*, *13*(9), 911–920. https://doi.org/10.1093/cercor/13.9.911

Kourtzi, Z., & Kanwisher, N. (2001). Representation of Perceived Object Shape by the Human Lateral Occipital Complex. *Science*, *293*(5534), 1506–1509. https://doi.org/10.1126/science.1061133

Koziol, L. F., Budding, D., Andreasen, N., D'Arrigo, S., Bulgheroni, S., Imamizu, H., Ito, M., Manto, M., Marvel, C., Parker, K., Pezzulo, G., Ramnani, N., Riva, D., Schmahmann, J., Vandervert, L., & Yamazaki, T. (2014). Consensus Paper: The Cerebellum's Role in Movement and Cognition. *The Cerebellum*, *13*(1), 151–177. https://doi.org/10.1007/s12311-013-0511-x

Krämer, U. M., Solbakk, A.-K., Funderud, I., Løvstad, M., Endestad, T., & Knight, R. T. (2013). The role of the lateral prefrontal cortex in inhibitory motor control. *Cortex*, *49*(3), 837–849. https://doi.org/10.1016/j.cortex.2012.05.003

Krigolson, O., & Heath, M. (2004). Background visual cues and memory-guided reaching. *Human Movement Science*, *23*(6), 861–877. https://doi.org/10.1016/j.humov.2004.10.011

Kritikos, A., & Brasch, C. (2008). Visual and tactile integration in action comprehension and execution. *Brain Research*, *1242*, 73–86. https://doi.org/10.1016/j.brainres.2008.04.081

Kuhtz-Buschbeck, J. P., Stolze, H., Jöhnk, K., Boczek-Funcke, A., & Illert, M. (1998). Development of prehension movements in children: A kinematic study. *Experimental Brain Research*, *122*(4), 424–432. https://doi.org/10.1007/s002210050530

Kumral, E., Ece Çetin, F., Deniz Çetin, Z., & Ekici, A. (2025). Visual and Cognitive Disorders Associated With Isolated Lingual Gyrus Infarctions. *The Journal of Neuropsychiatry and Clinical Neurosciences*, appi.neuropsych.20230182. https://doi.org/10.1176/appi.neuropsych.20230182

Kurkela, K., & Ritchey, M. (2024). Intrinsic functional connectivity among memory networks does not predict individual differences in narrative recall. *Imaging Neuroscience*, *2*, imag–2–00169. https://doi.org/10.1162/imag_a_00169

Ladwig, S., Sutter, C., & Müsseler, J. (2013). Intra- and intermodal integration of discrepant visual and proprioceptive action effects. *Experimental Brain Research*, *231*(4), 457–468. https://doi.org/10.1007/s00221-013-3710-2

Lancaster, J. L., Tordesillas-Gutiérrez, D., Martinez, M., Salinas, F., Evans, A., Zilles, K., Mazziotta, J. C., & Fox, P. T. (2007). Bias between MNI and Talairach coordinates analyzed using the ICBM-152 brain template. *Human Brain Mapping*, *28*(11), 1194–1205. https://doi.org/10.1002/hbm.20345

Land, M. F. (2006). Eye movements and the control of actions in everyday life. *Progress in Retinal and Eye Research*, *25*(3), 296–324. https://doi.org/10.1016/j.preteyeres.2006.01.002

Latora, V., & Marchiori, M. (2001). Efficient Behavior of Small-World Networks. *Physical Review Letters*, *87*(19), 198701. https://doi.org/10.1103/PhysRevLett.87.198701

Le, A., Monaco, S., Chen, Y., & Crawford, J. D. (2015). *Cortical mechanisms underlying the integration of transport and grip components for grasping*. Society for Neuroscience, Chicago.

Lebedev, M. A., & Nicolelis, M. A. L. (2017). Brain-Machine Interfaces: From Basic Science to Neuroprostheses and Neurorehabilitation. *Physiological Reviews*, *97*(2), 767–837. https://doi.org/10.1152/physrev.00027.2016

Lederman, S. J., & Wing, A. M. (2003). Perceptual judgement, grasp point selection and object symmetry. *Experimental Brain Research*, *152*(2), 156–165. https://doi.org/10.1007/s00221-003-1522-5

Lewald, J., & Ehrenstein, W. H. (2000). Visual and proprioceptive shifts in perceived egocentric direction induced by eye-position. *Vision Research*, *40*(5), 539–547. https://doi.org/10.1016/S0042-6989(99)00197-2

Lin, K., Wu, C., Lin, K., & Chang, C. (2008). Effects of Task Instructions and Target Location on Reaching Kinematics in People With and Without Cerebrovascular Accident: A Study of the Less-Affected Limb. *The American Journal of Occupational Therapy*, *62*(4), 456–465. https://doi.org/10.5014/ajot.62.4.456

Lohse, K. R., Jones, M., Healy, A. F., & Sherwood, D. E. (2014). The role of attention in motor control. *Journal of Experimental Psychology: General*, *143*(2), 930–948. https://doi.org/10.1037/a0032817

Luabeya, G. N., Le, A., Ghaderi, A. H., Musa, L., Monaco, S., Freud, E., & Crawford, J. D. (2026). Modular Integration of Auditory Instructions and Visual Cues into the Cortical Reach Network. *bioRxiv*. https://doi.org/https://doi.org/10.64898/2026.01.20.700205

Luabeya, G. N., Yan, X., Freud, E., & Crawford, J. D. (2024). Influence of gaze, vision, and memory on hand kinematics in a placement task. *Journal of Neurophysiology*, *132*(1), 147–161. https://doi.org/10.1152/jn.00362.2023

Lukos, J., Ansuini, C., & Santello, M. (2007). Choice of Contact Points during Multidigit Grasping: Effect of Predictability of Object Center of Mass Location. *The Journal of Neuroscience*, *27*(14), 3894–3903. https://doi.org/10.1523/JNEUROSCI.4693-06.2007

Madole, J. W., Buchanan, C. R., Rhemtulla, M., Ritchie, S. J., Bastin, M. E., Deary, I. J., Cox, S. R., & Tucker-Drob, E. M. (2023). Strong intercorrelations among global graph-theoretic indices of structural connectivity in the human brain. *NeuroImage*, *275*, 120160. https://doi.org/10.1016/j.neuroimage.2023.120160

Majdandžić, J., Grol, M. J., Van Schie, H. T., Verhagen, L., Toni, I., & Bekkering, H. (2007). The role of immediate and final goals in action planning: An fMRI study. *NeuroImage*, *37*(2), 589–598. https://doi.org/10.1016/j.neuroimage.2007.04.071

Manto, M., Bower, J. M., Conforto, A. B., Delgado-García, J. M., Da Guarda, S. N. F., Gerwig, M., Habas, C., Hagura, N., Ivry, R. B., Mariën, P., Molinari, M., Naito, E., Nowak, D. A., Oulad Ben Taib, N., Pelisson, D., Tesche, C. D., Tilikete, C., & Timmann, D. (2012). Consensus Paper: Roles of the Cerebellum in Motor Control—The Diversity of Ideas on Cerebellar Involvement in Movement. *The Cerebellum*, *11*(2), 457–487. https://doi.org/10.1007/s12311-011-0331-9

Marangon, M., Kubiak, A., & Króliczak, G. (2016). Haptically Guided Grasping. fMRI Shows Right-Hemisphere Parietal Stimulus Encoding, and Bilateral Dorso-Ventral Parietal Gradients of Object- and Action-Related Processing during Grasp Execution. *Frontiers in Human Neuroscience*, *9*. https://doi.org/10.3389/fnhum.2015.00691

Marchant, D. C. (2011). Attentional Focusing Instructions and Force Production. *Frontiers in Psychology*, *1*. https://doi.org/10.3389/fpsyg.2010.00210

Marcinowski, E. C., Nelson, E., Campbell, J. M., & Michel, G. F. (2019). The Development of Object Construction From Infancy Through Toddlerhood. *Infancy*, *24*(3), 368–391. https://doi.org/10.1111/infa.12284

Marotta, J. J., Keith, G. P., & Crawford, J. D. (2005). Task-Specific Sensorimotor Adaptation to Reversing Prisms. *Journal of Neurophysiology*, *93*(2), 1104–1110. https://doi.org/10.1152/jn.00859.2004

Marotta, J. J., Medendorp, W. P., & Crawford, J. D. (2003). Kinematic Rules for Upper and Lower Arm Contributions to Grasp Orientation. *Journal of Neurophysiology*, *90*(6), 3816–3827. https://doi.org/10.1152/jn.00418.2003

Marteniuk, R. G., Mackenzie, C. L., Jeannerod, M., Athenes, S., & Dugas, C. (1987). Constraints on human arm movement trajectories. *Canadian Journal of Psychology / Revue Canadienne de Psychologie*, *41*(3), 365–378. https://doi.org/10.1037/h0084157

Mason, A. H., & Bryden, P. J. (2007). Coordination and concurrency in bimanual rotation tasks when moving away from and toward the body. *Experimental Brain Research*, *183*(4), 541–556. https://doi.org/10.1007/s00221-007-1068-z

Mazziotta, J. C., Toga, A., Eans, A., Fox, P., & Lancaster, J. (1995). A probabilistic atlas of the human brain: Theory and rationale for its development. *NeuroImage*, *2*(2), 89–101. https://doi.org/https://doi.org/10.1006/nimg.1995.1012

McCarthy, P. (2025). *FSLeyes (1.15.0)*. https://doi.org/https://doi.org/10.5281/zenodo.15542963

McGuire, L. M. M., & Sabes, P. N. (2009). Sensory transformations and the use of multiple reference frames for reach planning. *Nature Neuroscience*, *12*(8), 1056–1061. https://doi.org/10.1038/nn.2357

McNamee, D., & Wolpert, D. M. (2019). Internal Models in Biological Control. *Annual Review of Control, Robotics, and Autonomous Systems*, *2*(1), 339–364. https://doi.org/10.1146/annurev-control-060117-105206

Medaglia, J. D. (2017). Graph Theoretic Analysis of Resting State Functional MR Imaging. *Neuroimaging Clinics of North America*, *27*(4), 593–607. https://doi.org/10.1016/j.nic.2017.06.008

Medendorp, W. P., & Crawford, J. D. (2002). Visuospatial updating of reaching targets in near and far space: *Neuroreport*, *13*(5), 633–636. https://doi.org/10.1097/00001756-200204160-00019

Medendorp, W. P., Goltz, H. C., Vilis, T., & Crawford, J. D. (2003). Gaze-Centered Updating of Visual Space in Human Parietal Cortex. *The Journal of Neuroscience*, *23*(15), 6209–6214. https://doi.org/10.1523/JNEUROSCI.23-15-06209.2003

Medina, J., Jax, S. A., & Coslett, H. B. (2020). Impairments in action and perception after right intraparietal damage. *Cortex*, *122*, 288–299. https://doi.org/10.1016/j.cortex.2019.02.004

Meredith, M. A., Wallace, M. T., & Stein, B. E. (1992). Visual, auditory and somatosensory convergence in output neurons of the cat superior colliculus: Multisensory properties of the tecto-reticulo-spinal projection. *Experimental Brain Research*, *88*(1), 181–186. https://doi.org/10.1007/BF02259139

Miller, E. K., & Cohen, J. D. (2001). An Integrative Theory of Prefrontal Cortex Function. *Annual Review of Neuroscience*, *24*(1), 167–202. https://doi.org/10.1146/annurev.neuro.24.1.167

Milner, A. D. (2017). How do the two visual streams interact with each other? *Experimental Brain Research*, *235*(5), 1297–1308. https://doi.org/10.1007/s00221-017-4917-4

Milner, A. D., Dijkerman, H. C., McIntosh, R. D., Rossetti, Y., & Pisella, L. (2003). Delayed reaching and grasping in patients with optic ataxia. In *Progress in Brain Research* (Vol. 142, pp. 225–242). https://doi.org/10.1016/S0079-6123(03)42016-5

Milner, T. E., Franklin, D. W., Imamizu, H., & Kawato, M. (2006). Central Representation of Dynamics When Manipulating Handheld Objects. *Journal of Neurophysiology*, *95*(2), 893–901. https://doi.org/10.1152/jn.00198.2005

Mishkin, M., & Ungerleider, L. G. (1982). Contribution of striate inputs to the visuospatial functions of parieto-preoccipital cortex in monkeys. *Behavioural Brain Research*, *6*(1), 57–77. https://doi.org/10.1016/0166-4328(82)90081-X

Modirrousta, M., & Fellows, L. K. (2008). Dorsal Medial Prefrontal Cortex Plays a Necessary Role in Rapid Error Prediction in Humans. *The Journal of Neuroscience*, *28*(51), 14000–14005. https://doi.org/10.1523/JNEUROSCI.4450-08.2008

Moerel, D., Rich, A. N., & Woolgar, A. (2024). Selective attention and decision-making have separable neural bases in space and time. *The Journal of Neuroscience*, e0224242024. https://doi.org/10.1523/JNEUROSCI.0224-24.2024

Monaco, S., Cavina-Pratesi, C., Sedda, A., Fattori, P., Galletti, C., & Culham, J. C. (2011). Functional magnetic resonance adaptation reveals the involvement of the dorsomedial stream in hand orientation for grasping. *Journal of Neurophysiology*, *106*(5), 2248–2263. https://doi.org/10.1152/jn.01069.2010

Monaco, S., Malfatti, G., Culham, J. C., Cattaneo, L., & Turella, L. (2020). Decoding motor imagery and action planning in the early visual cortex: Overlapping but distinct neural mechanisms. *NeuroImage*, *218*, 116981. https://doi.org/10.1016/j.neuroimage.2020.116981

Monaco, S., Menghi, N., & Crawford, J. D. (2024). Action-specific feature processing in the human cortex: An fMRI study. *Neuropsychologia*, *194*, 108773. https://doi.org/10.1016/j.neuropsychologia.2023.108773

Monaco, S., Sedda, A., Cavina-Pratesi, C., & Culham, J. C. (2015). Neural correlates of object size and object location during grasping actions. *European Journal of Neuroscience*, *41*(4), 454–465. https://doi.org/10.1111/ejn.12786

Mottolese, C., Richard, N., Harquel, S., Szathmari, A., Sirigu, A., & Desmurget, M. (2013). Mapping motor representations in the human cerebellum. *Brain*, *136*(1), 330–342. https://doi.org/10.1093/brain/aws186

Mountcastle, V. B., Lynch, J. C., Georgopoulos, A., Sakata, H., & Acuna, C. (1975). Posterior parietal association cortex of the monkey: Command functions for operations within extrapersonal space. *Journal of Neurophysiology*, *38*(4), 871–908. https://doi.org/10.1152/jn.1975.38.4.871

Mueller, S., & Fiehler, K. (2014). Gaze-dependent spatial updating of tactile targets in a localization task. *Frontiers in Psychology*, *5*. https://doi.org/10.3389/fpsyg.2014.00066

Mueller, S., & Fiehler, K. (2017). Gaze-centered coding of proprioceptive reach targets after effector movement: Testing the impact of online information, time of movement, and target distance. *PLOS ONE*, *12*(7), e0180782. https://doi.org/10.1371/journal.pone.0180782

Murata, A., Gallese, V., Luppino, G., Kaseda, M., & Sakata, H. (2000). Selectivity for the Shape, Size, and Orientation of Objects for Grasping in Neurons of Monkey Parietal Area AIP. *Journal of Neurophysiology*, *83*(5), 2580–2601. https://doi.org/10.1152/jn.2000.83.5.2580

Musa, L., Ghaderi, A., Chen, Y., & Crawford, J. D. (2025). *Spatial task instructions and global activation trends influence functional modularity in the cortical reach network*. Neuroscience. https://doi.org/10.1101/2025.03.20.644329

Musa, L., Yan, X., & Crawford, J. D. (2024). Instruction alters the influence of allocentric landmarks in a reach task. *Journal of Vision*, *24*(7), 17. https://doi.org/10.1167/jov.24.7.17

Naish, K. R., Reader, A. T., Houston-Price, C., Bremner, A. J., & Holmes, N. P. (2013). To eat or not to eat? Kinematics and muscle activity of reach-to-grasp movements are influenced by the action goal, but observers do not detect these differences. *Experimental Brain Research*, *225*(2), 261–275. https://doi.org/10.1007/s00221-012-3367-2

Neggers, S. F. W., & Bekkering, H. (1999). Integration of visual and somatosensory target information in goal-directed eye and arm movements. *Experimental Brain Research*, *125*(1), 97–107. https://doi.org/10.1007/s002210050663

Neggers, S. F. W., & Bekkering, H. (2000). Ocular Gaze is Anchored to the Target of an Ongoing Pointing Movement. *Journal of Neurophysiology*, *83*(2), 639–651. https://doi.org/10.1152/jn.2000.83.2.639

Nelson, W., & Mayhew, S. D. (2025). Investigating the Consistency of Negative BOLD Responses to Combinations of Visual, Auditory, and Somatosensory Stimuli and Their Modulation by the Level of Task Demand. *Human Brain Mapping*, *46*(4), e70177. https://doi.org/10.1002/hbm.70177

Nettekoven, C., Zhi, D., Shahshahani, L., Pinho, A. L., Saadon-Grosman, N., Buckner, R. L., & Diedrichsen, J. (2024). A hierarchical atlas of the human cerebellum for functional precision mapping. *Nature Communications*, *15*(1), 8376. https://doi.org/10.1038/s41467-024-52371-w

Newman, M. E. J. (2006). Modularity and community structure in networks. *Proceedings of the National Academy of Sciences*, *103*(23), 8577–8582. https://doi.org/10.1073/pnas.0601602103

Nicolas-Alonso, L. F., & Gomez-Gil, J. (2012). Brain Computer Interfaces, a Review. *Sensors*, *12*(2), 1211–1279. https://doi.org/10.3390/s120201211

Nowak, D. A., Topka, H., Timmann, D., Boecker, H., & Hermsdörfer, J. (2007). The role of the cerebellum for predictive control of grasping. *The Cerebellum*, *6*(1), 7. https://doi.org/10.1080/14734220600776379

Oldham, S., Fulcher, B., Parkes, L., Arnatkevičiūtė, A., Suo, C., & Fornito, A. (2019). Consistency and differences between centrality measures across distinct classes of networks. *PLOS ONE*, *14*(7), e0220061. https://doi.org/10.1371/journal.pone.0220061

Opoku-Baah, C., Schoenhaut, A. M., Vassall, S. G., Tovar, D. A., Ramachandran, R., & Wallace, M. T. (2021). Visual Influences on Auditory Behavioral, Neural, and Perceptual Processes: A Review. *Journal of the Association for Research in Otolaryngology*, *22*(4), 365–386. https://doi.org/10.1007/s10162-021-00789-0

Orban, G. A., Sepe, A., & Bonini, L. (2021). Parietal maps of visual signals for bodily action planning. *Brain Structure and Function*, *226*(9), 2967–2988. https://doi.org/10.1007/s00429-021-02378-6

Osiurak, F., Rossetti, Y., & Badets, A. (2017). What is an affordance? 40 years later. *Neuroscience & Biobehavioral Reviews*, *77*, 403–417. https://doi.org/10.1016/j.neubiorev.2017.04.014

Palejwala, A. H., Dadario, N. B., Young, I. M., O'Connor, K., Briggs, R. G., Conner, A. K., O'Donoghue, D. L., & Sughrue, M. E. (2021). Anatomy and White Matter Connections of the Lingual Gyrus and Cuneus. *World Neurosurgery*, *151*, e426–e437. https://doi.org/10.1016/j.wneu.2021.04.050

Papadatou-Pastou, M., Ntolka, E., Schmitz, J., Martin, M., Munafò, M. R., Ocklenburg, S., & Paracchini, S. (2020). Human handedness: A meta-analysis. *Psychological Bulletin*, *146*(6), 481–524. https://doi.org/10.1037/bul0000229

Park, I. S., Lee, N. J., & Rhyu, I. J. (2018). Roles of the Declive, Folium, and Tuber Cerebellar Vermian Lobules in Sportspeople. *Journal of Clinical Neurology*, *14*(1), 1. https://doi.org/10.3988/jcn.2018.14.1.1

Parry, R., Macias Soria, S., Pradat-Diehl, P., Marchand-Pauvert, V., Jarrassé, N., & Roby-Brami, A. (2019). Effects of Hand Configuration on the Grasping, Holding, and Placement of an Instrumented Object in Patients With Hemiparesis. *Frontiers in Neurology*, *10*, 240. https://doi.org/10.3389/fneur.2019.00240

Paulignan, Y., MacKenzie, C., Marteniuk, R., & Jeannerod, M. (1991). Selective perturbation of visual input during prehension movements. *Experimental Brain Research*, *83*, 502–512.

Paulun, V. C., Kleinholdermann, U., Gegenfurtner, K. R., Smeets, J. B. J., & Brenner, E. (2014). Center or side: Biases in selecting grasp points on small bars. *Experimental Brain Research*, *232*(7), 2061–2072. https://doi.org/10.1007/s00221-014-3895-z

Penfield, W., & Boldrey, E. (1937). SOMATIC MOTOR AND SENSORY REPRESENTATION IN THE CEREBRAL CORTEX OF MAN AS STUDIED BY ELECTRICAL STIMULATION. *Brain*, *60*(4), 389–443. https://doi.org/10.1093/brain/60.4.389

Perenin, M. T., & Vighetto, A. (1988). Optic ataxia: A specific disruption in visuomotor mechanisms: I. Different aspects of the deficit in reaching for objects. *Brain*, *111*, 643–674.

Petrides, M. (2014). Connectivity of the Core Language Areas. In *Neuroanatomy of Language Regions of the Human Brain* (pp. 139–174). Elsevier. https://doi.org/10.1016/B978-0-12-405514-8.50006-2

Pierce, J. E., & Péron, J. (2020). The basal ganglia and the cerebellum in human emotion. *Social Cognitive and Affective Neuroscience*, *15*(5), 599–613. https://doi.org/10.1093/scan/nsaa076

Pilacinski, A., Wallscheid, M., & Lindner, A. (2018). Human posterior parietal and dorsal premotor cortex encode the visual properties of an upcoming action. *PLOS ONE*, *13*(10), e0198051. https://doi.org/10.1371/journal.pone.0198051

Pisella, L., Gréa, H., Tilikete, C., Vighetto, A., Desmurget, M., Rode, G., Boisson, D., & Rossetti, Y. (2000). An 'automatic pilot' for the hand in human posterior parietal cortex: Toward reinterpreting optic ataxia. *Nature Neuroscience*, *3*(7), 729–736. https://doi.org/10.1038/76694

Pitzalis, S., Sereno, M. I., Committeri, G., Fattori, P., Galati, G., Tosoni, A., & Galletti, C. (2013). The human homologue of macaque area V6A. *NeuroImage*, *82*, 517–530. https://doi.org/10.1016/j.neuroimage.2013.06.026

Poldrack, R. A., Baker, C. I., Durnez, J., Gorgolewski, K. J., Matthews, P. M., Munafò, M. R., Nichols, T. E., Poline, J.-B., Vul, E., & Yarkoni, T. (2017). Scanning the horizon: Towards transparent and reproducible neuroimaging research. *Nature Reviews Neuroscience*, *18*(2), 115–126. https://doi.org/10.1038/nrn.2016.167

Pötter-Nerger, M., Reese, R., Steigerwald, F., Heiden, J. A., Herzog, J., Moll, C. K. E., Hamel, W., Ramirez-Pasos, U., Falk, D., Mehdorn, M., Gerloff, C., Deuschl, G., & Volkmann, J. (2017). Movement-Related Activity of Human Subthalamic Neurons during a Reach-to-Grasp Task. *Frontiers in Human Neuroscience*, *11*, 436. https://doi.org/10.3389/fnhum.2017.00436

Prado, J., Clavagnier, S., Otzenberger, H., Scheiber, C., Kennedy, H., & Perenin, M.-T. (2005). Two Cortical Systems for Reaching in Central and Peripheral Vision. *Neuron*, *48*(5), 849–858. https://doi.org/10.1016/j.neuron.2005.10.010

Price, C. J. (2012). A review and synthesis of the first 20years of PET and fMRI studies of heard speech, spoken language and reading. *NeuroImage*, *62*(2), 816–847. https://doi.org/10.1016/j.neuroimage.2012.04.062

Quinlan, D. J., & Culham, J. C. (2015). Direct comparisons of hand and mouth kinematics during grasping, feeding and fork-feeding actions. *Frontiers in Human Neuroscience*, *9*. https://doi.org/10.3389/fnhum.2015.00580

Radeau, M., & Bertelson, P. (1977). Adaptation to auditory-visual discordance and ventriloquism in semirealistic situations. *Perception & Psychophysics*, *22*(2), 137–146. https://doi.org/10.3758/BF03198746

Ran, Q., Jamoulle, T., Schaeverbeke, J., Meersmans, K., Vandenberghe, R., & Dupont, P. (2020). Reproducibility of graph measures at the subject level using resting-state fMRI. *Brain and Behavior*, *10*(8), 2336–2351. https://doi.org/10.1002/brb3.1705

Rand, M. K., Shimansky, Y., Stelmach, G. E., Bracha, V., & Bloedel, J. R. (2000). Effects of accuracy constraints on reach-to-grasp movements in cerebellar patients. *Experimental Brain Research*, *135*(2), 179–188. https://doi.org/10.1007/s002210000528

Rauschecker, J. P. (2011). An expanded role for the dorsal auditory pathway in sensorimotor control and integration. *Hearing Research*, *271*(1–2), 16–25. https://doi.org/10.1016/j.heares.2010.09.001

Rauschecker, J. P. (2018). Where, When, and How: Are they all sensorimotor? Towards a unified view of the dorsal pathway in vision and audition. *Cortex*, *98*, 262–268. https://doi.org/10.1016/j.cortex.2017.10.020

Rauschecker, J. P., & Tian, B. (2000). Mechanisms and streams for processing of "what" and "where" in auditory cortex. *Proceedings of the National Academy of Sciences*, *97*(22), 11800–11806. https://doi.org/10.1073/pnas.97.22.11800

Rearick, M. P., & Santello, M. (2002). Force synergies for multifingered grasping: Effect of predictability in object center of mass and handedness. *Experimental Brain Research*, *144*(1), 38–49. https://doi.org/10.1007/s00221-002-1024-x

Reichenbach, A., Bresciani, J.-P., Peer, A., Bülthoff, H. H., & Thielscher, A. (2011). Contributions of the PPC to Online Control of Visually Guided Reaching Movements Assessed with fMRI-Guided TMS. *Cerebral Cortex*, *21*(7), 1602–1612. https://doi.org/10.1093/cercor/bhq225

Rens, G., Figley, T. D., Gallivan, J. P., Liu, Y., & Culham, J. C. (2023). Grasping with a Twist: Dissociating Action Goals from Motor Actions in Human Frontoparietal Circuits. *The Journal of Neuroscience*, *43*(32), 5831–5847. https://doi.org/10.1523/JNEUROSCI.0009-23.2023

Rens, N., Bode, S., Burianová, H., & Cunnington, R. (2017). Proactive Recruitment of Frontoparietal and Salience Networks for Voluntary Decisions. *Frontiers in Human Neuroscience*, *11*, 610. https://doi.org/10.3389/fnhum.2017.00610

Revol, P., Rossetti, Y., Vighetto, A., Rode, G., Boisson, D., & Pisella, L. (2003). Pointing errors in immediate and delayed conditions in unilateral optic ataxia. *Spatial Vision*, *16*(3), 347–364. https://doi.org/10.1163/156856803322467572

Rice, N. J., Tunik, E., & Grafton, S. T. (2006). The Anterior Intraparietal Sulcus Mediates Grasp Execution, Independent of Requirement to Update: New Insights from Transcranial Magnetic Stimulation. *The Journal of Neuroscience*, *26*(31), 8176–8182. https://doi.org/10.1523/JNEUROSCI.1641-06.2006

Rizzolatti, G., & Luppino, G. (2001). The Cortical Motor System Review. *Neuron*, *31*, 889–901.

Rizzolatti, G., & Matelli, M. (2003). Two different streams form the dorsal visual system: Anatomy and functions. *Experimental Brain Research*, *153*(2), 146–157. https://doi.org/10.1007/s00221-003-1588-0

Roberts, J., Burkitt, J. J., Willemse, B., Ludzki, A., Lyons, J., Elliott, D., & Grierson, L. E. M. (2013). The influence of target context and early and late vision on goal-directed reaching. *Experimental Brain Research*, *229*(4), 525–532. https://doi.org/10.1007/s00221-013-3614-1

Rondi-Reig, L., Paradis, A.-L., Lefort, J. M., Babayan, B. M., & Tobin, C. (2014). How the cerebellum may monitor sensory information for spatial representation. *Frontiers in Systems Neuroscience*, *8*. https://doi.org/10.3389/fnsys.2014.00205

Rosenbaum, D. A., Cohen, R. G., Meulenbroek, R. G. J., & Vaughan, J. (2006). Plans for Grasping Objects. In M. L. Latash & F. Lestienne (Eds.), *Motor Control and Learning* (pp. 9–25). Kluwer Academic Publishers. https://doi.org/10.1007/0-387-28287-4_2

Rosenbaum, D. A., & Jorgensen, M. J. (1992). Planning macroscopic aspects of manual control. *Human Movement Science*, *11*(1–2), 61–69. https://doi.org/10.1016/0167-9457(92)90050-L

Rosenbaum, D. A., Van Heugten, C. M., & Caldwell, G. E. (1996). From cognition to biomechanics and back: The end-state comfort effect and the middle-is-faster effect. *Acta Psychologica*, *94*(1), 59–85. https://doi.org/10.1016/0001-6918(95)00062-3

Rossetti, Y., Pisella, L., & Vighetto, A. (2003). Optic ataxia revisited: *Experimental Brain Research*, *153*(2), 171–179. https://doi.org/10.1007/s00221-003-1590-6

Rossi, A. F., Pessoa, L., Desimone, R., & Ungerleider, L. G. (2009). The prefrontal cortex and the executive control of attention. *Experimental Brain Research*, *192*(3), 489–497. https://doi.org/10.1007/s00221-008-1642-z

Rost, K., Nowak, D. A., Timmann, D., & Hermsdörfer, J. (2005). Preserved and impaired aspects of predictive grip force control in cerebellar patients. *Clinical Neurophysiology*, *116*(6), 1405–1414. https://doi.org/10.1016/j.clinph.2005.02.015

Rowe, J. B., Toni, I., Josephs, O., Frackowiak, R. S. J., & Passingham, R. E. (2000). The Prefrontal Cortex: Response Selection or Maintenance Within Working Memory? *Science*, *288*(5471), 1656–1660. https://doi.org/10.1126/science.288.5471.1656

Rubinov, M., & Sporns, O. (2010). Complex network measures of brain connectivity: Uses and interpretations. *NeuroImage*, *52*(3), 1059–1069. https://doi.org/10.1016/j.neuroimage.2009.10.003

Salman, M. S. (2002). Topical Review: The Cerebellum: It's About Time! But Timing Is Not Everything-New Insights Into the Role of the Cerebellum in Timing Motor and Cognitive Tasks. *Journal of Child Neurology*, *17*(1), 1–9. https://doi.org/10.1177/088307380201700101

Schaefer, A., Kong, R., Gordon, E. M., Laumann, T. O., Zuo, X.-N., Holmes, A. J., Eickhoff, S. B., & Yeo, B. T. T. (2018). Local-Global Parcellation of the Human Cerebral Cortex from Intrinsic Functional Connectivity MRI. *Cerebral Cortex*, *28*(9), 3095–3114. https://doi.org/10.1093/cercor/bhx179

Scharoun, S. M., Scanlan, K. A., & Bryden, P. J. (2016). Hand and Grasp Selection in a Preferential Reaching Task: The Effects of Object Location, Orientation, and Task Intention. *Frontiers in Psychology*, *7*. https://doi.org/10.3389/fpsyg.2016.00360

Schenk, T., & Hesse, C. (2018). Do we have distinct systems for immediate and delayed actions? A selective review on the role of visual memory in action. *Cortex*, *98*, 228–248. https://doi.org/10.1016/j.cortex.2017.05.014

Schenk, T., & McIntosh, R. D. (2010). Do we have independent visual streams for perception and action? *Cognitive Neuroscience*, *1*(1), 52–62. https://doi.org/10.1080/17588920903388950

Schettino, L. F., Adamovich, S. V., & Poizner, H. (2003). Effects of object shape and visual feedback on hand configuration during grasping. *Experimental Brain Research*, *151*(2), 158–166. https://doi.org/10.1007/s00221-003-1435-3

Schieber, M. H. (2001). Constraints on Somatotopic Organization in the Primary Motor Cortex. *Journal of Neurophysiology*, *86*(5), 2125–2143. https://doi.org/10.1152/jn.2001.86.5.2125

Schmahmann, J. D. (2019). The cerebellum and cognition. *Neuroscience Letters*, *688*, 62–75. https://doi.org/10.1016/j.neulet.2018.07.005

Schuboe, A., Maldonado, A., Stork, S., & Beetz, M. (2008). *Subsequent actions influence motor control parameters of a current grasping action*. 389–394. https://doi.org/10.1109/ROMAN.2008.4600697

Schucht, P., Moritz-Gasser, S., Herbet, G., Raabe, A., & Duffau, H. (2013). Subcortical electrostimulation to identify network subserving motor control. *Human Brain Mapping*, *34*(11), 3023–3030. https://doi.org/10.1002/hbm.22122

Schulz, K. P., Bédard, A.-C. V., Czarnecki, R., & Fan, J. (2011). Preparatory activity and connectivity in dorsal anterior cingulate cortex for cognitive control. *NeuroImage*, *57*(1), 242–250. https://doi.org/10.1016/j.neuroimage.2011.04.023

Schütz, I., Henriques, D. Y. P., & Fiehler, K. (2013). Gaze-centered spatial updating in delayed reaching even in the presence of landmarks. *Vision Research*, *87*, 46–52. https://doi.org/10.1016/j.visres.2013.06.001

Schütz, I., Henriques, D. Y. P., & Fiehler, K. (2015). No effect of delay on the spatial representation of serial reach targets. *Experimental Brain Research*, *233*(4), 1225–1235. https://doi.org/10.1007/s00221-015-4197-9

Sedda, A., Monaco, S., Bottini, G., & Goodale, M. A. (2011). Integration of visual and auditory information for hand actions: Preliminary evidence for the contribution of natural sounds to grasping. *Experimental Brain Research*, *209*(3), 365–374. https://doi.org/10.1007/s00221-011-2559-5

Seegelke, C., Hughes, C. M. L., Schütz, C., & Schack, T. (2012). Individual differences in motor planning during a multi-segment object manipulation task. *Experimental Brain Research*, *222*(1–2), 125–136. https://doi.org/10.1007/s00221-012-3203-8

Seeley, W. W. (2019). The Salience Network: A Neural System for Perceiving and Responding to Homeostatic Demands. *The Journal of Neuroscience*, *39*(50), 9878–9882. https://doi.org/10.1523/JNEUROSCI.1138-17.2019

Seeley, W. W., Menon, V., Schatzberg, A. F., Keller, J., Glover, G. H., Kenna, H., Reiss, A. L., & Greicius, M. D. (2007). Dissociable Intrinsic Connectivity Networks for Salience Processing and Executive Control. *The Journal of Neuroscience*, *27*(9), 2349–2356. https://doi.org/10.1523/JNEUROSCI.5587-06.2007

Selen, L. P. J., & Medendorp, W. P. (2011). Saccadic updating of object orientation for grasping movements. *Vision Research*, *51*(8), 898–907. https://doi.org/10.1016/j.visres.2011.01.004

Shafer-Skelton, A., & Golomb, J. D. (2018). Memory for retinotopic locations is more accurate than memory for spatiotopic locations, even for visually guided reaching. *Psychonomic Bulletin & Review*, *25*(4), 1388–1398. https://doi.org/10.3758/s13423-017-1401-x

Shibata, M., Fuchino, Y., Naoi, N., Kohno, S., Kawai, M., Okanoya, K., & Myowa-Yamakoshi, M. (2012). Broad cortical activation in response to tactile stimulation in newborns. *NeuroReport*, *23*(6), 373–377. https://doi.org/10.1097/WNR.0b013e3283520296

Shirer, W. R., Ryali, S., Rykhlevskaia, E., Menon, V., & Greicius, M. D. (2012). Decoding Subject-Driven Cognitive States with Whole-Brain Connectivity Patterns. *Cerebral Cortex*, *22*(1), 158–165. https://doi.org/10.1093/cercor/bhr099

Shirinbayan, S. I., Dreyer, A. M., & Rieger, J. W. (2019). Cortical and subcortical areas involved in the regulation of reach movement speed in the human brain: An fMRI study. *Human Brain Mapping*, *40*(1), 151–162. https://doi.org/10.1002/hbm.24361

Siegel, J. S., Power, J. D., Dubis, J. W., Vogel, A. C., Church, J. A., Schlaggar, B. L., & Petersen, S. E. (2014). Statistical improvements in functional magnetic resonance imaging analyses produced by censoring high-motion data points. *Human Brain Mapping*, *35*(5), 1981–1996. https://doi.org/10.1002/hbm.22307

Singh, H., & Wulf, G. (2022). Mind over body: Creating an external focus for sport skills. *European Journal of Sport Science*, *22*(4), 610–616. https://doi.org/10.1080/17461391.2021.1887367

Singhal, A., Monaco, S., Kaufman, L. D., & Culham, J. C. (2013). Human fMRI Reveals That Delayed Action Re-Recruits Visual Perception. *PLoS ONE*, *8*(9), e73629. https://doi.org/10.1371/journal.pone.0073629

Smitha, K., Akhil Raja, K., Arun, K., Rajesh, P., Thomas, B., Kapilamoorthy, T., & Kesavadas, C. (2017). Resting state fMRI: A review on methods in resting state connectivity analysis and resting state networks. *The Neuroradiology Journal*, *30*(4), 305–317. https://doi.org/10.1177/1971400917697342

Snow, J. C., Pettypiece, C. E., McAdam, T. D., McLean, A. D., Stroman, P. W., Goodale, M. A., & Culham, J. C. (2011). Bringing the real world into the fMRI scanner: Repetition effects for pictures versus real objects. *Scientific Reports*, *1*(1), 130. https://doi.org/10.1038/srep00130

Sober, S. J., & Sabes, P. N. (2003). Multisensory Integration during Motor Planning. *The Journal of Neuroscience*, *23*(18), 6982–6992. https://doi.org/10.1523/JNEUROSCI.23-18-06982.2003

Sober, S. J., & Sabes, P. N. (2005). Flexible strategies for sensory integration during motor planning. *Nature Neuroscience*, *8*(4), 490–497. https://doi.org/10.1038/nn1427

Soechting, J. F., & Flanders, M. (1992). Moving in Three-Dimensional Space: Frames of Reference, Vectors, and Coordinate Systems. *Annual Review of Neuroscience*, *15*, 167–191. https://doi.org/10.1146/annurev.ne.15.030192.001123

Sokolov, A. A., Miall, R. C., & Ivry, R. B. (2017). The Cerebellum: Adaptive Prediction for Movement and Cognition. *Trends in Cognitive Sciences*, *21*(5), 313–332. https://doi.org/10.1016/j.tics.2017.02.005

Spampinato, D. A., Casula, E. P., & Koch, G. (2024). The Cerebellum and the Motor Cortex: Multiple Networks Controlling Multiple Aspects of Behavior. *The Neuroscientist*, *30*(6), 723–743. https://doi.org/10.1177/10738584231189435

Spence, C. (2007). Audiovisual multisensory integration. *Acoustical Science and Technology*, *28*(2), 61–70. https://doi.org/10.1250/ast.28.61

Sporns, O. (2002). Network analysis, complexity, and brain function. *Complexity*, *8*(1), 56–60. https://doi.org/10.1002/cplx.10047

Sporns, O., & Betzel, R. F. (2016). Modular Brain Networks. *Annual Review of Psychology*, *67*(1), 613–640. https://doi.org/10.1146/annurev-psych-122414-033634

Srinivasan, L., Asaad, W. F., Ginat, D. T., Gale, J. T., Dougherty, D. D., Williams, Z. M., Sejnowski, T. J., & Eskandar, E. N. (2013). Action Initiation in the Human Dorsal Anterior Cingulate Cortex. *PLoS ONE*, *8*(2), e55247. https://doi.org/10.1371/journal.pone.0055247

Stam, C. J., Van Straaten, E. C. W., Van Dellen, E., Tewarie, P., Gong, G., Hillebrand, A., Meier, J., & Van Mieghem, P. (2016). The relation between structural and functional connectivity patterns in complex brain networks. *International Journal of Psychophysiology*, *103*, 149–160. https://doi.org/10.1016/j.ijpsycho.2015.02.011

Starowicz-Filip, A., Prochwicz, K., Kłosowska, J., Chrobak, A. A., Myszka, A., Bętkowska-Korpała, B., & Kwinta, B. (2021). Cerebellar Functional Lateralization From the Perspective of Clinical Neuropsychology. *Frontiers in Psychology*, *12*, 775308. https://doi.org/10.3389/fpsyg.2021.775308

Steenhuis, R. E., & Goodale, M. A. (1988). The Effects of Time and Distance on Accuracy of Target-Directed Locomotion: Does an Accurate Short-Term Memory for Spatial Location Exist? *Journal of Motor Behavior*, *20*(4), 399–415. https://doi.org/10.1080/00222895.1988.10735454

Straube, B., Van Kemenade, B. M., Arikan, B. E., Fiehler, K., Leube, D. T., Harris, L. R., & Kircher, T. (2017). Predicting the Multisensory Consequences of One's Own Action: BOLD Suppression in Auditory and Visual Cortices. *PLOS ONE*, *12*(1), e0169131. https://doi.org/10.1371/journal.pone.0169131

Sun, S., Li, X., Zhu, J., Wang, Y., La, R., Zhang, X., Wei, L., & Hu, B. (2019). Graph Theory Analysis of Functional Connectivity in Major Depression Disorder With High-Density Resting State EEG Data. *IEEE Transactions on Neural Systems and Rehabilitation Engineering*, *27*(3), 429–439. https://doi.org/10.1109/TNSRE.2019.2894423

Tagliabue, M., & McIntyre, J. (2014). A modular theory of multisensory integration for motor control. *Frontiers in Computational Neuroscience*, *8*. https://doi.org/10.3389/fncom.2014.00001

Takeuchi, T. (1993). Auditory Information in Playing Tennis. *Perceptual and Motor Skills*, *76*(3_suppl), 1323–1328. https://doi.org/10.2466/pms.1993.76.3c.1323

Talati, A., Valero-Cuevas, F. J., & Hirsch, J. (2005). *Visual andTactile Guidance of Dexterous Manipulation Tasks: An fMR Study*. *101*.

Thach, W. T. (2014). Does the Cerebellum Initiate Movement? *The Cerebellum*, *13*(1), 139–150. https://doi.org/10.1007/s12311-013-0506-7

Therrien, A. S., & Bastian, A. J. (2015). Cerebellar damage impairs internal predictions for sensory and motor function. *Current Opinion in Neurobiology*, *33*, 127–133. https://doi.org/10.1016/j.conb.2015.03.013

Thomas, B. L., Karl, J. M., & Whishaw, I. Q. (2015). Independent development of the Reach and the Grasp in spontaneous self-touching by human infants in the first 6 months. *Frontiers in Psychology*, *5*. https://doi.org/10.3389/fpsyg.2014.01526

Thompson, A. A., & Henriques, D. Y. P. (2011). The coding and updating of visuospatial memory for goal-directed reaching and pointing. *Vision Research*, *51*(8), 819–826. https://doi.org/10.1016/j.visres.2011.01.006

Tomasi, D., Wang, G.-J., & Volkow, N. D. (2013). Energetic cost of brain functional connectivity. *Proceedings of the National Academy of Sciences*, *110*(33), 13642–13647. https://doi.org/10.1073/pnas.1303346110

Tomasi, D., Wang, R., Wang, G.-J., & Volkow, N. D. (2014). Functional Connectivity and Brain Activation: A Synergistic Approach. *Cerebral Cortex*, *24*(10), 2619–2629. https://doi.org/10.1093/cercor/bht119

Tomou, G., Baltaretu, B. R., Ghaderi, A., & Crawford, J. D. (2025). Saccades influence functional modularity in the human cortical vision network. *Scientific Reports*, *15*(1), 10683. https://doi.org/10.1038/s41598-025-95568-9

Tubaldi, F., Ansuini, C., Tirindelli, R., & Castiello, U. (2008). The Grasping Side of Odours. *PLoS ONE*, *3*(3), e1795. https://doi.org/10.1371/journal.pone.0001795

Tugac, N., Gonzalez, D., Noguchi, K., & Niechwiej-Szwedo, E. (2019). The role of somatosensory input in target localization during binocular and monocular viewing while performing a high precision reaching and placement task. *Experimental Eye Research*, *183*, 76–83. https://doi.org/10.1016/j.exer.2018.08.013

Turella, L., & Lingnau, A. (2014). Neural correlates of grasping. *Frontiers in Human Neuroscience*, *8*. https://doi.org/10.3389/fnhum.2014.00686

Turesky, T. K., Olulade, O. A., Luetje, M. M., & Eden, G. F. (2018). An fMRI study of finger tapping in children and adults. *Human Brain Mapping*, *39*(8), 3203–3215. https://doi.org/10.1002/hbm.24070

Umeda, T., Isa, T., & Nishimura, Y. (2019). The somatosensory cortex receives information about motor output. *Science Advances*, *5*(7), eaaw5388. https://doi.org/10.1126/sciadv.aaw5388

Ünal, A. B., Platteel, S., Steg, L., & Epstude, K. (2013). Blocking-out auditory distracters while driving: A cognitive strategy to reduce task-demands on the road. *Accident Analysis & Prevention*, *50*, 934–942. https://doi.org/10.1016/j.aap.2012.07.020

Valente, G., Castellanos, A. L., Hausfeld, L., De Martino, F., & Formisano, E. (2021). Cross-validation and permutations in MVPA: Validity of permutation strategies and power of cross-validation schemes. *NeuroImage*, *238*, 118145. https://doi.org/10.1016/j.neuroimage.2021.118145

Valyear, K. F., & Culham, J. C. (2010). Observing Learned Object-specific Functional Grasps Preferentially Activates the Ventral Stream. *Journal of Cognitive Neuroscience*, *22*(5), 970–984. https://doi.org/10.1162/jocn.2009.21256

Van De Kamp, C., & Zaal, F. T. J. M. (2007). Prehension is really reaching and grasping. *Experimental Brain Research*, *182*(1), 27–34. https://doi.org/10.1007/s00221-007-0968-2

Van Den Heuvel, M. P., & Hulshoff Pol, H. E. (2010). Exploring the brain network: A review on resting-state fMRI functional connectivity. *European Neuropsychopharmacology*, *20*(8), 519–534. https://doi.org/10.1016/j.euroneuro.2010.03.008

Van Den Heuvel, M. P., & Sporns, O. (2013). Network hubs in the human brain. *Trends in Cognitive Sciences*, *17*(12), 683–696. https://doi.org/10.1016/j.tics.2013.09.012

Van Pelt, S., & Medendorp, W. P. (2008). Updating Target Distance Across Eye Movements in Depth. *Journal of Neurophysiology*, *99*(5), 2281–2290. https://doi.org/10.1152/jn.01281.2007

Vannest, J. J., Karunanayaka, P. R., Altaye, M., Schmithorst, V. J., Plante, E. M., Eaton, K. J., Rasmussen, J. M., & Holland, S. K. (2009). Comparison of fMRI data from passive listening and active-response story processing tasks in children. *Journal of Magnetic Resonance Imaging*, *29*(4), 971–976. https://doi.org/10.1002/jmri.21694

Varoquaux, G., Raamana, P. R., Engemann, D. A., Hoyos-Idrobo, A., Schwartz, Y., & Thirion, B. (2017). Assessing and tuning brain decoders: Cross-validation, caveats, and guidelines. *NeuroImage*, *145*, 166–179. https://doi.org/10.1016/j.neuroimage.2016.10.038

Váša, F., & Mišić, B. (2022). Null models in network neuroscience. *Nature Reviews Neuroscience*, *23*(8), 493–504. https://doi.org/10.1038/s41583-022-00601-9

Vaziri, S., Diedrichsen, J., & Shadmehr, R. (2006). Why Does the Brain Predict Sensory Consequences of Oculomotor Commands? Optimal Integration of the Predicted and the Actual Sensory Feedback. *The Journal of Neuroscience*, *26*(16), 4188–4197. https://doi.org/10.1523/JNEUROSCI.4747-05.2006

Velji-Ibrahim, J., Crawford, J. D., Cattaneo, L., & Monaco, S. (2022). Action planning modulates the representation of object features in human fronto-parietal and occipital cortex. *European Journal of Neuroscience*, *56*(6), 4803–4818. https://doi.org/10.1111/ejn.15776

Vesia, M., Barnett-Cowan, M., Elahi, B., Jegatheeswaran, G., Isayama, R., Neva, J. L., Davare, M., Staines, W. R., Culham, J. C., & Chen, R. (2017). Human dorsomedial parieto-motor circuit specifies grasp during the planning of goal-directed hand actions. *Cortex*, *92*, 175–186. https://doi.org/10.1016/j.cortex.2017.04.007

Vesia, M., & Crawford, J. D. (2012). Specialization of reach function in human posterior parietal cortex. *Experimental Brain Research*, *221*(1), 1–18. https://doi.org/10.1007/s00221-012-3158-9

Vesia, M., Prime, S. L., Yan, X., Sergio, L. E., & Crawford, J. D. (2010). Specificity of Human Parietal Saccade and Reach Regions during Transcranial Magnetic Stimulation. *The Journal of Neuroscience*, *30*(39), 13053–13065. https://doi.org/10.1523/JNEUROSCI.1644-10.2010

Vesia, M., Yan, X., Henriques, D. Y., Sergio, L. E., & Crawford, J. D. (2008). Transcranial Magnetic Stimulation Over Human Dorsal–Lateral Posterior Parietal Cortex Disrupts Integration of Hand Position Signals Into the Reach Plan. *Journal of Neurophysiology*, *100*(4), 2005–2014. https://doi.org/10.1152/jn.90519.2008

Vingerhoets, G. (2014). Contribution of the posterior parietal cortex in reaching, grasping, and using objects and tools. *Frontiers in Psychology*, *5*. https://doi.org/10.3389/fpsyg.2014.00151

Virameteekul, S., & Bhidayasiri, R. (2022). We Move or Are We Moved? Unpicking the Origins of Voluntary Movements to Better Understand Semivoluntary Movements. *Frontiers in Neurology*, *13*, 834217. https://doi.org/10.3389/fneur.2022.834217

Vossel, S., Geng, J. J., & Fink, G. R. (2014). Dorsal and Ventral Attention Systems: Distinct Neural Circuits but Collaborative Roles. *The Neuroscientist*, *20*(2), 150–159. https://doi.org/10.1177/1073858413494269

Wagner, M. J., Kim, T. H., Kadmon, J., Nguyen, N. D., Ganguli, S., Schnitzer, M. J., & Luo, L. (2019). Shared Cortex-Cerebellum Dynamics in the Execution and Learning of a Motor Task. *Cell*, *177*(3), 669-682.e24. https://doi.org/10.1016/j.cell.2019.02.019

Wallace, M. T., Meredith, M. A., & Stein, B. E. (1998). Multisensory Integration in the Superior Colliculus of the Alert Cat. *Journal of Neurophysiology*, *80*(2), 1006–1010. https://doi.org/10.1152/jn.1998.80.2.1006

Wallace, M. T., Wilkinson, L. K., & Stein, B. E. (1996). Representation and integration of multiple sensory inputs in primate superior colliculus. *Journal of Neurophysiology*, *76*(2), 1246–1266. https://doi.org/10.1152/jn.1996.76.2.1246

Warren, J. E., Wise, R. J. S., & Warren, J. D. (2005). Sounds do-able: Auditory–motor transformations and the posterior temporal plane. *Trends in Neurosciences*, *28*(12), 636–643. https://doi.org/10.1016/j.tins.2005.09.010

Watts, D. J., & Strogatz, S. H. (1998). *Collective dynamics of 'small-world' networks*.

Weaverdyck, M. E., Lieberman, M. D., & Parkinson, C. (2020). Tools of the Trade Multivoxel pattern analysis in fMRI: A practical introduction for social and affective neuroscientists. *Social Cognitive and Affective Neuroscience*, *15*(4), 487–509. https://doi.org/10.1093/scan/nsaa057

Westwood, D. A., & Goodale, M. A. (2003). A haptic size-contrast illusion affects size perception but not grasping. *Experimental Brain Research*, *153*(2), 253–259. https://doi.org/10.1007/s00221-003-1599-x

Wheaton, L. A., & Hallett, M. (2007). Ideomotor apraxia: A review. *Journal of the Neurological Sciences*, *260*(1–2), 1–10. https://doi.org/10.1016/j.jns.2007.04.014

Wolpert, D. M., Ghahramani, Z., & Jordan, M. I. (1995). An Internal Model for Sensorimotor Integration. *Science*, *269*(5232), 1880–1882. https://doi.org/10.1126/science.7569931

Wong, W.-W., Chan, S.-T., Tang, K.-W., Meng, F., & Tong, K.-Y. (2013). Neural correlates of motor impairment during motor imagery and motor execution in sub-cortical stroke. *Brain Injury*, *27*(6), 651–663. https://doi.org/10.3109/02699052.2013.771796

Woodworth, R. S. (1899). Accuracy of voluntary movement. *The Psychological Review: Monograph Supplements*, *3*(3), i–114. https://doi.org/10.1037/h0092992

Worsley, K. J. (2001). Statistical analysis of activation images. In *Functional MRI: An Introduction to Methods*.

Xia, M., Wang, J., & He, Y. (2013). BrainNet Viewer: A Network Visualization Tool for Human Brain Connectomics. *PLoS ONE*, *8*(7), e68910. https://doi.org/10.1371/journal.pone.0068910

Yarkoni, T., Poldrack, R. A., Nichols, T. E., Van Essen, D. C., & Wager, T. D. (2011). Large-scale automated synthesis of human functional neuroimaging data. *Nature Methods*, *8*(8), 665–670. https://doi.org/10.1038/nmeth.1635

Yu, R., Han, B., Wu, X., Wei, G., Zhang, J., Ding, M., & Wen, X. (2023). Dual-functional Network Regulation Underlies the Central Executive System in Working Memory. *Neuroscience*, *524*, 158–180. https://doi.org/10.1016/j.neuroscience.2023.05.025

Zangemeister, W. H., & Stark, L. (1982). Types of Gaze Movement: Variable Interactions of Eye and Head Movements. *Experimental Neurology*, *77*, 563–577.

Zhu, J., Hasanbegović, H., Liu, L. D., Gao, Z., & Li, N. (2023). Activity map of a cortico-cerebellar loop underlying motor planning. *Nature Neuroscience*, *26*(11), 1916–1928. https://doi.org/10.1038/s41593-023-01453-x

APPENDIX I: AUTHOR CONTRIBUTIONS

CHAPTER 2

G.N.L.: Conceptualization, Investigation, Formal Analysis, Visualization, Writing - Original draft, Writing - review and editing. X.Y.: Conceptualization, Writing - review and editing. E.F.: Conceptualization, Writing - review and editing. J.D.C.: Conceptualization, Formal Analysis, Writing - review and editing.

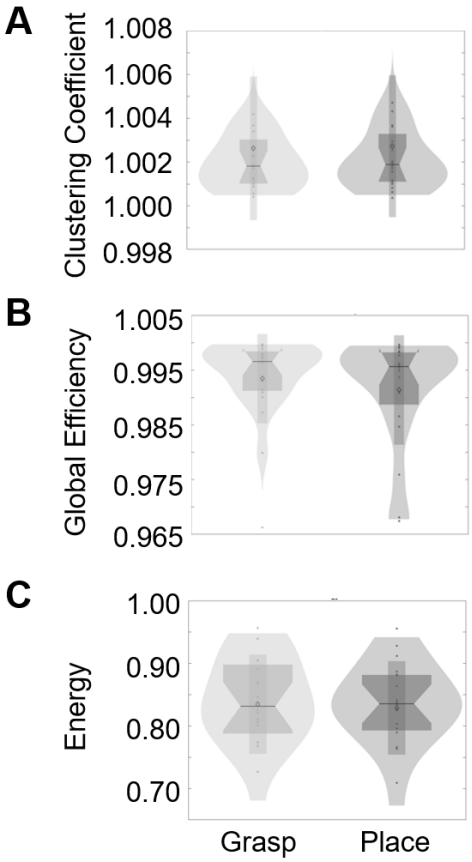
CHAPTER 3

G.N.L: Methodology, Investigation, Data curation, Formal Analysis, Conceptualization, Visualization, Writing - Original draft, Writing - review and editing. E.F.: Conceptualization, Methodology, Writing - review and editing. J.D.C: Conceptualization, Methodology, Writing - review and editing, Funding acquisition, Project administration, Supervision.

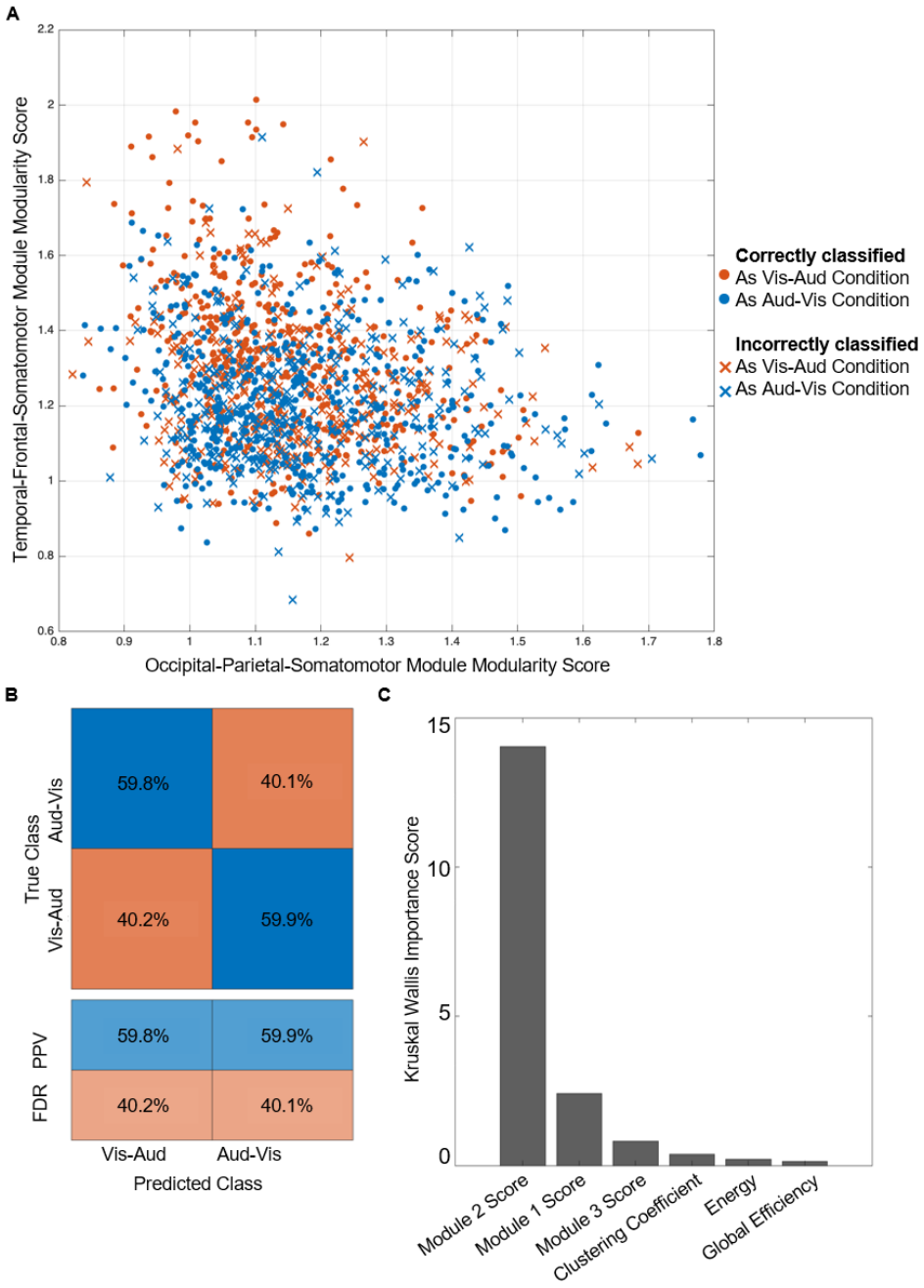
CHAPTER 4

G.N.L.: Data curation, Formal Analysis, Visualization, Writing - Original draft, Writing - review and editing. A.L.: Conceptualization, Investigation, Writing - review and editing. A.G.: Formal Analysis, Writing - review and editing. L.M.: Formal Analysis, Writing - review and editing. S.M.: Conceptualization, Writing - review and editing. E.F.: Writing - review and editing. J.D.C.: Conceptualization, Formal Analysis, Writing - review and editing.

APPENDIX II: SUPPLEMENTARY FIGURES



Supplementary Figure 3.1 Violin plots displaying distributions of normalized global network parameters: clustering coefficient (A), global efficiency (B), and energy (C). To normalize these global measures, they were divided by the global measure outputs obtained from a null model. In all three cases, our nonparametric test did not find any significant difference based on task (*grasp* vs *place*).



Supplementary Figure 3.1 Classifier Analysis represents the performance of the Narrow Neural Network classifier to differentiate between the Visual-Auditory Order (Vis-Aud) and Auditory-Visual Order (Aud-Vis). A) Scatterplot showing the distribution of modularity values from the top two predictors based on the Kruskal Importance Score (Module 2: Occipital-Parietal-Somatomotor Module and Module 1: Temporal-Frontal-Somatomotor Modularity Index). A circle represents a correctly predicted trial order, and a cross represents an incorrectly predicted trial order. B) displays the confusion matrix, comparing the predicted data point identity (Vis-Aud or Aud-Vis) with its true identity. The bottom panel table shows the positive predictive values (PPV) and false discovery rates (FDR) of the Grasp data (left column) and the Place data (right column). C) The Kruskal-Wallis importance scores of each feature were used to classify the order of cue

presentation. A higher value indicates greater separation between classes based on that feature – meaning the feature is more useful for classification.